UNIVERSIDADE FEDERAL DE SANTA CATARINA
CENTRO DE CIÊNCIAS AGRÁRIAS
PROGRAMA DE PÓS-GRADUAÇÃO EM RECURSOS GENÉTICOS VEGETAIS

Márcia Denise Rossarolla

Fisiologia da interação e mecanismos moleculares de resistência da videira (*Vitis vinifera)* ao *Plasmopara viticola* (BERK. & M. A. CURTIS) Berl. & De Toni

Florianópolis
2021

Márcia Denise Rossarolla

Fisiologia da interação e mecanismos moleculares de resistência da videira (*Vitis vinifera)* ao *Plasmopara viticola* (BERK. & M. A. CURTIS) Berl. & De Toni

Tese submetida ao Programa de Pós-Graduação em Recursos Genéticos Vegetais da Universidade Federal de Santa Catarina para a obtenção do título de Doutor em Ciências.
Orientador: Prof. Rubens Onofre Nodari, Dr.

Florianópolis
2021

Ficha de identificação da obra elaborada pelo autor,
através do Programa de Geração Automática da Biblioteca Universitária da UFSC.

Rossarolla, Márcia Denise
Fisiologia da interação e mecanismos moleculares e resistência da videira (*Vitis vinifera*) ao *Plasmopara viticola* (BERK. & M. A. CURTIS) Berl. & De Toni / Márcia Denise Rossarolla ; orientador, Rubens Onofre Nodari, 2021.
173 p.

Tese (doutorado) - Universidade Federal de Santa Catarina, Centro de Ciências Agrárias, Programa de Pós Graduação em Recursos Genéticos Vegetais, Florianópolis, 2021.

Inclui referências.

1. Recursos Genéticos Vegetais. 2. Vitis vinifera. 3. Imunidade vegetal. 4. Interação planta patógeno. 5. Resistência a doenças. I. Nodari, Rubens Onofre. II. Universidade Federal de Santa Catarina. Programa de Pós Graduação em Recursos Genéticos Vegetais. III. Título.

Márcia Denise Rossarolla

Fisiologia da interação e mecanismos moleculares de resistência da videira (*Vitis vinifera)* ao *Plasmopara viticola* (BERK. & M. A. CURTIS) Berl. & De Toni

O presente trabalho em nível de doutorado foi avaliado e aprovado por banca examinadora composta pelos seguintes membros:

Prof. Rubens Onofre Nodari, Dr.
Universidade Federal de Santa Catarina

Prof. Miguel Pedro Guerra, Dr.
Universidade Federal de Santa Catarina

Prof. Aparecido Lima da Silva, Dr.
Universidade Federal de Santa Catarina

Dr. Marco Antônio Dalbó, Dr.
EPAGRI – Videira

Certificamos que esta é a **versão original e final** do trabalho de conclusão que foi julgado adequado para obtenção do título de Doutora em Ciências.

ICP-Edu
Documento assinado digitalmente
Claudio Roberto Fonseca Sousa Soares
Data: 28/03/2021 11:16:45-0300
CPF: 501.085.575-53
Verifique as assinaturas em https://v.ufsc.br

Coordenação do Programa de Pós-Graduação

ICP-Edu
Documento assinado digitalmente
Rubens Onofre Nodari
Data: 28/03/2021 11:03:09-0300
CPF: 144.811.620-15
Verifique as assinaturas em https://v.ufsc.br

Prof. Rubens Onofre Nodari, Dr.
Orientador

Florianópolis, 2021

Dedico este trabalho a todos que me acompanharam durante a jornada do doutorado, aos meus pais, ao meu namorado, meus irmãos, aos familiares, amigos e professores que me apoiaram durante todo este caminho.

AGRADECIMENTOS

À Universidade Federal de Santa Catarina e ao PPG em Recursos Genéticos Vegetais docentes, discentes e colaboradores.

Ao Professor Rubens Onofre Nodari, pela confiança, amizade e apoio científico, pela valiosa oportunidade de trabalhar junto ao NEUVIN, meu coorientador do mestrado, e pela orientação durante todas as etapas do doutorado pelos ensinamentos e oportunidades proporcionados.

Ao Professor Miguel Pedro Guerra pela orientação, pelas contribuições durante todas as etapas deste trabalho, apoio científico ensinamentos e oportunidades proporcionadas.

Ao Professor Leocir José Welter, pela amizade, confiança e apoio científico, pela oportunidade de fazer parte do grupo de pesquisa desde a graduação até o doutorado, e pela valiosa colaboração durante as etapas do trabalho ensinamentos e oportunidades proporcionados, meu muito obrigado.

À secretária do PPG em Recursos Genéticos Vegetais Bernadete Ribas, a Livia, e ao técnico do laboratório LFDGV Frankilin e o engenheiro agrônomo André Ribeiro sempre dispostos a ajudar.

A toda minha família principalmente meus pais Osmar e Lenir, meus irmãos Marcio e Miriam, sobrinhos Bianca e Rian, pelo amor, confiança e apoio em todos os momentos;

Ao Tiago C. Tomazetti, amigo, colega de aula e de trabalho, pela contribuição no trabalho, pelo companheirismo de todos os momentos, principalmente nos intermináveis finais de semana no laboratório, pelo carinho e incentivo.

A Dr Henrique Pessoa e sua equipe do laboratório de LMFV da EMBRAPA UVA E VINHO pela parceria e colaboração e prestatividade no trabalho, agradeço também pelas amizades dos colegas da pousada da EMBRAPA.

Ao Dr Vanildo e Felipe do laboratório de Biotecnologia da UENF pela ajuda nas análises de proteomica e escrita do artigo.

Aos integrantes do LFDGV que estiveram presentes durante o tempo de realização de meu doutorado.

Ao Professor Aparecido pelo apoio e incentivo no trabalho e em todos os momentos do doutorado, sempre com uma palavra de incentivo e conforto.

Ao professor José Afonso Voltolini pela confiança, amizade e oportunidades proporcionados durante o doutorado e por desenvolver e implantar o projeto 'Tecnologias para o desenvolvimento da viticultura catarinense', a partir deste foi possível a realização desta tese e oportunidade de realizar uma parte do trabalho na Fondazione Edmund Mach/Trento/Itália.

Aos companheiros e amigos do NEUVIN (Núcleo de estudos da uva e do vinho), pela colaboração e incentivo nos trabalhos, parceria nas jantas e degustações.

Aos colaboradores e pesquisadores da Epagri que fazem parte do projeto "Avaliação vitivinícola de genótipos de videiras nas condições edafoclimáticas de Santa Catarina", André Luiz Kulkamp de Souza, Marco Antônio Dalbó, Vinicius Cagliari, Emilio Dela Bruna, Alberto Brighenti e Emilio Brighenti.

Ao professor Lirio Dal Vesco pela amizade, ensinamentos e por proporcionar o trabalho na unidade experimental da UFSC Curitibanos.

Ao Leonardo enólogo da Abreu Garcia e Dr Ernani pelas oportunidades e estadias na Vinícola Abreu Garcia.

Às instituições envolvidas no projeto que possibilitou, dentre outros avanços técnicos-cientificos, a elaboração desta tese, em especial a Fondazione Edmund Mach, que me acolheu para desenvolvimento de parte desta pesquisa, contudo, extensivo também às demais instituições que tornam possíveis estes avanços, UFSC, EPAGRI e Julius Kuhn Institut, muito obrigado pela parceria.

À CAPES pela concessão da bolsa de doutorado no Brasil, bem como, pelo período sanduíche na Itália.

À FAPESC e CNPq pelo apoio financeiro para desenvolvimento das atividades de pesquisa.

Vorrei ringraziare...

Il Dott. Marco Stefanini, per avermi dato la possibilità di svolgere una parte della mia tesi presso la Fondazione Edmund Mach, inserendomi nel suo gruppo di ricerca UGMGV oltre che per tutti gli insegnamenti, l'attenzione e per l'esempio professionale che mi ha dato. Desidero estendere la mia gratitudine a tutta la sua famiglia.

La Dott.ssa Urska, per la disponibilità dimostrata nell'eseguire le analisi metabolomica presso il suo laboratorio e per tutti gli utili insegnamenti.

I dottori Claudio Moser, Luca Zulini, La Dott.ssa Silvia Vezzulli per tutti gli insegnamenti, l'attenzione e l'esempio professionale.

I dottori Duilio Porro e Stefano per tutti gli insegnamenti, l'attenzione l'esempio professionale ed i momenti di confronto e discussione.

Tutti gli amici italiani: Giulia, Ramona, Domen, Cesar, Samuel, Paola, Nicola, Umberto, Benedetta, Simone, Giorgio, Camila, Francesco, Monica Colombo, Monica della Serra, Carlotta, Ayesha, Taba, Lorenzo, Stefano Piazza, Giulia Malacarne, Simone, Alice, Michele, Valerio, Diego, Silvano, grazie per i momenti piacevoli trascorsi insieme, per i momenti di gioia, per l'amicizia, l'affetto, la forza e la cordialità. “Ho vissuto alcuni dei momenti più belli della mia vita insieme a voi! Grazie immensamente.

A todos que contribuíram direta ou indiretamente para minha formação e concretização desta Tese.

À Deus e/ou pelas forças que me guiaram até aqui.

"*In vino veritas*"
Proverbio latino

RESUMO

A videira, uma das espécies frutíferas mais cultivadas mundialmente, apresenta suscetibilidade a diversos patógenos, destacando-se como principal causador de danos o míldio, (*Plasmopara viticola*). Locos de resistência contra este patógeno (*Rpv*) são descritos para outras espécies do gênero *Vitis*. *Rpv*s estão associados ao reconhecimento patogênico, provavelmente via *nucleotide-bind Leucine-rich repeat*, desencadeando reações celulares de imunidade, *Effector-Triggered Immunity* (ETI). A cascata de sinais ativada resulta na morte celular, inibindo o progresso do patógeno. Pouco se sabe quanto aos mecanismos moleculares ativados por *Rpv*s, atuando isoladamente ou piramidados. Portanto, o objetivo com esta tese de doutorado foi caracterizar, a nível celular, as interações entre plantas portadoras de Rpvs e o *P. viticola*. A tese divide-se em 3 capítulos, no primeiro é apresentado a cinética da expressão gênica para os genes JAZMONATE ZIM DOMAIN 1 (JAZ1) e JAZ3, MYC2, TOPLESS, PATHOGENESIS RELATED-1 (PR1) e PR10, NONEXPRESSOR OF PATHOGENESIS RELATED 1 (NPR1), WRKY70, AtMYB44, STILBENE SYNTHASE (STS), GLICOSILTRANSFERASE (GT) e RESVERATROL O-METHYLTRANSFERASE (ROMT), bem como, dos níveis hormonais para ácido jasmônico (AJ), ácido salicílico (AS), ácido abscísico (ABA), ácido giberélico (GA_4), ácido indolacético (AIA), zeatina (Z) e *trans*-zeatina-ribose (t-Z-R), em genótipos portadores de genes Rpvs expostos ao patógeno. Na avaliação da expressão gênica, foram utilizados genótipos contendo ausência de Rpv (genótipo suscetível), *Rpv3-1*, *Rpv1+Rpv3-1* e *Rpv3-3+Rpv10*. A quantificação hormonal foi feita nos mesmos genótipos e também no genótipo *Rpv3-1+Rpv3-3*. No segundo capítulo, é apresentado a expressão diferencial de proteínas, identificadas em culturas celulares, contendo *Rpv1+Rpv3-1*, *Rpv3-1* e rpv (suscetível), expostas ao patógeno. As culturas celulares foram obtidas a partir de calos foliares, mantidos em meio de cultura sólido e inoculados com *P viticola*, a coleta foi realizada em 24 horas após a inoculação. Os resultados apontam para a resposta de expressão diferencial de proteínas e processos biológicos nas células a partir de genótipos com resistência genética, resultando na indução de estresse oxidativo e morte celular, enquanto que no genótipo suscetível foi verificada maior quantidade de proteínas reguladas negativamente ou silenciadas com a inoculação do patógeno. O terceiro capítulo relata as atividades realizadas durante o período sanduíche na Fondazione Edmund Mach (FEM, Trento-IT). Foi desenvolvido uma avaliação temporal de uma pesquisa de médio prazo com o objetivo de conhecer o perfil metabólico de genótipos de videira contendo diferentes locos de resistência ao *P. viticola* quando expostos ao referido patógeno em distintos anos. Foram utilizados os genótipos

F12P127 (*Rpv3-1+Rpv3-3+Rpv10*) e F12P60 (*Rpv3-1+Rpv12*), além das cultivares Bianca (*Rpv3-1*) Jasmine (*Rpv12*) BC4 (*Rpv1*), Solaris (*Rpv3-3+Rpv10*), pertencentes a coleção de germoplasma da FEM. Foram quantificadas as expressões dos compostos primários, fenólicos, voláteis e lipídicos em 0, 12, 48 e 96 horas posterior a inoculação (hpi). A principal alteração metabólica ocorre nas primeiras horas, principalmente pela sinalização do estresse oxidativo e a indução da morte celular. Com os resultados obtidos nos três capítulos foi possível descrever fisiológica e bioquimicamente a interação da videira e o *P. viticola* nos níveis de expressão gênica, mudanças no perfil de proteínas e modulação dos compostos metabólicos, durante o processo de interação planta patógeno.

Palavras-chave: Genótipos PIWI. Interação planta patógeno. Expressão gênica. Proteômica. Metabolômica. Viticultura. Mildio.

ABSTRACT

Grapevine is one of the most cultivated fruit worldwide; however, it is susceptible to several pathogens, as downy mildew (*Plasmopara viticola*), which is one of the main grapevine pathogens. Resistance loci (*Rpv*) against this pathogen have been described for *Vitis* species. *Rpvs* are associated with pathogenic recognition, probably via nucleotide-bind Leucine-rich repeat, triggering cellular immune reactions, by Effector-Triggered Immunity (ETI), resulting in cell death, and inhibition of the pathogen's progress. Little is known about the molecular mechanisms activated by *Rpvs*, acting alone, or pyramided. The aim of the present work was to characterize the interactions between exposed plants carrying *Rpvs* and *P. viticola*. The thesis is composed by 3 chapters. In the first one it is presented the kinetics of the gene expression for the genes JAZMONATE ZIM DOMAIN 1 (JAZ1) and JAZ3, MYC2, TOPLESS, PATHOGENESIS RELATED-1 (PR1) and PR10, NONEXPRESSOR OF PATHOGENESIS RELATED 1 (NPR1), WRKY70, AtMYB44, STILBENE SYNTHASE (STS), GLYCOSTRANSFERASE (GT) and RESVERATROL O-METHYLTRANSFERASE (ROMT), as well as hormone levels for jasmonic acid (JA), salicylic acid (SA), abscisic acid (ABA), gibberellic acid (GA_4), indoleacetic acid (IAA), zeatin (Z) and trans-zeatin-ribose (tZR), in genotypes with *Rpvs* exposed to pathogen. For gene expression, genotypes containing *Rpv3-1*, *Rpv1+Rpv3-1* and *Rpv3-3+Rpv10* and *rpv* (susceptible) were used. For hormonal quantification, the genotype *Rpv3-1+Rpv3-3* was added. In the second chapter, it is presented the differential expression of proteins, identified in cell cultures, containing *Rpv1+Rpv3-1*, *Rpv3-1* and *rpv*, exposed to contamination with *P. viticola*. The cell cultures were obtained from leaf calluses, cultivated in gelled culture medium, and inoculated with *P. viticola*; the collection being performed 24 hours after inoculation. The results pointed out the differential expression of proteins and biological processes in cells from genotypes with genetic resistance, resulting in the induction of oxidative stress and cell death. In the susceptible genotype, a greater amount of negatively regulated or silenced proteins was observed with the pathogen inoculation. The third chapter reports activities carried out in the sandwich period at the Fondazione Edmund Mach (FEM, Trento-IT). Part of a research was developed with the objective of understand the metabolic profile of grapevine genotypes carrying different *Rpv* loci against when exposed to *P. viticola*. The genotypes F12P127 (*Rpv3-1+Rpv3-3+Rpv10*) and F12P60 (*Rpv3-1+Rpv12*) were used, in addition to the cultivars Bianca (*Rpv3-1*), Jasmine (*Rpv12*), BC4 (*Rpv1*), and Solaris (*Rpv3-3+Rpv10*), belonging to the germplasm collection FEM. The expressions of primary, phenolic, volatile and lipid compounds were quantified at 0,

12, 48 and 96 hours post inoculation (hpi). The main metabolic alteration occurs in the first hours, mainly by signaling oxidative stress and inducing cell death. The results obtained allowed the physiological and biochemical characterization of the interaction between grapevine and *P. viticola* in the levels of gene expression, changes in the protein profile and modulation of the metabolic compounds, during the pathogen plant interaction process.

Keywords: PIWI genotypes. Plant pathogen interaction. Gene expression. Proteomic. Metabolomic. Viticulture. Downy mildew.

LISTA DE FIGURAS

Revisão de literatura

Capítulo I

Capítulo III

LISTA DE TABELAS

Revisão de Literatura

Capítulo I

Capítulo II

LISTA DE ABREVIATURAS E SIGLAS

2,4-D: Ácido diclorofenóxiacético

µL: microlitro

µM: micro molar

ABA: Ácido abscísico, também valido na sigla em inglês 'Abscisic acid'

ADE: Água destilada esterilizada

AJ: Ácido Jasmônico

ANOVA: Análise de variância, na sigla em inglês '*analysis of variance*'

AS: Ácido Salicílico

avr: Avirulence – genes de avirulência presentes no patógeno

BAP: 6-Benzilamina Purina, também valido na sigla em inglês 'Benzylamino Purine'

BG40: β-GLUCOSIDASE 40

CC-NB-LRR: Coiled Coil Nucleotide Binding Leucine Rich Repeat

Cq: Cycle of quantification

CRRSP38: CYSTEINE-RICH REPEAT SECRETORY PROTEIN 38

DPI: Days Post Inoculation

DSD1: Da Silva e Doazan 1, meio de cultivo vegetal

EBL: epibrassinoesteroid

EF1-α: elongation factor 1-α

ETI: effector triggered immunity

g: gravidade da terra, considerado constante de 9,81 m s^{-2}

GA_3: Gibberellic acid 3 (Giberilina)

GA_4: Gibberellic acid 3 (Giberilina)

GAPDH: Glyceraldehyde-3-phosphate dehydrogenase

GC: Gas Chromatography

GT: Glicosiltransferase

HPI: Hours Post Inoculation

HR: Hypersensitivity

IAA: Indole-3-Acetic Acid

IBA: Indole Butyric Acid

JA: Jasmonic Acid

JAZ: Jasmonate-zim-domain

kDa: kilodaltons, equivalente a massa de mil daltons

KDE: Kernel Density Estimation

LC: liquid chromatography

LOD: Limit of detection

LOQ: Limit of quantification

MAP: Mitogen-activated protein

MAS: Marker-Assisted Selection

MeJA: Methyl Jasmonate

mM: millimolar

MS: Mass Spectrometry

NB-LRR: Nucleotide Binding Leucine Rich Repeat

ng: nanograma

NINJA: Novel Interactor of JAZ

NPR: non-expressor of pathogenesis-related

PAMP: Pathogen Associated Molecular Patterns

PC: Principal Component

PCA: Principal Component Analysis

PCR: Polymerase Chain Reaction

PIWI: em alemão *pilzwiderstandsfähigen Reben*, videira resistente a doenças fúngicas

PR: Pathogen Related

PTI: PAMP triggered immunity

QTL: quantitative trait loci

***R*-loci:** Resistance loci

***R*-loco:** Resistance loco

RNA: ribonucleic acid

ROMT: Resveratrol O-methyltransferase

ROS: Reactive Oxygen Species

***rpv*:** genótipo não portador de locos *Rpv*

Rpv: Resistance to *Plasmopara viticola*

RT-qPCR: Reverse Transcriptase – quantitative PCR

SA: Salicylic Acid

SCF-COI: SKP-Cullin-F-box protein

SDW: sterile distilled water

STS: Stilbene synthase

TIR-NB-LRR: toll/interleukin-1 receptor Nucleotide Binding Leucine Rich Repeat

TPL: proteína TOPLESS

tZR: trans-Zeatin-riboside

UGT43: UDP-GLYCOSYLTRANSFERASE 43-LIKE

UGT74E2: UDP-GLYCOSYLTRANSFERASE 74E2-LIKE

UHPLC: Ultra-High-Performance Liquid Chromatography

UPLC: Ultra-Performance Liquid Chromatography

Z: Zeatin

SUMÁRIO

1 ANTECEDENTES E JUSTIFICATIVA

O cultivo da videira (*Vitis vinifera*) é realizado a milênios e está permeado em diversas culturas e civilizações. Assim, a produção da uva, seja para produção de vinho ou consumo *in natura*, é parte da história humana. Atualmente, diversas regiões do mundo praticam a viticultura com diferentes finalidades e dentre as espécies do gênero Vitis, a *V. vinifera* destaca-se devido a sua qualidade obtida por um longo processo de domesticação que selecionou genótipos para o consumo humano.

O centro de domesticação e de diversidade da *V. vinifera* é conhecido como centro Euroasiático, estando geograficamente localizado a partir do crescente fértil até a Europa. Outros dois centros de diversidade do gênero *Vitis* são descritos, o centro Asiático, localizado na Ásia oriental e o centro Americano, localizado na América do norte.

A *V. vinifera* foi domesticada principalmente por apresentar alta qualidade das uvas e vinhos, em regiões climáticas que desfavoreciam o surgimento de patógenos, possuindo assim baixa resistência genética a uma gama de patógenos. Nos demais centros de diversidade, no entanto, a presença de patógenos favoreceu a seleção voltada para a resistência a doenças. Neste contexto, o cultivo da *V. vinifera* é impactado pela suscetibilidade a doenças, principalmente o míldio.

O míldio da videira é causado pelo cromista biotrófico obrigatório *Plasmopara viticola*, originário da América do Norte. Foi acidentalmente introduzido na Europa em meados do século XIX, com a importação de material vegetal de videiras de espécies silvestres. Desde então, sua disseminação tomou conta do continente e se espalhou pelo mundo. Até o momento a principal forma de manejo deste patógeno é realizado por meio de aplicações de agrotóxicos, sempre que as condições climáticas forem favoráveis ao surgimento da doença.

Em climas com elevada precipitação, favorecendo o molhamento foliar, como o sul do Brasil, o uso de agrotóxicos tem sido empregado na prática de forma preventiva e curativa, devido a elevada umidade do ar que mantem condições favoráveis durante praticamente todo o ciclo da videira. Neste contexto, programas de melhoramento genético têm buscado a introdução de resistência genética contra o *P. viticola* a partir de espécies de outros centros de diversidade da videira. A nomenclatura destes locos foi definida pelo termo inglês *Resistance Plasmopara viticola* (*Rpv*) seguida da numeração que reflete o momento em que o referido loco foi adicionado no banco de dados do catálogo internacional de variedades de videira (VIVC, www.vivc.de). Atualmente 31 *Rpv*'s são descritos na literatura, além de 7 haplótipos preditos

via análise de pedigree para o *Rpv3*, dos quais 3 estão descritos, nomeados respectivamente como *Rpv3-1*, *Rpv3-2* e *Rpv3-3*.

O mapeamento destes locos é realizado em estudos de análises de *Quantitative Trade Loci* (QTLs) e programas de melhoramento a nível global, tem priorizado incorporar em seus materiais, QTLs de maior efeito. *Rpv1* e *Rpv3,* originários de espécies do centro de diversidade americano, bem como, *Rpv10* e *Rpv12*, originários de espécies do centro de diversidade asiático, são os mais utilizados no melhoramento genético da videira. Melhoristas também vem adotando a combinação de *Rpv*s, técnica conhecida como piramidação; diversos estudos com *Rpv*s piramidados tem demonstrado o efeito aditivo dos genes utilizados. Esta estratégia também vem sendo utilizada para aumentar a durabilidade da resistência, uma vez que, patógenos que conseguiram superar a resistência de alguns *Rpv*s ainda não avirulentos em genótipos contendo outros *Rpv*s, dificultando que um patógeno seja capaz de superar a resistência conjunta de um genótipo piramidado, desde que diferentes genótipos em cultivo contenham diferentes combinações de genes *Rpv*.

O mecanismo de resistência genética ainda não é totalmente conhecido para todos os *Rpv*s. Contudo há fortes indícios da imunidade desencadeada por efetores (da sigla inglês ETI, *Effector Triggered Immunity*) via reconhecimento dos efetores patogênicos por receptores quinases do tipo *nucleotide binding leucine-rich repeat* (NB-LRR). Assim, a piramidação de *Rpv*s que reconhecem efetores diferentes ou desencadeiem a sinalização por vias alternativas, podem contribuir para a durabilidade da resistência.

Todavia, há poucos estudos que tratam da interação celular, entre planta e patógeno, com genótipos portadores de resistência genética, individualizados ou piramidados. Esta informação é importante para guiar estratégias de melhoramento genético visando aumentar a sustentabilidade e a durabilidade da resistência. Pesquisas realizadas apontam para o envolvimento de hormônios secundários, tais como jasmonatos e salicilatos e a produção de compostos fenólicos, destacando a indução de síntese de estilbenos, na sinalização patogênica, e na indução da morte celular, sintoma reconhecido como hipersensibilidade. Contudo, ainda são pouco conhecidos os efeitos da piramidação de genes de resistência oriundos de distintas fontes e suas atuações em termos de sinalização do patógeno, controle e produtos da expressão gênica. Neste contexto, avanços científicos na área molecular com a interação patógeno hospedeiro entre *P. viticola e V. vinífera* foram obtidos com a realização do presente estudo.

1.1 A VIDEIRA (*Vitis vinifera*)

A família *Vitaceae* possui cerca de 950 espécies distribuídas em 16 gêneros que são agrupados em 5 tribos (*Ampelopsideae, Cisseae, Cayratieae, Parthenocisseae* e *Viteae*), a tribo

Viteae possui espécies com ploidia 2*n* = 38 ou 40 e agrupa os gêneros *Vitis* e *Ampelocissus* (WEN et al., 2018a). O gênero *Vitis* surgiu a aproximadamente 32.6 a 48.6 milhões de anos e, a aproximadamente 18 milhões de anos foi subdividido em dois subgêneros, *Muscadinia* e *Vitis* (LIU et al., 2016b; WAN et al., 2013; WEN et al., 2018a).

O subgênero *Muscadinia* possui somente duas espécies, *V. popenoei* e *V. rotundifolia*, enquanto o subgênero *Vitis* possui maior diversidade, compreendendo em torno de 70 espécies, que estão distribuídas geograficamente em três centros de diversidade (MOORE, 1991; SAPORTA, 1879; WEN et al., 2018a, 2018b). Os centros Asiático e Americano apresentam a maior diversidade de espécies (LIU et al., 2016b; WAN et al., 2013), enquanto o centro de diversidade euroasiático possui somente a *V. vinifera* que pode ser dividida em subespécie silvestre (*V. vinifera* ssp. *sylvestris*) e domesticada (*V. vinifera* ssp. *sativa*) (EMANUELLI et al., 2013; LIANG et al., 2019; THIS; LACOMBE; THOMAS, 2006).

Dados moleculares e fenotípicos apontam para a origem geográfica da domesticação da *V. vinifera* entre o mar Cáspio e o mar Negro, mais precisamente no sul do Cáucaso, na região onde atualmente encontra-se a Georgia (IMAZIO et al., 2013; RIAZ et al., 2018). As principais características fenotípicas alteradas pela domesticação, da *V. vinifera* ssp. *sylvestris* para a *V. vinifera* ssp. *sativa* foram a mudança de plantas dioicas para hermafroditas; o formato das sementes, que são esféricas nas cultivares silvestres e piriformes nas espécies domesticadas, a redução na expressão de metabolitos secundários, como os estilbenos e a seleção de genes envolvidos na composição aromática do vinho (DUAN et al., 2015; EMANUELLI et al., 2010; RIAZ et al., 2018; TERRAL et al., 2010).

Apesar de, historicamente, a *V. vinifera* ssp. *sativa* ser propagada vegetativamente, por meio da produção de clones, é relatada elevada diversidade genética dentro da espécie, sendo descritos mais de 10.000 variedades domesticadas (EMANUELLI et al., 2013; LIANG et al., 2019). Contudo, devido a síndrome de domesticação e a ausência de coabitação com patógenos, genótipos de *V. vinifera*, via de regra, apresentam baixa resistência à patógenos, dentre eles, o *P. viticola*, agente casual do míldio e maior causador de danos na viticultura (AZIZ et al., 2020; BOSO et al., 2011; BUONASSISI et al., 2017a, 2017b; DEYETT et al., 2019; PIRRELLO et al., 2019, 2020).

1.2 O MÍLDIO DA VIDEIRA (*Plasmopara viticola*)

O míldio da videira é causado pelo patógeno *Plasmopara viticola*, que é considerado um dos dez principais oomicetos causadores de danos em plantas (KAMOUN et al., 2015). As perdas causadas pelo míldio na viticultura são significativas em quantidade, como em qualidade

(NOGUEIRA JÚNIOR et al., 2019; PONS et al., 2018). O ataque do patógeno, dependendo do órgão vegetal atingido, pode resultar no apodrecimento das inflorescências, brotações e cachos, além da perda de área foliar fotossinteticamente ativa e desfolhamento (ROSSI; CAFFI; GOBBIN, 2013). O patógeno é ainda mais problemático para o cultivo da videira em ambientes úmidos, devido a maior severidade da doença nestas condições e a dispersão de seus inóculos potencializada pela umidade (ROSSI; CAFFI, 2012).

Em estudo com 80 acessos de diferentes espécies do gênero *Vitis*, não foi reportada resistência ao míldio em acessos das espécies *V. vinifera* e *V. acerifolia* (CADLE-DAVIDSON, 2008). Curiosamente, regiões InDel, no braço longo do cromossomo 18, que flanqueiam o *Rpv3-1* (BELLIN et al., 2009; WELTER et al., 2007) e o *Rpv27* (SAPKOTA et al., 2019), são compartilhados por acessos da *V. acerifolia* (FORIA et al., 2018b). Um estudo com 120 acessos de diversas espécies do gênero *Vitis*, novamente apontou para a ausência de resistência genética ao míldio, em acessos de *V. acerifolia* (ZHAO et al., 2019). Por outro lado, em *V. vinifera* var. Mgaloblishvili, foram mapeados os locos *Rpv29*, *Rpv30* e *Rpv31*, que conferem resistência parcial ao *P. viticola*, nos cromossomos 14, 3 e 16, respectivamente (SARGOLZAEI et al., 2020).

O *P. viticola* é um cromista, biotrófico obrigatório (GRENVILLE-BRIGGS; WEST, 2005). Este oomiceto heterotálico possui forma reprodutiva dimórfica, formando esporos de forma sexuada e assexuada (GESSLER; PERTOT; PERAZZOLLI, 2011; ROSSI; CAFFI; GOBBIN, 2013). Na fase sexuada são necessários dois indivíduos com diferentes tipos de acasalamento (*mating types*), P1 e P2, ocorrendo a formação do oósporo a partir da fusão do oogônio (feminino) e anterídio (masculino) (GESSLER; PERTOT; PERAZZOLLI, 2011; WONG; BURR; WILCOX, 2001).

Os oósporos podem permanecer em dormência por mais de cinco anos, até atingir as condições ambientais favoráveis para a germinação, com temperatura entre 20 a 24°C e presença de água livre (ROSSI et al., 2008; ROSSI; CAFFI; GOBBIN, 2013). A partir da germinação dos oósporos, é formado o macroesporângio que, dependendo das condições ambientais, de temperatura, umidade e luminosidade, sobrevivem entre algumas horas a até mesmo alguns dias (BLASSER; WELTZIEN, 1979). Esporângios viáveis, na superfície vegetal, quando em presença de água livre, liberam de quatro a oito zoósporos (UNGER et al., 2007) os zoósporos do *P. viticola* são biflagelados e sensíveis a desidratação, necessitando de água livre para sua sobrevivência. Uma vez na folha, os zoósporos são guiados pelo hospedeiro, necessitando de um filme de água para nadarem até os estômatos, quando próximos das células guarda, emitem o flagelo, formando o tubo germinativo que penetra no estômato, colonizando

a câmara estomática (KIEFER et al., 2002; UNGER et al., 2007). O micélio inicia o crescimento pelo espaço intercelular no tecido do mesófilo foliar, formando haustórios que aumenta a superfície de contato com as células e facilita a troca molecular entre o patógeno e a planta parasitada (BURRUANO, 2000). Em um período que varia de 5 a 18 dias após a infecção, quando a reação planta patógeno for compatível e em ausência de luz azul, o *P. viticola* produz esporangióforos que carregam esporângios que contém zoósporos gerados assexuadamente responsáveis pela infecção secundária (LALANCETTE; ELLIS; MADDEN, 1988; LALANCETTE; MADDEN; ELLIS, 1988; RUMBOLZ et al., 2002).

Na espécie *V. labrusca*, que apresenta reação de incompatibilidade com o *P. viticola*, é reportada a desorientação na formação do tubo germinativo, evitando a penetração do mesmo na câmara estomática (NASCIMENTO-GAVIOLI et al., 2020). Em outras relações de incompatibilidade planta-patógeno, é reportada a atuação de mecanismos de defesa vegetal retardando o desenvolvimento do *P. viticola* a partir da penetração do tubo germinativo na câmara estomática, induzindo as reações de hipersensibilidade (KIEFER et al., 2002). Ainda há relatos da existência de depósitos de calose nas células adjacentes, representando uma barreira física para a penetração do patógeno no hospedeiro (GINDRO; PEZET; VIRET, 2003).

O manejo comumente realizado para esta doença tem sido a utilização de elevadas doses de fungicidas. Contudo, cenários de mudanças climáticas apontam para o aumento da necessidade de agrotóxicos para manejar a doença (SALINARI et al., 2006). Além disso, diversos estudos tem reportado o surgimento de isolados mutantes que desenvolvem resistência genética aos fungicidas em diversas partes do mundo (BAUDOIN et al., 2008; BLUM; WALDNER; GISI, 2010; CAMPBELL et al., 2020, 2021; CORIO-COSTET et al., 2011; MATASCI et al., 2008).

O sequenciamento genômico do *P. viticola* apontou que este oomiceto possui 17.014 genes preditos, dos quais, 1.301 foram anotados como envolvidos na produção de proteínas secretadas. Muitas destas estão envolvidas na interação planta-patógeno, atuando na célula vegetal como efetores (YIN et al., 2017).

1.3 INTERAÇÃO PLANTA-PATÓGENO

A relação entre o hospedeiro e o patógeno ocorre em diversos níveis. Em organismos eucariotos o reconhecimento do patógeno pelo hospedeiro ocorre via *Pattern recognition receptors* (PRRs), podendo ser diretamente via *Pathogen-associated molecular patterns* (PAMPs) ou indiretamente pela detecção dos ferimentos que sinalizam o ataque patogênico (JANEWAY; MEDZHITOV, 2002; MATZINGER, 2002; ZIPFEL; FELIX, 2005). PAMPs

são, normalmente proteínas, peptídeos ou carbohidratos, dentre outras moléculas, produzidas especificamente por determinado patógeno, permitindo o hospedeiro identificar a presença do mesmo pela detecção desta molécula.

O hospedeiro pode detectar as PAMPs por meio de proteínas do tipo PRR, desenvolvendo a imunidade desencadeada por PAMPS, *PAMP-triggered immunity* (PTI) (JONES; DANGL, 2006). O patógeno por sua vez, secreta proteínas de avirulência (Avr), que são efetores e tem por finalidade principal, inativar a PTI da planta hospedeira para facilitar a penetração e colonização dos tecidos (BOZKURT et al., 2012; KING et al., 2014; LIU et al., 2019a). Este mecanismo de supressão da resistência via efetores é conhecido por *effector-triggered susceptibility* (ETS) (JONES; DANGL, 2006). Os principais efetores intracelulares secretados por oomicetos são o N-terminal conservado Arg-x-Leu-Arg (RXLR) e o CRinkling and Necrosis (CRN) (CHEN et al., 2020; WAWRA et al., 2012).

Dentre os efetores encontrados no genoma do *P. viticola*, os tipos RXLR e CRN são também relatados com maior abundância (BRILLI et al., 2018; CHEN et al., 2020; YIN et al., 2017). Estes efetores são secretados pelo haustório do patógeno no início da interação com o hospedeiro e translocados para o interior da célula vegetal com ajuda de uma sequência de aminoácidos específicos RXLR-EER e LXLFLAK para RXLR e CRN, respectivamente (SCHORNACK et al., 2010; WHISSON et al., 2007). Secreção de efetores das famílias RXLR e CRN é frequentemente reportada em oomicetos (AMARO et al., 2017; BOZKURT et al., 2012), como, por exemplo, *Plasmopara halstedii* (GASCUEL et al., 2016), *Phytophthora parasitica* (ATTARD et al., 2014), *Phytophthora capsici* (STAM et al., 2013) e *Phytophthora infestans* (BOS et al., 2006), entre outros. Um estudo comparativo revelou a presença de 12 famílias de efetores RXLR compartilhadas entre *P. viticola e P. halstedii* além da presença de oito domínios CRN descritos em *P. infestans* (MESTRE et al., 2016), demonstrando que estes domínios são conservados entre os oomicetos e identificando também domínios que determinam a especificidade do hospedeiro.

Visando o aproveitamento de mecanismos de resistência genética, encontrados em outras espécies do gênero *Vitis*, programas de melhoramento da videira, tem buscado incorporar os caracteres de resistência em variedades viníferas via melhoramento genético, também com auxílio de técnicas moleculares para mapeamento de QTL's ligados a genes de resistência e incorporação dos mesmos via retrocruzamentos em seleção assistida por marcadores moleculares (BELLIN et al., 2009; MERDINOGLU et al., 2003; SCHWANDER et al., 2012; VENUTI et al., 2013; WELTER et al., 2007).

Na comparação do desenvolvimento da infecção do míldio em um genótipo contendo o gene de resistência *Rpv10* e outro com ausência de resistência, foi verificado, via microscopia de fluorescência, a deposição de calose nas células guardas das plantas *Rpv10+* (GINDRO; PEZET; VIRET, 2003). Também estão descrito na literatura resultados de estudos envolvendo mais de um gene de resistência piramidados; contudo, são ainda poucos os estudos que demonstram uma perspectiva de que a interação entre os genes de resistência ao míldio é do tipo aditiva, com maior eficiência da maquinaria de resistência quando em comparação a atuação dos genes isolados (NASCIMENTO-GAVIOLI et al., 2017; VENUTI et al., 2013). Assim, são necessários estudos mais aprofundados para elucidar a nível celular a interação entre estes genes, oriundos de distintas espécies de *Vitis.*

Com a utilização da microscopia eletrônica de transmissão, foi demonstrado que a penetração do míldio nos estômatos da videira, causa alteração no metabolismo de carboidratos do hospedeiro. A principal alteração verificada foi a redução do metabolismo de consumo do amido durante o período escuro, resultando na acumulação destes compostos nos cloroplastos (GAMM et al., 2011).

A ocorrência concomitante da desregulação do metabolismo e da sincronia do funcionamento das células guardas, provoca alterações nos mecanismos de fechamento estomático e eleva o tempo da planta com estômatos abertos, bem como, a condutância estomática. Esta desregulação leva a um possível *crosstalk* entre a infecção do míldio e a inativação ou alteração de algumas rotas hormonais da planta, como por exemplo o ácido abscísico, principal responsável pelo fechamento estomático (ALLÈGRE et al., 2007). Contudo, não se exclui a possibilidade de o míldio estar envolvido na alteração de concentrações em outros hormônios que indiretamente também estão envolvidos no processo de regulação estomática, como auxinas, citocininas, brassinoesteroides, salicilatos, jasmonatos e etileno (DASZKOWSKA-GOLEC; SZAREJKO, 2013).

Durante o processo de penetração das hifas no hospedeiro, ocorre um processo de reconhecimento bioquímico celular entre o cromista e a planta (GUERREIRO et al., 2016; MERZ et al., 2015), o que inclui a ocorrência de mudanças substanciais no citoesqueleto das células do patógeno. Iniciando-se assim a formação das hifas primárias na orientação de penetração na cavidade estomacal (RIEMANN et al., 2002). No hospedeiro tem sido verificado mudanças substanciais no metabolismo celular, que é mais pronunciada em células contendo genes de resistência (VENUTI et al., 2013; WANG et al., 2017b).

Estas mudanças resultam na complexa modulação do metabolismo de defesa vegetal, alterando imediatamente o conteúdo proteico da célula e iniciando a expressão de proteínas

relacionadas a defesa, como as *PR-proteínas* visando combater o patógeno ou dificultar seu avanço (MILLI et al., 2012). Dentre os compostos do metabolismo gerados durante o processo de reconhecimento do patógeno pela planta, a síntese de estilbenos é amplamente discutida na literatura, estando envolvida com diversos eventos que causam estresse para a planta (SHI et al., 2014). Esta afirmação é sustentada por inúmeros estudos que destacam a *upregulation* do metabolismo de fitoalexinas, principalmente a síntese de estilbenos durante ataques de fitopatógenos (ALONSO-VILLAVERDE et al., 2011; CHONG; POUTARAUD; HUGUENEY, 2009; DERCKS; CREASY, 1989; PEZET et al., 2003, 2004; RICHTER et al., 2006; SCHNEE; VIRET; GINDRO, 2008; WANG et al., 2017b).

A quantificação de polifenóis e estilbenos mostrou que o pterostilbeno foi especificamente acumulado em folhas pré-tratadas com o elicitor Benzotiadiazol (BTH), um indutor da resistência sistêmica adquirida e associado à eficácia biológica e aumentos significativos nos transcritos do gene das proteínas PR (DUFOUR et al., 2013). Outro estudo, utilizando diretamente o jasmonato como elicitor em culturas celulares de *V. vinífera* demonstrou que este hormônio vegetal é um ativador da síntese de estilbenos, como resveratrol e piceid (TAURINO et al., 2015). Além dos jasmonatos, que apresentam influência direta com a ativação dos mecanismos bioquímicos promotores da sinalização dos estilbenos.

Os hormônios vegetais, ácido abscísico e salicilatos também estão aparentemente envolvidos na cascata de regulação de sinais induzindo a resistência da videira ao míldio (PERAZZOLLI et al., 2008; WANG et al., 2017b). Em genótipos com os genes piramidados, *Rpv1* e *Rpv3*, foi verificada maior resistência em comparação a genótipos com somente um dos genes de resistência. Estes genes atuam no período pós-inoculação e elevam a atividade do metabolismo antioxidante em resposta ao estímulo oxidativo do apoplasto (NASCIMENTO-GAVIOLI et al., 2017).

O processo de sinalização da doença é complexo e, mesmo com diversos estudos envolvendo o assunto, este não está completamente elucidado. As respostas metabólicas desencadeadas nas rotas bioquímicas celulares são responsáveis por uma série de alterações no perfil metabólico citoplasmático (CHITARRINI et al., 2017) e envolvem principalmente a ativação de proteínas de respostas patogênicas (PR – proteínas) e a elevação dos teores de espécies reativas de oxigênio, bem como, em alguns casos, o depósito de calose (GINDRO; PEZET; VIRET, 2003; MERZ et al., 2015; MESTRE et al., 2017). Estes processos desencadeiam sinais bioquímicos que resultam na morte celular (CHOUDHURY et al., 2017), descrita na literatura como reação de hipersensibilidade (HR); desta forma, impedindo ou

dificultando o progresso da doença em genótipos resistentes (HARA-NISHIMURA; HATSUGAI, 2011; HOFIUS et al., 2011).

Reações de resistência ocorrem em magnitude variável durante o estágio de latência, estágio seguinte a colonização da folha, durante o qual a hifa cresce na fase abaxial da folha, sem causar sintomas visíveis da doença. O tempo e a intensidade da reação da planta é altamente governado pelo genoma, pois a reação de resistência apresenta estabilidade de expressão em diferentes condições ambientais (CADLE-DAVIDSON, 2008; STAUDT; KASSEMEYER, 1995). Em acessos resistentes de videiras da América do Norte foi verificado que a reação de resistência ocorre após o contato estabelecido do haustório com as células do mesofilo (DÍEZ-NAVAJAS et al., 2008; JÜRGES et al., 2009; POLESANI et al., 2010).

A coevolução do míldio com diferentes mecanismos de resistência da videira resultou na formação de patógenos com maior especificidade para cada espécie hospedeira (ROUXEL et al., 2013). O desenvolvimento de protocolos de infecção controlada e novos avanços nas abordagens utilizando ferramentas "omicas" tem elucidado o funcionamento dos mecanismos de defesa desencadeados na videira em resposta ao ataque de *Plasmopara viticola* (BUONASSISI et al., 2017b). O conhecimento dos mecanismos moleculares envolvidos na interação de plantas e patógenos é de fundamental importância para o desenvolvimento de estratégias que melhor explorem os mecanismos de resistência dos vegetais (JONES; DANGL, 2006).

A indução da morte celular é um mecanismo comumente observado em genótipos contendo *Rpv*'s. Este evento, evita o avanço do patógeno biotrófico, impedindo maiores danos no tecido hospedeiro. No entanto, alguns estudos de interação planta patógeno, tem relatado a produção de supressores da morte celular por parte do patógeno, impedindo, ou reduzindo a efetividade do mecanismo de resistência na planta (GÓMEZ-ZELEDÓN; SPRING, 2018; XIANG et al., 2016). Nas regiões genômicas onde são encontrados os locos *Rpv*'s, é frequentemente relatado a existência de proteínas ricas em repetições de lucinas do tipo Nucleotide-Binding Site Leucine Rich Repeat (NB-LRR) (FEECHAN et al., 2013; SARGOLZAEI et al., 2020; SCHWANDER et al., 2012; VENUTI et al., 2013; ZYPRIAN et al., 2016). Esta família de proteínas é responsável por identificar efetores patogênicos e desencadear a *Effector-Triggered Immunity* (ETI), conforme demonstrado na Figura 1 (ALBERT et al., 2015; DANGL; JONES, 2001).

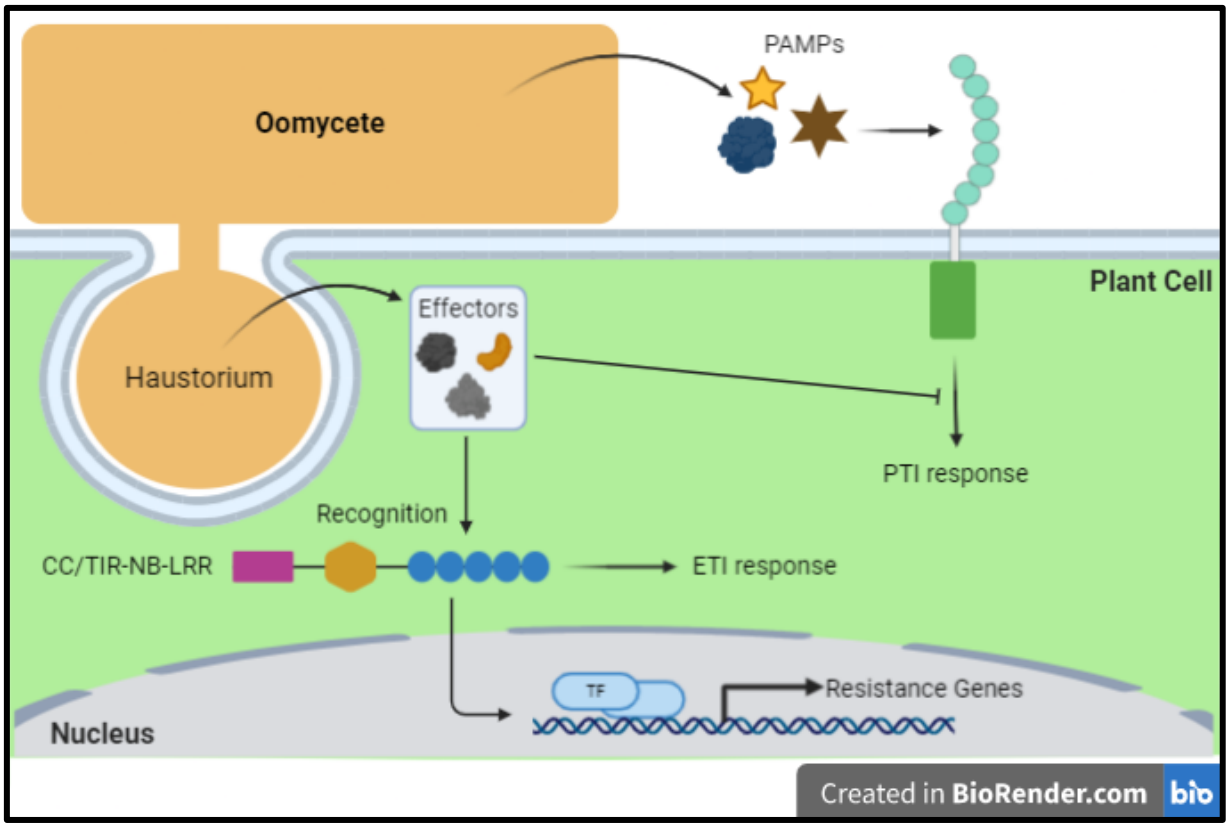

Figura 1. Interação planta-patógeno. O reconhecimento ocorre via receptores transmembranas, de *Pathogen-Associated Molecular Patterns* (PAMPs), secretados pelo oomiceto no apoplasto, que desencadeiam a *PAMP-Triggered Immunity* (PTI). Para bloquear a PTI, o oomiceto forma haustórios, aumentando a superfície de contato com a célula do hospedeiro e secreta efetores, promovendo a *Effector Triggered Susceptibility* (ETS). Hospedeiros que apresentam resistência a este patógeno, desenvolveram mecanismos celulares de reconhecimentos destes efetores patogênicos, via *Coiled-coil* (CC-) ou *Toll Interleukin 1 Receptor* (TIR-) nucleotide bind leucine rich repeat (NB-LRR) que promovem a ativação de vias de resistência celular ao oomiceto, via *Effector Triggered Immunity* (ETI).

O *Rpv1* é descrito como uma região altamente repetitiva, sendo constituída em 50% por elementos transponíveis. A região possui, dentre outras 31 sequências codificantes de proteínas potencialmente funcionais, uma família de genes codificantes de proteínas putativas do tipo toll interleukin 1 receptor nucleotide-binding leucine rich repeat (TIR-NB-LRR) (FEECHAN et al., 2013), responsáveis pelo início da cascata de sinal induzindo o sistema de defesa da célula vegetal (SWIDERSKI; BIRKER; JONES, 2009; VAN ECK; BRADEEN, 2018). Além disso, a presença do gene SUBTILISIN-LIKE PROTEASE SBT5.3 (XM_010659200.1), um regulador da morte celular programada, corrobora com a observação de hipersensibilidade como resposta neste R-loco (FIGUEIREDO et al., 2016; FIGUEIREDO; SOUSA SILVA; FIGUEIREDO, 2018).

O *Rpv3* está localizado em uma região igualmente rica em sequencias NB-LRR, juntamente às LRR-kinase receptor-like, que são responsáveis por ativar a cascata de sinais resultando na indução da expressão de genes PR (pathogenesis-related), com destaque para a atuação do gene PR-1 (CASAGRANDE et al., 2011). Este processo resulta também na morte celular programada, gerando a reação de hipersensibilidade desencadeada pela presença do *P. viticola*. A hipersensibilidade é uma reação também verificada em genótipos contendo o *Rpv10*, neste loco é também verificado abundancia de sequencias NB-LRR, além da presença de uma proteína transmembranar ankyrin-like, genes ligados a *Systemic Acquired Resistance* (SAR), um fator de transcrição responsável pela sinalização de estresse por etileno e genes ligados a rota dos salicilatos, reguladores da ativação de genes PR (CAO et al., 1994; LE HENANFF et al., 2009; SCHWANDER et al., 2012; SHARMA; PANDEY, 2016).

Um estudo do loco *Rpv3*, reporta a presença de um gene candidato do tipo NB-LRR, na posição VIT_18s0041g01790 (ZYPRIAN et al., 2016). Nesta mesma posição (LOC100256747), no genoma de referência PN40024 está anotado o gene *TMV RESISTANCE PROTEIN N*, gene este que também está associado ao mecanismo de resistência a doenças. Outros genes da mesma família são reportados no cromossomo 15, ligados ao *Rpv25* que é herdado da espécie asiática *V. amurensis* (LIN et al., 2019).

Em estudo envolvendo genômica estrutural e funcional do loco *Rpv12*, são relatados 13 CC-NBS-LRR (coiled-coil-NBS-LRR), a uma distância de aproximadamente 0,24 cM do epicentro do referido R-Loco (VENUTI et al., 2013). Os autores também relataram que estas famílias de CC-NBS-LRR ocupam uma região de 600 kb, estando intercaladas com outros genes com funções não relacionadas, como Asparagina Sinthase B, Cytochromo P450 89A2 e Hypothetical protein coding region (VENUTI et al., 2013). O mesmo padrão de associação entre famílias de genes NBS-LRR e R-Loci é relatado para o *Rpv10*, que provém do mesmo ancestral do *Rpv12* (SCHWANDER et al., 2012).

Para o R-Loco *Rpv3-3*, foi recentemente desenvolvido um estudo abrangendo a abordagem da genômica estrutural, genômica funcional e metabolômica (VEZZULLI et al., 2019). Os autores relatam a associação entre o *Rpv3-3* e a ativação de diversos genes associados com a resistência, principalmente ligados ao metabolismo dos estilbenos, metabolismo lipídico, especialmente envolvido na síntese dos jasmonatos, bem como, o metabolismo dos salicilatos, conforme evidenciado pela atuação dos genes da família WRKY (ZHANG et al., 2019a). Estes resultados corroboram com os relatados em estudos anteriores com o *Rpv3*, que apontou a hipersensibilidade como resposta do mecanismo de resistência, sendo resultado da morte

celular proveniente da síntese de proteínas PR acionadas pelas vias de jasmonatos e salicilatos (CASAGRANDE et al., 2011).

Ainda se tratando do *Rpv3*, em uma abordagem de metabolômica visando descobrir biomarcadores para o patossistema entre planta – patógeno, o principal grupo de moléculas metabólicas diferencialmente detectadas foram os estilbenos (CHITARRINI et al., 2017). Este resultado demonstra a complexidade da interação entre a planta e o patógeno, assim como, demonstra a importância da rota dos estilbenos nos estudos envolvendo este patossistema.

Estudos que relatam a interação entre R-Locos, como a piramidação *Rpv3+Rpv12* (VENUTI et al., 2013) e *Rpv3-3+Rpv10* (VEZZULLI et al., 2019) apontam para um efeito aditivo. Esta evidência foi corroborada por estudo do transcriptôma no genótipo piramidado Rpv3+Rpv10 (FRÖBEL et al., 2019). No estudo referido, foi contrastado 416 genes diferencialmente expressos exclusivos para o genótipo piramidado seis horas após a inoculação com o patógeno (*P. viticola*). Contudo, a principal via metabólica alterada trata-se da rota dos estilbenos, evidenciando a importância desta via metabólica em estudos mais focados.

Conforme relatado, estudos da genômica estrutural já mapearam fisicamente os R-Loci associados com a resistência ao míldio (Tabela 1), além disto muitos estudos de genômica funcional vêm sendo publicados atualmente, conforme relatado no levantamento bibliográfico onde são apresentados os pontos centrais da interação entre *V. vinifera* e *P. viticola* concentra-se nas vias do metabolismo lipídico, percursor dos jasmonatos (WANG et al., 2018b), via dos salicilatos e por fim, a via de atuação dos estilbenos. Ainda convém salientar que a quantificação de genes específicos, via RT-qPCR é utilizado por autores com foco na interação entre a videira e o patógeno *P. viticola* (GUERREIRO et al., 2016; ZHAO et al., 2019).

Tabela 1 – Genótipos portadores (em negrito) dos locos associados à resistência da videira (*V. vinifera*) ao míldio (*Plasmopara viticola*) descritos na literatura

Loco	Cr	Position (MB)	Parental I	Parental II	Espécie doadora	Referência
Rpv1	12	10,3	Syrah	**28-8-78**	*Muscadinia rotundifolia*	MERDINOGLU et al. (2003)
Rpv2	18		Cabernet Sauvignon	**8624**	*M. rotundifolia*	WIEDEMANN-MERDINOGLU et al. (2006)
Rpv3	18		**Regent**	Lemberger		WELTER et al. (2007)
	18	24,9 – 26,9	Chardonnay	**Bianca**		BELLIN et al. (2009)
	18	26,9	**Regent**	Red Globe		VAN HEERDEN et al. (2014)
Rpv3-1	18	25,9 – 26,9	GF.GA-47-42	**Villard blanc**	*V. rupestris*	ZYPRIAN et al. (2016)
Rpv3-2	18	25,9 – 26,9	**GF.GA-47-42**	Villard blanc	*V. rupestris* ou *V. lincecumii*	
Rpv3-3	18	25,9 – 26,9	**Merzling**	Teroldego		VEZZULLI et al. (2019)
Rpv4	4	4,7 – 5,2	**Regent**	Lemberger		WELTER et al. (2007)
Rpv5	9	4,0	Cabernet Sauvignon	**Gloire de Montpellier**	*V. riparia*	MARGUERIT et al. (2009)
Rpv6	12	20,4				
Rpv7	7	11,4	Chardonnay	**Bianca**		BELLIN et al. (2009)
Rpv8	14	6,6	**Ruprecht**	**Ruprecht**	*V. amurensis*	BLASI et al. (2011)
Rpv9	7	16,6	Moscato Bianco	**W63**	*V. riparia*	MOREIRA et al. (2011)
Rpv10	9	3,7	Gf.Ga-52-42	**Solaris**	*V. amurensis*	SCHWANDER et al. (2012)
Rpv11	5	4,1				
Rpv12	14	8,0 – 10,1	**99-1-48**	Pinot noir		VENUTI et al. (2013)
			Cabernet Sauvignon	**20/3**		
Rpv13	12	10,0	Moscato Bianco	**W63**	*V. riparia*	MOREIRA et al. (2011)
Rpv14	5	20,2	Gf.V3125	**Börner**	*V. cinerea*	OCHSSNER; HAUSMANN; TÖPFER (2016)
Rpv15	18		**DVIT2027**	F2-35	*V. piasezkii*	PAP et al. (em preparação)
Rpv16						
Rpv17	8	11,7	B38	**Horizon**		DIVILOV et al. (2018)
Rpv18	11	15,4				
Rpv19	14	29,5	**B38**	Horizon	*V. rupestris*	
Rpv20	6	0,9	**Horizon**	B9		
Rpv21	7	2,1	**Horizon**	B9		
Rpv22	2	2,1 – 3,5	**Shuang Hong**	Cabernet Sauvignon	*V. amurensis*	FU et al. (2020)
Rpv23	15				*V. amurensis*	
Rpv24	18				*V. amurensis*	
Rpv25	15	3,0 – 3,9	Red Globe	**Shuangyou**	*V. amurensis*	LIN et al. (2019)
Rpv26	15	14,7 – 15,0				
Rpv27	18	24,6 – 26,0	**Norton**	Cabernet Sauvignon	*V. aestivalis*	SAPKOTA et al. (2019)
Rpv28	10	1,2 – 1,3	**B38**	*V. riparia* HP-1	*V. rupestris*	BHATTARAI et al. (2020)

Continua...

Continuação

Loco	Chr	Position (MB)	Parental I	Parental II	Espécie doadora	Referência
Rpv29	14	21,6	**Mgaloblishvili**	**Mgaloblishvili**	*V. vinifera*	SARGOLZAEI et al. (2020)
Rpv30	3	16,2	**Mgaloblishvili**	**Mgaloblishvili**	*V. vinifera*	SARGOLZAEI et al. (2020)
Rpv31	16	21,4	**Mgaloblishvili**	**Mgaloblishvili**	*V. vinifera*	SARGOLZAEI et al. (2020)

Adaptado de MAUL et al. (2020).

1.4 RESPOSTA AO ESTRESSE BIÓTICO

1.4.1 Resistência Sistemática Adquirida

O termo Resistência Sistêmica Adquirida (SAR) surgiu pela primeira vez em 1933 em uma revisão de trabalhos a respeito da existência de mecanismos de imunidade fisiológica em plantas (CHESTER, 1933). O conceito ganhou maior visibilidade a partir de trabalhos desenvolvidos com o vírus do mosaico do tabaco (TMV), onde foi observado que após a segunda inoculação do vírus na mesma folha, as lesões foram menores em comparação àquelas geradas na primeira inoculação (ROSS; BOZARTH, 1960). Os autores inicialmente consideraram como resistência induzida e, somente com a repetição do trabalho, com avaliações envolvendo outras partes da planta, como flores e outras folhas, a resistência gerada foi considerada como SAR (ROSS, 1961).

Aproximadamente uma década mais tarde, foi desenvolvido um estudo baseado no perfil proteico comparativo de amostras expressando ou não a SAR onde foi verificado acúmulo de proteínas em folhas inoculadas ou induzidas à resistência (VAN LOON; VAN KAMMEN, 1970). Estas proteínas, inicialmente desconhecidas, foram nomeadas posteriormente de PATHOGENESIS-RELATED que são definidas como proteínas vegetais induzidas em situações de interação com patógenos ou relacionadas (ANTONIW et al., 1980). Posteriormente, estas proteínas foram agrupadas em famílias de acordo com suas características (VAN LOON et al., 1994), cuja classificação proposta na época, foi mantida (Tabela 2).

Em estudo visando conhecer a molécula sinalizadora, responsável pela indução da SAR, em decorrência da inoculação de *Colletotrichum* em cucurbitáceas, foi verificado que o sinal se movia do porta-enxerto para o enxerto, mas a recíproca não ocorreu (DEAN; KUĆ, 1986). Os autores também verificaram que a retirada das folhas onde a resistência foi induzida, reduzia a resistência em novas folhas, sugerindo que a folha infectada era a fonte do “sinal” para SAR, além do que, este “sinal”, até então desconhecido, não era remobilizado ou produzido em folhas sistemicamente protegidas (DEAN; KUĆ, 1986).

A SAR é definida como a resposta de defesa vegetal adquirida de forma sistêmica, podendo ser induzida de diversas formas, como a interação com patógenos, via PAMPs, resultando no acumulo de proteínas de defesa vegetal em tecidos diversos daquele afetado pelo dano (ONAGA; WYDRA, 2016; PONCE DE LEÓN; MONTESANO, 2013). A atuação da SAR, também confere proteção quantitativa contra diversos microrganismos, de forma similar à imunização em mamíferos, embora os mecanismos subjacentes sejam diferentes (STICHER; MAUCH-MANI; MÉTRAUX, 1997). A ativação da SAR foi inicialmente associada aos

hormônios salicilatos (SA) (DURRANT; DONG, 2004), entretanto, ao longo das descobertas foram sendo reveladas outras possíveis vias de ativação (BERNSDORFF et al., 2016; MITTLER; BLUMWALD, 2015; VAN DER ENT et al., 2018).

Tabela 2. PATHOGENESIS-RELATED PROTEÍNAS descritas na literatura e suas classificações, adaptado de (ALI et al., 2018; VAN LOON et al., 1994)

Família	Função	Espécie Fonte	Referência
PR1	Antifúngico	*Nicotiana. tabacum*	(ANTONIW et al., 1980)
PR2	B-1,3-glucanase	*N. tabacum*	(ANTONIW et al., 1980)
PR3	Kitinase	*N. tabacum*	(LOON, 1981)
PR4	Antifúngico	*N. tabacum*	(LOON, 1981)
PR5	Antifúngico	*N. tabacum*	(LOON, 1981)
PR6	Inibidor de proteínase	*Solanum lycopersicum*	(GREEN; RYAN, 1972)
PR7	Endoproteínase	*S. lycopersicum*	(VERA; CONEJERO, 1988)
PR8	Kitinase	*Cucumis sativus*	(MÉTRAUX; STREIT; STAUB, 1988)
PR9	Peroxidase	*N. tabacum*	(LAGRIMINI et al., 1987)
PR10	Ribonuclease-*like*	*Petroselinum crispum*	(SOMSSICH et al., 1986)
PR11	Kitinase	*N. tabacum*	(MELCHERS et al., 1994)
PR12	Defesa	*Raphanus raphanistrum*	(TERRAS et al., 1995)
PR13	Tionina	*Arabidopsis thaliana*	(EPPLE; APEL; BOHLMANN, 1995)
PR14	Transporte de lipídeos	*Hordeum vulgare*	(GARCÍA-OLMEDO et al., 1995)
PR15	Oxalato oxidase	*H. vulgare*	(ZHANG; COLLINGE; THORDAL-CHRISTENSEN, 1995)
PR16	Oxidase-*like*	*H. vulgare*	(WEI et al., 1998)
PR17	Antifúngico e antiviral	*N. tabacum*	(OKUSHIMA et al., 2000)

No cenário científico atual, há um debate quanto as relações entre os hormônios e demais moléculas do metabolismo vegetal. Estudos recentes demonstram a interdependência e o *crosstalk* existente entre estas moléculas e as complexas vias de regulação. Quando se trata da interação entre planta e patógeno o cenário é ainda mais complexo, envolvendo a regulação do sistema de defesa vegetal e a interação com o microrganismo invasor. Assim, como já apontado pelos primeiros estudos com SAR e reafirmado por estudos recentes, as condições ambientais exercem influência na atuação do mecanismo de indução da resistência e também na sinalização da doença (KLESSIG et al., 2018; ROSS, 1961; SHAH; ZEIER, 2013).

A descrição da rota do AS permite compreender como ocorre a expressão da SAR. Todavia, na rota de indução das PR proteínas e, consequentemente da SAR, existe um gene regulando a via de sinalização, que foi então nomeado de NONEXPRESSER OF PR (NPR1). Os mutantes neste gene não respondiam a presença de indutores da SAR, como o AS, mesmo quando aplicado de forma exógena (CAO et al., 1994). A função do NPR1, como regulador da SAR via ativação da rota dos salicilatos, foi corroborada por outros estudos (DING et al., 2020;

DONG, 2004). Recentemente, foi demonstrada a atuação de outros genes com esta mesma função, como o fator de transcrição *TEOSINTE BRANCHED 1, CYCLOIDEA, PCF1* (TCP), contribuindo para redundância na ativação da SAR (LI et al., 2018).

Em paralelo, um estudo buscando conhecer domínios proteicos conservados no genoma de aveia, revelou a presença de um peptídeo conservado com a sequência DGYxWRKYGQKxxKxxxxPRxYxx, que foi classificado como parte de uma proteína do tipo DNA-binding; contudo sua função não foi inicialmente descrita com precisão (RUSHTON et al., 1995). Por conta do seu domínio altamente conservado, este peptídeo foi chamado posteriormente de WRKY e foi mais tarde associada com a resposta de defesa vegetal (WANG et al., 1998).

A existência de uma interdependência entre o fator de transcrição WRKY e a SAR foi esclarecida anos mais tarde, quando foi observado que esta molécula atua na cascata de sinal do NPR1, que por sua vez era conhecido pela sua função como regulador da resposta de proteínas PR na via de sinalização dos AS (YU; CHEN; CHEN, 2001). No entanto, o entendimento dos mecanismos de regulação da indução da SAR ficou mais complexo a partir da descoberta de que o NPR1 possuí também o papel de modulador do *crosstalk* entre as rotas metabólicas de sinalização dos AS e dos Jasmonatos (JA), onde a presença do NPR1 promove a atuação dos AS, enquanto o mutante npr1 não ativa a via dos AS, mas sim a via dos JA (SPOEL et al., 2003).

Neste contexto, estudos envolvendo a SAR em arroz (*Oryza sativa*), visando elucidar melhor o contexto de funcionamento destas rotas, apontavam para resultados contrastantes, enquanto era observado que o aumento da expressão do NPR1 e, consequentemente, da atuação dos AS, elevou a resistência a patógenos (YUAN et al., 2007) . Foi também constatado que vias alternativas de indução da resistência eram possíveis, não envolvendo necessariamente a dependência de NPR1 (SHIMONO et al., 2007). A análise de transcritos, utilizando tecidos distais de cevada (*Hordeum vulgare*), revelou que a SAR nesta espécie provavelmente está associada ao ácido jasmônico, etileno e ABA, em vez do AS (DEY et al., 2014).

Neste contexto, novos estudos foram surgindo demonstrando a presença da atuação de outros mecanismos percursoras da resistência, principalmente a oxidação do apoplasto, indicando a atuação de peróxidos, gerados pela atividade de radicais livres (MAMMARELLA et al., 2015; O'BRIEN et al., 2012). Assim, foi proposto que espécies reativas de oxigênio (ROS) e glutationa (GSH) estão envolvidas como sinalizadoras pela via de atuação dos AS (HERRERA-VÁSQUEZ; SALINAS; HOLUIGUE, 2015). Em contraponto, foi proposta uma classificação das vias de indução da SAR em dois seguimentos, o primeiro envolvendo as vias

em resposta aos AS e sinalizadas pelo NPR1, enquanto no outro seguimento estão a indução por via de radicais livres, em especial as ROS e GSH (GAO et al., 2015). Considerando-se ainda a atuação do AS, a fronteira do conhecimento atual está no entendimento das relações do SA com o ácido N-hydroxypipecolico e no papel que esta molécula tem na SAR, devido a sua atuação como estimuladora dos AS e indutora de respostas de hipersensibilidade contra oomicetos (HARTMANN et al., 2018; HARTMANN; ZEIER, 2019).

Por outro lado, estudos têm também explorado a atuação de outras moléculas como responsáveis pela indução da SAR, como os AJ e principalmente seu equilíbrio com o etileno. Este mecanismo de ação é principalmente caracterizado pelo deposito de calose como via de defesa principalmente contra patógenos necróticos (GAUTAM; NANDI, 2018). O deposito de calose é relatado como forma de defesa contra o ataque de *Plasmopara viticola*, patógeno biotrófico causador do míldio, na variedade Solaris (*V. vinifera*), portadora dos locos de resistência *Rpv3-3+Rpv10* (GINDRO; PEZET; VIRET, 2003).

Este comportamento pode ser explicado pelo perfil de expressão dos genes ligados à resistência em videira, onde a atuação dos AJ que em outras espécies estão predominante ligados a doenças necrotróficas, apresentam atuação ativa no controle de doenças biotróficas como o míldio (GUERREIRO et al., 2016). Além disso, o principal sinalizador de resistência a estresses bióticos ou abióticos em videira são os estilbenos, principalmente o resveratrol (JIAO et al., 2016; OLIVIER; SPRING; GINDRO, 2018). Molécula esta que pode ser sintetizada pela via de atuação dos AS como dos AJ, mesmo estes últimos aparentemente possuindo maior influência no sistema de defesa imunológico da videira (PAOLACCI et al., 2017).

Para esclarecer melhor como funciona a atuação destes mecanismos já descritos na videira, atualmente estão anotados 49 genes ligados a PR proteínas para esta espécie (Tabela 3), disponível no GeneBank (https://www.ncbi.nlm.nih.gov/). Na literatura são citados alguns estudos com organismos geneticamente modificado para estes genes (ALI et al., 2018). A família gênica para expressão das THAUMATIN-LIKE PROTEIN (TLP) desempenham diversos papéis nas respostas de plantas a estresses bióticos ou abióticos, sendo consideradas PR proteínas por conferirem resistência a uma ampla gama de doenças.

Em estudo avaliando a atuação de 33 genes *VvTPL*, isolados a partir de *V. vinifera*, em plantas desafiadas com antracnose (*Elsinoe ampelina*), oídio (*Erysiphe necator*) ou *Botrytis cinerea*, é descrito a expressão diferenciada do *TPL29*. Posteriormente, este gene foi isolado da espécie portadora de resistência a doenças, *V. quinquangularis* (VqTPL29), e transferido para plantas de *Arabidopsis thaliana*, que passaram a expressar também resistência a estes patógenos, com exceção do *B. cinerea*. Este estudo demonstra ainda que a ação do *VqTPL29*

está relacionado com as vias metabólicas dos salicilatos, jasmonatos e etileno (YAN et al., 2017). Além disso, o estudo desenvolvido com a variedade Zhuoshan-1, da espécie *V. amurensis*, do centro de diversidade asiático, portadora de resistência ao míldio (*P. viticola*), foi doadora do gene *VaTPL* para a *V. vinifera* Thompson Seedless, que passou a também expressar resistência a este patógeno (HE et al., 2017).

A transferência de genes ligados a PR-proteínas permitiu verificar o sucesso na expressão de resistência ao oídio. Neste caso, o gene *VpPR4-1* identificado no genótipo Baihe 35-1, da espécie *V. pseudoreticulata*, também do centro de diversidade asiático, e portadora de elevada resistência esta doença, foi transferido para a variedade suscetível Red Globe (*V. vinifera*), resultando no aumento da resistência a esta doença no genótipo receptor do gene (DAI et al., 2016). Do mesmo doador foi isolado o gene VpPR10 e transferido para a variedade suscetível Thompson Seedless, de *V. vinifera* cujas plantas resultantes e expostas ao míldio demonstraram resistência a este patógeno (SU et al., 2018).

Tabela 3. Proteínas relacionadas a patogênese (PR-proteínas) anotadas no genoma de *V. vinifera* PN40024[1]

Descrição	**Loco**	**Cr.***	**Posição****
PATHOGENESIS-RELATED PROTEIN 5-LIKE	LOC104879326	1	4,9 Mb
PATHOGENESIS-RELATED PROTEIN 1-LIKE	LOC100265128	3	8,9 Mb
BASIC FORM OF PATHOGENESIS-RELATED PROTEIN 1-LIKE	LOC100265141	3	8,9 Mb
PATHOGENESIS-RELATED LEAF PROTEIN 6	LOC100242852	3	8,9 Mb
BASIC FORM OF PATHOGENESIS-RELATED PROTEIN 1	LOC100247990	3	8,9 Mb
PATHOGENESIS-RELATED LEAF PROTEIN 4	LOC100258405	3	8,9 Mb
PATHOGENESIS-RELATED LEAF PROTEIN 6	LOC100253281	3	8,9 Mb
BASIC FORM OF PATHOGENESIS-RELATED PROTEIN 1-LIKE	LOC100251550	3	9,0 Mb
BASIC FORM OF PATHOGENESIS-RELATED PROTEIN 1	LOC100232880	3	9,0 Mb
BASIC FORM OF PATHOGENESIS-RELATED PROTEIN 1-LIKE	LOC109122343	3	9,0 Mb
PATHOGENESIS-RELATED PROTEIN	LOC100258414	3	9,0 Mb
BASIC FORM OF PATHOGENESIS-RELATED PROTEIN 1	LOC100263556	III	9,1 Mb
PATHOGENESIS-RELATED LEAF PROTEIN 6-LIKE	LOC100241292	3	9,1 Mb
PATHOGENESIS-RELATED PROTEIN 1	LOC100246419	3	9,1 Mb
BASIC FORM OF PATHOGENESIS-RELATED PROTEIN 1	LOC100251560	3	9,1 Mb

Continua

Continuação...

Descrição	**Loco**	**Cr***	**Posição****

BASIC FORM OF PATHOGENESIS-RELATED PROTEIN 1	LOC100256689	3	9,1 Mb
BASIC FORM OF PATHOGENESIS-RELATED PROTEIN 1-LIKE	LOC100249795	3	9,3 Mb
BASIC FORM OF PATHOGENESIS-RELATED PROTEIN 1	LOC100242451	3	11,3 Mb
PATHOGENESIS-RELATED PROTEIN 5-LIKE	LOC104879199	4	21,0 Mb
PATHOGENESIS-RELATED PROTEIN STH-2	LOC100263738	5	1,2 Mb
PATHOGENESIS-RELATED PROTEIN 10.3-LIKE	LOC100256795	5	1,2 Mb
PATHOGENESIS-RELATED PROTEIN 10.3-LIKE	LOC100261887	5	1,2 Mb
PATHOGENESIS-RELATED PROTEIN 10.3	LOC100267074	5	1,3 Mb
PATHOGENESIS-RELATED PROTEIN 10	LOC100249884	5	1,3 Mb
PATHOGENESIS-RELATED PROTEIN 10.4	LOC100260133	5	1,3 Mb
PATHOGENESIS-RELATED PROTEIN 10.5	LOC100243040	5	1,3 Mb
PATHOGENESIS-RELATED PROTEIN 10.6	LOC100248161	5	1,3 Mb
PATHOGENESIS-RELATED PROTEIN 10.7	LOC100253292	5	1,3 Mb
PATHOGENESIS-RELATED PROTEIN 10.9	LOC100246600	5	1,3 Mb
PATHOGENESIS-RELATED PROTEIN 10.8	LOC100258426	5	1,3 Mb
PATHOGENESIS-RELATED GENES TRANSCRIPTIONAL ACTIVATOR PTI6	LOC100246641	6	9,0 Mb
PATHOGENESIS-RELATED PROTEIN STH-21	LOC100264209	7	3,5 Mb
PATHOGENESIS-RELATED PROTEIN STH-21-LIKE	LOC100258821	7	3,5 Mb
PATHOGENESIS-RELATED PROTEIN 1C	LOC100258474	8	13,9 Mb
PATHOGENESIS-RELATED GENES TRANSCRIPTIONAL ACTIVATOR PTI5	LOC100264074	10	1,8 Mb
PATHOGENESIS-RELATED HOMEODOMAIN PROTEIN	LOC100262260	11	16,8 Mb
PATHOGENESIS-RELATED PROTEIN PR-1	LOC100265073	11	19,4 Mb
PATHOGENESIS-RELATED PROTEIN PR-1-LIKE	LOC100256515	11	19,4 Mb
PATHOGENESIS-RELATED PROTEIN 5-LIKE	LOC100257979	13	23,2 Mb
PATHOGENESIS-RELATED PROTEIN 5	LOC100252836	13	23,2 Mb
PATHOGENESIS-RELATED PROTEIN PR-4	LOC100255405	14	7,6 Mb
PATHOGENESIS-RELATED PROTEIN PR-4	LOC100260476	14	7,6 Mb
PATHOGENESIS-RELATED PROTEIN 5-LIKE	LOC109124076	15	13,9 Mb
PATHOGENESIS-RELATED PROTEIN 5	LOC100254811	15	14,0 Mb
PATHOGENESIS-RELATED PROTEIN 5-LIKE	LOC109124044	15	14,2 Mb
PATHOGENESIS-RELATED GENES TRANSCRIPTIONAL ACTIVATOR PTI6	LOC100255049	15	18,4 Mb
PATHOGENESIS-RELATED PROTEIN 5	LOC100259225	18	3,4 Mb
PATHOGENESIS-RELATED PROTEIN PRB1-3-LIKE	LOC104878449		*Indefinido*

[1](JAILLON et al., 2007; VELASCO et al., 2007); *Cromossomo; **Posição em megabases (Mb) do loco responsável pela expressão da proteína no genoma da videira (*V. vinifera*) PN40024.

1.4.2 Sinalização de estilbenos

Genes envolvidos na sinalização dos estilbenos apresentam-se governados por fatores ainda não completamente elucidados; contudo, o papel fundamental tem sido atribuído a ação do jasmonato (TAURINO et al., 2015). O principal gene responsável pela síntese de estilbenos é *Stilbene Synthase* (*STS*), que foi isolado em 71 eventos, cujas sequências estão depositadas na base de dados do GenBank (NCBI, https://www.ncbi.nlm.nih.gov).

Dentre as sequências depositadas, alinhadas ao genoma da videira, este gene é observado em dois cromossomos distintos do genoma; no cromossomo 10 (gb | NC_012016.3) posição 16.507.942 pb e uma família de 19 *STS* no cromossomo 16 (gb | NC_012022.3) localizada entre 12.636.838 pb e 16.710.281 pb (JAILLON et al., 2007; VELASCO et al., 2007). Contudo, estudos anteriores recomendaram estudar a expressão dos genes posicionados entre 16.430.808 pb e 16.493.234 pb (WANG et al., 2007).

Os estilbenos são as principais fitoalexinas produzidas pela videira. Dentre os estilbenos o resveratrol é o principal composto estudado, devido a este composto estar no topo da cascata de sinais que envolve a regulação das vias de estresse (JEANDET et al., 2002). No entanto, o pterostilbeno é relatado como a molécula com maior potencial de proteção da videira contra estresse biótico, sendo até 10 vezes mais eficiente que o resveratrol para ação contra a germinação dos esporângios do *P. viticola* (JEANDET et al., 2002).

A síntese do pterostilbeno é realizada a partir da acetilação da molécula de resveratrol, processo este realizado pelo *resveratrol O-methyltransferase* (*ROMT*). É relatado na anotação do genoma da videira que este gene está presente em uma pequena família localizada no cromossomo 12 (gb | CAO69896, gb | CAO69893, gb | CAO69817 e gb | CAO69813) (JAILLON et al., 2007; VELASCO et al., 2007); no entanto, há indícios de que outros alelos deste gene, podem estar presentes em diferentes genótipos (LASSNIGG et al., 2004). A expressão do *ROMT* é induzida logo após a expressão do gene *STS* em situações de inoculação com o *P. viticola* (SCHMIDLIN et al., 2008). Fato que se deve a sua função de acetilação do resveratrol tornando este em um pterostilbeno, com maior eficiência no combate ao estresse biótico (JEANDET et al., 2002).

Outra via de transformação do resveratrol é a glicosilação, regulada pelo gene *Resveratrol/hydroxycinnamic acid O-glucosyltransferase* (HALL; DE LUCA, 2007), localizado no cromossomo 3, que regula a produção do piceid, outra molécula do grupo dos estilbenos com maior potencial antioxidante em comparação ao resveratrol (MIKULSKI; MOLSKI, 2010). Contudo, a síntese de piceid, mesmo induzida em situações de estresse biótico, é comumente relacionada ao estresse abiótico, principalmente a exposição à luz ultravioleta (LIU et al., 2013; SCHMIDLIN et al., 2008).

1.4.3 Sinalização de jasmonatos

A biossíntese dos jasmonatos está vinculada ao metabolismo dos lipídios (LIECHTI; FARMER, 2002), partindo da oxidação de ácidos graxos poli-insaturados, principalmente o ácido linoleico, ácido linolênico, ácido hexadecatrienoico, por sua abundância nas membranas

do cloroplasto. O processo oxidativo ocorre comumente livre de reações enzimáticas, contudo, a via de biossíntese pode ser estimulada a partir da ação da atividade das enzimas lipoxigenase ou α-dioxigenase. O processo de síntese deste hormônio inicia nos cloroplastos e é finalizado nos peroxissomos (SCHALLER; STINTZI, 2009). Os Jasmonatos, em suas distintas conjugações, possuem papel na regulação da sinalização de estresses envolvendo injurias mecânicas ou ataques patogênicos (FENG et al., 2003).

Dentre os genes envolvidos na cascata de sinal promovida pela ação dos jasmonatos, papel importante tem sido denotado ao fator de transcrição *basic helix-loop-helix Leu zipper* (*MYC2*). Primeiramente descrito em *Arabidopsis thaliana*, como *AtMYC2* (LORENZO et al., 2004), por meio do uso de mutantes para o gene, foi verificado que as plantas *myc2* apresentavam maior resistência a fungos necrotroficos; contudo a resposta de regeneração aos danos mecânicos é prejudicada.

Outros estudos demonstraram que o *MYC2* está presente em outras posições no genoma, com diferentes alelos, podendo desempenhar papeis distintos. A principal função deste fator de transcrição é o seu papel como repressor de genes relacionados a defesa contra patógenos, principalmente *PDF1.2*, *CHIB/PR3* e *HEL/PR4*. No entanto, também é atribuído ao *MYC2* o *crosstalk* com a via metabólica de outros hormônios, como ácido abscísico e etileno (ANDERSON et al., 2004; LORENZO et al., 2004)

Devido à complexidade do metabolismo celular em que está envolvido o jasmonato, diversas vias de regulação são descritas para este hormônio. Dentre estas, a principal via descrita é pela autorregulação via uma família de enzimas denominadas como *jasmonate ZIM domain protein* (JAZ), que estão envolvidas em um sistema de *looping* de autorregulação negativa com as proteínas do fator de transcrição MYC2, bem como, de seus diferentes alelos descritos na literatura (CHINI et al., 2007; FERNÁNDEZ-CALVO et al., 2011). Por este mecanismo, a ativação do *JAZ* induz a regulação negativa da síntese de jasmonatos, por outro lado, a degradação das enzimas JAZ no proteossoma libera as proteínas MYC2 e eleva a ativação do jasmonato (CHINI et al., 2009; HOO; HOWE, 2009; THINES et al., 2007).

Na família do *JAZ* são descritos 12 genes em Arabidopsis, onde os estudos elucidaram o funcionamento destes genes. Dentre os genes desta família, o *JAZ 1* e *JAZ 3* destacam-se pela principal atividade e interação com todos os demais genes. Devido a isto, estudos envolvendo a regulação do metabolismo de jasmonatos têm denotado maior importância para detalhar a atuação destes genes nos sistemas biológicos (HOO; HOWE, 2009; THINES et al., 2007).

As proteínas JAZ têm demonstrado *crosstalk* com outras vias metabólicas mediadas por agentes distintos. Exemplo disso é a repressão da atividade de enzimas Topless (TPL)

realizada com auxílio da proteína adaptadora denominada Novel interactor of JAZ (NINJA) (CAUSIER et al., 2012; DE GEYTER et al., 2012; PAUWELS et al., 2010). O gene *TOPLESS* é responsável por uma série de eventos bioquímicos dentro do metabolismo vegetal, estando envolvido em eventos como a floração, resposta ao estresse, sinalização hormonal e, devido a esta interação, é também considerado um agente da regulação entre a sinalização de auxinas e jasmonatos (CAUSIER et al., 2012).

1.4.4 Sinalização de salicilatos

São conhecidas duas diferentes rotas de biossíntese do ácido salicílico. A primeira é conhecida como a rota do isocorismato e a outra é a rota da fenilalanina amônia-liase. Ambas as vias iniciam na mesma molécula precursora, o isocorismato, e por fim completam a síntese do ácido salicílico na via metabólica do shikimato (DEMPSEY et al., 2011). Este hormônio apresenta papel fundamental no envolvimento com mecanismos de sinalização do estresse em plantas, atuando em alguns casos como indutor da resistência adquirida (SHAH, 2003).

As vias de sinalização da defesa vegetal induzidas pelo ácido salicílico não são lineares, pois possuem diversas interações com outros componentes de diversas rotas metabólicas. Muitos mecanismos podem ativar a síntese do ácido salicílico, contudo nem todos estes estão completamente elucidados. A principal via de ativação relatada para este hormônio é por meio da ativação do gene *NON-EXPRESSOR OF PR1* (*NPR1*) (SHAH, 2003).

O *NPR1* é relatado em estudos como gene ativado em sistemas celulares em condições de estresse biótico (HADWIGER, 2009). Contudo, em trabalho com inoculação de míldio em plantas de videira resistente e suscetível a este patógeno, não foram verificadas diferenças nos níveis de expressão deste gene, enquanto o *STS* apresentou até 20 vezes maior expressão, se comparado com o momento anterior a inoculação (LE HENANFF et al., 2009). Estes dados demonstram que, mesmo com a atuação do ácido salicílico na indução da defesa contra estresse biótico, na videira maior atenção deve ser dada a via do jasmonato e dos estilbenos.

2 OBJETIVOS

2.1 OBJETIVO GERAL

Caracterizar em nível celular e molecular, as interações entre genótipos de videira (*V. vinifera*) portadores de *R*-locos e o patógeno *P. viticola* e descrever os possíveis mecanismos envolvidos na biossíntese da resistência do hospedeiro ao patógeno.

2.2 OBJETIVOS ESPECIFICOS

1. Avaliar a cinética de expressão de genes associados, a sinalização da defesa e a reação de incompatibilidade entre genótipos de videira e o *P. viticola*.
2. Descrever as alterações no perfil de expressão de proteínas em células de *V. vinifera* contendo *Rpvs* em resposta a reação de incompatibilidade com o *P. viticola*.
3. Elucidar a cinética das alterações metabólicas em decorrência da interação incompatível entre o hospedeiro (*V. vinifera*) e o patógeno (*P. viticola*), com resistência promovida por diferentes *R*-locos.

3 CAPÍTULO I – THE INTERPLAY OF GENE DEFENSE EXPRESSION AND HORMONES IN GRAPEVINE GENOTYPES CARRYING GENETIC RESISTANCE AGAINST *Plasmopara viticola*

Este capítulo encontra-se formatado de acordo com as normas para publicação e foi submetido ao periódico “Vitis”.

The interplay of gene defense expression and hormones in grapevine genotypes carrying genetic resistance against *Plasmopara viticola*

3.1 ABSTRACT

The present study aimed at to investigate defense related pathways during *Plasmopara viticola* infection in *Vitis vinifera* carrying different resistance loci. Gene expression analysis from genes involved in the pathway of pathogen effector recognition and downstream signaling, using *Rpv3-1*, *Rpv1+Rpv3-1*, *Rpv3-3+Rpv10*, and susceptible (*no Rpv*) genotypes were performed. In addition, we carried out hormonal quantification analysis for jasmonic acid (JA), salicylic acid (SA), abscisic acid (ABA), indole-3-acetic acid (IAA), and trans-zeatin-ribose (tZR) using the same listed genotypes and another variety containing *Rpv3-1+Rpv3-2*. The samples were collected from plants cultivated in *in vitro*. All genotypes were inoculated with *Plasmopara viticola* sporangia, while in the control plants water was used without inoculum. The evaluation was performed at 0, 1, 3, 5, and 7 days post inoculation (DPI) for gene expression, and 0, 3, 5, and 7 DPI for hormonal quantification. The results showed an interaction between genotype and time post inoculation for the main gene expression and hormonal pathway linked with the pathogenic signaling. Overall, the results pointed out the influence of hormonal signaling by both salicylate and jasmonate pathways. The role of stilbenes acting against the pathogen at different times was also evidenced. Changes in the expression of genes linked to cell defense were observed in all evaluated genotypes; however, genotypes with R-loci responded more quickly, activating mechanisms of cell death, resulting in symptoms of hypersensitivity.

Key words: *Vitis vinifera*, *Plasmopara viticola*, PIWI cultivars, Vitiviniculture, Disease resistance, Plant breeding, Gene expression

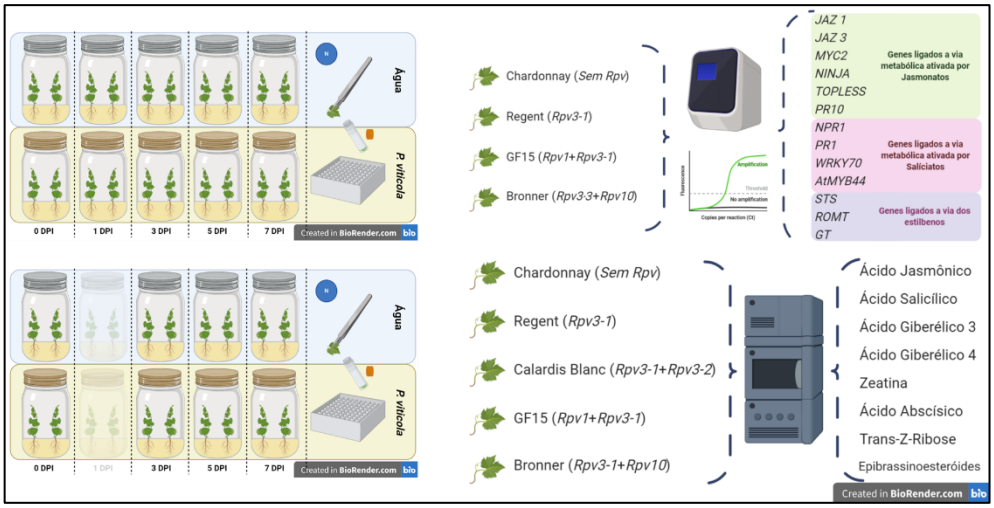

3.2 INTRODUCTION

Grapevine downy mildew is caused by the biotrophic heterothallic oomycete pathogen *Plasmopara viticola* (Berk. and Curt.) Berl. & de Toni. This is one of the most challenging diseases in viticulture worldwide, since it can negatively affect the grape quality and yield; also the phytosanitary treatments increase production costs and may result in negative impacts on the environment and human health (GESSLER; PERTOT; PERAZZOLLI, 2011; TAYLOR; COOK, 2018). In the second half of the 19th century, *P. viticola*, originally from North America, was introduced into Europe, from where it was disseminated throughout the world (GESSLER; PERTOT; PERAZZOLLI, 2011).

The pathogen caused a devastation of European viticulture since the cultivated *V. vinifera* is commonly susceptible to *P. viticola*. However, resistance to *P. viticola* (*Rpv*) loci, inherited from American and Asian *Vitis* species, was localized by quantitative trait loci (QTL) analysis (MAUL ET AL., 2020). The first *Rpv* (*Rpv1*) mapped on chromosome 12 came from *Muscadinia rotundifolia* (2n=40), a species developed at the American diversity center (MERDINOGLU et al., 2003). Another *Rpv*-locus commonly used in breeding programs is the *Rpv3* (ZINI et al., 2019). This *Rpv*-locus is also from the American diversity center, and it was mapped on chromosome 18; until now three haplotypes from *Rpv3* were known and stimulate different host resistance responses to downy mildew infection.

Rpv3-1 is the most common, and the first *Rpv3* haplotype described (ZINI et al., 2019). It was inherited from *V. rupestris* (2n=38) and was transferred from the hybrid Seibel 4614 and mapped from the cvs. 'Regent' and 'Bianca' (BELLIN et al., 2009; WELTER et al., 2007). The *Rpv3-2* was genetically mapped from the hybrid GF.GA-47-42 segregant population inherited from *V. rupestris* or *V. lincecumii* (ZYPRIAN et al., 2016). Until now, *Rpv3-3 was* the latest published haplotype from the *Rpv3* locus, inherited from *V. labrusca* or *V. riparia, and* was mapped from the hybrid Noah, in the segregant population between 'Merzling' and 'Teroldego' (VEZZULLI et al., 2019). Other *Rpv3* haplotypes are also predicted by pedigree analysis, from *V. labrusca*, *V. riparia,* and *V. rupestris* (DI GASPERO et al., 2012). The *Rpv10* locus is found on chromosome 9, inherited from *V. amurensis*, sourced from the Asian diversity center, and mapped from cv. Solaris (SCHWANDER et al., 2012).

All *Rpv* loci individually confer partial resistance to *P. viticola*, varying in intensity (BOVE et al., 2019; BOVE; ROSSI, 2020; POSSAMAI et al., 2020). However, when two or more *Rpv* loci are combined in the same plant it commonly results in additional genetic interactions, increasing the level of resistance (KOSEV et al., 2017; SAIFERT et al., 2018; SCHWANDER et al., 2012; VENUTI et al., 2013; ZINI et al., 2019). However, there are also reports about lower resistance levels in pyramided genotypes in comparison with other ones (SAIFERT et al., 2018; ZINI et al., 2019), suggesting the role of minor QTLs. The plant reaction against the pathogen development may change in time, and mechanisms of action depend on host susceptibility to the disease. In the PIWI (from the German world Pilzwiderstandsfähigen that means grapevine disease resistance) cv. Solaris (*Rpv3-3+Rpv10*) (MAUL ET AL., 2020) the presence of callose deposits in the guard cells of the stomata was reported (GINDRO; PEZET; VIRET, 2003). In addition, structural modifications in the stomata cells were reported to hinder or prevent the pathogen penetration of the *V. labrusca* cv. Bordô (NASCIMENTO-GAVIOLI et al., 2020).

Rpv1 was cloned from *M. rotundifolia* (*MrRPV1*) and was the first *Rpv* gene characterized by function. The results demonstrate the involvement of nucleotide-binding domains and leucine-rich repeats (NB-LRR) in this gene, and the similarity with NB-LRR cluster for the same locus present in the *V. vinifera* genome (FEECHAN et al., 2013). The presence of NB-LRR was also reported in the major *Rpv* loci (CASAGRANDE et al., 2011; FEECHAN et al., 2013; MERDINOGLU et al., 2003; SAPKOTA et al., 2019; SCHWANDER et al., 2012; VENUTI et al., 2013; WELTER et al., 2007). NB-LRR proteins are codified by *R*-genes and directly or indirectly recognize pathogen effectors, resulting in the downstream activation of defense pathways in plants and animals (LOLLE; STEVENS; COAKER, 2020; POSTEL; KEMMERLING, 2009). This resistance mechanism is called effector-triggered immunity (ETI) (JONES; DANGL, 2006).

Up until now, it is well known that *Vitis* resistance relies on indirect recognition of the pathogen effector by the N-terminal domain of NB-LRRs (FEECHAN et al., 2013; SARGOLZAEI et al., 2020; SCHWANDER et al., 2012; VENUTI et al., 2013). This domain may be a Toll interleukin-1 receptor (TIR-NB-LRR), or a coiled-coil (CC) protein–protein interaction domain (CC-NB-LRR) (CASAGRANDE et al., 2011; FEECHAN et al., 2013; KORTEKAMP et al., 2008; POLESANI et al., 2008). TIR domains present higher rates of mutations and greater functional constraints, owing to this domain specializing in race-specific pathogens and their fast evolution (BELLIN et al., 2009; CANNON et al., 2002). However, non-TIR domains, such as CC, are evolutionarily more stable and consecutively less-adapted from biotic threats (CANNON et al., 2002).

Vitis species from continental Asia, carrying CC-NB-LRR, can recognize downy mildew (ZHANG et al., 2018), due to the cohabitation with other *Plasmopara* species from the Asian continent, such as *P. cissii* and *P. amurensis* (DICK, 2002; VENUTI et al., 2013). Additive effects in the resistance are reported using combinations *Rpv1+Rpv3*, *Rpv3+Rpv10* and *Rpv3+Rpv12*, in bioassays (CHITARRINI et al., 2020; EIBACH et al., 2007; SAIFERT et al., 2018; SCHWANDER et al., 2012; VENUTI et al., 2013), or in field conditions (ZANGHELINI et al., 2019). Both domains (TIR and CC) can recognize the same pathogen by different effectors, and this can be useful for increasing the resistance durability in the host plants (CHEN et al., 2016; LI et al., 2017b; PEART et al., 2005; SINAPIDOU et al., 2004).

The pyramiding of complementary *Rpv* loci contributes to the sustainable resistance (MERDINOGLU et al., 2018), once *Rpv3*-mediated resistance breakdown by *avrRpv3*$^{-}$ isolates has been reported (CASAGRANDE et al., 2011; DELMOTTE et al., 2014; PERESSOTTI et

al., 2010). The presence of *Rpv12*, a CC-NB-LRR type receptor, recognizes *avrRpv3*$^{-}$ pathogen effectors and maintains the resistance in *Rpv3*+*Rpv12* genotypes (VENUTI et al., 2013).

Successful pathogen recognition leads to the activation of signal transduction pathways involving MAP (Mitogen Activated Protein) kinases and WRKY transcription factors, which in turn trigger primary immune responses such as the accumulation of pathogenesis related (PR) proteins, reactive oxygen species (ROS), or phytoalexins, and may result in a hypersensitive response (HR) that prevents pathogen development (ASAI et al., 2002; DEVENDRAKUMAR; LI; ZHANG, 2018; RASMUSSEN et al., 2012; SARRIS et al., 2015). However, recently ETI was reported in partial resistance loci from Georgian *V. vinifera* access without HR response (SARGOLZAEI et al., 2020).

The performance of *Rpv* loci is commonly linked to the recognition of the pathogen by specific receptors (FEECHAN et al., 2013; THOMMA; NÜRNBERGER; JOOSTEN, 2011). Thus, activating WRKY transcription factors and starting the signal transduction induces the downstream activation of the expression of gene-linked cell death pathways (FRÖBEL et al., 2019; HOFMANN, 2019; HORSEFIELD et al., 2019; SARRIS et al., 2015). Generally, the activated defense pathway involves pathogen-related (PR) gene activation, especially PR1, because of their relationship with the salicylic induction pathway (MÉNARD et al., 2004; ZEIER et al., 2004), which can also involve primary metabolic compounds and stilbenes (ALI et al., 2012; KORTEKAMP, 2006).

The salicylic acid (SA) pathway is a plant cell defense inductor against biotrophic pathogens, such as *P. viticola*. However, challenging grapevine cells with mildews also activate the jasmonate pathway (BELHADJ et al., 2006; GUERREIRO et al., 2016; POLESANI et al., 2010). This activation is ascribed to the lipid oxidation on the attacked cells, thus launching jasmonate synthesis, which culminates in a hyper-sensibility response against biotrophic pathogens (CHOUDHURY et al., 2017).

The interplay between SA and JA in defense response pathways is mainly regulated by *AtMYB44* and *WRKY70* (SHIM et al., 2013; SHIM; CHOI, 2013; ÜLKER; SHAHID MUKHTAR; SOMSSICH, 2007). Commonly, the role of antagonist by these hormones is reported (SHIM et al., 2013). However, during the ETI, JA can be activated by SA receptors, such as NPR3 and NPR4, resulting in a conjunct action by these hormones (LIU et al., 2016a).

Based on this context, the objective of the present work was to elucidate the interplay between salicylic and jasmonic acid pathways, and the kinetic of gene defense expression related to these hormones and the stilbenes pathway during downy mildew infection in genotypes carrying *R-loci* to downy mildew resistance.

3.3 MATERIAL AND METHODS

3.3.1 Plant material

Hormonal quantification was performed using the susceptible cv. Chardonnay (*V. vinifera*) and the PIWI cvs. Regent, Calardis Blanc, Bronner, and the advanced breeding selection GF.2004.0043.015 (thereafter called GF15), kindly provided by the grapevine breeding program of Julius Kühn-Institut – Germany. The resistant genotypes contain the *Rpv3-1, Rpv3-1+Rpv3-2*, *Rpv3-3+Rpv10*, and *Rpv1+Rpv3-1* loci, respectively. All genotypes, except Calardis Blanc, were also used in the gene expression analysis.

3.3.2 In vitro plant cultivation

To ensure less influence from the environment, the experiment was carried out in *in vitro* conditions. All genotypes were introduced *in vitro* from nodal segments and maintained in *in vitro* conditions, using a DSD1 culture medium (SILVA; DOAZAN, 1995) added to sucrose (2%). Two plantlets were maintained in each cultivation flask (300 mL), supplied with 50 mL of culture medium, in a room temperature of 25 °C with a 16 h light photoperiod.

3.3.3 Downy mildew propagation and inoculation

Young leaves from the susceptible cv. Cabernet Sauvignon, exhibiting typical downy mildew symptoms, were collected from an experimental unsprayed vineyard from the EPAGRI (Empresa de Pesquisa Agropecuária e Extensão Rural de Santa Catarina) experimental station of Videira - Santa Catarina (Brazil). Leaf discs containing the sporulating lesions were collected and maintained at -20 °C until being used. Seven days before setting up the experiment, the sporangia were activated and cultivated on leaf discs excised from young leaves from susceptible cv. Chardonnay under *in vitro* conditions. Previously, the Chardonnay leaves were disinfected by a solution of sodium hypochlorite (1%) for 2 min, followed by a triple wash with sterile distilled water (SDW).

Five leaf discs of 1.6 cm in diameter were placed on each 15 cm diameter Petri plate containing SDW-soaked filter paper, using the abaxial side up. The inoculum was defrosted in cold SDW and immediately sprayed on the leaf discs, using a 500 µL plate^{-1}. The Petri plates were sealed and stored in the dark at a room temperature of 25 °C. One day after inoculation (DPI) droplets were removed from the leaf disc and the cultivation was maintained under the same temperature conditions with a 16 h light photoperiod for the next six days, when the sporangia were collected in sterile water. The sporangia suspension was then adjusted to the

concentration of $5x10^4$ sporangia mL^{-1}. All the procedures were performed in the flow chamber using previously sterilized materials.

A single droplet of the sporangia suspension was applied to the abaxial side of all mature leaves of the *in vitro* plants of all five genotypes. Leaves of the control plants were inoculated only with SDW. After inoculation, the flasks were sealed and kept in the absence of light at 25 °C for 24 h and afterwards maintained at the same room temperature in a 16 h light photoperiod. The experiment was completely randomized, with three replications and five flasks (10 plants) per repetition.

3.3.4 Expression of resistance-related genes

A sample (200 mg) of fresh leaves was collected at five different times after inoculation (0, 1, 3, 5, and 7 DPI) from plants of each repetition. The collected leaves were immediately frozen in liquid nitrogen and remained at -80 °C until use. RNA extraction and purification were performed using the commercial kit SV Total RNA Isolation System (Promega, Madison, WI, USA), according to the manufacturer's recommendations. The quality of the RNA was confirmed by electrophoresis on agarose gel [1.5%], denatured with formamide and stained with Gelred [1X]. Quantification was obtained using a Nanodrop 1000 spectrophotometer (ThermoFisher Scientific) and the concentration of all samples was standardized to 10 ng μL^{-1}.

Reverse transcriptase quantitative PCR (RT-qPCR) reactions were carried out using GoTaq Master Mix RT-qPCR Systems (Promega, Madison, WI, USA), according the manufacturer's recommendations, in a StepOnePlus thermocycler (Thermofisher, CA, USA). The expression of genes associated with the jasmonate and salicylate signaling pathways was quantified, together with the endogenous control *Actinia*, *EF1-α*, *GAPDH* and *Ubiquitin* (Table 1). The primer efficiency was established using six points of a 1:10 dilution. All reactions were performed in technical duplicate. The two endogenous controls that showed the least variation between treatments were selected to normalize the expression of the resistance-related genes. The $E^{\Delta\Delta Ct}$ (LIVAK; SCHMITTGEN, 2001) relative quantification method was used to determine the relative expression, using 0 (zero) DPI as a reference.

Table 1. Oligonucleotide sequences for gene expression analysis, by Sybr RT-qPCR from genes related to defense to pathogens and signaling pathway.

Gene	Gene function	GenBank access	Oligonucleotides forward and reverse	Reference
		Housekeeping genes		
Actinia	Housekeeping gene		F:CTTGCATCCCTCAGCACCTT	

		AC969944	R:TCCTGTGGACAATGGATGGA	(REID et al., 2006)
EF1-α	Housekeeping gene	XM_002279562.2	F:CTCCAAGTCCAGGTATGATG R:CAGAGATTGGAACAAAGGGG	(WANG et al., 2018a)
GAPDH	Housekeeping gene	EF192466	F:TCAAGGTCAAGGACTCTAACACC R:CCAACAACGAACATAGGAGCA	(MONTEIRO et al., 2013)
Ubiquitin	Housekeeping gene	EC929411	F: GAGGGTCGTCAGGATTTGGA R:GCCCTGCACTTACCATCTTTAAG	(REID et al., 2006)
		Jasmonic acid related genes		
JAZ 1	Repressor of JA responses	XM_002272327.3	F: CAACCCAAAGCTCAACAAAG R: TAAGTGGGAGTGGACAAGAT	(GUERREIRO et al., 2016)
JAZ 3	Repressor of JA responses	XM_002282652.2	F: TCCCTCCTGTAAGTCCCAAT R: TCCCCATAAAACCATCACCT	(GUERREIRO et al., 2016)
MYC 2	Transcriptional activator of light, ABA, and JA signaling pathways	XM_002280217.2	F: ATGCATTGCGAGCTGTTGTG R: TCTGCCTCGGTGTTAGTTTC	(GUERREIRO et al., 2016)
NINJA	Negative regulator of JA responses	XM_002283943.2	F: AAATTCGGGGGATCTGGTTC R: TGGATTGGCATGCTCTTCAC	(GUERREIRO et al., 2016)
TOPLESS	Negative regulator of jasmonate responses	XM_002268229.1	F: TCGGGATGGATGATTCTACA R: GGCAAGGCCAGTTATTCTC	(GUERREIRO et al., 2016)
PR10	Pathogenesis-related protein	HS075818	F:GTTTTGACTGACGGCGTTGA R:TGGTGTGGTACTTGCTGGTGTT	(GUERREIRO et al., 2016)
		Salicylic acid related genes		
NPR 1	Positive regulate of SA signaling	XM_002281439.2	F: ATGGATGCCGATGACTTA R: TCCTTGTACCTCCTCTTCTT	(GUERREIRO et al., 2016)
PR 1	Defense against pathogens	XM_002273752.2	F:AAAAATGGGGTTGTGTAGGAG R:TGTTGTGAGCATTGAGGTAGT	(GUERREIRO et al., 2016)
WRKY70	Regulator of SA and JA pathway	XM_002275365.2	F: GCCACCATACTTGCAGAGAT R:CAGACCCAACCATATTATTAG	(GUERREIRO et al., 2016)
AtMYB44	Regulator of SA and JA pathway	XM_002284979.2	F: CAACGGTTTCGGGTCATAAT R: GTTCTCGGCACTGGTCTAT	(GUERREIRO et al., 2016)
		Stilbenes related genes		
STS	Phytoalexins production	DQ459351.1	F: GAGTTCTTGTGGTGTGCTCTG R: GCTGCTGAGACAAGCTGGAAG	(WANG et al., 2018a)
ROMT	Biosynthesis of pterostilbene	FM178870.1	F: CTCGACCCAATTTTAACTAAACCA R: TCATTGAAGGAATTGTTGAGCTG	(WANG et al., 2018a)
GT	O-glucosyltransferase	DQ832169.1	F: GAAGTATGATGAAATCGCCAGC R: TATTCAATGACTTCGGGTTCCAG	(WANG et al., 2018a)

3.3.5 Hormonal analysis

A sample (500 mg) of fresh leaves was collected at four different times after inoculation (0, 3, 5, and 7 DPI), immediately frozen in liquid nitrogen and maintained at -80 °C until the hormonal extraction. The experiment was completely randomized, with three replications and five flasks (10 plants) per repetition. The hormonal quantification was adapted

from the protocol described by Fraga et al. (2016). The samples were ground using pestle and mortar in liquid nitrogen. Afterwards, 500 mg of the ground sample were transferred to a 15 mL tube containing extraction solution (acetonitrile:methanol:formic acid 50:45:5 v/v). Then $MgSO_4$, NaCl, $Na_3C_6H_5O_7$. $2H_2O$, $C_6H_6Na_2O_7$.1,5 H_2O (4:1:1:0.5) and 4 mL of extraction solution were added to each tube, maintained in a pendulum shaker (Labnet Rocker 25) for 24 h at 4 °C (inside a refrigerator). The samples were vortexed, and immediately centrifuged at 3026 *g* for 30 min at 4 °C. The supernatant was transferred to another 15 mL tube and kept at -20 °C. Three mL of the extraction solution was added to each tube with the precipitate from the first extraction. The samples were vortexed and returned to the pendulum shaker for 24 h twice, then the samples were centrifuged at 3026 *g* for 30 min at 4 °C. The supernatant was concentrated under vacuum, using Concentrator *Plus* (Eppendorf, USA). The pellets were suspended in 1 mL of 1 mol L^{-1} formic acid and vortexed. The purification of resuspended extracts was carried out using SPE (solid-phase extraction) columns (Waters Oasis MCX 150 mg, USA), according to the manufacturer's instructions. The eluent of each sample was newly concentrated, the pellet was resuspended in 200 µL methanol and filtered through a 0.22 µm PTFE filter. In each set of processed samples, a vial with a standard solution of 1000 ng mL^{-1} of the set of hormones analyzed, and a vial with only Milli-Q water, were used as references. Samples were then analyzed by LC–MS/MS consisting of an Acquity UPLC™ System (Waters, USA) quaternary pump equipped with an autosampler (7.5 µL of injection volume). The column used was Acquity UPLC BEH C18 (2.1 × 50 mm, 1.7 µm) (Waters, USA) and the mobile phase in the chromatographic separation consisted of eluent A (1 mM ammonium acetate and 0.1% formic acid in water) and eluent B (1 mM ammonium acetate and 0.1% formic acid in acetonitrile). The gradient used was 1% B until 1 min, followed by a linear increase up to 6 min reaching 38% B, followed by 100% B until 8.5 min as a cleaning step, and finally changing to the initial 1% B condition up to 9 min. The flow rate was 0.3 ml min^{-1} and the column temperature was 40 °C. A Waters Xevo™ triple quadrupole mass spectrometer system (MS/MS) with an ESI interface was used in tandem MS analyses with the following conditions: capillary voltage, 2.7 kV; source temperature, 150 °C; desolvation temperature, 400 °C; desolvation gas flow, 800 L h^{-1}; cone gas flow, 50 L h^{-1}. Cone voltage (V, in +/- modes) and collision energy (eV) were optimized to MS/MS detection of each hormone (fragmentation patterns), as follows: IAA (176>130 m/z), +18 V, 12 eV; IAA-d2 (178>132 m/z), +18 V, 12 eV; Z (220>136 m/z), +18 V, 12 eV; tZR (352>220 m/z), +25 V, 22 eV; EBL (481,5>445,1 m/z), +20 V, 10 eV; SA (137>93 m/z), -25 V, 13 eV; JA (209>59 m/z), -24 V, 13 eV; ABA (137>93 m/z), -20 V, 12 eV; GA4 (331>257 m/z), -30 V, 20 eV; GA_3

(345>239 m/z), -60 V, 14 eV. The multiple reaction monitoring (MRM) mode was applied in this analysis. Concentrations of 5, 10, 50, 100, 250, 500, and 1000 ng mL^{-1} were prepared in three separate dilutions in methanol to obtain the standard curve, and the analysis/quantification of each dilution was performed in duplicate. The quantification was achieved using TargetLynx™ software (Waters, USA), with a limit of detection (LOD) greater than three, and a limit of quantification (LOQ) greater than 10. The recovery efficiency and matrix effect were determined with standard spikes (1000 ng $sample^{-1}$ of all hormones) in a group of samples during the extraction and detection steps. All variations in recovery and matrix effect were considered in the final concentration of each hormone.

3.3.6 Statistical analysis

Clustering analysis with the gene expression kinetic were performed using the neighbor-joining grouping method based on the Euclidean distance between the genotypes (SAITOU; NEI, 1987), and presented in a heatmap. The hormone quantification data was used in a pairwise comparison using t-test (α=0.05); the means were represented in line graphs and a two-factorial analysis was carried out with DPI (0, 3, 5, and 7 DPI) and genotypes, using ANOVA (α=0.05); when significant, the means were separated using a Tukey test (α=0.05). The data was also considered to perform two principal component analyses (PCA), for gene expression and for hormonal content. We performed a collinearity test and variables with significant correlation were discarded from PCA that was performed using normalized data. The two main PCs were presented in a Kernel density estimation (KDE) and plotted in 2D graphic to compare the control vs. the inoculated. The statistical analysis of the data was performed using R language (R CORE TEAM, 2019) and the figures generated using Python 3 language.

3.4 RESULTS

3.4.1 Expression analysis

Among the endogenous controls tested, *Actinia* and *Ubiquitina* were chosen to normalize the expression of the target genes, due to their lower expression variation among the treatments, measured from the standard deviation of Cq (quantification cycle) in the samples. Among the target genes, *NINJA* was discarded from the analysis due to inconsistent results, such as an absence of amplification signal and low efficiency, probably as a result of difficulties in ringing the oligonucleotides used as primers with the template strips.

High correlation was observed between *GT* and *JAZ3*, and between *PR1*, *PR10* and *STS* expression patterns. Therefore, *JAZ3*, *PR10* and *STS* data was removed from the multivariate analysis. For PCA constructed by gene expression data, PC1 represented 40.5% and PC2 16.1% of the variance. *MYC2*, *AtMYB44* and *PR1* presented a high correlation with PC1, while PC2 was mainly loaded by *TPL* and *WRKY70* (Figure 1).

According to the data obtained, the n*o Rpv* genotype presents a significant change in showing higher values in PC2 7 DPI, suggesting a higher expression of the *TPL* and *WRKY70* genes. The *Rpv3-1* genotype presents a strong change in the gene expression at 3 DPI, suggesting an elevation of *TPL*, *WRKY70,* and *ROMT* expression and at 5 DPI, when NPR1 and PR1 were more expressed. However, significant changes arose at 7 DPI, suggesting a higher expression of *GT* and *AtMYB44* genes. This behavior was more accentuated at 7 DPI in the *Rpv3-3+Rpv10* genotype, although, unlike the others, no positive values were observed in PC2, suggesting that *ROMT*, *TPL,* and *WRKY70* gene expression was not up-regulated along the pathogen life cycle in this genotype. On the other hand, the *Rpv1+Rpv3-1* genotype showed significant changes in the PC1, from 1 DPI, varying between positive and negative values in the PC2 (Figure S1 A).

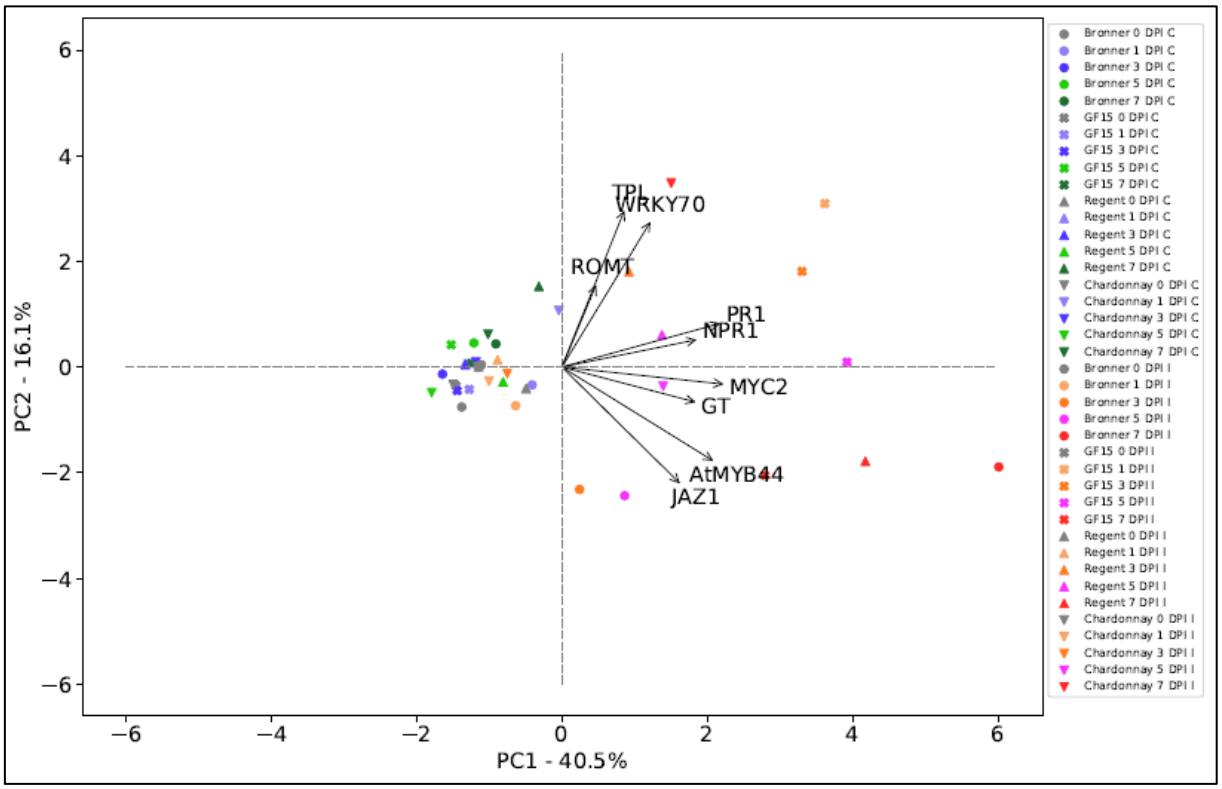

Figure 1. Principal component analyses based on the gene expression data from grapevine leaves inoculated (I) or control (C) with *Plasmopara viticola* to the genotypes: 1. *Rpv3-1+Rpv3-2* (cv. Calardis blanc), 2. *Rpv1+Rpv3-1* (GF15), 3. *Rpv3-3+Rpv10* (cv. Bronner), 4. *Rpv3-1* (cv. Regent), and 5. *No Rpv* (cv. Chardonnay).

JAZ1 and *JAZ3* expression were strongly induced from 1 DPI in the genotypes containing pyramided *Rpv* loci, especially *JAZ1* gene in the *Rpv3-3+Rpv10* genotype for the contrasting with n*o Rpv* and *Rpv3-1* genotypes (Figure 2). The *MYC2* gene was up-regulated in all evaluated times for *Rpv1+Rpv3-1* genotype, up-regulated from 3 DPI in *Rpv3-1* genotype, and up-regulated only in 7 DPI for n*o Rpv* and *Rpv3-3+Rpv10* genotypes. Like *MYC2*, the genes *PR1*, *PR10*, *WRKY70*, *STS,* and *GT* were up-regulated from 1 DPI in the *Rpv1+Rpv3-1* genotype. Interestingly, in all genotypes, the *GT* was most up-regulated regarding the *ROMT*, and the STS was up-regulated only in the *Rpv1+Rpv3-1* genotype (Figure 2).

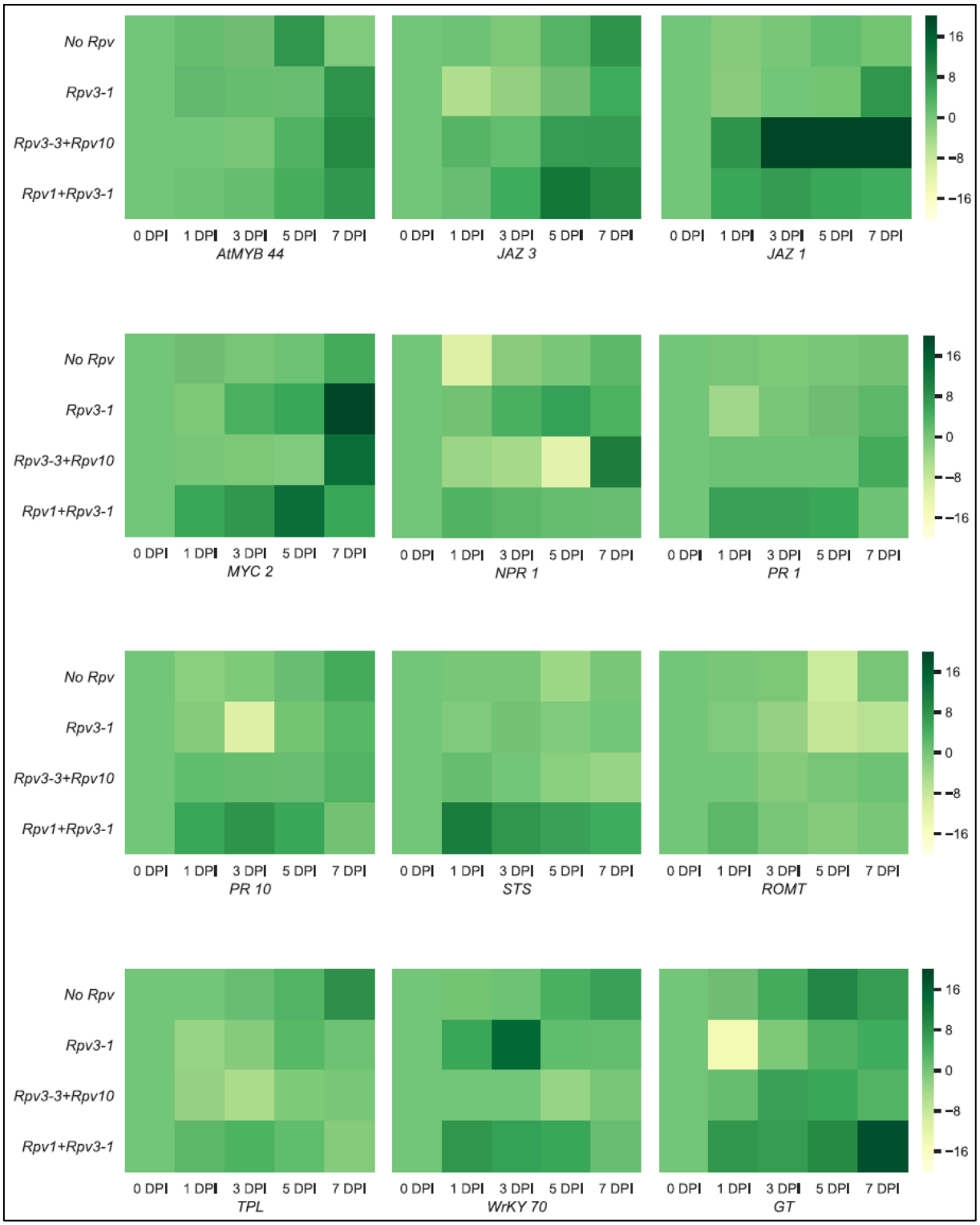

Figure 2. Heatmap demonstrating the fold change in the gene expression kinetics by defense pathway genes in grapevine genotypes with different resistance levels: 1. *Rpv3-1+Rpv3-2* (cv. Calardis blanc), 2. *Rpv1+Rpv3-1* (GF15), 3. *Rpv3-3+Rpv10* (cv. Bronner), 4. *Rpv3-1* (cv. Regent), and 5. *No Rpv* (cv. Chardonnay) elicited by inoculation with *Plasmopara viticola*. Scale bars represent the fold of change for each gene in each genotype regarding 0 DPI.

Regarding kinetic results, at 1 DPI, *JAZ1* and *PR10* were up-regulated in the pyramidated genotypes. While *NPR1*, *PR1*, *STS*, *ROMT,* and *TPL* were up-regulated only in the *Rpv1+Rpv3-1* genotype, WRKY70 was up-regulated in the *Rpv3-1* and *Rpv1+Rpv3-1* genotypes. In addition, PR1 and GT were down-regulated in the *Rpv3-1* genotype, while no significant changes were observed in the n*o Rpv* genotype. Furthermore, at 3 DPI, *JAZ3* was up-regulated in the *Rpv1+Rpv3-1* genotype and *JAZ1* was up-regulated in the pyramidated genotypes, *MYC2* and *NPR1* were up-regulated in the *Rpv3-1* and *Rpv1+Rpv3-1* genotypes, and NPR1 was down-regulated in the *Rpv3-3+Rpv10* genotype. *PR1* and *PR10* were up-regulated in the *Rpv1+Rpv3-1* and down-regulated in the *Rpv3-1*, while *WRKY70* was strongly up-regulated in this genotype.

The behavior of the gene expression demonstrates that the largest difference to the others was exhibited by the *Rpv1+Rpv3-1* genotype, while the genotype without *Rpv* (n*o Rpv*) and with only one resistance gene, *Rpv3-1*, clustered together (Figure S2). The cluster analysis makes evident the addictive effect between the *Rpv* loci in the plant cell gene expression during the *P. viticola* infection.

3.4.2 Hormonal quantification

Among the target hormones, epibrassinolide (EBL) and gibberellic acid 3 (GA_3) did not reach the limit of detection by the methodology employed. In addition, gibberellic acid 4 (GA_4) was detected only in the uninoculated genotype containing *,3-1+Rpv3-2* at 3 and 5 DPI, and inoculated *Rpv3-1* at 5 DPI (Figure S3 A). In the susceptible genotype (*no Rpv*), the single hormonal change occurred at 3 DPI, when the reduction in the concentration of IAA was found (Table S1, Figure S3 B). The *Rpv3-3+Rpv10* genotype showed a reduction in ABA expression levels at 3 and 5 DPI (Figure 3); similar behavior was observed in the *Rpv3-1* genotype at 5 DPI, when at the same time, the amount of tZR decreased (Figure 4). This result contrasts with the presence of a greater amount of tZR, also at 5 DPI revealed by the *Rpv3-1+Rpv3-2*.

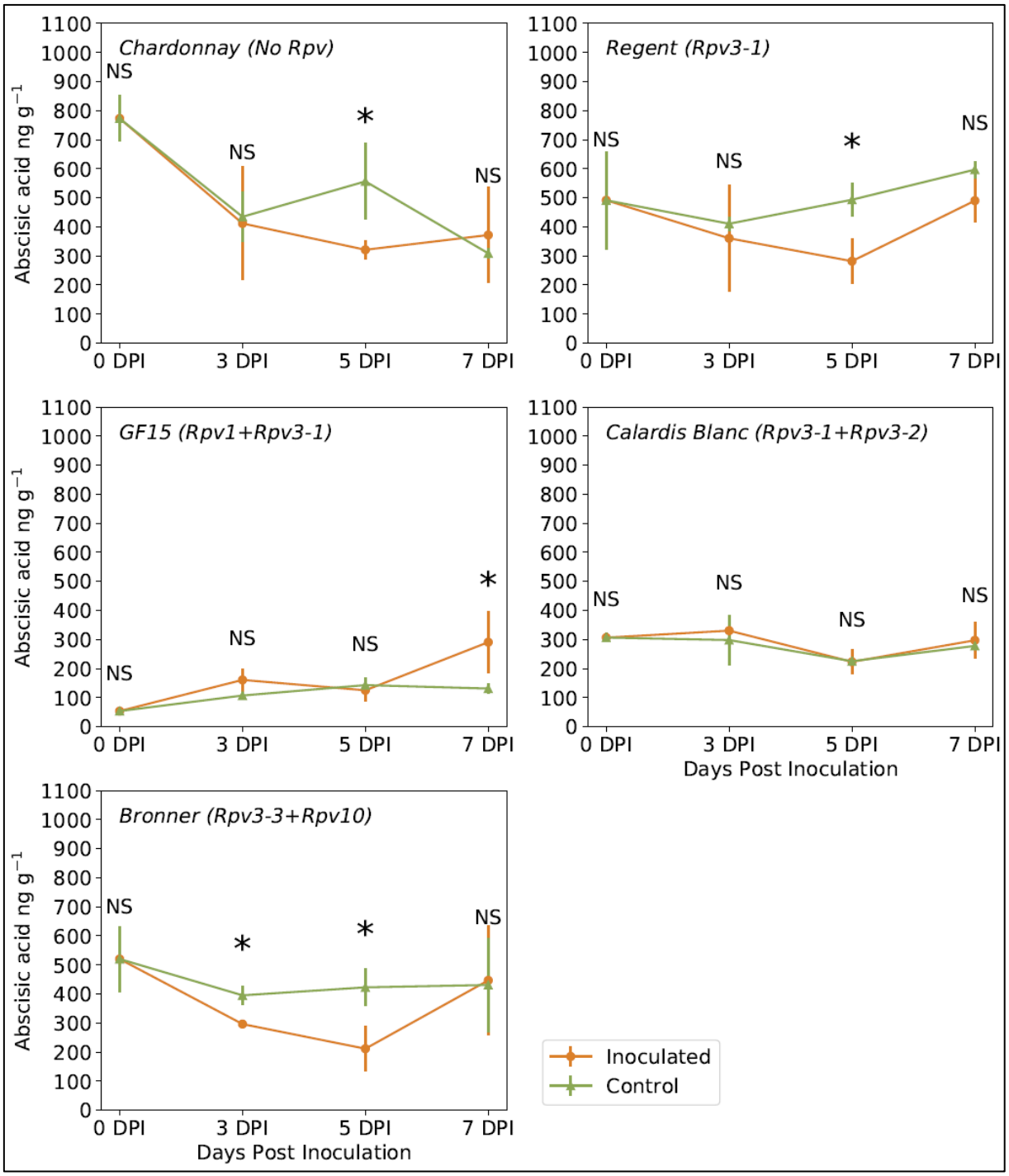

Figure 3. Kinetics of abscisic acid (ABA) concentration in grape leaf tissue inoculated with P. *viticola* in genotypes with different levels resistant against downy mildew and susceptible (Chardonnay – n*o Rpv*). Pairwise comparison controlled and inoculated conditions, columns with identical letters in the same day are not statistically different by t test (P<0.05).

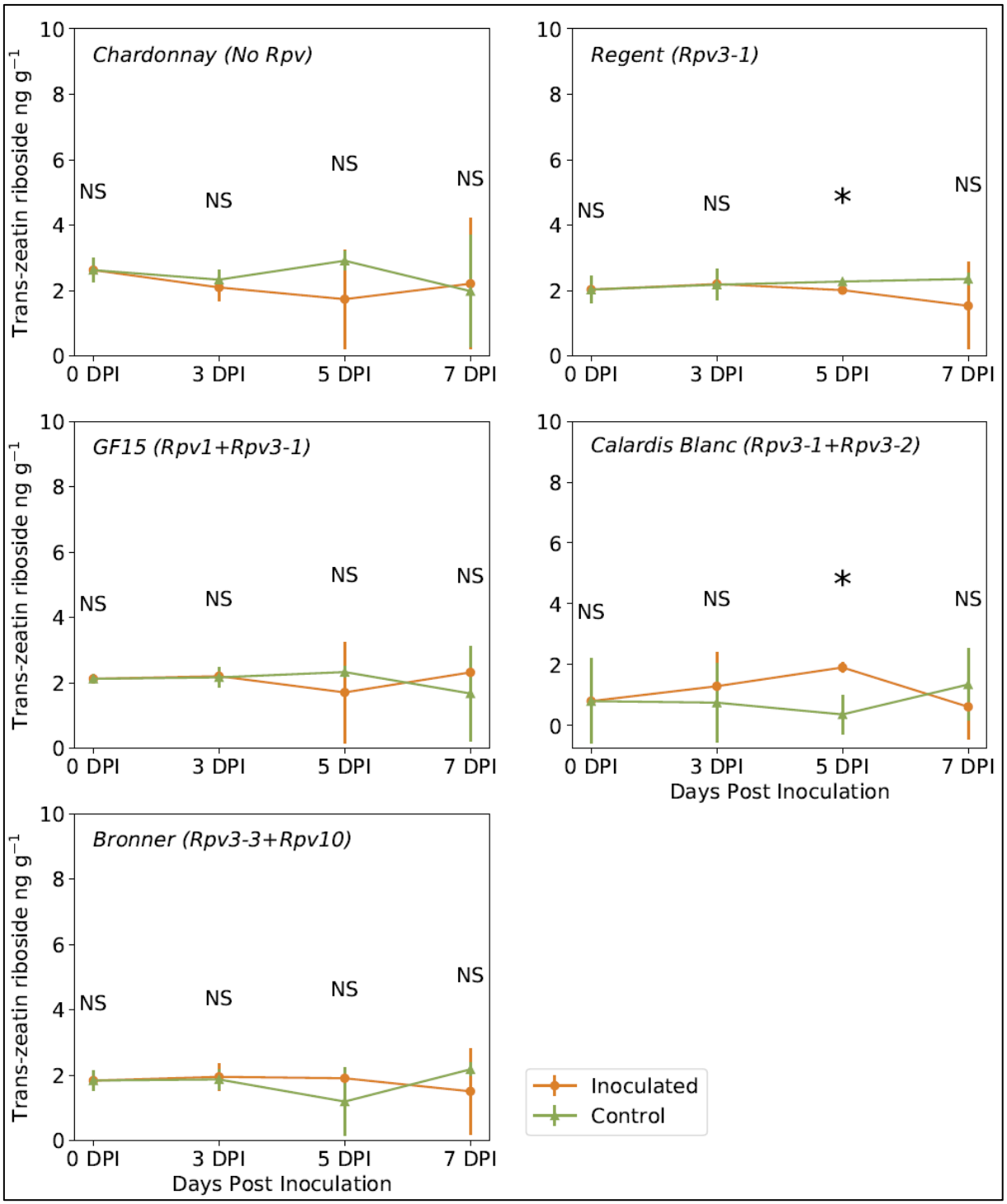

Figure 4. Kinetics of trans-Zeatin ribose (tZR) concentration in grape leaf tissue inoculated with P. *viticola* in genotypes with different levels resistant against downy mildew and susceptible (Chardonnay – n*o Rpv*). Pairwise comparison controlled and inoculated conditions, columns with identical letters in the same day are not statistically different by t test (P<0.05).

The highest concentrations of SA were observed at 3 DPI in the *Rpv3-1+Rpv3-2* genotype and at 7 DPI in the Rpv1+*Rpv3-1* genotype (Figure 5). The concentrations of the other hormones JA and Z did not show any significant differences between samples inoculated or not

with the *P. viticola* pathogen, in all tested genotypes, during the bioassay evaluation period (Figures S3 C and D).

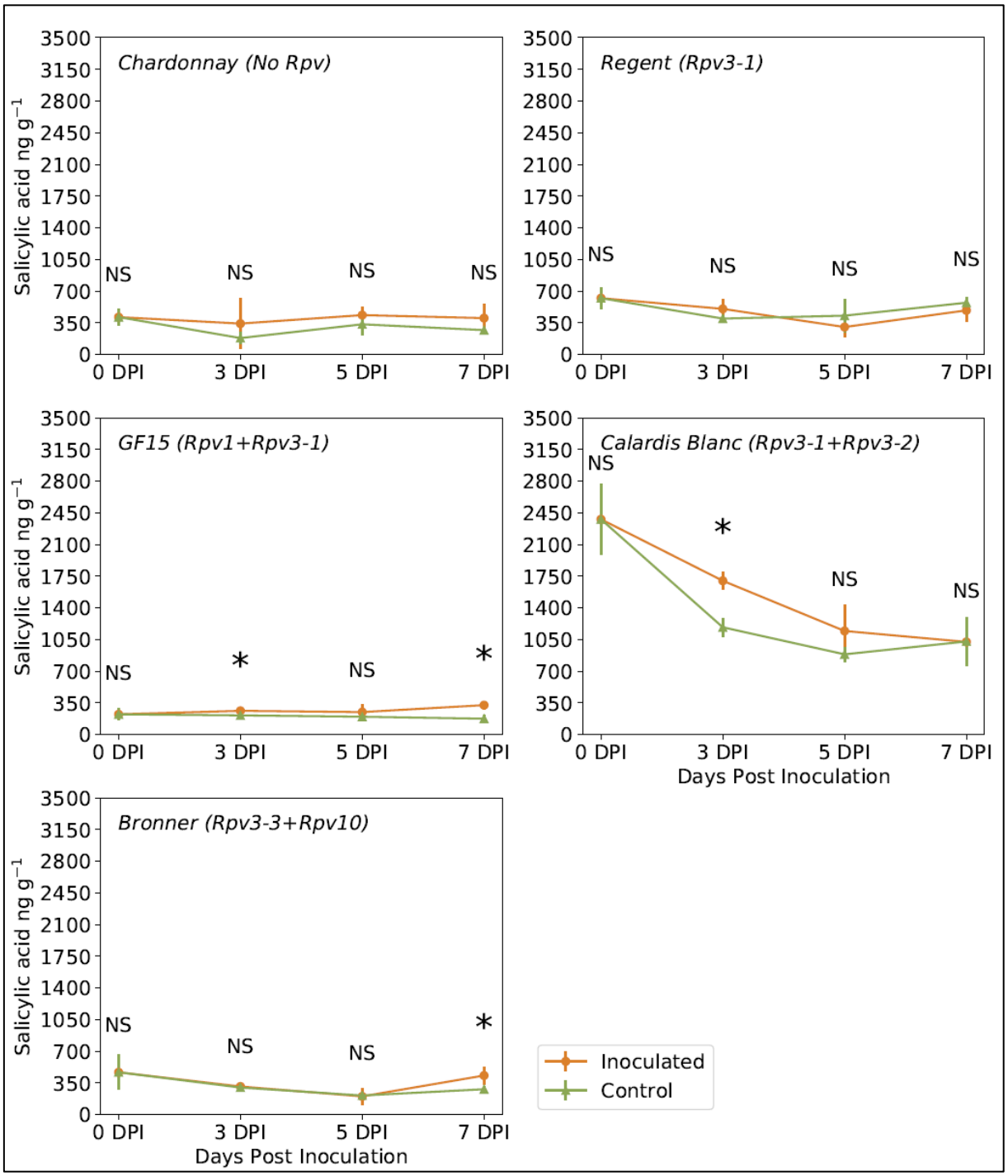

Figure 5. Kinetics of salicylic acid (SA) concentration in grape leaf tissue inoculated with P. *viticola* in genotypes with different levels resistant against downy mildew and susceptible (Chardonnay – *no Rpv*). Pairwise comparison controlled and inoculated conditions, columns with identical letters in the same day are not statistically different by t test (P<0.05).

Significant positive correlation coefficients were found between the concentrations of tZR and SA, tZR and GA_4 and to JA and IAA. Thus, tZR, GA_4 and IAA were discarded from

the multivariate analysis. The two PCs shown (Figure 6 and S1 B) represent 51.4% of the variation; PC1 primarily separated the genotype *Rpv3-1+Rpv3-2* from the others, while PC2 primarily separated, at some points, the inoculated treatment in contrast to the control.

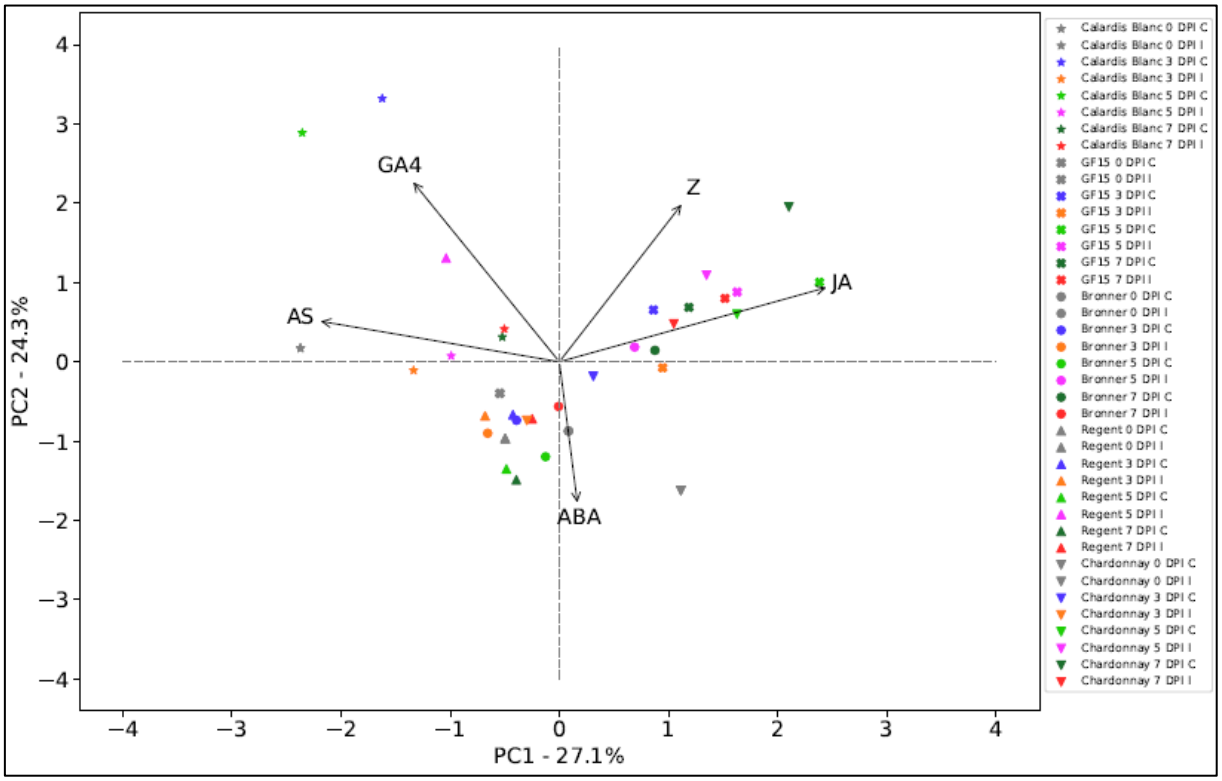

Figure 6. Principal component analyses based on the concentration of the hormones salicylic acid (SA), jasmonic acid (JA), abscisic acid (ABA), gibberellic acid 4 (GA4) and zeatin (Z) in grapevine leaves inoculated (I) or control (C) with *Plasmopara viticola* to the genotypes: 1. *Rpv3-1+Rpv3-2* (cv. Calardis blanc), 2. *Rpv1+Rpv3-1* (GF15), 3. *Rpv3-3+Rpv10* (cv. Bronner), 4. *Rpv3-1* (cv. Regent), and 5. *No Rpv* (cv. Chardonnay).

3.5 DISCUSSION

3.5.1 Gene expression patterns

The distribution of the genotypes obtained from the PCA analysis with gene expression data showed the different responses of the resistance genotypes and the susceptible genotype, mainly in pyramided genotypes (Figure 1). In the resistant genotypes, contrasting the inoculated with the control, differences in PCA were found from the first days after inoculation (Figure S1A). However, in the susceptible genotype, this change was only observed at 7 DPI, on the last day of evaluation. Incompatible interaction occurs mainly in the pyramided genotypes that present stronger alterations across the evaluated period.

The results showed that *NPR1* was positively regulated in the *Rpv1+Rpv3-1* genotype, from 1 DPI, also coinciding with the increase in *PR1* expression. The positive regulation of *NPR1* expression is associated with SAR and ETI and the induction of *PR* gene expression

(DURRANT; DONG, 2004; GAO et al., 2015; WU et al., 2014). These results demonstrate the association of the salicylate pathway acting as a resistance inducer in the *Rpv1+Rpv3-1* genotype. The no *Rpv* genotype showed an extremely late activation of the same pathway (Figure 2). In the same way, the overexpression of the *WRKY70* was observed in the susceptible genotype only at 5 and 7 DPI. Possibly, this activation is associated with *AtMYB44* increased levels. These results make evident that the susceptible genotype presents late molecular changes, resulting in the compatible plant pathogen reaction.

The *AtMYB44* regulates the defense response by transcriptional activation of the downstream gene *WRKY70* (SHIM; CHOI, 2013). In the present study, the evaluated genotypes showed a late activation of *AtMYB44*. However, the *WRKY70* gene was also independently activated by *NPR1* (SHIM et al., 2013), as also happened with the *Rpv3-1* and *Rpv1+Rpv3-1* genotypes. The *Rpv3-3+Rpv10* genotype showed late activation of the *AtMYB44* and down-regulated *NPR1*, resulting in a lower change of the WRKY70 level expression and late activation of the *PR* genes (*PR1* and *PR10*). However, this genotype presented a higher expression of *JAZ* genes, mainly *JAZ3*.

The *WRKY70* transcription factor has several roles in plant metabolism, such as negative regulation of leaf senescence processes (ÜLKER; SHAHID MUKHTAR; SOMSSICH, 2007; ÜLKER; SOMSSICH, 2004), *PR1* gene inducing (WITHERS; DONG, 2016), and pathogen resistance inducing the programed cell death (ZOU et al., 2013). This gene plays a central role as a regulator repressing the jasmonic acid pathway and activating the salicylic acid pathway (LI; BRADER; PALVA, 2004; LI et al., 2019). However, there is a functional redundancy in this crosstalk: the SA still actively repress JA-responsive pathways in wrky70 knock-out mutants (LI et al., 2019).

Upstream of the *WRKY70* expression there are the *NPR1* and *AtMYB44* genes (CAARLS; PIETERSE; VAN WEES, 2015; SHIM et al., 2013; SHIM; CHOI, 2013). *AtMYB44* also acts in several other pathways, playing an important role in controlling stomatal closure in response to abiotic stresses (JUNG et al., 2008). The *NPR1* is an SA receptor that acts as a transcriptional coactivator, whereas NPR3 and NPR4 act as transcriptional corepressors of the SA downstream pathway (DING et al., 2018). The presence of SA activates the *NPR1* and induces the *WRKY70* to start the *PR1* expression (DING et al., 2018; LI et al., 2019). The *NPR1* also acts in the cytoplasm, and in *npr1* nuclear plants, the NPR1 may play the role of SA-activator and JA-repressor (LI et al., 2019; SPOEL et al., 2003, 2009).

The *MYC2* transcription factor has several roles, acting in plant development and defense (MAJOR et al., 2017; WANG; YAO; WANG, 2020). Related to the resistance

pathway, the *MYC2* is reported as a PR10 inductor, repressed by JAZ genes and therefore induced by JA (GUERREIRO et al., 2016; HE et al., 2018a; ZHANG et al., 2017). This occurs due to the JAZ degradation by jasmonate-isoleucine (*JA-Ile*) releasing the *TOPLESS* (TPL) and MYC2 (PAUWELS; GOOSSENS, 2011). One of the results of the effective action of the jasmonate pathway is the production of the PR10 protein.

Our results present a contrast between the evaluated genotypes for the *PR10* gene expression, just one day after inoculation, at which time the gene was significantly upregulated in the pyramidated genotypes (Figure 2). The *Rpv1+Rpv3-1* genotype was able to produce the greatest change for this gene expression, which remained high in the next evaluated times. In contrast, the other genotypes showed a reduction in the expression value of the PR10 gene, presenting late activation after the pathogen life cycle (Figure 2).

The activation of the *JAZ* family evaluated genes (*JAZ1* and *JAZ3*) also presented a contrast between the genotypes. *Rpv3-3+Rpv10* showed the most differentiated behavior from the other genotypes, specifically *JAZ1*, with an increase in expression at 1 DPI and a maintenance of high expression until the end of the bioassay. A similar result was obtained for the *Rpv1+Rpv3-1* genotype, whereas the n*o Rpv* and the *Rpv3* genotypes showed little down regulation in expression, except for *Rpv3-1* at 7 DPI, which showed an increase in the expression of this gene.

The JAZ proteins are a family induced and repressed by the jasmonate action, maintaining a balance of the signal of this hormone (DEMIANSKI; CHUNG; KUNKEL, 2012). The gene expression control occurs through the link with coronatine-insensitive 1 (*COI1*), which is part of the SKP-Cullin-F-box protein (*SCF*) complex, acting as a co-receptor for *JA-Ile*, an active form of jasmonate (SHEARD et al., 2010). From the connection of the *JAZ* family proteins with *COI1*, the process of ubiquitination of them starts and, consequently, the inhibition of jasmonate happens as demonstrated in Figure 7 (GUERREIRO et al., 2016; PAUWELS; GOOSSENS, 2011; WASTERNACK; HAUSE, 2013).

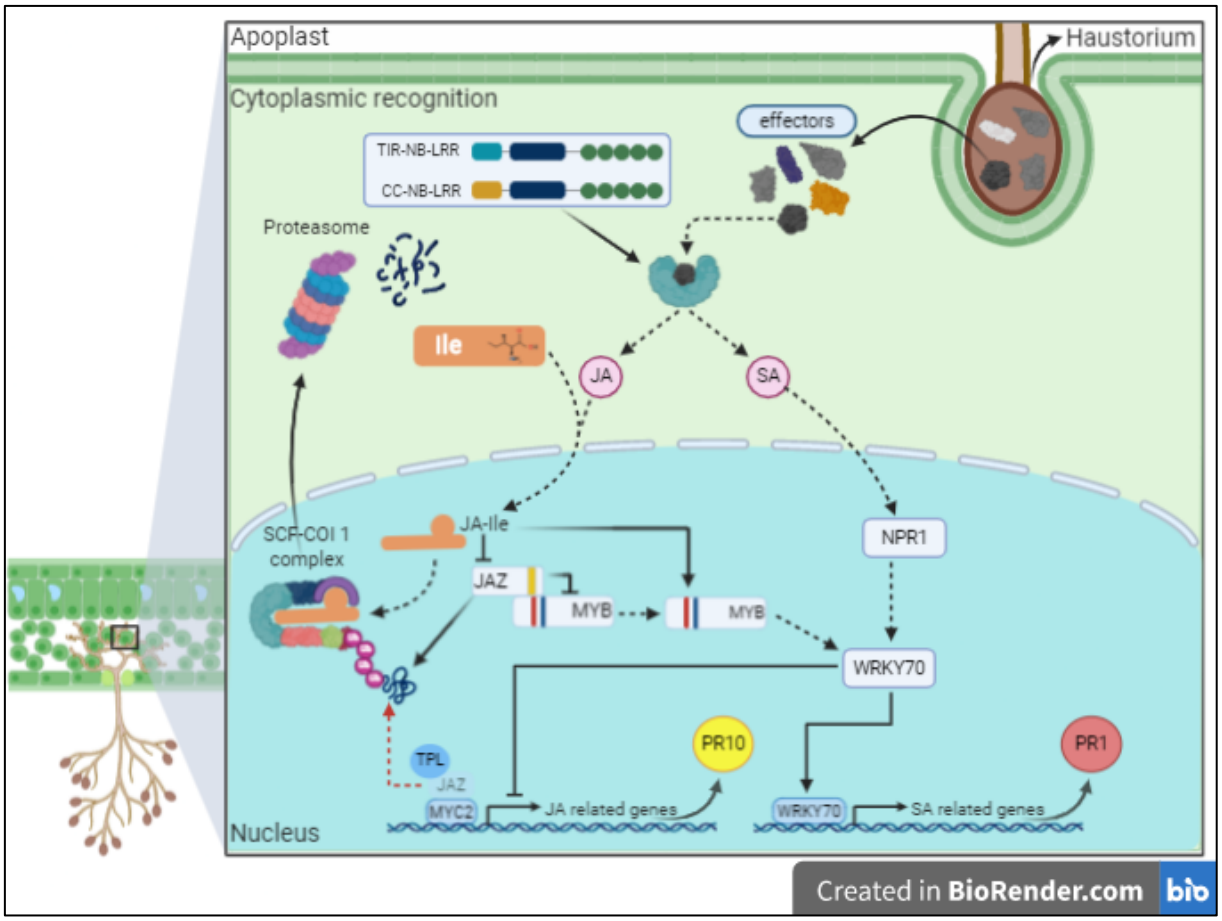

Figure 7. Proposed model for the interplay between effector triggered immunity activated by JA and SA induced hormones. Pathogen effectors recognized by Tool/interleukin-1 receptor (TIR) or coiled-coil (CC), nucleotide-binding site (NB) leucine rich repeat (LRR), activating the salicylic acid (SA) or jasmonate acid (JA) pathway, SA activates the nuclear expression of NPR1 that triggers the WRKY70 transcription factor. WRKY70 acts as an antagonist of the JA pathway activating SA related genes, resulting in the PR protein expression, mainly PR1. However, the JA pathway joins with isoleucine (JA-Ile) to activate the SCF-COI 1 complex inducing the jasmonate zim domain (JAZ) protein ubiquitination and their degradation on the proteasome, inducing the MYB, releasing the TOPLESS (TPL) and activating the MYC2, starting the expression of genes related to JA, primarily PR10.

GF15 (*Rpv1+Rpv3-1*) showed greater expression than cv. Bronner (*Rpv3-3+Rpv10*), indicating that there is an alteration to signaling between the genes of this family depending on the studied locus of resistance. The behavior of the n*o Rpv* genotype is also noteworthy, showing an increase in expression at 7 DPI, showing the extremely late reaction triggered by the compatible reaction plant pathogen.

Despite cv. Bronner (*Rpv3-3+Rpv10*) having a greater expression of *JAZ*, indicating early activation of the jasmonate pathway, it was not expressed in the downstream. Based on the gene expression kinetics, this genotype did not show signs of increased expression of *TOPLESS* at any time after inoculation. Meanwhile, the change in the expression of *MYC2* was

verified only at 7 DPI in the cv. Bronner (Figure 2). These results contrast with the increase of *PR10* expression at 1 DPI, suggesting two hypotheses to be further tested: in the genotype containing *Rpv3-3+Rpv10* (i) there is the role of an alternative pathway for the performance of jasmonates, regardless of the action of the *TOPLESS* and *MYC2* genes or (ii) the activity of these two genes occurred before 1 DPI and their expression was immediately normalized.

The genotype that did carry at least one resistant allele showed a constant increase in the *TOPLESS* expression, with greater accumulation at 7 DPI. However, the pyramid genotype *Rpv1+Rpv3-1* had high levels of *TOPLESS* and *MYC2* expression at 1 DPI, corroborating the results obtained for the *JAZ* genes family. While the presence of *Rpv3-1* promoted a behavior similar to the genotype containing the locus *Rpv3-3+Rpv10*, in which *TOPLESS* expression was initially low, it increased up to 5 DPI, while *MYC2* showed a constant increase in levels of expression during the evaluated period.

The expression profile of the genes linked to the route of the stilbenes was influenced by the different R-loci. The results obtained in the present study demonstrate that in the susceptible genotype the expression of the stilbene synthase (*STS*) was reduced from the first day after inoculation, presenting the lowest value at 5 DPI, returning to the initial values at 7 DPI. The genotype that carries the resistance locus *Rpv3-1* (cv. Regent) showed alternative behavior: a decrease of transcription (1 and 5 DPI), with a reduction of approximately 50% in the expression of the *STS*, and an increase (3 and 7 DPI) when the expression of *STS* in inoculated plants did not differ from that of uninoculated plants. Compared to the others, the genotype with *Rpv1+Rpv3-1* induced greater expression of the *STS* gene from 1 DPI and remained elevated throughout the evaluation period. The cv. Bronner that contained *Rpv3-3+Rpv10* showed an increase in *STS* expression by 1 DPI.

Similarly, we did not find a clear pattern between the expression of *Resveratrol O-methyltransferase* (ROMT) in distinct PIWI genotypes. The cv. Regent (*Rpv3-1*) showed a constant reduction in *ROMT* expression reaching values of approximately 10 % of the expression at 5 DPI, like the result obtained in the susceptible genotype. The *ROMT* gene within GF-15 (*Rpv1+Rpv3-1*) also showed greater expression at 1 DPI, but in 3DPI their expression level returned to normal and was suppressed at 5 DPI. As in *Rpv1+Rpv3-1*, *Rpv3-3+Rpv10* showed an increase in *STS* expression by 1 DPI; however, this was not different from the control treatment since the same pattern was verified in the expression of the *ROMT* gene. *STS* expression was normalized to 3 DPI, the same period in which the *ROMT* gene was suppressed to less than 50% of the expression observed at the beginning of the experiment. In the 5 and 7 DPI evaluations, the *STS* gene was suppressed, while the *ROMT* gene normalized expression.

In the cv. Chardonnay (n*o Rpv* genotype) genotype, *ROMT* showed no change in expression levels at 1 DPI, being suppressed at 3 and 5 DPI and returning to the initial expression values at 7 DPI.

The *GT* gene, responsible for the resveratrol glycosylation and for producing piceid (a molecule that is less aggressive to the action of the pathogen) showed an increase in expression up to 5 DPI, the moment of sporulation of the pathogen in the cv. Chardonnay *(no Rpv*). However, *GT* gene expression was reduced to approximately 7% at 1 DPI, normalized at 3 DPI, but was higher at 5 and 7 DPI in cv. Regent (*Rpv3-1*). In the GF-15 (*Rpv1+Rpv3*-1) the *GT* gene expression, as well as *STS*, was induced from 1 DPI, reaching maximum values at 7 DPI (*GT*) and 1 DPI (*STS*).

The coding gene for stilbene synthase (*STS*) is responsible for the synthesis of stilbenes; mainly resveratrol, which is responsible for cellular resistance to pathogens and other abiotic stresses (Zamboni et al. 2009). Compared with the control lines, the concentration of trans-resveratrol and other stilbene compounds were significantly higher in the transgenic lines (Cheng et al. 2016). This result was obtained with the insertion of the *STS* gene from *V. quinquangularis*, which had a higher content of resveratrol. The authors also verified a correlation between transgenic lines with high resveratrol content and high resistance to powdery mildew (CHENG et al., 2016).

Within the cell, the resveratrol can be transformed to other molecules. Resveratrol can also be methylated and transformed into pterostilbene, through the action of the product of the expression of the *Resveratrol O-methyltransferase* (*ROMT*) gene, induced by the action of jasmonate and responsible for suppressing the attack of pathogens (MARTÍNEZ-MÁRQUEZ et al., 2016; SCHMIDLIN et al., 2008; XU et al., 2018). The glycosylation of resveratrol is an alternative pathway for the molecule, resulting in its transformation into piceid, a process that is normally observed during the ripening of the grapes, as well as with exposure to ultraviolet radiation (AOKI et al., 2015; MA et al., 2019; XU et al., 2019a). The opposite process can also occur through the deglycolization of the piceid (KUO et al., 2016).

The review of the results revealed that the pyramided genotype with the *Rpv1+Rpv3-1* genes showed earlier responses in relation to the other evaluated genotypes. In the same way, the results obtained for the genotype *Rpv3-3+Rpv10* suggest an early JA activation (earlier than 1 DPI) resulting in the JAZ degradation followed by the activation of *JAZ* expression, to normalize the JAZ level. However, genotypes with only one Rpv locus present behavior close to the susceptible genotype.

3.5.2 Hormonal patterns

The reduction of the ABA concentration of genotypes containing *Rpv3-1* (Regent) and *Rpv3-3+Rpv10* (Bronner) after mildew inoculation is possibly linked to the balance of this hormone and the performance of the protein ubiquitination complex (BUESO et al., 2014). In another pathosystem, the performance of *RING-type E3 ubiquitin ligase*, a negative regulator of ABA, was observed for cellular defense against the attack of the biotrophic pathogen *Erysiphe necator*, causal agent of powdery mildew in grapevines (WANG et al., 2017a; WANG; YAO; WANG, 2020). The ABA balance hypothesis is in accordance with the reported performance of the ubiquitination process involving pathogen associated molecular patterns triggered immunity (PAMP-PTI), resulting in the signalization of the programmed cell death, as hypersensitivity responses caused by the activation of ETI by NBS-LRR genes (DUPLAN; RIVAS, 2014; MARINO; PEETERS; RIVAS, 2012).

Nevertheless, IAA plays many roles in the plant metabolism, although controversial results were reported in studies considering plant cell defense. Sometimes IAA is reported as a resistance inductor through systematic acquired resistance (SAR) inducing quitinases expression that acts as pathogen related (PR) proteins (VAN LOON; VAN STRIEN, 1999); however, this hormone is also reported as a resistance suppressor while IAA silencing is reported as a PAMP act (DENANCÉ et al., 2013; KARASOV et al., 2017). In our evaluations, IAA concentration was downregulated, only at 3 DPI on the susceptible genotype.

The activation of genes linked to the salicylate route was verified in all evaluated genotypes; however, *Rpv3-1+Rpv3-2*, but not the others, present an alteration in the kinetic of this hormone quantification (Table S1). The early response from the *Rpv3-1+Rpv3-2* genotype can be associated with the potential additive effect obtained from the haplotypes Rpv3-1 and Rpv3-2 combination. However, this hypothesis is not supported by the SA kinetics that present a decreasing response over the evaluated times. Our results are in agreement with the behavior of greater resistance induction in pyramided genotypes *Rpv3-1+Rpv3-2* (e.g. 'Calardis Blanc') compared to *Rpv3-1* genotypes (e.g. 'Regent') in controlled conditions (EISENMANN et al., 2019). Yet, until now, this statement is contradictory in field conditions (ZANGHELINI et al., 2019).

Unlike for the other hormones, there is no established knowledge regarding the involvement of Trans-zeatin-riboside in plant defense mechanisms. Nevertheless, a report suggests that this molecule favors the expression of salicylate route genes, promoting the synthesis of *PR1* and increasing resistance in some pathosystems (CHOI et al., 2011). However, the changes demonstrate that there is possibly an effect due to the genetic background

associated with the observed variation. The genotypes carrying different *Rpv3* haplotypes revealed contrasting results. The effect of the genetic background associated with the *Rpv3* genotypes modulating the genetic resistance response to downy mildew is described in the literature (FORIA et al., 2018a). Thus, the background genetic of the genotypes used for this work can be acting on the results obtained, due to the heterozygous nature of the grapevine and the different origins of each *Rpv* loci.

3.6 CONCLUSIONS

Genotypes with distinct resistance haplotypes combinations against *P. viticola* triggered differentiated activated defense pathways. Early defense responses were reported to pyramided genotypes.

The *Rpv3-1* genotype presents a SA activation pathway. While the same genotype pyramided with *Rpv1* shows more expressive changes, in both SA and JA metabolic pathways. Differently, the *Rpv3-3+Rpv10* genotype shows a predict JA activation pathway.

The stilbenes pathway was activated in all inoculated plants, demonstrating the involvement of these molecules in the defense pathways for these genotypes.

The susceptible genotype showed alterations in the expression of genes associated with resistance; however, these are triggered late after the cycle of *P. viticola* causes the damage.

Futures studies can be developed with new genotypes aiming to describe the effect of isolated genes and predict the genetic effect in each combination.

Acknowledgments

We are grateful to the Coordenação de Aperfeiçoamento de Pessoal de Nível Superior (CAPES) for scholarship to MDR, and, to Conselho Nacional de Desenvolvimento Científico e Tecnológico (CNPq) for financial support and scholarships to RON (Proj 423476/ 2018-1), and to MPG (Proc. 302798/2018-8 and 407974/2018-0) and to the Fundação de Amparo à Pesquisa e Inovação de Santa Catarina (FAPESC) for financial support (Proj. TO2017 TR1844). We thankful to EPAGRI for kindly allowed us to collect plant samples.

3.7 SUPPLEMENTAL MATERIAL

Figure S1 A. Kernel density estimative according the two Principal Components (PC1 and PC2) derived from PCA, showing the gene expression levels in grapevine in no treated leaves (control – blue) and inoculated leaves, with *Plasmopara viticola* (inoculated – red) in genotypes with different resistance levels: 1 – *Rpv3-1+Rpv3-2* (cv. Calardis blanc), 2 – *Rpv1+Rpv3-1* (GF15), 3 – *Rpv3-3+Rpv10* (cv. Bronner), 4 – *Rpv3-1* (cv. Regent), and 5 – *No Rpv* (cv. Chardonnay). **B.** Kernel density estimative according the two Principal Components (PC1 and PC2) derived from PCA, showing the hormonal concentration for Salicylic acid (SA), Jasmonic acid (JA), Abscisic acid (ABA), Gibberellic acid 4 (GA4) and Zeatin (Z) in grapevine in no treated leaves (control – blue) and inoculated leaves, with *Plasmopara viticola* (inoculated – red) in genotypes with different resistance levels: 1 – *Rpv3-1+Rpv3-2* (cv. Calardis blanc), 2 – *Rpv1+Rpv3-1* (GF15), 3 – *Rpv3-3+Rpv10* (cv. Bronner), 4 – *Rpv3-1* (cv. Regent), and 5 – *No Rpv* (cv. Chardonnay).

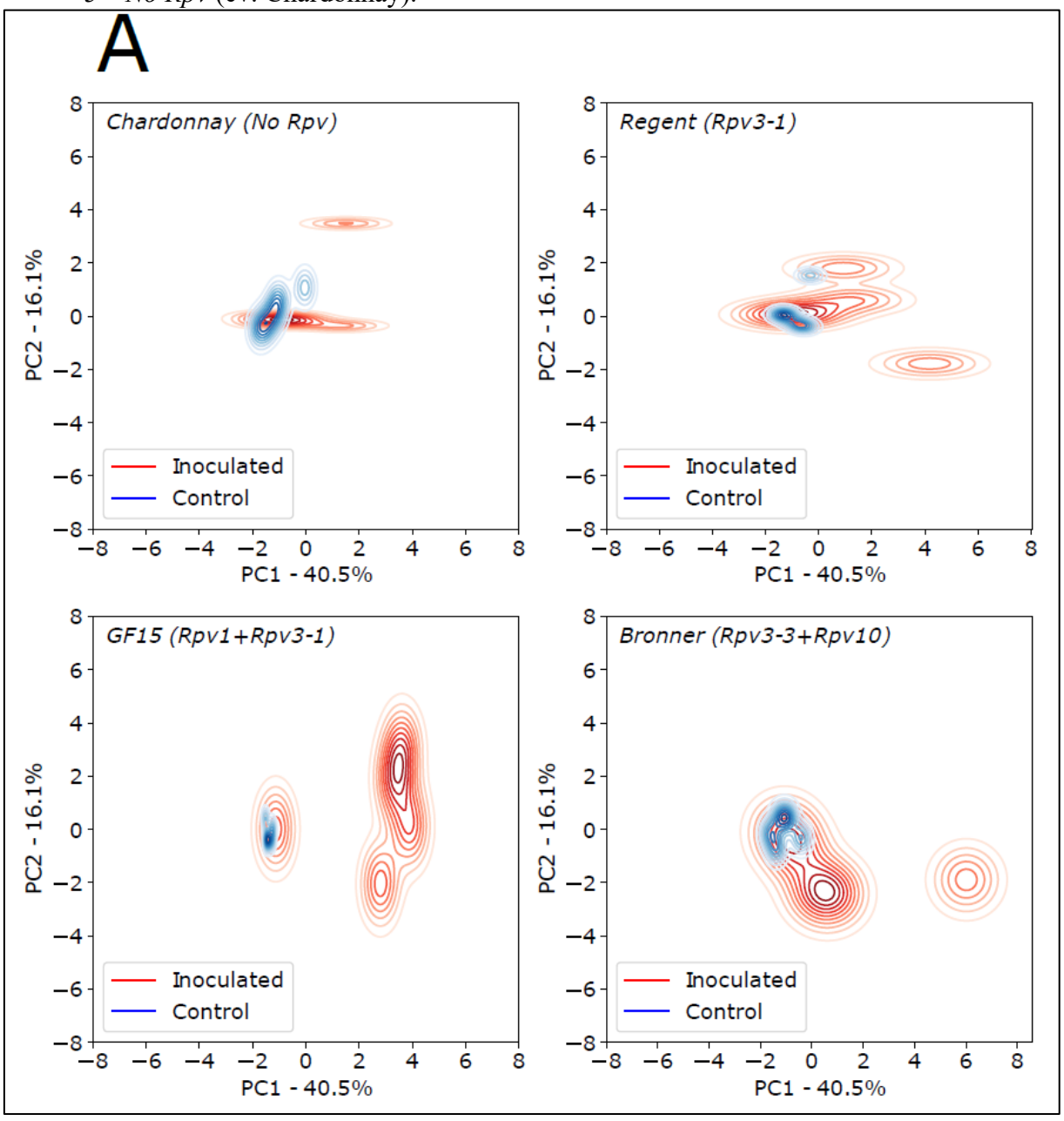

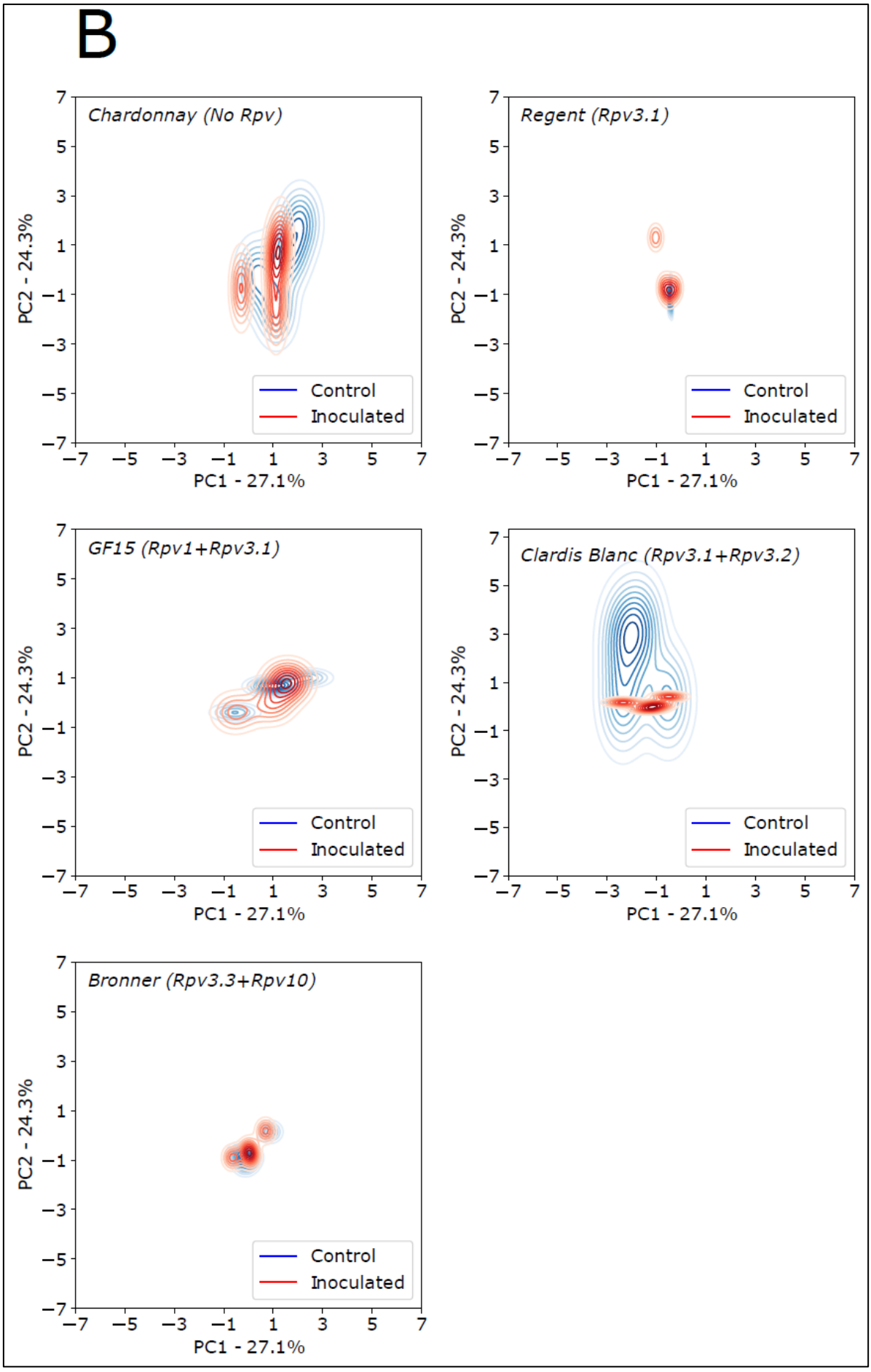
B
Chardonnay (No Rpv)
Regent (Rpv3.1)
GF15 (Rpv1+Rpv3.1)
Clardis Blanc (Rpv3.1+Rpv3.2)
Bronner (Rpv3.3+Rpv10)
Control
Inoculated
PC1 - 27.1%
PC2 - 24.3%

Figure S2. Clustering of grapevine Chardonnay and PIWI genotypes Regent (Rpv3-1), GF15 (Rpv1+Rpv3-1) and Bronner (Rpv3-3+Rpv10) based on the Euclidian distance of the gene expression by the genes AtMYB44, JAZ3, JAZ1, MYC2, NPR1, PR1, PR10, STS, ROMT, TPL, WRKY70 and GT, occurred at 1, 3, 5 and 7 days post inoculation with *Plasmopara viticola*.

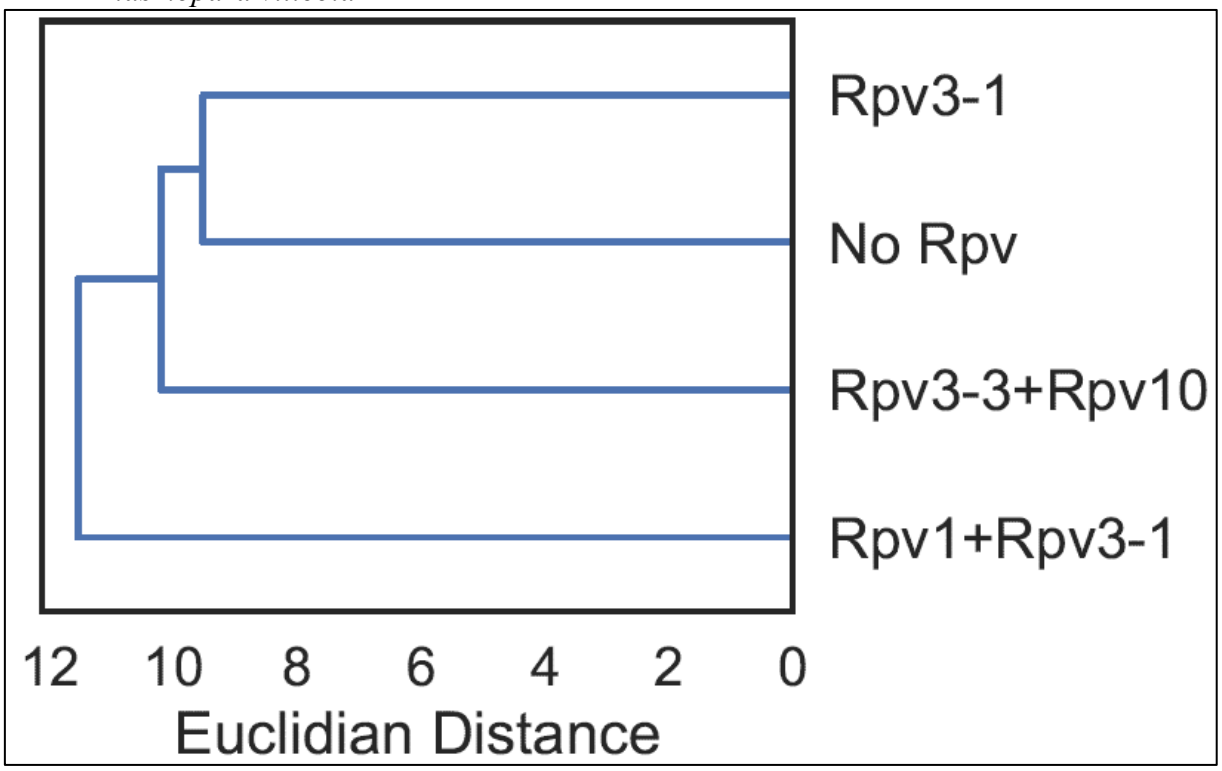

Figure S3 A. Kinetics of Gibberellic acid 4 (GA_4) concentration in grape leaf tissue inoculated with P. *viticola* in genotypes with different levels resistant against downy mildew. Pairwise comparation controlled and inoculated conditions, columns with identical letter in the same day are not statically different by t test ($P<0.05$). **B.** Kinetics of Indoleacetic acid (IAA) concentration in grape leaf tissue inoculated with P. *viticola* in genotypes with different levels resistant against downy mildew and susceptible (Chardonnay – *No Rpv*). Pairwise comparation controlled and inoculated conditions, columns with identical letter in the same day are not statically different by t test ($P<0.05$). **C**. Kinetics of Jasmonic acid (JA) concentration in grape leaf tissue inoculated with P. *viticola* in genotypes with different levels resistant against downy mildew and susceptible (Chardonnay – *No Rpv*). Pairwise comparation controlled and inoculated conditions, columns with identical letter in the same day are not statically different by t test ($P<0.05$). **D.** Kinetics of Zeatin (Z) concentration in grape leaf tissue inoculated with P. *viticola* in genotypes with different levels resistant against downy mildew and susceptible (Chardonnay – *No Rpv*). Pairwise comparation controlled and inoculated conditions, columns with identical letter in the same day are not statically different by t test ($P<0.05$).

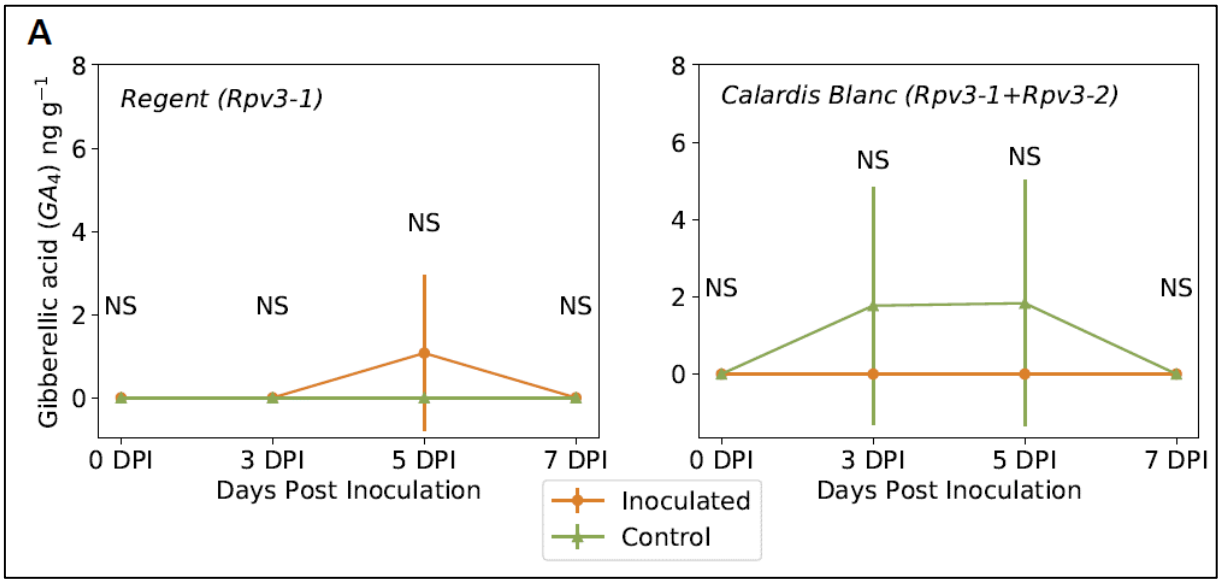

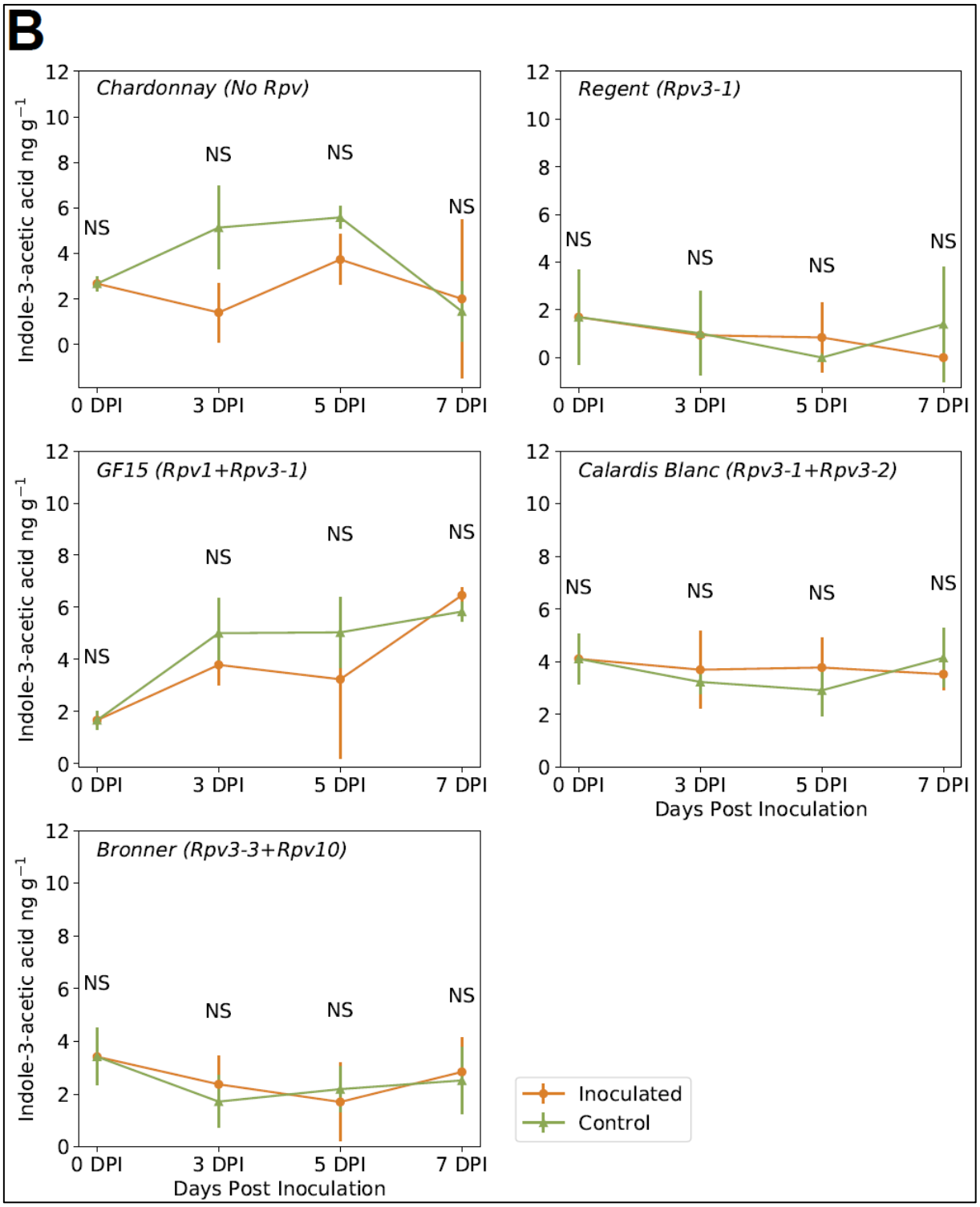
B
Chardonnay (No Rpv)
Regent (Rpv3-1)
GF15 (Rpv1+Rpv3-1)
Calardis Blanc (Rpv3-1+Rpv3-2)
Bronner (Rpv3-3+Rpv10)
Indole-3-acetic acid ng g^{-1}
NS
0 DPI
3 DPI
5 DPI
7 DPI
Days Post Inoculation
Inoculated
Control

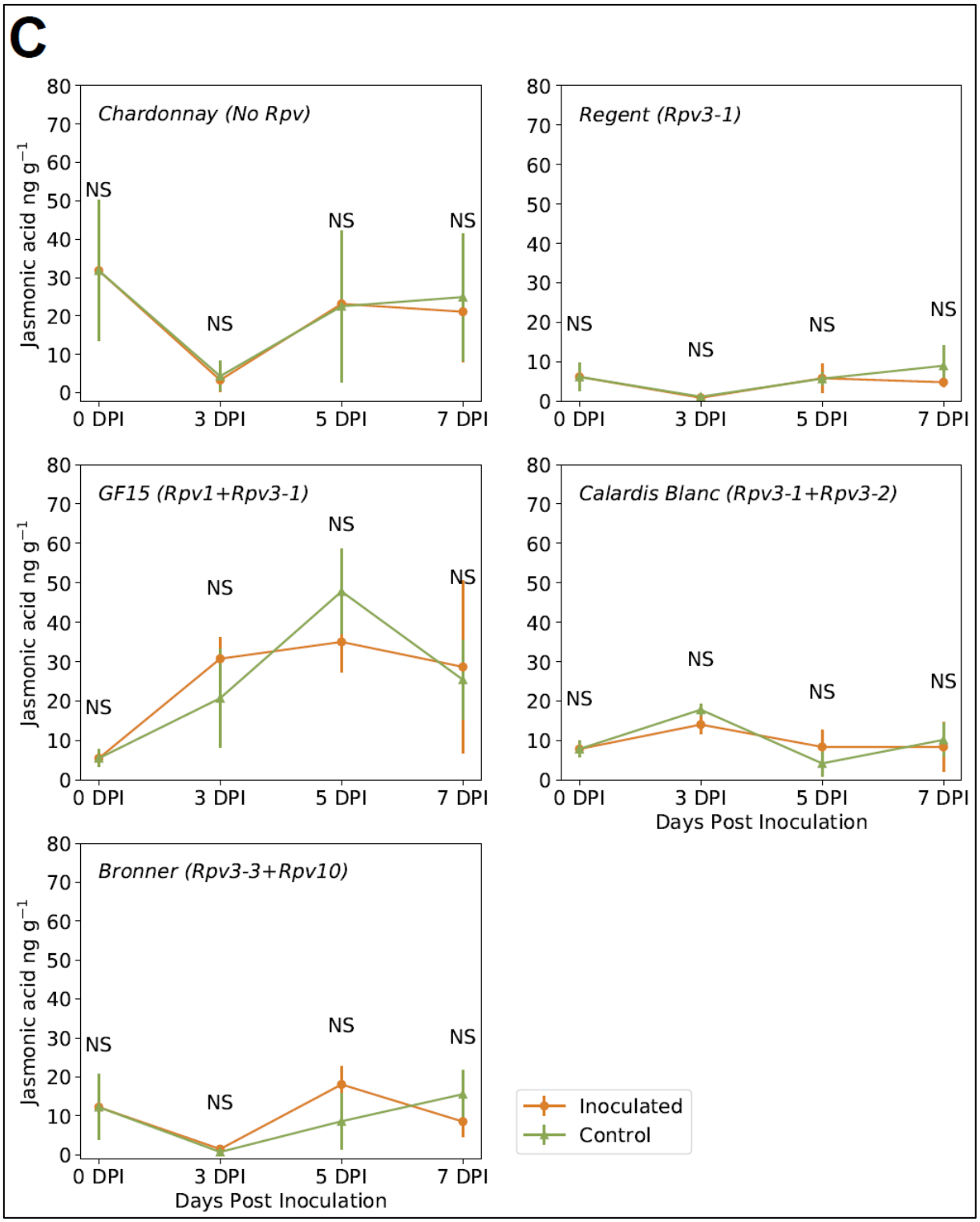
C
Chardonnay (No Rpv)
Regent (Rpv3-1)
GF15 (Rpv1+Rpv3-1)
Calardis Blanc (Rpv3-1+Rpv3-2)
Bronner (Rpv3-3+Rpv10)
Jasmonic acid ng g⁻¹
0 DPI
3 DPI
5 DPI
7 DPI
Days Post Inoculation
NS
Inoculated
Control

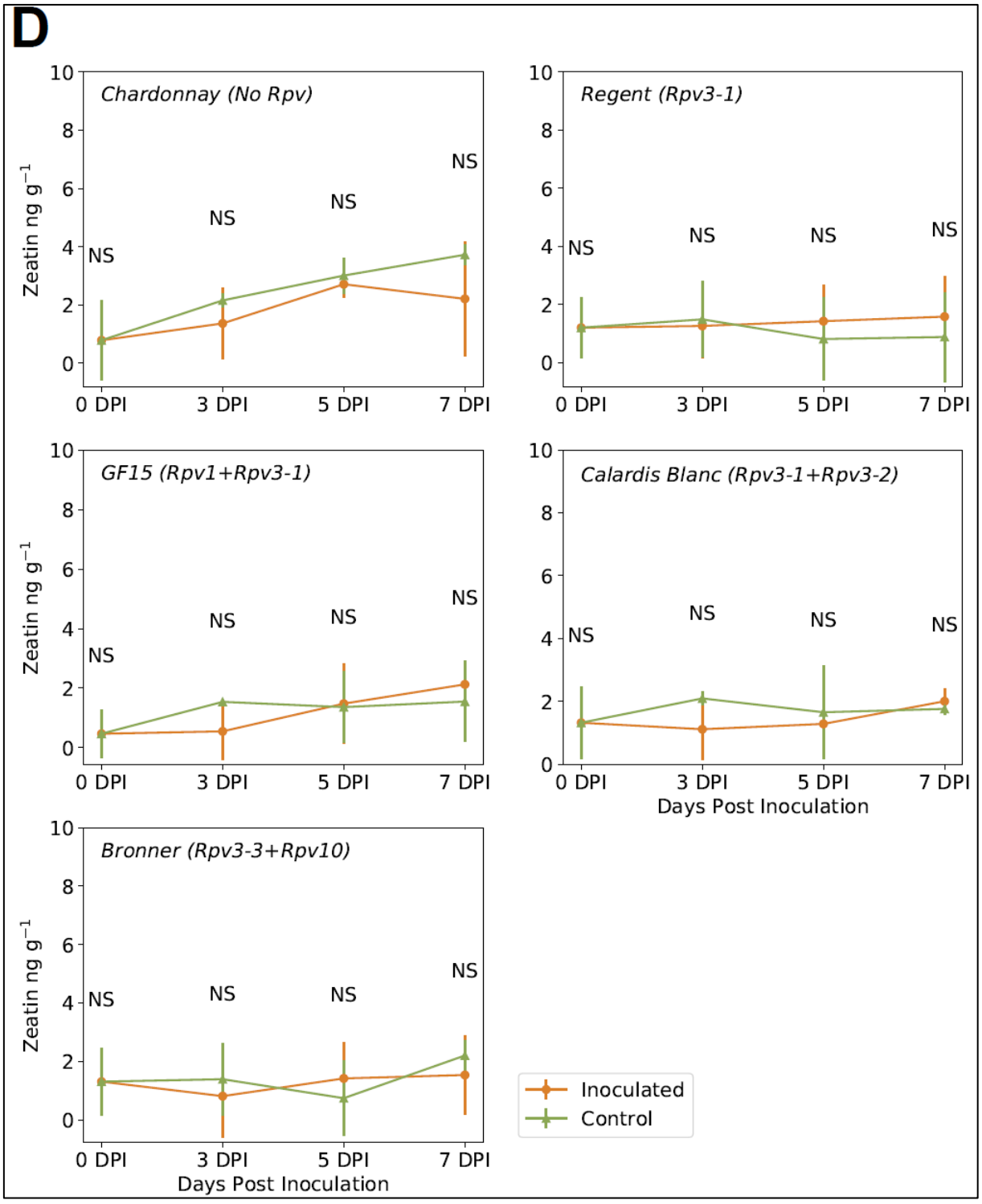
D
Chardonnay (No Rpv)
Regent (Rpv3-1)
GF15 (Rpv1+Rpv3-1)
Calardis Blanc (Rpv3-1+Rpv3-2)
Bronner (Rpv3-3+Rpv10)
Zeatin ng g^{-1}
0 DPI
3 DPI
5 DPI
7 DPI
NS
Days Post Inoculation
Inoculated
Control

Table S1. kinetic of plant hormones expression in 0, 3, 5, and 7 days post inoculation (DPI) with *Plasmopara viticola* oospore, in in vitro cultivated leaves of *V. vinifera* carrying different genetic resistance loci, Rpv3-1+Rpv3-2, Rpv3-3+Rpv10, Rpv3-1, and without genetic resistance (No Rpv). Means followed by the same capital letters in the collumns and lowercase letters in the lines, dont present statisticaly differences by tukey test (α=0.05).

	0 DPI	3 DPI	5 DPI	7 DPI
		Indole-3-acetic acid (ng g^{-1})		
Chardonnay (*rpv*)	2.68 aAB	1.41 aAB	3.74 aAB	2.01 aAB
Regent (*Rpv3-1*)	1.70 aB	0.94 aB	0.84 aB	0.00 aB
GF15 (*Rpv1+Rpv3-1*)	1.67 aA	3.79 aA	3.24 aA	6.46 aA
Calardis Blanc (*Rpv3-1+Rpv3-2*)	4.11 aA	3.70 aA	3.78 aA	3.53 aA
Bronner (*Rpv3-3+Rpv10*)	3.42 aAB	2.37 aAB	1.70 aAB	2.84 aAB
		Abscisic acid (ng g^{-1})		
Chardonnay (*rpv*)	773.12 aA	411.79 bA	321.17 bA	371.95 bA
Regent (*Rpv3-1*)	491.60 aB	360.74 aA	281.93 aA	490.26 aA
GF15 (*Rpv1+Rpv3-1*)	53.50 aC	160.82 aA	125.02 aA	290.66 aA
Calardis Blanc (*Rpv3-1+Rpv3-2*)	306.42 aB	330.38 aA	223.12 aA	297.14 aA
Bronner (*Rpv3-3+Rpv10*)	520.19 aB	296.35 abA	211.51 bA	446.75 aA
		trans-Zeatin-Ribose (ng g^{-1})		
Chardonnay (*rpv*)	2.62 aA	2.09 aA	1.73 aA	2.21 aA
Regent (*Rpv3-1*)	2.03 aA	2.20 aA	2.01 aA	1.53 aA
GF15 (*Rpv1+Rpv3-1*)	2.12 aA	2.20 aA	1.71 aA	2.32 aA
Calardis Blanc (*Rpv3-1+Rpv3-2*)	0.80 aA	1.29 aA	1.91 aA	0.62 aA
Bronner (*Rpv3-3+Rpv10*)	1.84 aA	1.95 aA	1.91 aA	1.51 aA
		Salicylic acid (ng g^{-1})		
Chardonnay (*rpv*)	412.44 aBC	340.68 aB	434.58 aB	401.31 aB
Regent (*Rpv3-1*)	621.66 aB	503.43 aB	302.49 aB	486.81 aB
GF15 (*Rpv1+Rpv3-1*)	223.21 aC	261.75 aB	247.68 aB	324.43 aB
Calardis Blanc (*Rpv3-1+Rpv3-2*)	2378.28 aA	1698.81 bA	1144.06 cA	1023.19 cA
Bronner (*Rpv3-3+Rpv10*)	467.59 aBC	310.50 aB	200.97 aB	431.76 aB
		Jasmonic acid (ng g^{-1})		
Chardonnay (*rpv*)	31.83 aA	3.31 bB	23.16 aAB	21.12 aAB
Regent (*Rpv3-1*)	6.23 aB	0.92 aB	5.88 aB	4.86 aB
GF15 (*Rpv1+Rpv3-1*)	5.56 bB	30.79 aA	35.05 aA	28.72 aA
Calardis Blanc (*Rpv3-1+Rpv3-2*)	7.90 aB	14.10 aAB	8.44 aB	8.43 aB
Bronner (*Rpv3-3+Rpv10*)	12.25 aB	1.49 aB	18.08 aAB	8.55 aB
		Zeatin (ng g^{-1})		
Chardonnay (*rpv*)	0.79 aA	1.37 aA	2.71 aA	2.21 aA
Regent (*Rpv3-1*)	1.21 aA	1.27 aA	1.43 aA	1.59 aA
GF15 (*Rpv1+Rpv3-1*)	0.47 aA	0.55 aA	1.48 aA	2.13 aA
Calardis Blanc (*Rpv3-1+Rpv3-2*)	1.32 aA	1.12 aA	1.29 aA	2.01 aA
Bronner (*Rpv3-3+Rpv10*)	1.31 aA	0.81 aA	1.42 aA	1.54 aA

4 CAPÍTULO II – GENETIC RESISTANCE AGAINST *Plasmopara viticola* PRODUCES DIFFERENTS PROTEOMICS PROFILE IN *Vitis vinifera* CELL CULTURES

Este capítulo encontra-se formatado de acordo com as normas para submissão ao periódico "Plant Science".

Genetic resistance against *Plasmopara viticola* produces different proteomics profile in *Vitis vinifera* cell cultures

4.1 ABSTRACT

One of the most important fruit crops around the world, the grapevine production is affected for several pathogens, being *P. viticola,* causal agent of downy mildew disease, the most important one. Genetic resistance against this pathogen was incorporated by breeding programs, which developed PIWI cultivars that combine high quality and disease resistance. The present work aimed at to identify proteins associated with the resistance against the *Plasmopara viticola* in genotypes *Rpv3-1* and *Rpv1+Rpv3-1*. Genotypes from grapevine breeding program of Federal University of Santa Catarina were used as explant donator to induced cell cultures. The population was genotyped in a marker-assisted selection workflow and were selected one genotype without *Rpv* loci (*rpv*), one *Rpv3-1* and another one *Rpv1+Rpv3-1*. Cell cultures were inoculated with *P. viticola* oospore and collected 24 hours post inoculation to proteomic analysis. Mass spectrophotometry was carried out and functional annotation was made using Blast2go software. The collected data pointed for 410 differently expressed proteins, highlighting to STILBENE SYNTHASE, the most upregulated protein in any treatment. The proteomic profile changed in any genotype when cell cultures were inoculated with the pathogen, however differently according the genotype host. Some proteins were unique for resistant genotypes; however, we highlight the INDOLE-3-ACETIC ACID-AMINO SYNTHETASE (GH3-1) that was up-regulated in both resistant genotypes and down-regulated in the susceptible genotype. Furthermore, the CYSTEINE-RICH REPEAT SECRETORY PROTEIN 38 (CRRSP38) is potentially related with the resistance in the pyramided genotype. To the best of our knowledge, this is the first report of proteomic data from grapevine cell cultures from pyramided *Rpv* loci.

Keywords: Downy mildew, cell cultures, embryogenic, disease resistance, vitiviniculture.

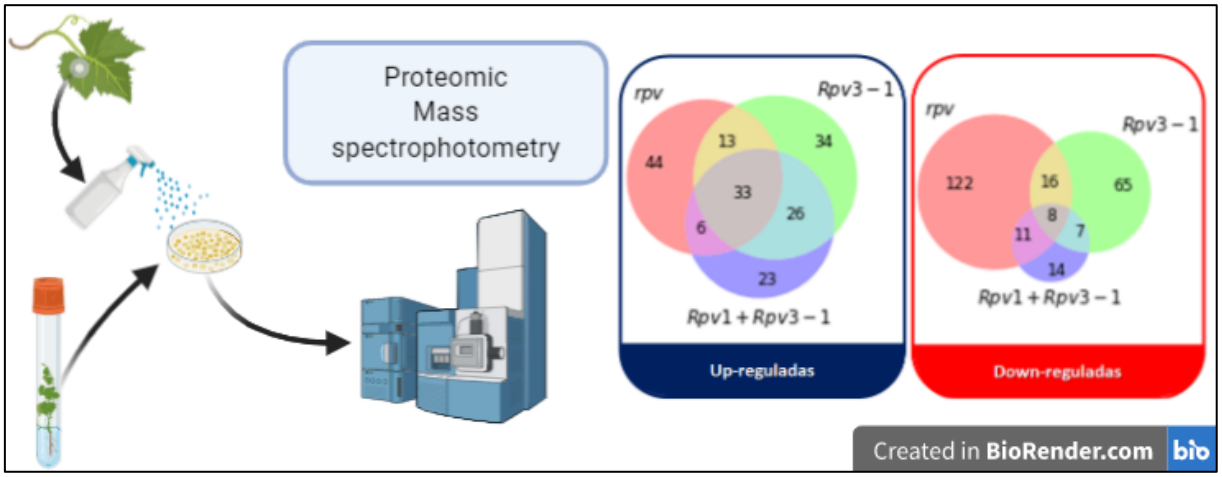

4.2 INTRODUCTION

The grapevine (*V. vinifera*) is one of the oldest and major fruit crops worldwide; however, in general this species renders high susceptibility against pathogens, and normally intensive phytochemical treatments are required (PIRRELLO et al., 2019; VALLEJO et al., 2019). In contrast, other *Vitis* species, from the American and Asiatic diversity center, have many resistances (*R*) loci against some pathogens. These *R*-loci has been intensively mapped,

by QTL analysis and introduced in the *V. vinifera* genome by breeding programs (EIBACH et al., 2006; MAUL ET AL., 2020).

This methodology was largely employed to the development of new *V. vinifera* cultivars combining high fruit quality and *R*-loci inherited from several *Vitis* species. These cultivars are named as PIWI cultivars, from the German words' initial "*pilzwiderstandsfähigen Reben*" that means grapevine resistance against fungal diseases.

One of the most important pathogens in grapevine culture is the *Plasmopara viticola*, the causal agent of downy mildew, that causes quality and quantity losses in grapevine production, with several economic damages (TAYLOR; COOK, 2018). *P. viticola* is a chromist, oomycete, and behave as a biotrophic pathogen (GRENVILLE-BRIGGS; WEST, 2005). Thus, grapevine breeders did mapping *R*-loci against the downy mildew aiming to incorporate the genetic resistance in *V. vinifera* genotypes and to develop PIWI cultivars resistant against the *P. viticola* (EIBACH et al., 2006; RUEHL et al., 2015; TÖPFER et al., 2011). This *R-loci* were named as *Rpv* followed by the number of the mapped loci, cataloged in the VIVC data bank (https://www.vivic.de) (MAUL ET AL., 2020); until now 31 *Rpv*s were published and only *Rpv29*, *Rpv30* and *Rpv31* were mapped as a partial resistance from *V. vinifera* (SARGOLZAEI et al., 2020).

Due the importance of the downy mildew in the grapevine culture, several researches were developed in order to characterized the proteomic profile of the plant pathogen interaction with susceptible and resistance genotypes (FIGUEIREDO et al., 2017; LEMAÎTRE-GUILLIER et al., 2017; MILLI et al., 2012; NASCIMENTO-GAVIOLI et al., 2017; PALMIERI et al., 2012; ROSSIN et al., 2015). However, there is no research data reported exclusively for the cellular response.

To consider the cell response, it is necessary to employ cell culture. Moreover, it is important to developed studies involving pyramid genotypes, to better understand the behavior of the resistance in these genotypes. In the present work the overall aim was to identify proteins that might be associated with the cell resistance against the *Plasmopara viticola* in genotypes carrying no *Rpv* (*rpv*), *Rpv3-1*, and *Rpv1+Rpv3-1*.

4.3 MATERIAL AND METHODS

4.3.1 Plant material

Three full-sibs of *V. vinifera* were selected from a grapevine breeding population, obtained from the self-pollination of a heterozygous breeding line for *Rpv1+Rpv3-1*. The individuals were selected by Marker Assisted Selection (MAS) (SÁNCHEZ-MORA et al.,

2017) and one haplotype without *Rpv* (*rpv*), one with *Rpv3-1* and the third one with *Rpv1+Rpv3-1* were selected to this work.

The plants were growth in greenhouse conditions and nodal segments were used to regenerate *in vitro* plants using test tubes with 50 mL DSD1 culture medium (SILVA; DOAZAN, 1995), supplemented with 20 g L^{-1} sucrose and 2 g L^{-1} phytagel®. The pH of the culture medium was adjusted to 6.4 before phytagel was added. The cultures were maintained in controlled environment with 16 h photoperiod and 22 to 25 °C. Young leaves from these *in vitro* plants were used to cell line induction.

4.3.2 Induction and proliferation of cell cultures

The protocol to obtain cell cultures from *V. vinifera* cultivars followed the methodologies described by Das et al. (2002) and Gray and Mortensen (1987). In brief, young leaves (3rd to 5th) from plants grown *in vitro* were used as explant to obtain cell cultures. These leaves were sectioned into four parts and added in the Petri dishes (90 x 15 mm) containing 25 mL of the culture medium. The saline solution of the culture medium was based on the formulation DSD1 (SILVA; DOAZAN, 1995), supplemented 20 g L^{-1} sucrose, BAP [1 µM], 2,4-D [2,5 µM] and 2 g L^{-1} Phytagel, the pH was adjusted to 6.4 before Phytagel was added. The explants were maintained for 60 days in controlled environment conditions with no light source and at a 25 °C.

4.3.3 Plant cell cultures

After the cell culture establishment, the cultures were transferred to a new Petri dish containing 25 mL of the multiplication culture medium, composed by basal saline solution DSD1 (SILVA; DOAZAN, 1995), supplemented with 20 g L^{-1} sucrose, BAP [1 µM], 2,4-D [1.5 µM] and 2 g L^{-1} Phytagel. The cultures were maintained in the same environmental conditions as before until the cell mass was approximately twice the initial aliquot.

At this stage, cell cultures were split in different Petri dishes, cultivated in the same condition as before and histomorphologically evaluated by means double staining with acetocarmin (embryogenic cells stain in red), and Evans blue (tubular cells stain in blue).

4.3.4 *P. viticola* inoculation

The *P. viticola* was cultivated on leaves of cv. ‘Chardonnay’ kept *in vitro* and the sporulation was collected in sterile distilled water (SDW), then the solution was adjusted to 10^5 sporangia mL^{-1} and used to inoculation. The cell cultures used for this challenge were kept in Petri dishes contain the multiplication culture medium as described before. In the control treatment it was applied 100 µL SDW by Petri dish and in the inoculated treatment was applied 100 µL of the inoculum solution in each Petri dish. It was used five Petri dishes for each

genotype. In 24 hours post-inoculation (HPI) the cell cultures from three random dishes were lyophilized under frozen conditions, kept at -80 °C until proteomic analysis was carried out in the Biotechnology Lab of the Universidade Estadual do Norte Fluminense.

4.3.5 Protein extraction

Samples of cell cultures were prepared in biological triplicates (500 mg of lyophilized material). The proteins were extracted using the TCA/acetone precipitation method (DAMERVAL et al., 1986). The samples were macerated with liquid nitrogen with the aid of a mortar and a pistil. The samples were resuspended in 1 mL of chilled extraction buffer containing 10% (w/v) trichloroacetic acid (TCA; SigmaChemical Co., St. Louis, MO) in acetone with 20 mM dithiothreitol (DTT; GE Healthcare) vortexed for 30 min at 8 °C and left at -20 °C for 1 h for protein precipitation. The mixture was centrifuged at 16,000g for 30 min at 4 °C. The resulting pellets were washed three times with cold acetone plus 20 mM DTT, vortexed for 30 s and centrifuged for 5 min at 4 ºC, for each wash. The samples were air dried, resuspended in 1 mL of buffer containing 7 M urea (GE Healthcare, Little Chalfont, UK), 2 M thiourea (GE Healthcare), 2% Triton X-100 (GE Healthcare), 1% DTT, 1 mM phenylmethylsulfonyl fluoride (PMSF; Sigma-Aldrich) and complete protease inhibitor cocktail (Roche Diagnostics, Mannheim, Germany) and incubated for 30 min on ice. The samples were then vortexed at 8 °C for 30 min and centrifuged at 16,000g for 20 min at 4 °C. The supernatants were collected, and the protein concentrations were determined using the 2-D Quant kit (GE Healthcare, Piscataway, NJ, USA).

4.3.6 Protein digestion

For the protein digestion, 100 µg of extracted proteins from each biological replicate were precipitated using the methanol/chloroform method to remove any interference from the samples before digestion with trypsin (NANJO et al., 2012). After the protein precipitation, the samples were resuspended in a 7 M urea/2 M thiourea solution for proper suspension. Tryptic protein digestion (1:100 enzyme:protein, V5111, Promega, Madison, USA) was performed using the filter-aid sample preparation (FASP) (WIŚNIEWSKI et al., 2009), with modifications. (BURRIEZA et al., 2019). Before starting digestion, an integrity test was carried out to check for damaged filter units (HERNANDEZ-VALLADARES et al., 2016), so only the working units were used. After that, protein aliquots were added to the Microcon-30 kDa filter units Merck Millipore (Darmstadt, HE, Germany) (LIPECKA et al., 2016), washed with 200 µl of 50 mM ammonium bicarbonate (Sigma-Aldrich) (solution A) and centrifuged at 12,000g for 15 min at 25 °C (unless stated otherwise, all centrifugation steps were performed under this condition). This step was repeated once for complete removal of urea before protein reduction.

Afterwards, 100 µL of 50 mM DTT, freshly made in solution A, was added, vortexed and incubated for 20 min at 60 °C (1 min agitation and 4 min resting, at 47g). Then 200 µl of 8 M urea in 50 mM ammonium bicarbonate (solution B) was added, and centrifuged for 15 min. For protein alkylation, 100 µL of 50 mM iodoacetamide (GE Healthcare) freshly prepared in solution B, was added, gently vortexed and incubated for 20 min at 25 °C in the absence of light (1 min agitation and 19 min resting, at 47g). Next, 200 µl of solution B was added and centrifuged for 15 min. This step was repeated once. Then, 200 µl of solution A was added and centrifuged for 15 min. This step was repeated twice. Approximately 50 µl of the sample should remain in the last washing. For protein digestion, 20 µl of 0.2% (v/v) RapiGest (Waters, Milford, CT, USA) and 25 µl of trypsin solution (enzyme 1:100: protein), V511, were added, gently vortexed and incubated for 18 h at 37 °C (1 min agitation and 4 min resting at 47g). For peptide elution, the filter units were transferred to new microtubes and centrifuged for 10 min, then 50 µl of solution A was added and centrifuged for 15 min. This step was repeated once. For RapiGest precipitation and trypsin inhibition, 5 µl of 15% TFA was added, gently vortexed and incubated for 30 min at 37 °C. Then, samples were centrifuged for 15 min and the supernatants were collected and vacuum dried. The peptides were resuspended in 50 µl of a solution of 95% water, 5% acetonitrile and 0.1% formic acid (Sigma-Aldrich). The resulting peptides were quantified by the $A_{205\ nm}$ protein and peptide method, using a NanoDrop 2000C spectrophotometer (Thermo Fisher Scientific, MA, USA).

4.3.7 Mass spectrometry analysis

A nanoAcquity UPLC coupled to a Synapt G2-Si HDMS mass spectrometer (Waters, Manchester, United Kingdom) was used for ESI-LC-MS/MS. The runs consisted of three biological replicates of 1 µg of digested proteins. During separation, samples were loaded onto the nanoAcquity UPLC 5 µm C18 trap column (180 µm x 20 mm) at 5 µl/min for 3 min and then onto the nanoAcquity HSS T31 1.8 µm analytical reversed phase column (75 µm x 150 mm) at 400 nL min^{-1}, with a column temperature of 45 ºC. For peptide elution, a binary gradient was used, with the mobile phase A (water and 0.1% formic acid) and the mobile phase B (acetonitrile and 0.1% formic acid). The gradient elution started at 7% B, then ramped from 7% B to 40% B until 92.72 min, then remained at 99.9% until to 106.00 min, then decreased to 7% B until 106.1 min, and finally remained at 7% B until the end of the experiment at 120 min. Mass spectrometry was performed in positive and resolution mode (V mode), 35,000 FWHM, with ion mobility and independent-data acquisition mode (HDMSE). The ion mobility wave was adjusted to a velocity of 600 m s^{-1}; the transfer collision energy ramped from 19 V to 55 V in high-energy mode; the cone and capillary voltages were 30 V and 2750 V, respectively; and

the source temperature was 70 °C. In TOF parameters, the scan time was set to 0.5 s in continuum mode with a mass range from 50 to 2000 Da. The human [Glu1]-fibrinopeptide B (Sigma-Aldrich) at 100 fmol l^{-1} was used as an external calibrant and lock mass acquisition was performed every 30 s. Mass spectra were acquired by MassLynx v4.0 software.

4.3.8 Proteomic data analysis

For spectral processing and database searching, the ProteinLynx Global Server (PLGS; version 3.0.2) (Waters, USA) and the ISSOQuant workflow software (DISTLER et al., 2014, 2016) were used. The PLGS was processed using a low-energy threshold of 150 (counts), an elevated-energy threshold of 50 and an intensity threshold of 750. In addition, the analysis was performed using the following parameters: two missed cleavages, a minimum fragment ion per peptide equal to 3, a minimum fragment ion per protein equal to 7, a minimum peptide per protein equal to 2, fixed modifications of carbamidomethyl and variable modifications of oxidation and phosphoryl. The false discovery rate was set to a maximum of 1%. The proteomics data were processed against the grapevine protein database from Uniprot (https://www.uniprot.org/proteomes/UP000009183).

The comparative label-free quantification analysis was performed using the ISOQuant software, by using previously described settings and algorithms (DISTLER et al., 2014, 2016). Briefly, the analysis included retention time alignment, exact mass retention time and ion mobility spectrometry clustering as well as data normalization and protein homology filtering. ISOQuant annotates the resulting feature clusters by evaluating consensus peptide identifications and identification probabilities. Protein identification parameters in ISOQuant were set to a false discovery rate of 1%, a peptide score greater than six, a minimum peptide length of six amino acids, and at least two peptides per protein. Label-free quantification was estimated using the TOP3 quantification approach, followed by the multidimensional normalization process implemented within ISOQuant (DISTLER et al., 2014).

After ISOQuant analysis, only the proteins that were either present or absent (for unique proteins) in all three biological replicates of each inoculated/control comparison were considered for differential abundance analysis. Data were analyzed using Student's t-test (two-tailed). Proteins with p-values lower than 0.05 were considered up-regulated if the log2 of fold change was greater than 0.5 and down-regulated if the log2 of the fold change was lower than -0.05. Finally, for functional annotation, the differentially regulated proteins were blasted against the non-redundant (nr) plants/viridiplantae_protein_sequences database by using the OmicsBox software (Blast2Go).

To identify the functionally grouped network associated to the differentially regulated proteins, the enrichment analysis was carried out using ClueGO plugin into Cytoscape software. The gene IDs referring to the regulated proteins in each genotype were used as reference set entry for the enrichment analysis. The hypergeometric test with Binjamini-Hochberg correction was used to assess enrichment categories in the Gene Ontology (GO) domains 'Biological process'. In the resultant graph, the functional grouping was evaluated with the %Genes/Term using the kappa statistic. Pairs of terms (nodes) with a kappa value of at least 0.5 related to edges in the network. The STRING actions (activation, inhibition, expression, and post-translational modification) scores were used to connect nodes (proteins) in the network.

4.3.9 Statistical analysis

The experiment testing the effect of the *P. viticola* in the cell cultures of three genotypes, was completely randomized factorial design with three biological replicates represented by three Petri dishes and three colonies of 200 mg fresh matter per Petri dish for each genotype. The resulting data were submitted to analysis of variance (ANOVA), and the means were compared using the t-test (Significant level, $P<0.01$) using the statistical software R (R CORE TEAM, 2019). Additionally, we constructed a principal component analysis (PCA) with no redundant data, proteins pairwise comparation were carried out. Pairs with Pearson correlation higher than |0.80| only one of both proteins was maintained. These analyses were carried using Python 3 (https://www.python.org/).

4.4 RESULTS

4.4.1 Comparative proteomics analysis

The comparative proteomic analysis identified 1084 proteins, among these, 410 were differently expressed with the *P. viticola* inoculation in at least one genotype (Table S1). In the pyramided genotype, 128 proteins were differently expressed with the inoculation. In *Rpv3-1* genotype, 202 proteins were differently expressed after inoculation and 253 proteins in the susceptible genotype. In pyramided genotype, 18 proteins were unique and 70 up-regulated after inoculation. For the *Rpv3-1* genotype, 27 proteins were unique and 79 up-regulated with inoculation. Although the larger number of differently expressed protein in the susceptible genotype, only 24 of these were identified as unique and 72 up-regulated with the pathogen inoculation.

A range of 33 and 8 proteins were up- or down-regulated for all three genotypes, respectively. In addition, 83 proteins were up-regulated exclusively in the resistance genotypes. Out of them, 26 proteins were up-regulated in both *Rpv3-1* and *Rpv1+Rpv3-1*. In the susceptible genotype, we found 122 proteins exclusively downregulated, in contrast, 86 proteins were

down-regulated exclusively to resistance genotypes. Moreover, the pyramided genotype was the only one that present more up-regulated than down-regulated protein (Figure 1).

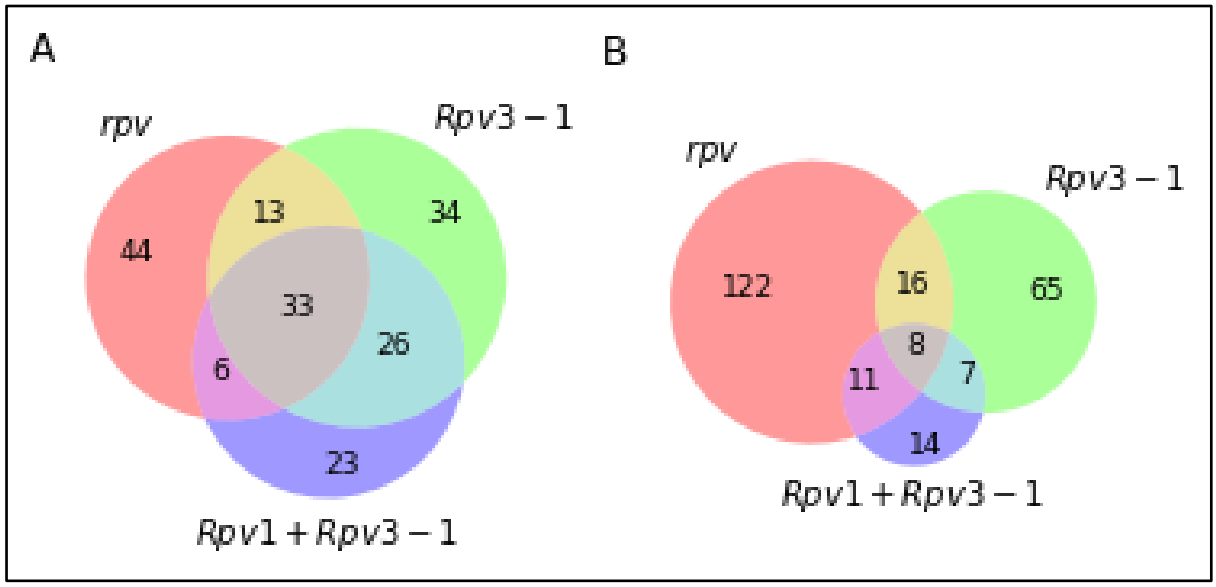

Figure 1. Venn diagram showing differentially expressed proteins in cell cultures from *Vitis vinifera* genotypes with different resistance loci against *Plasmopara viticola* (*Rpv*), among these, no resistance (*rpv*), *Rpv3-1* and *Rpv1+Rpv3-1*. A) number of up-regulated proteins; B) number of down-regulated proteins.

We found 140 proteins without Pearson correlation higher than |0.8|, thus, these proteins were used to make the PCA, that represented 32.3% from total variation from the two firsts components (PC1 and PC2). All genotypes present higher PC2 values in inoculated conditions, mainly the susceptible, that have highest PC2 values. In contrast, the pyramided genotype present negative PC2 values in both treatments. Resistant genotypes presented lower PC1 values when inoculated. In the other hand, higher PC1 values were reported from the susceptible genotype in the same condition (Figure 2).

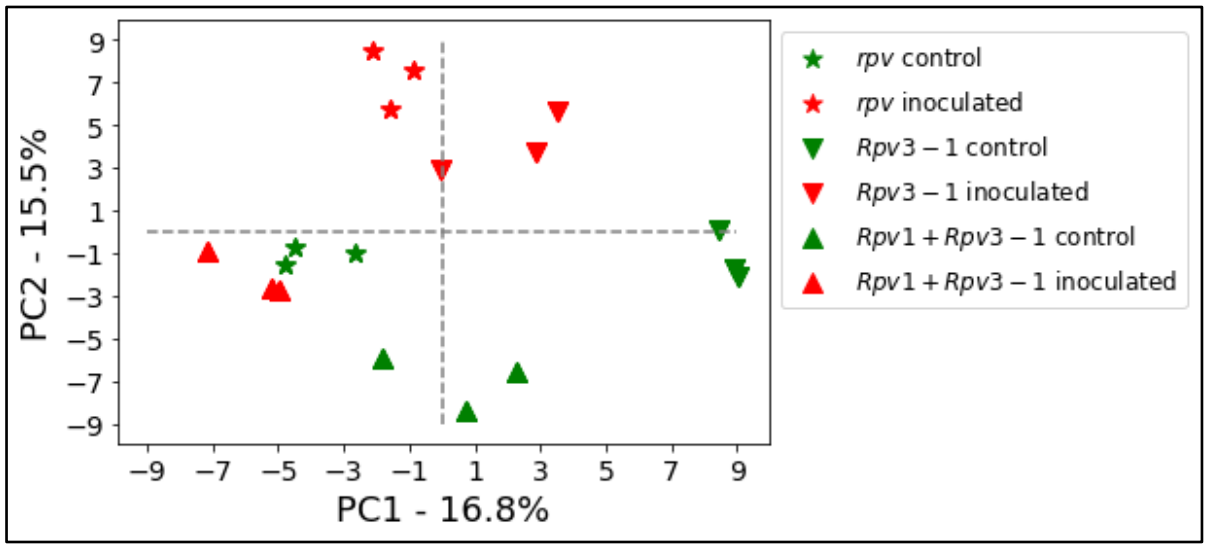

Figure 2. Principal component analysis with the two most representative dimension (PC1 and PC2) explained 70.5% of the total variation from the expression data of 1084 proteins expressed in cell cultures from *Vitis vinifera* genotypes with different resistance loci against *Plasmopara viticola* (*Rpv*), no resistance (*rpv*), *Rpv3-1* and *Rpv1+Rpv3-1* genotypes, with (red) and without (green) pathogen inoculation.

4.4.2 Genotype specific proteomic profile with P. viticola inoculation

In the inoculated pyramided genotype, three proteins were exclusively identified and do not found in *Rpv3-1* or *rpv* genotypes, including the Putative laccase-9 (A5AUN7); Phenylalanine ammonia-lyase-like (PAL-like) (D7TCJ8) and Laccase-15-like (F6I290) isoforms. For the up-regulated proteins, were identified 19 proteins in this genotype and unchanged in the others genotypes after inoculation, such as three isoforms of Beta-xylosidase/alpha-L-arabinofuranosidase 2 (F6I6S2; D7U8Q0 and F6I6R4) (Xy12) and three isoforms of ATP synthase (D7T300; D7UA89 and A5AY42).

Additionally, we highlight the identification of the proteins Cysteine-rich repeat secretory protein 38 (F6HIL6) (CRRSP38), Acidic endochitinase (F6H6H8), lignin-forming anionic peroxidase (D7TAI3), DNA damage-repair/toleration protein DRT100 (F6HBA8), UDP-glucuronic acid decarboxylase 6 (A5BIN1) and Ketose-bisphosphate aldolase class-ii family protein isoform 1 (F6GSN7) which was up-regulated in pyramided genotype and unchanged in the others genotypes, indicating an important role of these proteins for pyramided resistance, being a potential resistance related protein in this genotype.

Moreover, we found nine proteins abundant up-regulated, at least tenfold increase with the inoculation, in the pyramided genotype. Two isoform of phenylalanine ammonia-lyase (513.0 and 205.6-fold), two isoform of stilbene synthase (STS), one unique to this genotype (34.1-fold) and other expressed in all genotypes (24.9-fold), putative laccase-9 (33.7-fold), lignin-forming anionic peroxidase (27.2-fold), laccase-15-like (11.6-fold), trans-cinnamate 4-monooxygenase (11.5-fold), and bifunctional nitrilase/nitrile hydratase nit4b (11.2-fold).

In the genotype *Rpv3-1* fewer proteins were identified (1046). However, more proteins were differently expressed (202) and ten proteins were exclusively expressed in the *Rpv3-1* genotype. Among these, ras-related protein raba4d and inositol oxygenase 2-like were unique to inoculated treatment, while levodione reductase was, up-regulated with the *P. viticola* inoculation. Furthermore, α-dioxygenase 1-like was up-regulated for *Rpv3-1* genotype and unique in the inoculated pyramided genotype. In the other hand, tubulin β-1 chain was suppressed with the *P. viticola* inoculation, down-regulated in *Rpv3-1* and unique to the control in the pyramided genotype.

Considering the most abundant up-regulated proteins, at least tenfold changed, eight proteins were reported to *Rpv3-1*, the highest changed was reported in the putative lactase-9 (44.2-fold) and in the STS (29.5-fold). Beside these, three isoform of major allergen Pru av1, endochitinase ep3, lignin-forming anionic peroxidase, and stem-specific protein tsjt1-like. The *Rpv3-1* was the only genotype with highest down-regulated proteins (at least tenfold lower expression), these were two isoform of heat schock protein 83 (34.7 and 7.6-fold).

Additionally, we found 72 proteins exclusively from resistant genotypes (*Rpv3-1* and *Rpv1+Rpv3-1*), among these, arogenate dehydratase/prephenate dehydratase 6, chloroplastic-like; endochitinase ep3; patatin-like protein 2; stilbene synthase 4 and laccase-15-like were expressed only in *P. viticola* inoculated treatment, and lignin-forming anionic peroxidase, pectinesterase 2, osmotin-like protein; 3-dehydroquinate synthase, chloroplastic were up-regulated with the inoculation. These results pointed to the possible relation between these proteins and the resistance conferred by *Rpv3-1* haplotype.

In addition, two isoforms of the protein indole-3-acetic acid-amino synthetase (GH3-1) (F6HSW and F6H697) were identified up-regulated in both resistant genotypes and down-regulated or unchanged in the susceptible genotype. This data point to this protein can be a key in the resistant response.

The susceptible genotype presented the fewer number of proteins (990), however, the largest number of differently expressed proteins (253). Addicting, only eight proteins were exclusively expressed in this genotype, among these, udp-glycosyltransferase 74e2-like (UGT74E2-LIKE) and udp-glycosyltransferase 43-like (UGT43-LIKE) were down-regulated and β-glucosidase 40 (BG40) was completely suppressed with the *P. viticola* inoculation, the others were unchanged. Five proteins were abundant up-regulated (at least tenfold increase) in the susceptible genotype, stilbene synthase (STS); three major allergen pru av 1 and endochitinase ep3 that was 26.8, 20.0, 13.5, 11.3, 11.4-fold change respectively, with the *P. viticola* inoculation.

4.4.3 Ontological Enrichment Analysis

To determine the biological pathways associated with the differentially regulated proteins, we performed the enrichment analysis in the GO biological process. This analysis allowed the identification of five enriched biological processes considering the regulated proteins of pyramided genotype, 16 for *Rpv3-1* and 21 for susceptible genotype.

Among the metabolic pathway changed by the *P. viticola* inoculation, in the pyramided genotype, the regulation of protein serine/threonine phosphatase activity and cinnamic acid biosynthetic process presented 43.9 and 37.9% of the total variation, respectively. Others three

metabolic pathway were affected in this genotype: chorismate biosynthetic process (9.1%), phenylpropanoid metabolic process (7.6%), and aminoglycan metabolic process (1.5%) (Figure 3A).

In the *Rpv3-1* L-phenylalanine metabolic process was the most affected biological process, with 19.6% of the total protein changed. regulation of protein serine/threonine phosphatase activity (15.5%), chorismate biosynthetic process (14.2%) and hydrogen peroxide catabolic (13.5%) were also hardly affected. Beside these, others 12 biological processes presented 37.2% of the total alteration from this genotype (Figure 3B).

In the susceptible genotype the cinnamic acid biosynthetic process and the regulation of protein serine/threonine phosphatase activity were the main biological process affected with the inoculation, presenting 21,7 and 19.9% of the total variation, respectively. Beside these, approximately 30% of the variation was due the biological processes like as the regulation of cellular pH (8.7%), hydrogen peroxide catabolic (8.1%), aminoglycan catabolic and chorismate biosynthetic process 6.8% each one. The others 28% of the variation was due translation initiation complex (5.0%), detoxification (4.4%), pectinesterase inhibitor activity (3.1%), oxidoreductase activity acting on single donors with incorporation of molecular oxygen, ‘de novo’ posttranslational protein folding and water transmembrane transporter activity with 2.5% each one, monosaccharide metabolic process, oxidoreductase activity acting on NAD(P)H quinone or similar compound as acceptor, glutathione metabolic process and defense response to fungus with 1.2% each one and response to nitrogen compound, proteasome-mediated ubiquitin-dependent protein catabolic process, structural constituent of cytoskeleton, nucleoside diphosphate metabolic process and glutamine family amino acid metabolic process responsible for 0.6% of the total variation, each one (Figure 3C).

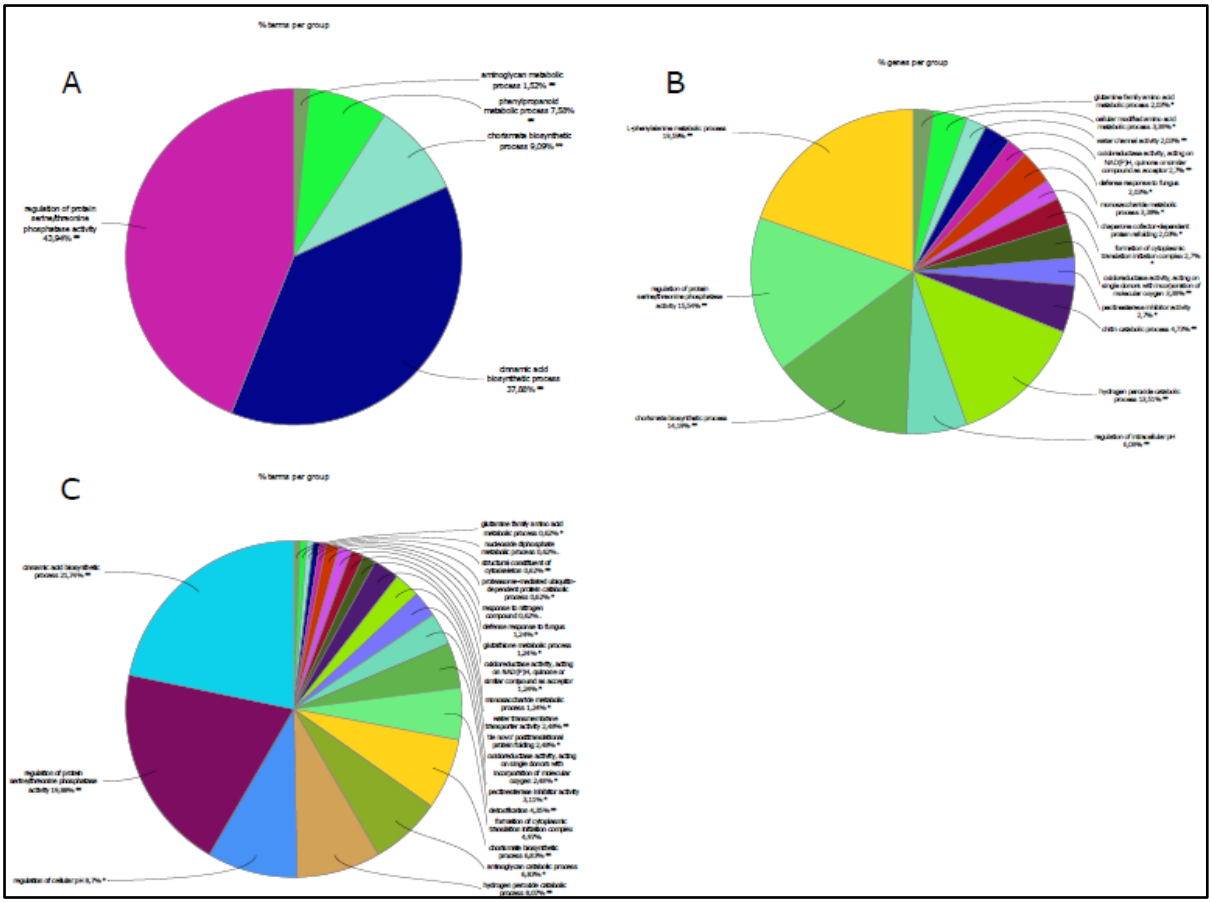

Figure 3. Biological processes affected by *Plasmopara viticola* inoculation in *Vitis vinifera* cell cultures for three genotypes with different genetic resistance loci, A) *Rpv1+Rpv3-1*, B) *Rpv3-1* e; C) *rpv*. The values in percentage represent the partition of the total variance of the metabolic pathway up- or down-regulated due the *P. viticola*; *represent that the alteration was significant at least 5% (α=0.05) and **represent that the alteration was significant at least 1% (α=0.01).

4.4.4 Biological processes network interactions

The network of biological processes up-regulated in the pyramided genotype pointed to five networks, four of them interconnected. The arabinan metabolic process was the unique biological processes network not connected with the other networks. While the cinnamic acid biosynthetic process network was the unique connected with all others network and the unique connected with the chorismate biosynthetic process. The linked between the networks cinnamic acid biosynthetic process, regulation of protein serine/threonine phosphatase activity and hydrogen peroxide catabolic process was only due the protein VIT_04s0044g01130 (Figure 4).

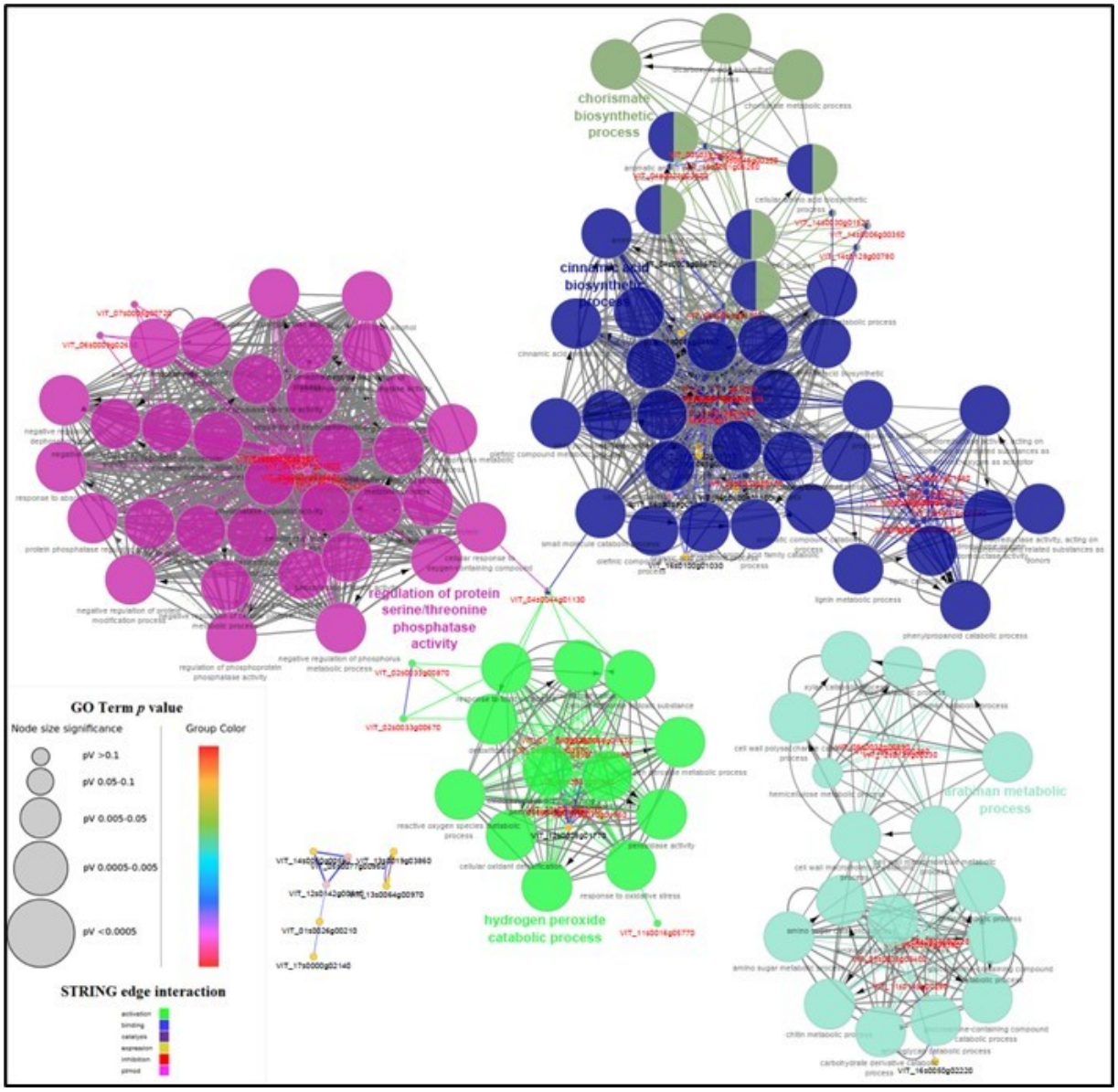

Figure 4. Networks of processes up-regulated or unique for inoculated treatment, in *Vitis vinifera* cell cultures carrying the genotype *Rpv1+Rpv3-1* after 24 hours post inoculation with *Plasmopara viticola*. Each circle represents one bioprocess, and the connection lines represent the linked of them. The color of each circle represents the pathway associated with the bioprocess and the size of the circle represent the statistical significance of the expression.

In the *Rpv3-1*, the interaction networks were more complex, involving nine up-regulated or unique to *P. viticola* inoculation networks. The networks chorismate biosynthetic process, hydrogen peroxidase catabolic process and oxidoreductase activity, acting on single donors with incorporation of molecular oxygen were only connected with a network linked with bioprocesses involving the secondary metabolism. Beside these, the network involving the regulation of protein serine/threonine phosphatase activity other involving pectinesterase inhibitor activity were interconnected. The other networks were unconnected, there are,

aminoglycan catabolic process, nucleoside diphosphatase metabolic process and glutathione metabolic process (Figure 5).

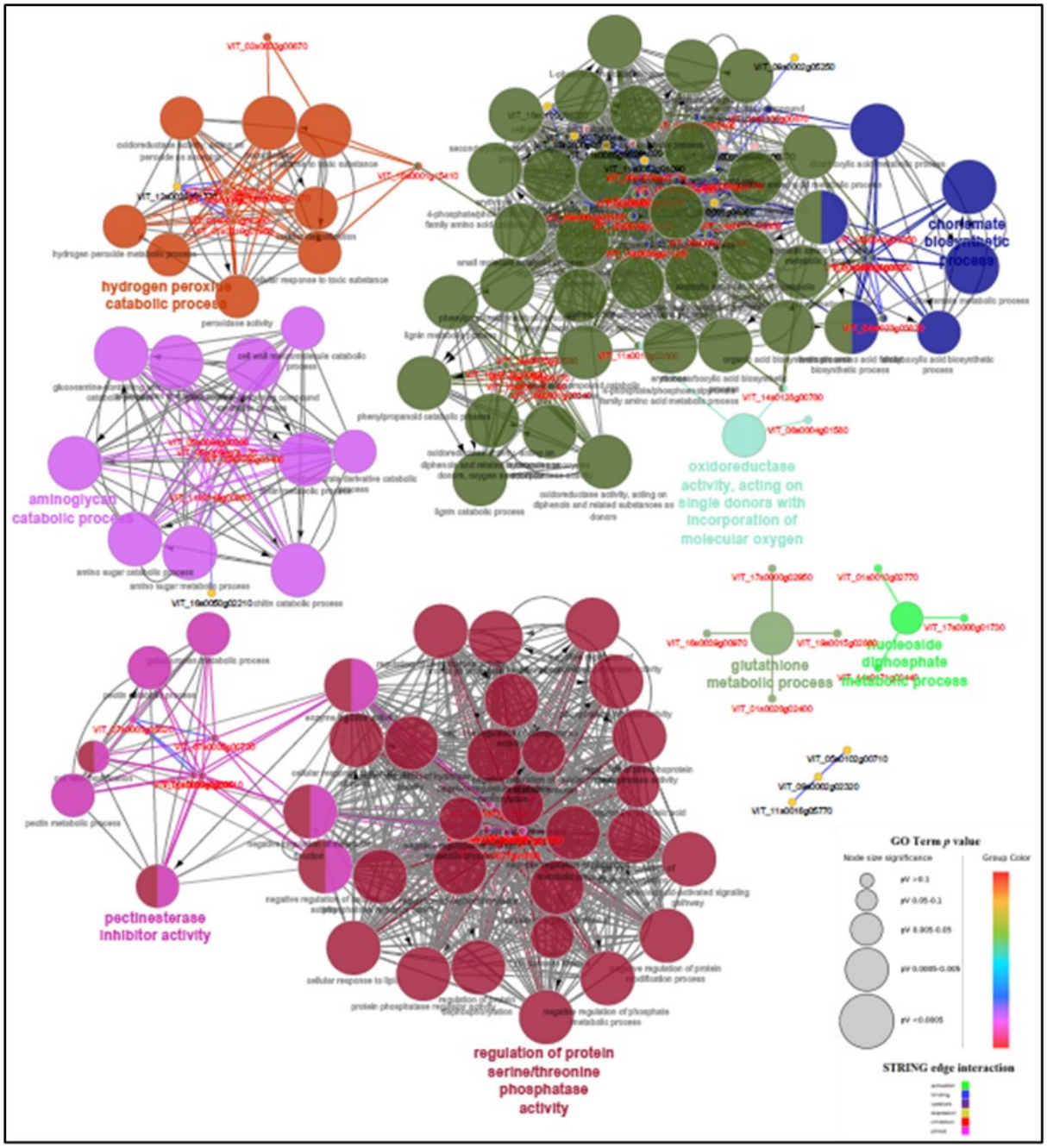

Figure 5. Networks of processes up-regulated or unique for inoculated treatment, in *Vitis vinifera* cell cultures carrying the genotype *Rpv3-1* after 24 hours post inoculation with *Plasmopara viticola*. Each circle represents one bioprocess, and the connection lines represent the linked of them. The color of each circle represents the pathway associated with the bioprocess and the size of the circle represent the statistical significance of the expression.

Unlike the resistance genotypes, the networks to the susceptible genotype, presented fewer interaction. In this genotype we found five networks of biological processes up-regulated or unique to the inoculated treatment. The regulation of protein serine/threonine phosphatase

activity was the network with more significative up-regulated bioprocess. The aminoglycan metabolic process, chorismate biosynthetic process, and phenylpropanoid metabolic process were only connected with the cinnamic acid biosynthetic process (Figure 6).

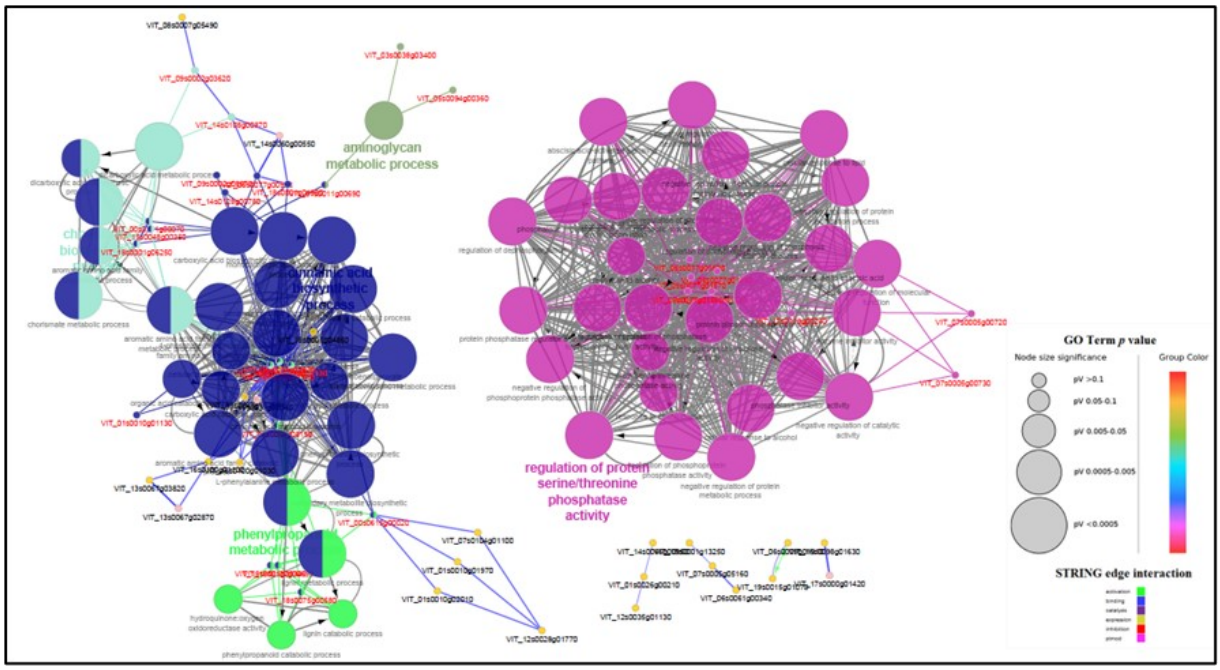

Figure 6. Networks of processes up-regulated or unique for inoculated treatment, in *Vitis vinifera* cell cultures that no carried genetic resistance after 24 hours post inoculation with *Plasmopara viticola*. Each circle represents one bioprocess, and the connection lines represent the linked of them. The color of each circle represents the pathway associated with the bioprocess and the size of the circle represent the statistical significance of the expression.

4.4.5 Down-regulated biological processes

The resistant genotypes presented also fewer biological processes down-regulated in comparison to susceptible genotype. Four unconnected interactions networks were obtained with down-regulated processes to resistant genotypes, these networks involved processes such as the formation of cytoplasmatic translation initiation complex, structural constituent of cytoskeleton, pyrophosphate hydrolysis-driven proton transmembrane transporter activity, cellular response to oxidase stress, and lignin biosynthetic process (Figure S1).

In contrast, to the susceptible genotype it was obtained four connected networks of down-regulated process. This result point to a much more complex interaction, the major biological process down-regulated were oxidoreductase activity, acting on the aldehyde or oxo group of donors, NAD or NADP as acceptor, energy derivation by oxidation of organic compounds, proteasome-mediated ubiquitin-dependent protein catabolic and the purine

ribonucleotide biosynthetic process. This last one responsible by the integration of all networks down-regulated in the compatible interaction plant pathogen (Figure S1).

4.5 DISCUSSION

4.5.1 Pattern Response

In all genotypes 33 proteins were commonly up-regulated proteins; these proteins probably are linked to the innate immune system of the cell (MACHO; ZIPFEL, 2014). The main changed protein in all genotypes was the STILBENE SYNTHASE. This protein is responsible for the host and nonhost defense response (YU et al., 2005). The overexpression of the STILBENE SYNTHASE lead to increase of the resveratrol levels in the cells (HE et al., 2018b) and the resistance against several pathogens (CLUZET; MÉRILLON; RAMAWAT, 2020; YU et al., 2019). In addition, five BET V 1 DOMAIN-CONTAINING proteins were also up-regulated in all evaluated genotypes. These proteins plays one essential role in the cell defense pathway and in the programmed cell death due biological stress (CHATTERJEE; CHAKRABORTY; DAS, 2019; KHAFIF et al., 2017). These results pointed to a baseline of the plant pathogen interaction, the stilbene production and the programmed cell death. Although activated in all cell cultures, BET V 1 DOMAIN-CONTAINING proteins were activated more intensity in the resistant genotypes.

4.5.2 *Rpv1+Rpv3-1* related resistance proteins

The proteins PUTATIVE LACCASE-9; PAL-like and LACCASE-15-LIKE were unique for the *Rpv1+Rpv3-1* genotype and expressed only with the *P. viticola* inoculation. The overexpression of PUTATIVE LACCASES was also reported in yeast elicited *Medicago truncatula* cell suspensions and was related with the polymerization of phenolics (LEI et al., 2010). Some PUTATIVE LACCASES proteins, synthetized by fungus, are reported as a lignin degradation (KIM et al., 2018), in the other hand, plants LACCASES are reported as act in the lignin synthesis (GAVNHOLT; LARSEN, 2002; HOFFMANN et al., 2020).

The diverse plant LACCASES perform different and no redundant functions (CAI et al., 2006). The LACCASE-15-LIKE are related with the oxidative polymerization of flavonoids, particularly proanthocyanidins (CAI et al., 2006; POURCEL et al., 2005). Proanthocyanidins are commonly found in the grape seeds, can be monomeric or from polymers and have an important role in the plant defense associated with the pathogenesis-related genes (FENG et al., 2020; RAUF et al., 2019; UNUSAN, 2020).

Such as LACCASES enzymes PAL is also related with the lignin synthesis, involved in the phenylpropanoid metabolic pathway (DOUGLAS, 1996; SUN et al., 2020) and

associated with the russet color in the grape (XU et al., 2019b). Furthermore, PAL is related with the salicylic acid pathway, converting phenylalanine to trans-cinnamic acid (GUAN et al., 2019) and in the synthesis of anthocyanins (Zhang et al. 2019). Functionally, PAL is related with the plant resistance against pathogens (XUE et al., 2019), and promoting the early flowering (Zhang et al. 2020), among other activities related to the secondary metabolism (XU et al., 2019b). In *V. vinifera* *Vv*PAL-like contains the W-box domain promoter and was characterized as an enzyme responsive to salicylic and jasmonic acid, acting in the wounding/pathogen response (JIU et al., 2016).

The expression of CRRSP38 in the resistance genotypes, as well as up-regulated in the pyramidated genotype, showed that this protein is related to the defense pathway in this genotype. The CRRSP is a secretory protein that acts in the apoplast and is related with pathogen recognition (CHEN et al., 2018). Moreover, the CRRSP expression is regulated by the *WRKY* transcription factor, that plays a crucial role in inducible resistance (RAINERI et al., 2015; SHIMONO et al., 2007). These results suggesting that the CRRSP38 is related with the pyramided *Rpv1+Rpv3-1* genotype.

4.5.3 *Rpv3-1* related resistance proteins

The *Rpv3-1* resistance response is probably associated with the GH3.1 expression. The family of this protein is also reported as a resistance induced in rice against bacterial blight and fungal blast (HU et al., 2008). The function of the GH3.1 protein, as well as the GH3 family proteins, is to reduce the auxin response in the tissue (STASWICK et al., 2005; ZHANG et al., 2007). Auxin is essential for the plant development, however, can be associated with the plant susceptibility, due the loosening the cell wall (GONZÁLEZ-LAMOTHE et al., 2012). Two genes from the GH3 family were reported in rice as an antagonist of the auxin response, inducing the plant resistance independent of jasmonic or salicylic acid signaling (DING et al., 2008; FU et al., 2011).

4.5.4 *rpv* response

The largest number of down-regulated proteins in the *rpv* genotype is probably due the largest impact of the fungus in the cell line. This affirmation is corroborated by the proteins unique expressed in this genotype, the UGT74E2-LIKE and UGT43-LIKE down-regulated, as well as the BG suppression can be related with the damage. UGTs are regulated by the MeJA pathway (CAO et al., 2015) and play multiple roles in the plant metabolism, can be related to plant architecture (BIAN et al., 2016). However, these enzymes are mainly related to the plant defense pathways (Song et al. 2019; Kim et al. 2006). Such as, the flavonoid biosynthesis (Jones et al. 2003; Kim et al. 2006; Vogt and Jones 2000), reactive oxygen species (ROS) (WANG et

al., 2020), and the balance by single and conjugated auxins IAA and IBA (TOGNETTI et al., 2010).

The ROS play an important role in the plant cell death (CZARNOCKA; KARPIŃSKI, 2018), a mechanism to avoid the biotrophic pathogen development, due the hypersensitive response (COLL; EPPLE; DANGL, 2011). The UGT74E2 play an important role in the ABA and auxin hormonal interaction and tolerance to abiotic stress (TOGNETTI et al., 2010; WANG et al., 2020). In the same way BG is related with the ABA pathway (ACANDA et al., 2020). Thus, the UGTs down-regulation and BG suppression result in a potential damage to the plant defense system. In special for stomata closure that can be increased the susceptibility.

4.6 CONCLUSION

Taken together the results of the present work showed that cell cultures from grapevine genotypes with genetic resistance against *P. viticola* presented lower down-regulated proteins in 24 hpi in comparation to susceptible genotype. The STILBENE SYNTHASE enzyme shown to plays a crucial role in the cell defense against the *P. viticola* infection, in all evaluated genotypes; however, the pyramided genotype *Rpv1+Rpv3-1* presents more isotypes of this enzyme up-regulated comparatively to other ones. The INDOLE-3-ACETIC ACID-AMINO SYNTHETASE plays an important role in the cell defense when the *Rpv3-1* is present. On the other hand, CYSTEINE-RICH REPEAT SECRETORY PROTEIN 38 revealed an important role in the pyramided genotype, probably due the *Rpv1* effect. To the best of our knowledge this is the first report of proteomic data using grapevine cell cultures from genotypes containing pyramided *Rpv* loci. News studies can apply a kinetic approach to determine in which moment the effect of the *P. viticola* inoculation is recognized in each genotype and the first changes in the cell responses.

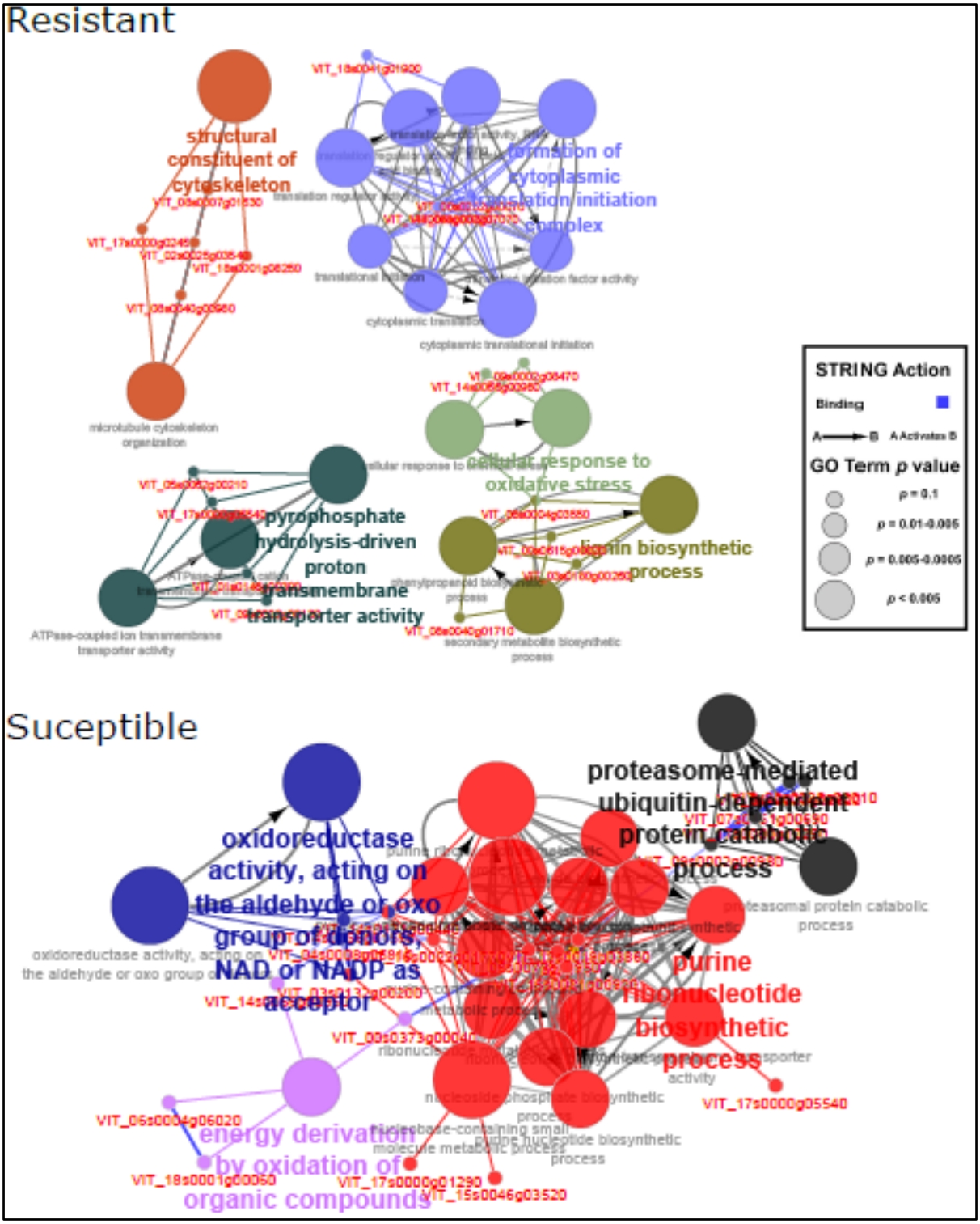

Figure S1. Networks of processes down-regulated or unique for no inoculated treatment, in *Vitis vinifera* resistances genotypes (*Rpv1+Rpv3-1* and *Rpv3-1*) with incompatible interaction plant pathogen, and susceptible genotype (*rpv*) with compatible interaction plant pathogen, in cell cultures after 24 hours post inoculation with *Plasmopara viticola*.

Table S1. Differentially expressed proteins with the *Plasmopara viticola* inoculation in three genotypes of *V. vinifera* cell cultures after 24 hours post inoculation

Accession	Reported Peptides	Description	Blast2Go Description	Rpv1+Rpv3-1 (PV/control)	Rpv3-1 (PV/control)	rpv (PV/control)
P51071	15	Stilbene synthase 3	stilbene synthase	UP	UP	UP
D7SY74	11	Bet_v_1 domain-containing protein	major allergen Pru av 1	UP	UP	UP
D7SY76	12	Bet_v_1 domain-containing protein	major allergen Pru av 1	UP	UP	UP
A5AJB3	4	Chitin-binding type-1 domain-containing protein	Endochitinase EP3	UP	UP	UP
F6H6U6	19	Bet_v_1 domain-containing protein	major allergen Pru av 1	UP	UP	UP
F6H0X2	16	Phospho-2-dehydro-3-deoxyheptonate aldolase	phospho-2-dehydro-3-deoxyheptonate aldolase 1, chloroplastic-like	UP	UP	UP
D7TAI2	16	Peroxidase	lignin-forming anionic peroxidase	UP	UP	UP
F6H527	3	FAD-binding PCMH-type domain-containing protein	tetrahydrocannabinolic acid synthase-like	UP	UP	UP
D0VBC7	8	3-phosphoshikimate 1-carboxyvinyltransferase	3-phosphoshikimate 1-carboxyvinyltransferase 2	UP	UP	UP
F6HZ63	3	Pectinesterase	probable pectinesterase/pectinesterase inhibitor 7	UP	UP	UP
E0CRG5	6	Aminotran_1_2 domain-containing protein	bifunctional aspartate aminotransferase and glutamate/aspartate-prephenate aminotransferase	UP	UP	UP
F6I347	8	Abhydrolase_3 domain-containing protein	probable carboxylesterase 8	UP	UP	UP
D7U9N6	4	Uncharacterized protein	pirin-like protein	UP	UP	UP
Q546P8	7	Chitinase	Basic endochitinase	UP	UP	UP
F6GZ23	8	Flavodoxin-like domain-containing protein (Fragment)	probable NAD(P)H dehydrogenase (quinone) FQR1-like 1	UP	UP	UP
F6HZ10	15	Lipoxygenase	probable linoleate 9S-lipoxygenase 5	UP	UP	UP
F6GYA5	11	Laccase	putative laccase-9	UP	UP	UP
D7UE87	9	DUF3700 domain-containing protein	stem-specific protein TSJT1-like	UP	UP	UP
F6HJB8	11	Laccase	laccase-15-like	UP	UP	Unique no-rpv_PV
A5BRL4	8	Uncharacterized protein	trans-cinnamate 4-monooxygenase	UP	UP	Unique no-rpv_PV
F6H6U9	7	Bet_v_1 domain-containing protein	Major allergen Pru ar 1	UP	UP	Unique no-rpv_PV
F6H9P8	4	Uncharacterized protein	cytochrome P450 CYP73A100-like	UP	UP	Unique no-rpv_PV
F6HNF5	8	Phenylalanine ammonia-lyase	Phenylalanine ammonia-lyase	UP	UP	Unique no-rpv_PV
F6HJA9	5	Laccase	laccase-15 isoform X1	UP	UP	Unique no-rpv_PV

F6HEB2	19	Phenylalanine ammonia-lyase	phenylalanine ammonia-lyase	UP	UP	UNCHANGED
D7U0Q3	7	Aminotran_1_2 domain-containing protein	Aromatic aminotransferase ISS1	UP	UP	UNCHANGED
D7T541	2	Glyco_18 domain-containing protein	acidic mammalian chitinase	UP	UP	UNCHANGED
F6GXF5	9	Uncharacterized protein	4-coumarate--CoA ligase 2-like	UP	UP	UNCHANGED
F6HG55	4	ADK_lid domain-containing protein	adenylate kinase 4	UP	UP	UNCHANGED
D7TSJ8	10	Glutamine synthetase	glutamine synthetase	UP	UP	UNCHANGED
F6HKR7	4	LEA_2 domain-containing protein	NDR1/HIN1-Like protein 3	UP	UP	UNCHANGED
A5AS18	10	Flavodoxin-like domain-containing protein	probable NAD(P)H dehydrogenase (quinone) FQR1-like 1	UP	UP	UNCHANGED
F6HSW4	27	Uncharacterized protein	probable indole-3-acetic acid-amido synthetase GH3.1	UP	UP	UNCHANGED
F6HHB0	4	Uncharacterized protein	probable galactinol--sucrose galactosyltransferase 6 isoform X2	UP	UP	UNCHANGED
F6HR33	26	Phenylalanine ammonia-lyase	phenylalanine ammonia-lyase	UP	UP	UNCHANGED
D7U3W2	12	CN hydrolase domain-containing protein	bifunctional nitrilase/nitrile hydratase NIT4B	UP	UP	UNCHANGED
F6H697	14	Uncharacterized protein	probable indole-3-acetic acid-amido synthetase GH3.1	UP	UP	DOWN
F6HG22	9	Peroxidase	lignin-forming anionic peroxidase	UP	UP	-
F6HAA1	9	Pectinesterase	pectinesterase 2	UP	UP	-
F6GV28	5	Uncharacterized protein	osmotin-like protein	UP	UP	-
D7SNV6	2	DHQ_synthase domain-containing protein	3-dehydroquinate synthase, chloroplastic	UP	UP	-
F6HPC0	6	Uncharacterized protein	glutathione S-transferase U10-like	Unique Rpv1+Rpv3_SPV	UP	UNCHANGED
D7TWT2	8	Uncharacterized protein	alpha-dioxygenase 1-like	Unique Rpv1+Rpv3_PV	UP	-
D7U634	5	Epimerase domain-containing protein	cinnamoyl-CoA reductase 1	UNCHANGED	UP	UP
F6H7X8	5	AAI domain-containing protein	PREDICTED: uncharacterized protein LOC104882174	UNCHANGED	UP	UP
E0CVR9	9	Uncharacterized protein	L-ascorbate oxidase homolog	UNCHANGED	UP	UP
F6HQ75	9	Peptidase A1 domain-containing protein	basic 7S globulin	UNCHANGED	UP	UP
F6GUG1	3	Dirigent protein	Dirigent protein 7	UNCHANGED	UP	UP
A5BPT8	14	Phenylalanine ammonia-lyase	phenylalanine ammonia-lyase	UNCHANGED	UP	UP
F6HUH2	10	Uncharacterized protein	thaumatin-like protein 1	UNCHANGED	UP	UP

D7SXW6	8	Uncharacterized protein	Basic secretory protease	UNCHANGED	UP	UP
D7U0U9	2	AAA domain-containing protein	26S protease regulatory subunit 8 homolog A	UNCHANGED	UP	Unique no-rpv_SPV
F6I447	2	Oxidored_FMN domain-containing protein	putative 12-oxophytodienoate reductase 11	UNCHANGED	UP	Unique no-rpv_PV
F6I390	11	Pectinesterase	pectinesterase 2	UNCHANGED	UP	UNCHANGED
D7U9P1	4	AAI domain-containing protein	putative lipid-transfer protein DIR1	UNCHANGED	UP	UNCHANGED
F6H4I9	3	PKS_ER domain-containing protein	alcohol dehydrogenase 1B	UNCHANGED	UP	UNCHANGED
F6H6B6	6	C2 domain-containing protein	protein SRC2 homolog	UNCHANGED	UP	UNCHANGED
F6GTS9	4	Uncharacterized protein	probable glutathione S-transferase	UNCHANGED	UP	UNCHANGED
D7SGV3	3	ADK_lid domain-containing protein	adenylate kinase 4	UNCHANGED	UP	UNCHANGED
D7SJL8	21	Peroxidase	peroxidase 4-like	UNCHANGED	UP	UNCHANGED
D7U3E6	6	Pectate lyase	probable pectate lyase 8	UNCHANGED	UP	UNCHANGED
A5B8T3	19	PfkB domain-containing protein	probable fructokinase-4	UNCHANGED	UP	UNCHANGED
D7SZX9	7	Uncharacterized protein	Glutelin type-A 3	UNCHANGED	UP	UNCHANGED
F6HY25	3	Uncharacterized protein	Beta-fructofuranosidase, insoluble isoenzyme CWINV1	UNCHANGED	UP	UNCHANGED
D7TBE3	4	Uncharacterized protein	acid phosphatase 1-like	UNCHANGED	UP	UNCHANGED
D7UBG8	13	Glyceraldehyde-3-phosphate dehydrogenase	glyceraldehyde-3-phosphate dehydrogenase 2, cytosolic	UNCHANGED	UP	UNCHANGED
F6GV85	3	Uncharacterized protein	Ubiquitin-associated and SH3 domain-containing protein	UNCHANGED	UP	UNCHANGED
F6H0F0	4	Uncharacterized protein	TOM1-like protein 4	UNCHANGED	UP	UNCHANGED
F6HVD5	8	Peptidase A1 domain-containing protein	aspartyl protease AED3-like	UNCHANGED	UP	UNCHANGED
F6HLB4	7	Glutamate dehydrogenase	Glutamate dehydrogenase 1	UNCHANGED	UP	DOWN
F6HR64	2	Uncharacterized protein	putative 3-oxoacyl-[acyl-carrier-protein] reductase	UNCHANGED	UP	-
D7TG84	3	Uncharacterized protein	expansin-like B1	UNCHANGED	UP	-
D7SLA2	5	Lipoxygenase domain-containing protein	probable linoleate 9S-lipoxygenase 5	UNCHANGED	UP	-
D7TW88	4	3-hydroxy-3-methylglutaryl coenzyme A synthase	hydroxymethylglutaryl-CoA synthase	UNCHANGED	UP	-
F6H2N4	5	Uncharacterized protein	epidermis-specific secreted glycoprotein EP1-like	UNCHANGED	UP	-
E0CQN2	7	Uncharacterized protein	alcohol dehydrogenase I	UNCHANGED	UP	-
F6HYK6	12	Uncharacterized protein	heat shock 70 kDa protein	-	UP	Unique no-rpv_SPV

F6HEA4	5	Uncharacterized protein	Glutathione transferase GST 23	-	UP	Unique no-rpv_PV
D7SVM9	2	Uncharacterized protein	levodione reductase	-	UP	-
D7TQ86	5	ADF-H domain-containing protein	actin-depolymerizing factor 2	UP	Unique Rpv3_SPV	Unique no-rpv_PV
F6HCP2	5	Glycosyltransferase	anthocyanidin 5,3-O-glucosyltransferase	UNCHANGED	Unique Rpv3_SPV	UNCHANGED
D7SI06	2	Uncharacterized protein	protein EDS1	UNCHANGED	Unique Rpv3_SPV	-
F6H1N2	10	Peroxidase	peroxidase N1	-	Unique Rpv3_SPV	-
F6HBK3	7	Aminotran_1_2 domain-containing protein	LL-diaminopimelate aminotransferase, chloroplastic	-	Unique Rpv3_SPV	-
F6I4L5	9	Uncharacterized protein	luminal-binding protein 5-like	-	Unique Rpv3_SPV	-
F6HEB5	19	Phenylalanine ammonia-lyase	phenylalanine ammonia-lyase	UP	Unique Rpv3_PV	Unique no-rpv_PV
F6HEB3	19	Phenylalanine ammonia-lyase	phenylalanine ammonia-lyase	UP	Unique Rpv3_PV	Unique no-rpv_PV
F6HP23	12	Uncharacterized protein	stilbene synthase	UP	Unique Rpv3_PV	Unique no-rpv_PV
F6HVX2	6	Laccase	laccase-14	UP	Unique Rpv3_PV	UNCHANGED
A5BT39	8	Glyco_hydro_18 domain-containing protein	acidic endochitinase	Unique Rpv1+Rpv3_SPV	Unique Rpv3_PV	DOWN
D7TAH8	7	Peroxidase	lignin-forming anionic peroxidase	Unique Rpv1+Rpv3_PV	Unique Rpv3_PV	Unique no-rpv_SPV
F6H0R8	5	Uncharacterized protein	7-deoxyloganetin glucosyltransferase-like	Unique Rpv1+Rpv3_PV	Unique Rpv3_PV	Unique no-rpv_PV
F6H0R9	6	Uncharacterized protein	7-deoxyloganetin glucosyltransferase-like	Unique Rpv1+Rpv3_PV	Unique Rpv3_PV	Unique no-rpv_PV
F6HM09	5	FAD-binding PCMH-type domain-containing protein	berberine bridge enzyme-like 8	Unique Rpv1+Rpv3_PV	Unique Rpv3_PV	Unique no-rpv_PV
A5C109	6	Bet_v_1 domain-containing protein	major allergen Pru ar 1-like	Unique Rpv1+Rpv3_PV	Unique Rpv3_PV	Unique no-rpv_PV
F6HJL1	9	Phospho-2-dehydro-3-deoxyheptonate aldolase	phospho-2-dehydro-3-deoxyheptonate aldolase 2, chloroplastic	Unique Rpv1+Rpv3_PV	Unique Rpv3_PV	Unique no-rpv_PV
F6HIR9	5	Uncharacterized protein	stilbene synthase	Unique Rpv1+Rpv3_PV	Unique Rpv3_PV	Unique no-rpv_PV
F6H8X2	4	Uncharacterized protein	Glutelin type-A 3	Unique Rpv1+Rpv3_PV	Unique Rpv3_PV	UNCHANGED
A5BWG3	2	Arogenate dehydratase	arogenate dehydratase/prephenate dehydratase 6, chloroplastic-like	Unique Rpv1+Rpv3_PV	Unique Rpv3_PV	-
F6HB09	3	Chitin-binding type-1 domain-containing protein	endochitinase EP3	Unique Rpv1+Rpv3_PV	Unique Rpv3_PV	-
F6HD62	2	Patatin	Patatin-like protein 2	Unique Rpv1+Rpv3_PV	Unique Rpv3_PV	-
F6HP33	11	Chal_sti_synt_N domain-containing protein	Stilbene synthase 4	Unique Rpv1+Rpv3_PV	Unique Rpv3_PV	-

F6HWB2	7	Laccase	laccase-15-like	Unique Rpv1+Rpv3_PV	Unique Rpv3_PV	-
F6I3A9	3	Uncharacterized protein	ATPase 10, plasma membrane-type isoform X2	UNCHANGED	Unique Rpv3_PV	UP
F6H5T9	9	Uncharacterized protein	Malate dehydrogenase, chloroplastic	UNCHANGED	Unique Rpv3_PV	Unique no-rpv_PV
D7TPD8	4	Uncharacterized protein	putative isomerase BH0283	UNCHANGED	Unique Rpv3_PV	UNCHANGED
D7SUD7	11	Aspartate aminotransferase	aspartate aminotransferase, cytoplasmic	UNCHANGED	Unique Rpv3_PV	DOWN
F6I523	6	Uncharacterized protein	putative glutathione S-transferase	UNCHANGED	Unique Rpv3_PV	-
F6H1B0	3	Uncharacterized protein	uncharacterized acetyltransferase At3g50280-like	-	Unique Rpv3_PV	Unique no-rpv_PV
F6HXW9	5	Germin-like protein	Auxin-binding protein ABP19a	-	Unique Rpv3_PV	UNCHANGED
A5AWW7	2	Uncharacterized protein	ras-related protein RABA4d	-	Unique Rpv3_PV	-
D7TBD4	4	Uncharacterized protein	inositol oxygenase 2-like	-	Unique Rpv3_PV	-
A5B473	6	Uncharacterized protein	calmodulin-7-like isoform X2	UP	UNCHANGED	UP
F6GUV7	23	Tubulin beta chain	tubulin beta-2 chain-like	UP	UNCHANGED	UP
D7U3V0	13	CN hydrolase domain-containing protein	bifunctional nitrilase/nitrile hydratase NIT4B	UP	UNCHANGED	UP
F6HPN3	3	Uncharacterized protein	Aldehyde dehydrogenase family 2 member B7, mitochondrial	UP	UNCHANGED	Unique no-rpv_PV
D7TAI3	8	Peroxidase	Lignin-forming anionic peroxidase	UP	UNCHANGED	UNCHANGED
F6H6H8	8	Glyco_hydro_18 domain-containing protein	Acidic endochitinase	UP	UNCHANGED	UNCHANGED
A5AY42	5	ATP synthase subunit d, mitochondrial	ATP synthase subunit d, mitochondrial	UP	UNCHANGED	UNCHANGED
F6GXY6	11	Peroxidase	cationic peroxidase 1-like	UP	UNCHANGED	UNCHANGED
F6HBA8	6	DRT100-like protein	DNA damage-repair/toleration protein DRT100	UP	UNCHANGED	UNCHANGED
D7UA89	10	Uncharacterized protein	ATP-citrate synthase alpha chain protein 2	UP	UNCHANGED	UNCHANGED
F6GWS4	9	Peroxidase	peroxidase 72	UP	UNCHANGED	UNCHANGED
F6H6U5	10	Bet_v_1 domain-containing protein	major allergen Pru av 1	UP	UNCHANGED	UNCHANGED
F6HWL2	8	Uncharacterized protein	calnexin homolog	UP	UNCHANGED	UNCHANGED
A5BIN1	14	NAD(P)-bd_dom domain-containing protein	UDP-glucuronic acid decarboxylase 6	UP	UNCHANGED	UNCHANGED
D7T300	2	Uncharacterized protein	ATP synthase subunit O, mitochondrial	UP	UNCHANGED	UNCHANGED
F6GSN7	15	Uncharacterized protein	Ketose-bisphosphate aldolase class-II family protein isoform 1	UP	UNCHANGED	UNCHANGED
D7TUP8	7	Cysteine synthase	cysteine synthase	UP	UNCHANGED	UNCHANGED

D7T8G1	2	Annexin	annexin D5	UP	UNCHANGED	UNCHANGED
F6I6S2	20	Fn3_like domain-containing protein	beta-xylosidase/alpha-L-arabinofuranosidase 2	UP	UNCHANGED	UNCHANGED
D7U8Q0	25	Fn3_like domain-containing protein	beta-xylosidase/alpha-L-arabinofuranosidase 2	UP	UNCHANGED	UNCHANGED
F6I6R4	23	Fn3_like domain-containing protein	beta-xylosidase/alpha-L-arabinofuranosidase 2	UP	UNCHANGED	UNCHANGED
F6HIL6	3	Uncharacterized protein	cysteine-rich repeat secretory protein 38	UP	UNCHANGED	-
D7U4F6	20	Uncharacterized protein	alcohol dehydrogenase 1	UP	UNCHANGED	-
F6HUC8	16	Tubulin beta chain	tubulin beta chain-like	Unique Rpv1+Rpv3_SP V	UNCHANGED	UNCHANGED
F6GVV2	9	Uncharacterized protein	UDP-arabinopyranose mutase 1	Unique Rpv1+Rpv3_SP V	UNCHANGED	-
F6GWA3	10	Uncharacterized protein	cell division cycle protein 48 homolog	UNCHANGED	UNCHANGED	UP
F6H766	7	Uncharacterized protein	Peptidase S8/S53 domain-containing protein	UNCHANGED	UNCHANGED	UP
F6H6M7	2	Uncharacterized protein	Cleavage and polyadenylation specificity factor subunit 2	UNCHANGED	UNCHANGED	UP
F6I0V8	3	Uncharacterized protein	lysM domain-containing GPI-anchored protein 2	UNCHANGED	UNCHANGED	UP
F6HF82	7	UDP-glucose 6-dehydrogenase	UDP-glucose 6-dehydrogenase 5-like	UNCHANGED	UNCHANGED	UP
F6HEL7	4	AAI domain-containing protein	putative lipid-transfer protein DIR1	UNCHANGED	UNCHANGED	UP
F6H5A0	2	Peptidase A1 domain-containing protein	aspartyl protease family protein 2	UNCHANGED	UNCHANGED	UP
F6HK38	10	Uncharacterized protein	elongation factor 1-gamma	UNCHANGED	UNCHANGED	UP
F6HZ64	13	Pectinesterase	pectinesterase-like	UNCHANGED	UNCHANGED	UP
A5ASF9	3	Profilin	profilin-1	UNCHANGED	UNCHANGED	UP
F6I5L8	6	Prohibitin	prohibitin-3, mitochondrial	UNCHANGED	UNCHANGED	UP
D7SVJ2	7	V-type proton ATPase subunit C	V-type proton ATPase subunit C	UNCHANGED	UNCHANGED	UP
F6HLQ8	2	Pyruvate kinase	pyruvate kinase 1, cytosolic	UNCHANGED	UNCHANGED	UP
A5BEF3	4	AAA domain-containing protein	26S proteasome regulatory subunit 4 homolog A	UNCHANGED	UNCHANGED	UP
F6H0Y3	5	Uncharacterized protein	PREDICTED: uncharacterized protein LOC100254028 isoform X2	UNCHANGED	UNCHANGED	UP
F6GTE2	23	Uncharacterized protein	UDP-arabinopyranose mutase 3	UNCHANGED	UNCHANGED	UP
D7U0C2	8	Malic enzyme	NADP-dependent malic enzyme-like	UNCHANGED	UNCHANGED	UP

F6HGH4	22	6-phosphogluconate dehydrogenase, decarboxylating	6-phosphogluconate dehydrogenase, decarboxylating 3	UNCHANGED	UNCHANGED	UP
D7SJS7	3	Uncharacterized protein	Gamma-interferon-inducible lysosomal thiol reductase	UNCHANGED	UNCHANGED	UP
A5AML5	4	Thioredoxin	thioredoxin H-type-like	UNCHANGED	UNCHANGED	UP
F6GUF4	3	Uncharacterized protein	formate--tetrahydrofolate ligase	UNCHANGED	UNCHANGED	UP
E0CV68	7	Importin N-terminal domain-containing protein	importin subunit beta-1	UNCHANGED	UNCHANGED	UP
A5ATD8	6	Cytochrome b5 heme-binding domain-containing protein	cytochrome b5	UNCHANGED	UNCHANGED	UP
D7T475	8	Chalcone-flavonone isomerase family protein	chalcone isomerase	UNCHANGED	UNCHANGED	UP
E0CSL3	2	Uncharacterized protein	3-deoxy-manno-octulosonate cytidylyltransferase, mitochondrial	UNCHANGED	UNCHANGED	UP
F6HW71	2	Uncharacterized protein	kunitz trypsin inhibitor 2	UNCHANGED	UNCHANGED	UP
F6HLD8	32	Uncharacterized protein	heat shock cognate 70 kDa protein 2	UNCHANGED	UNCHANGED	UP
F6I731	3	Uncharacterized protein	putative UDP-rhamnose:rhamnosyltransferase 1	UNCHANGED	UNCHANGED	UP
A5BYS8	2	Calcineurin B-like protein 02	calcineurin B-like protein 3	UNCHANGED	UNCHANGED	UP
F6HL98	9	LRRNT_2 domain-containing protein	polygalacturonase-inhibiting protein	UNCHANGED	UNCHANGED	UP
F6H0V3	39	Uncharacterized protein	acetyl-CoA carboxylase 1-like	UNCHANGED	UNCHANGED	UP
D7SYK8	24	Uncharacterized protein	ATP-citrate synthase beta chain protein 2	UNCHANGED	UNCHANGED	UP
F6HUY0	7	Isocitrate dehydrogenase [NADP]	isocitrate dehydrogenase [NADP]	UNCHANGED	UNCHANGED	UP
D7TP57	6	Peroxidase	peroxidase 3	UNCHANGED	UNCHANGED	UP
D7SKD8	3	Uncharacterized protein	oxysterol-binding protein-related protein 3C	UNCHANGED	UNCHANGED	UP
F6GUN2	5	Uncharacterized protein	Mitochondrial dicarboxylate/tricarboxylate transporter DTC	UNCHANGED	UNCHANGED	UP
F6I0S6	7	SSD domain-containing protein	Niemann-Pick C1 protein isoform X2	UNCHANGED	UNCHANGED	UP
F6HXR4	4	Uncharacterized protein	acetylornithine aminotransferase, mitochondrial	UNCHANGED	UNCHANGED	UP
F6I687	3	Uncharacterized protein	basic endochitinase-like	UNCHANGED	UNCHANGED	Unique no-rpv_SPV
F6GWB7	3	Uncharacterized protein	Glucan endo-1,3-beta-glucosidase	UNCHANGED	UNCHANGED	Unique no-rpv_SPV
D7U2I5	4	Uncharacterized protein	Calcium-dependent phosphotriesterase superfamily protein	UNCHANGED	UNCHANGED	Unique no-rpv_SPV
D7T7L7	2	Uncharacterized protein	Phosphoenolpyruvate carboxykinase	UNCHANGED	UNCHANGED	Unique no-rpv_SPV
F6H755	7	Uncharacterized protein	subtilisin-like protease SBT3.5	UNCHANGED	UNCHANGED	Unique no-rpv_SPV

D7SJX8	2	Peptidyl-prolyl cis-trans isomerase	peptidyl-prolyl cis-trans isomerase CYP20-1	UNCHANGED	UNCHANGED	Unique no-rpv_SPV
D7TCM2	2	Acetyltransferase component of pyruvate dehydrogenase complex	dihydrolipoyllysine-residue acetyltransferase component 2 of pyruvate dehydrogenase complex, mitochondrial-like	UNCHANGED	UNCHANGED	Unique no-rpv_SPV
D7SN09	15	Endoglucanase	endoglucanase 9-like	UNCHANGED	UNCHANGED	Unique no-rpv_SPV
D7U9L4	4	Aldo_ket_red domain-containing protein	probable aldo-keto reductase 2	UNCHANGED	UNCHANGED	Unique no-rpv_SPV
D7TM87	3	Uncharacterized protein	Alpha-D-phosphohexomutase superfamily	UNCHANGED	UNCHANGED	Unique no-rpv_SPV
F6H316	2	Uncharacterized protein	DEAD-box ATP-dependent RNA helicase 56	UNCHANGED	UNCHANGED	Unique no-rpv_SPV
D7TXC7	3	Uncharacterized protein	flowering locus K homology domain-like isoform X1	UNCHANGED	UNCHANGED	Unique no-rpv_PV
A5BEM8	12	Uncharacterized protein	glyoxylate/succinic semialdehyde reductase 1	UNCHANGED	UNCHANGED	DOWN
A5C3G7	7	Uncharacterized protein	gamma carbonic anhydrase 1, mitochondrial	UNCHANGED	UNCHANGED	DOWN
E0CSN8	9	DUF3700 domain-containing protein	stem-specific protein TSJT1-like	UNCHANGED	UNCHANGED	DOWN
E0CQT6	13	Uncharacterized protein	L-ascorbate oxidase homolog	UNCHANGED	UNCHANGED	DOWN
F6GTQ4	7	Uncharacterized protein	28 kDa ribonucleoprotein, chloroplastic-like	UNCHANGED	UNCHANGED	DOWN
D7TA18	11	Uncharacterized protein	PREDICTED: uncharacterized protein LOC100247879	UNCHANGED	UNCHANGED	DOWN
A5C6H7	35	Sucrose synthase	sucrose synthase SusA1	UNCHANGED	UNCHANGED	DOWN
D7TB63	3	Uncharacterized protein	Nucleosome assembly protein 1;2	UNCHANGED	UNCHANGED	DOWN
F6GWF3	12	Serine hydroxymethyltransferase	serine hydroxymethyltransferase 4	UNCHANGED	UNCHANGED	DOWN
F6GSG7	26	Glyceraldehyde-3-phosphate dehydrogenase	glyceraldehyde-3-phosphate dehydrogenase, cytosolic	UNCHANGED	UNCHANGED	DOWN
F6HRJ2	7	ACOX domain-containing protein	peroxisomal acyl-coenzyme A oxidase 1	UNCHANGED	UNCHANGED	DOWN
D7T9I6	11	Proteasome subunit alpha type	proteasome subunit alpha type-2-A	UNCHANGED	UNCHANGED	DOWN
A5CAL1	4	Uncharacterized protein	hydroxyphenylpyruvate reductase-like	UNCHANGED	UNCHANGED	DOWN
F6HSN5	7	Uncharacterized protein	2-hydroxyacyl-CoA lyase	UNCHANGED	UNCHANGED	DOWN
F6HE11	13	Dihydrolipoyl dehydrogenase	dihydrolipoyl dehydrogenase 1, mitochondrial	UNCHANGED	UNCHANGED	DOWN
F6GUP8	5	Uncharacterized protein	pyruvate decarboxylase 2	UNCHANGED	UNCHANGED	DOWN
F6I5U5	11	Pyruvate kinase	pyruvate kinase 1, cytosolic-like	UNCHANGED	UNCHANGED	DOWN
F6GT51	6	Uncharacterized protein (Fragment)	MtN19-like protein, putative isoform 2	UNCHANGED	UNCHANGED	DOWN

F6HZF1	15	Uncharacterized protein	pectin acetylesterase 3	UNCHANGED	UNCHANGED	DOWN
F6I0A4	19	Fe2OG dioxygenase domain-containing protein	2-oxoglutarate-dependent dioxygenase DAO	UNCHANGED	UNCHANGED	DOWN
F6GSQ2	10	Glutamine synthetase	glutamine synthetase	UNCHANGED	UNCHANGED	DOWN
A5AX75	16	14_3_3 domain-containing protein	14-3-3-like protein GF14 kappa	UNCHANGED	UNCHANGED	DOWN
F6HXC8	32	Phospholipase D	Phospholipase D alpha 1	UNCHANGED	UNCHANGED	DOWN
F6I407	32	Uncharacterized protein	patellin-3-like	UNCHANGED	UNCHANGED	DOWN
D7TJZ9	4	Coatomer subunit zeta	coatomer subunit zeta-1-like	UNCHANGED	UNCHANGED	DOWN
D7U2H8	14	Calreticulin	calreticulin	UNCHANGED	UNCHANGED	DOWN
D7T1V9	7	Uncharacterized protein	embryo-specific protein ATS3B-like	UNCHANGED	UNCHANGED	DOWN
D7SIR1	5	Uncharacterized protein	agmatine deiminase	UNCHANGED	UNCHANGED	DOWN
D7SHU4	18	Aldedh domain-containing protein	aldehyde dehydrogenase family 2 member B4, mitochondrial-like	UNCHANGED	UNCHANGED	DOWN
F6H2P8	3	Uncharacterized protein	protein DJ-1 homolog B-like	UNCHANGED	UNCHANGED	DOWN
D7TYZ1	10	T-complex protein 1 subunit eta	T-complex protein 1 subunit eta	UNCHANGED	UNCHANGED	DOWN
F6H0C4	11	Uncharacterized protein	Phosphoprotein ECPP44	UNCHANGED	UNCHANGED	DOWN
F6I0I5	28	Uncharacterized protein	Actin-7	UNCHANGED	UNCHANGED	DOWN
F6I7K1	2	ATP-dependent 6-phosphofructokinase	ATP-dependent 6-phosphofructokinase 2	UNCHANGED	UNCHANGED	DOWN
D7TIZ5	21	Pyruvate kinase	pyruvate kinase 1, cytosolic	UNCHANGED	UNCHANGED	DOWN
E0CSC9	3	Uncharacterized protein	Homogentisate 1,2-dioxygenase	UNCHANGED	UNCHANGED	DOWN
F6HKH3	24	Uncharacterized protein	Enolase	UNCHANGED	UNCHANGED	DOWN
D7SLM9	12	Uncharacterized protein	ruBisCO large subunit-binding protein subunit beta, chloroplastic	UNCHANGED	UNCHANGED	DOWN
D7UC33	4	Uncharacterized protein	(+)-neomenthol dehydrogenase	UNCHANGED	UNCHANGED	DOWN
D7TAG7	5	GRAM domain-containing protein	GEM-like protein 5	UNCHANGED	UNCHANGED	DOWN
D7TZN7	2	FMN hydroxy acid dehydrogenase domain-containing protein	peroxisomal (S)-2-hydroxy-acid oxidase GLO4	UNCHANGED	UNCHANGED	DOWN
D7THC6	6	Neutral ceramidase	neutral ceramidase	UNCHANGED	UNCHANGED	DOWN
F6H1L2	20	Tubulin beta chain	tubulin beta chain	UNCHANGED	UNCHANGED	DOWN
F6H9T6	11	Succinate-semialdehyde dehydrogenase	succinate-semialdehyde dehydrogenase, mitochondrial	UNCHANGED	UNCHANGED	DOWN
F6I1A2	4	Uncharacterized protein	cysteine protease RD19A-like	UNCHANGED	UNCHANGED	DOWN
F6GT74	11	Uncharacterized protein	malate dehydrogenase, chloroplastic	UNCHANGED	UNCHANGED	DOWN

D7TVE6	4	Uncharacterized protein	probable polygalacturonase	UNCHANGED	UNCHANGED	DOWN
D7TM77	15	PfkB domain-containing protein	adenosine kinase 2	UNCHANGED	UNCHANGED	DOWN
D7UCE5	3	AB hydrolase-1 domain-containing protein	Proline iminopeptidase	UNCHANGED	UNCHANGED	DOWN
D7U3V2	10	CN hydrolase domain-containing protein	Bifunctional nitrilase/nitrile hydratase NIT4B	UNCHANGED	UNCHANGED	DOWN
D7SYR7	19	Aminotran_1_2 domain-containing protein	Glutamate--glyoxylate aminotransferase 2	UNCHANGED	UNCHANGED	DOWN
F6GWM3	2	Uncharacterized protein	cold shock domain-containing protein 3-like	UNCHANGED	UNCHANGED	DOWN
D7SNX7	2	VWFA domain-containing protein	26S proteasome non-ATPase regulatory subunit 4 homolog	UNCHANGED	UNCHANGED	DOWN
F6HLL0	5	C-CAP/cofactor C-like domain-containing protein	TBCC domain-containing protein 1	UNCHANGED	UNCHANGED	DOWN
D7SNS5	9	Uncharacterized protein	selenium-binding protein 1	UNCHANGED	UNCHANGED	DOWN
F6H710	15	Uncharacterized protein	galactokinase	UNCHANGED	UNCHANGED	DOWN
F6GV26	32	Uncharacterized protein	heat shock cognate 70 kDa protein 2	UNCHANGED	UNCHANGED	DOWN
F6HYG1	26	Uncharacterized protein	heat shock 70 kDa protein 15-like	UNCHANGED	UNCHANGED	DOWN
D7TQM9	2	Isocitrate dehydrogenase [NAD] subunit, mitochondrial	isocitrate dehydrogenase [NAD] catalytic subunit 5, mitochondrial	UNCHANGED	UNCHANGED	DOWN
D7SQ37	17	Xylose isomerase	xylose isomerase	UNCHANGED	UNCHANGED	DOWN
F6H0X3	18	14_3_3 domain-containing protein	14-3-3-like protein	UNCHANGED	UNCHANGED	DOWN
F6GZK7	5	PB1 domain-containing protein	PB1 domain containing protein	UNCHANGED	UNCHANGED	DOWN
D7T227	29	Uncharacterized protein	enolase	UNCHANGED	UNCHANGED	DOWN
F6GUN1	22	Tubulin alpha chain	tubulin alpha-3 chain	UNCHANGED	UNCHANGED	DOWN
F6H740	28	Fn3_like domain-containing protein	putative beta-D-xylosidase	UNCHANGED	UNCHANGED	DOWN
D7TFS7	8	Uncharacterized protein	ras-related protein Rab7	UNCHANGED	UNCHANGED	DOWN
D7TJL0	9	14_3_3 domain-containing protein	14-3-3-like protein D isoform X1	UNCHANGED	UNCHANGED	DOWN
E0CQR2	17	Aamy domain-containing protein	1,4-alpha-glucan-branching enzyme 1, chloroplastic/amyloplastic-like	UNCHANGED	UNCHANGED	DOWN
A5AG34	4	Uncharacterized protein	protein EXORDIUM-like 2	UNCHANGED	UNCHANGED	DOWN
F6GY71	17	Uncharacterized protein	pyruvate decarboxylase 2	UNCHANGED	UNCHANGED	DOWN
D7TJI9	20	Uncharacterized protein	pyruvate decarboxylase 1	UNCHANGED	UNCHANGED	DOWN
D7SSM6	7	Flavodoxin-like domain-containing protein	probable NAD(P)H dehydrogenase (quinone) FQR1-like 1	UNCHANGED	UNCHANGED	DOWN
A5B3K2	10	Uncharacterized protein	plasma membrane-associated cation-binding protein 1	UNCHANGED	UNCHANGED	DOWN

F6HJJ4	6	Uncharacterized protein	malate dehydrogenase, glyoxysomal	UNCHANGED	UNCHANGED	DOWN
F6H0C8	4	Uncharacterized protein	T-complex protein 1 subunit beta	UNCHANGED	UNCHANGED	DOWN
D7SM33	2	ATP-synt_DE_N domain-containing protein	ATP synthase subunit delta', mitochondrial	UNCHANGED	UNCHANGED	DOWN
F6HWA5	4	Laccase	laccase-15-like	UNCHANGED	UNCHANGED	DOWN
E0CSF7	4	Uncharacterized protein	D-amino-acid transaminase, chloroplastic-like	UNCHANGED	UNCHANGED	DOWN
D7TA35	4	Usp domain-containing protein	universal stress protein PHOS32	UNCHANGED	UNCHANGED	DOWN
F6GST8	4	Uncharacterized protein	SNF1-related protein kinase regulatory subunit gamma-1	UNCHANGED	UNCHANGED	DOWN
D7TWS2	11	Aldedh domain-containing protein	aldehyde dehydrogenase family 2 member B7, mitochondrial-like	UNCHANGED	UNCHANGED	DOWN
A5AEH1	19	14_3_3 domain-containing protein	14-3-3-like protein	UNCHANGED	UNCHANGED	DOWN
F6HLJ7	2	Uncharacterized protein	enoyl-[acyl-carrier-protein] reductase [NADH], chloroplastic-like	UNCHANGED	UNCHANGED	DOWN
D7TFL3	12	Uncharacterized protein	calnexin homolog	UNCHANGED	UNCHANGED	DOWN
F6HNI6	16	Elongation factor 1-alpha	elongation factor 1-alpha	UNCHANGED	UNCHANGED	DOWN
F6HA09	3	Aminotran_5 domain-containing protein	serine--glyoxylate aminotransferase	UNCHANGED	UNCHANGED	DOWN
D7SUX4	3	Aldedh domain-containing protein	NADP-dependent glyceraldehyde-3-phosphate dehydrogenase	UNCHANGED	UNCHANGED	DOWN
F6HJM9	27	Uncharacterized protein	actin-7	UNCHANGED	UNCHANGED	DOWN
D7TVK9	8	PCI domain-containing protein	26S proteasome non-ATPase regulatory subunit 8 homolog A	UNCHANGED	UNCHANGED	DOWN
D7TMY3	5	PKS_ER domain-containing protein	Sorbitol dehydrogenase	UNCHANGED	UNCHANGED	DOWN
D7U090	9	Uncharacterized protein	mitochondrial-processing peptidase subunit alpha-like	UNCHANGED	UNCHANGED	DOWN
F6H0K5	12	Peptidase A1 domain-containing protein	aspartic proteinase Asp1 isoform X2	UNCHANGED	UNCHANGED	DOWN
D7TS82	15	Uncharacterized protein	3-ketoacyl-CoA thiolase 2, peroxisomal	UNCHANGED	UNCHANGED	DOWN
D7U016	5	Uncharacterized protein	Nucleosome assembly protein 1;2	UNCHANGED	UNCHANGED	DOWN
A5BNR6	3	Uncharacterized protein	2-alkenal reductase (NADP(+)-dependent)	UNCHANGED	UNCHANGED	DOWN
D7U252	8	Uncharacterized protein	glutathione S-transferase	UNCHANGED	UNCHANGED	DOWN
F6HCU9	41	HATPase_c domain-containing protein	heat shock cognate protein 80	UNCHANGED	UNCHANGED	DOWN
D7TY99	10	Uncharacterized protein	kunitz trypsin inhibitor 2	UNCHANGED	UNCHANGED	DOWN
A5B6U5	5	Proliferating cell nuclear antigen	proliferating cell nuclear antigen	UNCHANGED	UNCHANGED	DOWN
F6GSW1	11	Uncharacterized protein	UDP-arabinopyranose mutase 1-like	DOWN	UNCHANGED	Unique no-rpv_SPV

F6HKH5	2	C2H2-type domain-containing protein	histone deacetylase HDT1	DOWN	UNCHANGED	Unique no-rpv_SPV
F6GTM7	18	Adenosylhomocysteinase	adenosylhomocysteinase	DOWN	UNCHANGED	Unique no-rpv_SPV
F6I512	4	GST N-terminal domain-containing protein	putative glutathione S-transferase	DOWN	UNCHANGED	UNCHANGED
D7TE47	10	AB hydrolase-1 domain-containing protein	bifunctional epoxide hydrolase 2	DOWN	UNCHANGED	UNCHANGED
F6HU86	17	Starch synthase, chloroplastic/amyloplastic	granule-bound starch synthase 1, chloroplastic/amyloplastic	DOWN	UNCHANGED	UNCHANGED
F6H675	4	Uncharacterized protein	3-oxo-Delta(4,5)-steroid 5-beta-reductase-like	DOWN	UNCHANGED	UNCHANGED
D7SHA5	3	PCI domain-containing protein	26S proteasome non-ATPase regulatory subunit 6 homolog	DOWN	UNCHANGED	UNCHANGED
F6GZW5	2	WPP domain-containing protein	MFP1 attachment factor 1-like	DOWN	UNCHANGED	UNCHANGED
D7TZ77	4	Uncharacterized protein	glycerol kinase	DOWN	UNCHANGED	UNCHANGED
A5ALB2	4	Proteasome subunit alpha type	proteasome subunit alpha type-6	DOWN	UNCHANGED	UNCHANGED
F6HQC6	10	Abhydrolase_3 domain-containing protein	probable carboxylesterase 2	DOWN	UNCHANGED	DOWN
F6H144	4	TPR_REGION domain-containing protein	N-terminal acetyltransferase A, auxiliary subunit	DOWN	UNCHANGED	DOWN
F6H5V8	11	Uncharacterized protein	PREDICTED: uncharacterized protein At5g39570	DOWN	UNCHANGED	DOWN
D7SKR5	15	PEROXIDASE_4 domain-containing protein	L-ascorbate peroxidase, cytosolic	DOWN	UNCHANGED	DOWN
F6H5B8	6	Uncharacterized protein	T-complex protein 1 subunit epsilon	DOWN	UNCHANGED	DOWN
F6HQR1	9	NAC-A/B domain-containing protein	nascent polypeptide-associated complex subunit alpha-like protein 1	DOWN	UNCHANGED	DOWN
A5B8K3	6	Glutaredoxin domain-containing protein	glutaredoxin	DOWN	UNCHANGED	DOWN
F6HNM6	3	SHSP domain-containing protein	17.3 kDa class I heat shock protein-like	DOWN	UNCHANGED	-
F6HC36	4	Chalcone-flavonone isomerase family protein	chalcone isomerase	-	UNCHANGED	Unique no-rpv_SPV
F6HUM9	18	HATPase_c domain-containing protein	heat shock protein 83	Unique Rpv1+Rpv3_SPV	DOWN	Unique no-rpv_SPV
F6H6N8	3	Tubulin domain-containing protein	Tubulin beta-1 chain	Unique Rpv1+Rpv3_SPV	DOWN	-
F6HZD0	11	Uncharacterized protein	ADP-ribosylation factor	UNCHANGED	DOWN	UP
F6GZT1	4	Uncharacterized protein	SKP1-like protein 1B	UNCHANGED	DOWN	UP
F6HX64	15	Uncharacterized protein	pleiotropic drug resistance protein 1	UNCHANGED	DOWN	Unique no-rpv_SPV
D7STL2	2	Uncharacterized protein	UPF0587 protein C1orf123 homolog	UNCHANGED	DOWN	Unique no-rpv_SPV
F6HTC8	2	Uncharacterized protein	tobamovirus multiplication protein 2A-like	UNCHANGED	DOWN	UNCHANGED

Q2HZF5	5	Aquaporin PIP2	Aquaporin PIP2-7	UNCHANGED	DOWN	UNCHANGED
F6I5I7	5	Methylenetetrahydrofolate reductase	methylenetetrahydrofolate reductase 2-like	UNCHANGED	DOWN	UNCHANGED
F6HRX1	2	Uncharacterized protein	acetyl-CoA acetyltransferase, cytosolic 1	UNCHANGED	DOWN	UNCHANGED
F6HXM9	2	PKS_ER domain-containing protein	Quinone oxidoreductase 1	UNCHANGED	DOWN	UNCHANGED
F6HQ84	4	Uncharacterized protein	Leucine-rich repeat family protein, putative	UNCHANGED	DOWN	UNCHANGED
F6HRW7	6	Uncharacterized protein	monothiol glutaredoxin-S17	UNCHANGED	DOWN	UNCHANGED
D7TEW7	2	26S proteasome non-ATPase regulatory subunit 1 homolog	26S proteasome non-ATPase regulatory subunit 1 homolog A	UNCHANGED	DOWN	UNCHANGED
F6HBY3	9	Nudix hydrolase domain-containing protein	nudix hydrolase 3	UNCHANGED	DOWN	UNCHANGED
F6I0F7	2	PMEI domain-containing protein	cell wall / vacuolar inhibitor of fructosidase 2	UNCHANGED	DOWN	UNCHANGED
A5C9Q0	3	Usp domain-containing protein	universal stress protein PHOS32-like	UNCHANGED	DOWN	UNCHANGED
D7T2N7	9	Uncharacterized protein	desiccation-related protein At2g46140	UNCHANGED	DOWN	UNCHANGED
F6HS75	2	Eukaryotic translation initiation factor 3 subunit E	eukaryotic translation initiation factor 3 subunit E	UNCHANGED	DOWN	UNCHANGED
A5C3A3	4	Xyloglucan endotransglucosylase/hydrolase	probable xyloglucan endotransglucosylase/hydrolase protein 23	UNCHANGED	DOWN	UNCHANGED
E0CQS1	8	Protein kinase domain-containing protein	probable serine/threonine-protein kinase At4g35230	UNCHANGED	DOWN	UNCHANGED
A5B4N7	2	V-type proton ATPase subunit F	V-type proton ATPase subunit F	UNCHANGED	DOWN	UNCHANGED
F6GTM6	2	Uncharacterized protein	programmed cell death protein 4	UNCHANGED	DOWN	UNCHANGED
D7TZC8	2	PKS_ER domain-containing protein	Quinone oxidoreductase 1	UNCHANGED	DOWN	UNCHANGED
F6H2N7	7	Uncharacterized protein	phosphoenolpyruvate carboxylase, housekeeping isozyme	UNCHANGED	DOWN	UNCHANGED
F6HUM8	10	Pectate_lyase_3 domain-containing protein	probable polygalacturonase	UNCHANGED	DOWN	UNCHANGED
D7SIH5	13	Plasma membrane ATPase	ATPase 11, plasma membrane-type	UNCHANGED	DOWN	UNCHANGED
F6HDN6	8	Lipoxygenase	probable linoleate 9S-lipoxygenase 5	UNCHANGED	DOWN	UNCHANGED
D7UA22	8	Uncharacterized protein	pyrophosphate-energized vacuolar membrane proton pump 1-like	UNCHANGED	DOWN	UNCHANGED
D7TR34	2	Uncharacterized protein	potassium transporter 7	UNCHANGED	DOWN	UNCHANGED
D7TVX5	6	Uncharacterized protein	puromycin-sensitive aminopeptidase isoform X1	UNCHANGED	DOWN	UNCHANGED
D7TQ09	7	X8 domain-containing protein	glucan endo-1,3-beta-glucosidase 7-like	UNCHANGED	DOWN	UNCHANGED
F6I0Z8	4	Plasma membrane 22 aquaporin	probable aquaporin PIP2-8	UNCHANGED	DOWN	UNCHANGED

B6VJW7	2	ATPase subunit 8	ATPase subunit 8 (mitochondrion)	UNCHANGED	DOWN	UNCHANGED
F6HX23	2	Coatomer subunit beta'	coatomer subunit beta'-2 isoform X1	UNCHANGED	DOWN	UNCHANGED
D7SJV3	37	Clathrin heavy chain	clathrin heavy chain 1	UNCHANGED	DOWN	UNCHANGED
A5AT05	7	Serine/threonine-protein phosphatase	serine/threonine-protein phosphatase PP2A catalytic subunit	UNCHANGED	DOWN	UNCHANGED
F6H5F0	7	Uncharacterized protein	ADP,ATP carrier protein 3, mitochondrial	UNCHANGED	DOWN	UNCHANGED
F6HAU1	4	Uncharacterized protein	BAG family molecular chaperone regulator 7	UNCHANGED	DOWN	UNCHANGED
D7SM13	2	Uncharacterized protein	Heterogeneous nuclear ribonucleoprotein Q	UNCHANGED	DOWN	UNCHANGED
D7T959	9	Uncharacterized protein	ubiquitin receptor RAD23c-like	UNCHANGED	DOWN	UNCHANGED
F6GW96	3	Uncharacterized protein	alpha-L-fucosidase 1	UNCHANGED	DOWN	UNCHANGED
F6HBF2	5	Uncharacterized protein	ADP,ATP carrier protein 1, mitochondrial	UNCHANGED	DOWN	UNCHANGED
F6HW60	9	PB1 domain-containing protein	Retrovirus-related Pol polyprotein from transposon RE1	UNCHANGED	DOWN	UNCHANGED
F6HKY1	22	Tubulin beta chain	tubulin beta-2 chain	UNCHANGED	DOWN	UNCHANGED
D7TQS4	11	Carboxypeptidase	serine carboxypeptidase-like 45	UNCHANGED	DOWN	UNCHANGED
A5ACP0	29	Clathrin heavy chain	clathrin heavy chain 1	UNCHANGED	DOWN	UNCHANGED
D7U4X1	8	Protein kinase domain-containing protein	probable serine/threonine-protein kinase At4g35230	UNCHANGED	DOWN	UNCHANGED
F6I1A3	4	Purple acid phosphatase	purple acid phosphatase	UNCHANGED	DOWN	UNCHANGED
D7T9F2	6	Uncharacterized protein	PREDICTED: uncharacterized protein LOC100266416	UNCHANGED	DOWN	UNCHANGED
D7TN04	8	Abhydrolase_3 domain-containing protein	carboxylesterase 1-like	UNCHANGED	DOWN	UNCHANGED
D7U4N2	7	ANK_REP_REGION domain-containing protein	Ankyrin repeat domain-containing protein 2B	UNCHANGED	DOWN	UNCHANGED
D7T6Q0	2	DLH domain-containing protein	endo-1,3;1,4-beta-D-glucanase-like isoform X1	UNCHANGED	DOWN	DOWN
Q0MX16	6	Putative aquaporin	probable aquaporin PIP1-2	UNCHANGED	DOWN	DOWN
D7UAM1	11	Uncharacterized protein	Farnesyl pyrophosphate synthase 1	UNCHANGED	DOWN	DOWN
E0CTI4	8	26S proteasome non-ATPase regulatory subunit 2 homolog	26S proteasome non-ATPase regulatory subunit 2 homolog A	UNCHANGED	DOWN	DOWN
D7SLU3	4	Uncharacterized protein	T-complex protein 1 subunit alpha	UNCHANGED	DOWN	DOWN
Q5PXH0	5	Aquaporin	probable aquaporin PIP2-5	UNCHANGED	DOWN	DOWN
F6HAP8	9	Abhydrolase_3 domain-containing protein	carboxylesterase 1-like	UNCHANGED	DOWN	DOWN
F6HXK4	34	Plasma membrane ATPase	ATPase 10, plasma membrane-type	UNCHANGED	DOWN	DOWN

F6I455	8	Uncharacterized protein	elongation factor 1-gamma	UNCHANGED	DOWN	DOWN
Q4U339	4	Putative hexose transporter	monosaccharide-sensing protein 2	UNCHANGED	DOWN	DOWN
F6HXL1	8	Proteasome subunit alpha type	proteasome subunit alpha type-5	UNCHANGED	DOWN	DOWN
F6GZH5	5	Uncharacterized protein	heat shock cognate protein 80-like	UNCHANGED	DOWN	DOWN
D7T6P4	4	Glutamine synthetase	glutamine synthetase leaf isozyme, chloroplastic	UNCHANGED	DOWN	-
D7TQZ8	6	FMN hydroxy acid dehydrogenase domain-containing protein	peroxisomal (S)-2-hydroxy-acid oxidase GLO1 isoform X1	UNCHANGED	DOWN	-
D7TD95	2	AMP-binding domain-containing protein	long chain acyl-CoA synthetase 8	UNCHANGED	DOWN	-
F6HJ77	3	Uncharacterized protein	indole-3-acetic acid-amido synthetase GH3.17-like	UNCHANGED	DOWN	-
F6I4J3	2	Uncharacterized protein	Glutamate--tRNA ligase, cytoplasmic	UNCHANGED	DOWN	-
D7SVA4	2	Eukaryotic translation initiation factor 3 subunit M	eukaryotic translation initiation factor 3 subunit M-like	UNCHANGED	DOWN	-
F6HGX6	4	LRRNT_2 domain-containing protein	leucine-rich repeat extensin-like protein 4	UNCHANGED	DOWN	-
F6I3Y0	2	Uncharacterized protein	UDP-glycosyltransferase 88F3	UNCHANGED	DOWN	-
D7SV75	3	Eukaryotic translation initiation factor 3 subunit B	eukaryotic translation initiation factor 3 subunit B-like	UNCHANGED	DOWN	-
F6HF87	5	14_3_3 domain-containing protein	14-3-3-like protein GF14 iota	UNCHANGED	DOWN	-
A5ATG8	29	Tubulin beta chain	Tubulin beta-1 chain	DOWN	DOWN	Unique no-rpv_SPV
D7SN28	5	Uncharacterized protein	60S acidic ribosomal protein P2B	DOWN	DOWN	UNCHANGED
F6H3X3	9	Peroxidase	peroxidase 55-like	DOWN	DOWN	UNCHANGED
F6HHQ0	7	Uncharacterized protein	fasciclin-like arabinogalactan protein 2	DOWN	DOWN	UNCHANGED
F6HHR8	2	HipN domain-containing protein	FAM10 family protein At4g22670-like	DOWN	DOWN	UNCHANGED
F6GSK4	19	Tubulin beta chain	Tubulin beta-4 chain	DOWN	DOWN	DOWN
F6HEM4	5	C2 domain-containing protein	Calcium-dependent lipid-binding family protein isoform 1	DOWN	DOWN	DOWN
D7TT38	7	Uncharacterized protein	ubiquitin receptor RAD23d isoform X1	DOWN	DOWN	DOWN
D7T4Z4	2	Uncharacterized protein	Chaperonin like	DOWN	DOWN	DOWN
F6HDM0	6	DUF3700 domain-containing protein	stem-specific protein TSJT1	DOWN	DOWN	DOWN
A5BZF5	19	Tubulin alpha chain	alpha tubulin 1	DOWN	DOWN	DOWN
F6HX55	19	Uncharacterized protein	pleiotropic drug resistance protein 1	DOWN	DOWN	-
D7T467	3	Uncharacterized protein	protein MANNAN SYNTHESIS-RELATED 1	DOWN	DOWN	-

D7U4B6	2	RING-type domain-containing protein	E3 ubiquitin-protein ligase RGLG3 isoform X1	-	DOWN	Unique no-rpv_SPV
D7UBZ3	3	PKS_ER domain-containing protein	cinnamyl alcohol dehydrogenase 1	-	DOWN	DOWN
F6HMF5	2	Xyloglucan endotransglucosylase/hydrolase	xyloglucan endotransglucosylase/hydrolase 2-like	-	DOWN	-
D7TAH9	6	Peroxidase	lignin-forming anionic peroxidase	UP	-	Unique no-rpv_PV
F6HU90	2	Uncharacterized protein	subtilisin-like protease SBT3.5 isoform X1	Unique Rpv1+Rpv3_SPV	-	UNCHANGED
F6HQC8	10	Abhydrolase_3 domain-containing protein	probable carboxylesterase 2	Unique Rpv1+Rpv3_PV	-	UNCHANGED
A5AUN7	3	Laccase	putative laccase-9	Unique Rpv1+Rpv3_PV	-	-
D7TCJ8	3	Phenylalanine ammonia-lyase	phenylalanine ammonia-lyase-like	Unique Rpv1+Rpv3_PV	-	-
F6I290	8	Laccase	laccase-15-like	Unique Rpv1+Rpv3_PV	-	-
F6H2N2	2	Uroporphyrinogen decarboxylase	Peptide-N4-(N-acetyl-beta-glucosaminyl)asparagine amidase A	UNCHANGED	-	UP
A5AEI0	2	Chlorophyll a-b binding protein, chloroplastic	chlorophyll a-b binding protein P4, chloroplastic	UNCHANGED	-	Unique no-rpv_PV
F6HUX3	2	DUF1421 domain-containing protein	protein enabled	UNCHANGED	-	DOWN
E0CSR0	2	Uncharacterized protein	PREDICTED: uncharacterized protein LOC100246927	UNCHANGED	-	DOWN
D7ST12	4	PKS_ER domain-containing protein	probable mannitol dehydrogenase	DOWN	-	UP
F6HF75	2	Uncharacterized protein	Beta-glucosidase 40	-	-	Unique no-rpv_SPV
F6HAY4	2	Uncharacterized protein	UDP-glycosyltransferase 74E2-like	-	-	DOWN
D7T128	2	Glycosyltransferase	UDP-glycosyltransferase 43-like	-	-	DOWN

5 CAPÍTULO III – Alterações metabólicas na interação incompatível entre genótipos de videira portando genes de resistência e o *Plasmopara viticola*

Este capítulo refere-se as atividades realizadas durante o período de doutorado sanduíche na Fondazione Edmund Mach (Trento, Itália).

Alterações metabólicas na interação incompatível entre genótipos de videira portando genes de resistência e o *Plasmopara viticola*

Resumo: A interação metabolômica entre a videira (*Vitis vinifera*) e o patógeno causador do míldio (*Plasmopara viticola*) tem sido relatada em alguns estudos. Contudo, poucos deles reportaram a interação incompatível, causada pela presença de locos de resistência no genoma do hospedeiro e não há relatos de estudos com o uso de genótipos hospedeiros com locos de resistência piramidados. No presente trabalho o objetivo foi caracterizar o perfil metabólico de genótipos de videira contendo diferentes haplótipos associados com a resistência ao *P. viticola* quando expostos ao míldio, em condições controladas. Foram utilizados os genótipos F12P127 (*Rpv3-1+Rpv3-3+Rpv10*) e F12P60 (*Rpv3-1+Rpv12*), além das cultivares Bianca (*Rpv3-1*) Jasmine (*Rpv12*) BC4 (*Rpv1*), Solaris (*Rpv3-3+Rpv10*), pertencentes a coleção de germoplasma da Fondazione Edmund Mach (FEM, Trento, IT). A inoculação foi realizada com um isolado coletado a partir de uma vinifera suscetível, aplicado em solução de 1 X 10^6 esporângios mL^{-1} diluídos em ADE. As coletas para análise química dos compostos metabólicos foram realizadas em 0, 12, 48 e 96 horas posterior a inoculação (hpi) e a análise metabolômica foi realizada na FEM, utilizando protocolos estabelecidos para os compostos primários, fenólicos, voláteis e lipídicos. Verificou-se que a alteração nos compostos metabólicos, em resposta a interação incompatível da *V. vinifera* com o *P. viticola* ocorre nas primeiras horas após a inoculação. A resposta metabólica foi heterogênea, pois em cada genótipo estudado a alteração em metabólitos foi diferente entre os genótipos, apesar de padrão similar no contexto geral. A resposta metabólica para a interação incompatível entre *V. vinifera* e *P. viticola* nas primeiras horas após a inoculação aponta para a indução da morte celular como mecanismo de hipersensibilidade nos genótipos estudados.
Palavras-chave: *Vitis vinifera*, Genótipos PIWI, Metabolômica, resistência genética.

5.1 INTRODUÇÃO

O míldio da videira, causado pelo oomiceto, biotrófico obrigatório *P. viticola*, possui elevada capacidade de adaptação a distintas condições ambientais e do hospedeiro (DELMOTTE et al., 2014). Este é o principal causador de danos na viticultura, responsável pela adoção de intensas aplicações de agrotóxicos no cultivo da videira (BATTISTON et al., 2019; THUERIG et al., 2018), causando elevados prejuízos econômicos (TAYLOR; COOK, 2018) e ambientais (MARINHO et al., 2020; VALLEJO et al., 2019; VIVEROS SANTOS et al., 2018), ameaçando a sustentabilidade da cadeia produtiva.

O impacto do *P. viticola* é também refletido na composição química do vinho. Um estudo caracterizando os compostos aromáticos de vinhos das cultivares Cabernet Sauvignon e Merlot demonstrou que a presença do míldio está associada ao surgimento de compostos *off-flavor*, como a reminiscência de frutas herbáceas e cozidas, além de maior concentração de lactonas, aldeídos e metoxipirazinas (PONS et al., 2018). Em outro estudo, empregando a metabolômica para descrever a interação do *P. viticola* com a videira observou-se a presença de alguns compostos lipídios, tais como ceramidas e derivados de ácido araquidônico e eicosapentaenoico, que podem ser utilizados como biomarcadores da presença do patógeno (NEGREL et al., 2018).

A metabolômica busca estudar o maior número de metabólitos possíveis dentro de um sistema (CEVALLOS-CEVALLOS et al., 2009). Esta técnica tem sido cada vez mais frequente no estudo de interações entre plantas e patógenos (CHEN; MA; CHEN, 2019). Na videira, estudos utilizando a metabolômica foram conduzidos descrevendo interações de compatibilidade com patógenos (HONG et al., 2012; LEMAITRE-GUILLIER et al., 2020), inclusive com o míldio (BILLET et al., 2020). Estudos com interações incompatíveis também foram efetuados com genótipos portando o loco Rpv3-1 (associado com a resistência ao míldio), em condições controladas (ALI et al., 2012; CHITARRINI et al., 2017). Estes estudos evidenciam que o emprego da metabolômica tem ganhado espaço nos últimos anos como facilitadora do processo de seleção no melhoramento genético da videira para resistência a patógenos, como o *P. viticola* (BUONASSISI et al., 2017a).

Com base neste contexto, o objetivo com o presente trabalho foi caracterizar o perfil metabólico de genótipos de videira contendo diferentes haplótipos associados com a resistência ao *P. viticola* quando expostos ao referido patógeno, em condições controladas.

5.2 MATERIAL E MÉTODOS

5.2.1 Material vegetal

Para este estudo foram utilizadas as linhas avançadas do programa de melhoramento genético da videira da Fondazione Edmund Mach (FEM) F12P127 (*Rpv3-1+Rpv3-3+Rpv10*) e F12P60 (*Rpv3-1+Rpv12*), além das cultivares Bianca (*Rpv3-1*) Jasmine (*Rpv12*) BC4 (*Rpv1*), Solaris (*Rpv3-3+Rpv10*) e Pinot Noir (*rpv*), esta última com ausência de locos associados com a resistência genética ao *P. viticola*. As plantas utilizadas no experimento foram geradas a partir de material propagativo coletado de matrizes oriundas da coleção de germoplasma da FEM, em San Michele all'Adige (Trento, Itália, 46° 12' 0" N, 11° 8' 0" L), mantidas em campo de cultivo aberto.

Estacas lenhosas com três gemas, coletadas no período hibernal (n = 45) foram submetidas ao enraizamento em vasos contendo substrato comercial, na ausência de fitorreguladores. A irrigação foi fornecida via sistema de gotejamento para evitar o surgimento natural do míldio, favorecido pelo molhamento foliar. Quando as plantas apresentaram ao menos 12 folhas na brotação principal, foram separadas em 3 grupos homogêneos para cada genótipo e cada grupo homogêneo representou uma réplica biológica. Foram mantidas no experimento somente as plantas saudáveis, sem evidências de doenças foliares, para serem então inoculadas com o *P. viticola*.

5.2.2 Inoculação do míldio

A inoculação do *P. viticola* nas plantas selecionadas ao acaso foi realizada via pulverização foliar. Para isto, esporos do *P. viticola* foram coletados a partir de folhas em um vinhedo não tratado com agrotóxicos e imediatamente congelados a -20 °C. Antes da montagem do experimento, estes esporos foram descongelados em água e aplicado em discos foliares obtidos a partir de folhas jovens de *V. vinifera* e propagados *in vitro* por 14 dias.

Para a propagação do patógeno, foram utilizadas placas de Petri com 15 cm de diâmetro, onde foi acomodado uma lâmina de papel filtro, embebido em água destilada esterilizada (ADE). Logo, os discos foliares foram cortados, utilizando um fura-rolhas de 1.1 cm de diâmetro, a partir de folhas previamente desinfetadas em hipoclorito de sódio 0.8%, seguido de tríplice lavagem em ADE. Todo o material utilizado foi previamente esterilizado em autoclave a 121 °C por 15 min. Os discos foliares foram depositados com a face abaxial voltada para cima, onde for aplicado, via pulverização, 100 µL da solução contendo esporos do *P. viticola* em suspensão. As placas de Petri contendo os discos inoculados foram acondicionadas em câmara de crescimento a 21 °C e ausência de luminosidade nas primeiras 24 h. As gotículas foram removidas das folhas utilizando papel filtro e as placas foram novamente vedadas e mantidas em câmara de crescimento nas mesmas condições de temperatura e fotoperíodo de 16 h.

Aos 14 dias após a inoculação, os discos foliares que apresentaram esporulação abundante foram lavados em ADE gelada e a solução de esporos foi utilizada para o experimento. As plantas foram inoculadas com uma solução de 1 X 10^6 esporângios mL^{-1} diluídos em ADE, foram utilizados 10 mL $planta^{-1}$. Estas foram mantidas em casa de vegetação nas condições previamente descritas.

5.2.3 Preparação e coleta das amostras

As amostras foram coletadas em quatro pontos de avaliação no tempo, 0, 12, 48 e 96 horas posterior a inoculação (HPI). Foram consideradas para amostragem, a terceira a quinta folha, coletada a partir do ápice da planta, coletada aleatoriamente em cada uma das replicatas biológicas. As folhas amostradas foram imediatamente congeladas em nitrogênio líquido e mantidas em -80 °C até o preparo das e extração dos metabólitos.

5.2.4 Extração e análise de compostos primários

A extração dos compostos primários foi realizada de acordo com protocolo estabelecido para plantas (FIEHN et al., 2008), com algumas modificações para a extração destes compostos a partir de folhas de videira (CHITARRINI et al., 2017). Resumidamente, 0,1 g de folhas frescas maceradas foi submetida a extração pela adição de 1 mL de solvente de

extração a frio (-20 °C) composto de isopropanol/acetonitrila/água (3:3:2, v/v/v). Uma alíquota de 20 µL de uma solução contendo palmítico-D3, nicotínico-D4 e glicose-D7 (1000 mg $^{-1}$) foi adicionado como padrão interno. A mistura de extração foi agitada em vórtex por 10 s, agitada por 5 min a 4 °C e centrifugada a 12.000 g por 2 min a 5 °C. Uma segunda extração foi realizada seguindo o mesmo procedimento. Os dois sobrenadantes foram unidos e ressuspensos em volume final de 5 mL de solvente de extração. Uma alíquota de 250 µL de sobrenadante foi adicionado em um microtubo de 1,5 mL e seco em N_2. A fase solida remanescente foi ressuspensa em 500 µL de acetonitrila/água (50:50, v/v), submetido ao vortex por 10 s, sonicado e centrifugado a 12.000 g por 2 min. O sobrenadante foi então transferido para um microtubo de 1,5 mL e novamente seco em N_2. O extrato seco foi submetido a derivatização, primeiro pela adição de 20 µL de cloridrato de metoxamina em piridina (20 mg mL^{-1}) para inibir a ciclização de açúcares redutores e agitado a 30 °C por 1 h. Em seguida foi adicionado 80 µL de N-metil-Ntrimetilsilil-trifluoroacetamida com 1% de trimetilclorossilano para trimetrilsililação dos prótons ácidos e agitado por 30 min a 37 °C. Finalmente, foram adicionados 5 µL de uma solução contendo decano heptadecano (1 g L^{-1}) para monitorar a análise cromatográfica e as condições instrumentais. O extrato derivatizado foi então transferido para os *vials* e 1 µL deste foi injetado para análise no GC/MS.

5.2.5 Extração e análise de lipídios

A análise lipídica foi realizada utilizado método otimizado para tecido foliar de videira (CHITARRINI et al., 2017), sugerido a partir de modificações do método de extração de Folch (DELLA CORTE et al., 2015; FOLCH; LEES; SLOANE, 1957). Sucintamente, 300 µL de metanol foram adicionados a 100 mg de folhas maceradas, a mistura foi agitada em vortex por 30 s, em seguida, foram adicionados 600 µL de clorofórmio contendo hidroxil tolueno butilado (500 mg L^{-1}) e 10 µL do padrão interno (ácido docosahexaenóico 100 µg mL^{-1}), as amostras foram homogeneizadas por 1 h a 60 rpm em agitador orbital. Foi então adicionado 250 µL de água e as amostras foram centrifugadas a 3600 g por 10 min. A camada inferior, rica em lipídeos, foi recolhida e reextraída por adição de 400 µL de clorofórmio/metanol/água (86:14:1, v/v/v). As amostras foram novamente centrifugadas a 3600 rpm por 10 min e a camada inferior, rica em lipídeos foi coletada. Ambas as frações de clorofórmio foram fundidas e evaporadas em N_2. As amostras foram ressuspensas em 300 µL de acetonitrila/2-propanol/água (65:30:5, v/v/v) contendo o colesterol padrão interno em concentração de 1 µg mL^{-1} e transferidas para um *vial*. A separação foi realizada utilizando um UHPLC Dionex 3000 (ThermoFisher Scientific, Alemanha). Com uma coluna RP Ascentis Express (15 cm x 2.1 mm; 2.7 µm C18), seguindo um gradiente linear multipasso de 30 min. O sistema UHPLC foi acoplado a um

espectrômetro de massa triplo-quadrupolo API 5500 (Applied Biosystems/MDS Sciex) equipado com uma fonte de ionização por electrospray (ESI). Os compostos foram identificados com o auxílio do software Analyst com base em seu verdadeiro padrão de referência, tempo de retenção e qualificador de íon quantificador, usando as curvas de calibração expressos em mg kg^{-1} de folhas frescas.

5.2.6 Extração e análise de componentes fenólicos

Para a determinação dos compostos fenólicos foi empregado um protocolo desenvolvido para frutas (VRHOVSEK et al., 2012), com adaptações para tecido foliar da videira (CHITARRINI et al., 2017). Folhas frescas foram trituradas e uma alíquota de 100 mg foi adicionada a 400 µL de clorofórmio e 600 µL de metanol/água (2:1, v/v). uma alíquota de 20 µL de ácido gentísico (50 mg L^{-1}) e ácido rosmarínico (50 mg L^{-1}) foram adicionados como padrões internos. A mistura de extração foi agitada por 15 min em agitador orbital e posteriormente centrifugada por 5 min a 15000 g a 4 °C. A fase aquosa-metanólica superior foi coletada e reservada. A extração foi repetida por adição de 600 µL de metanol/água (2:1, v/v) e 200 µL de clorofórmio, seguido de centrifugação por 5 min a 15000 g a 4 °C. A fase aquosa-metanólica foi recolhida e combinada com a anterior e foram evaporadas em N_2. As amostras foram ressuspensas em 500 µL de metanol/água (1:1, v/v). As amostras foram ressuspensas em 500 µL de metanol/água (1:1, v/v), centrifugadas e transferidas cuidadosamente para um *vial*. A análise cromatográfica foi realizada em sistema Waters Acquity UPLC (Milford), com coluna Waters Acquity HSS T3 (100 mm x 2,1 mm; 1,8 µm). A detecção por espectrometria de massa foi realizada em detector de espectrômetro de massa triplo-quadrupolo Waters Xevo (Milford) com uma fonte de ionização por electrospray (ESI). Os compostos foram identificados com base em seu padrão de referência, tempo de retenção e qualificador e íon quantificador, para a quantificação foi utilizada a curva de calibração e expressos como mg kg^{-1} de folhas frescas. O processamento de dados foi realizado usando o software Waters MassLynx V4.1.

5.2.7 Extração e análise de compostos voláteis

Os compostos voláteis foram extraídos por microextração em fase sólida, utilizando um metodologia estabelecida para tecidos de videira (CHITARRINI et al., 2017; MATARESE et al., 2014; SALVAGNIN et al., 2016). A extração foi realizada com 100 mg de folhas frescas adicionadas em frascos de vidro de 10 mL, contendo 2 mL de tampão (100 mM Na_2HPO_4 e 50 mM de ácido cítrico pH 5,0), 200 mg de NaCl e 5 µL de 1-heptanol (25 mg L^{-1}) como padrão interno. As amostras foram mantidas a 60 °C por 20 min e os compostos no *headspace* foram capturados por 35 min a 60 °C. Um cromatógrafo de gás Trace GC Ultra acoplado a um espectrômetro de massa (EM) Quantum XLS (Thermo Electron Corporation, Estados Unidos)

foi utilizado para separar os compostos, equipado com uma coluna Stabilwax® DA de sílica fundida (30 m x 0,25 mm x 0,25 μm) (Restek Corporation, Estados Unidos). O *headspace* foi amostrado utilizando fibra de 2 cm DVB/CAR/PDMS 50/30 μm (Supelco, Estados Unidos). Os compostos foram dessorvidos na entrada do cromatógrafo de gás a 250°C por 4 min. O detector do EM foi operado no modo de varredura, na faixa de massa de *40 a 450 m/z*, com tempo de varredura de 0,2 s e a linha de transferência para o sistema EM foi mantida a 250 °C. O processamento de dados foi realizado utilizando o software XCALIBUR^{TM} v.2.2. Para a identificação de compostos voláteis foi utilizado a letra "A" para compostos com espectro de massa e tempo de retenção comparáveis aos do padrão puro; "B" para aqueles com correspondência de RI em uma coluna de fase semelhante com o banco de dados NIST MS Search 2.0 e; "C" para aqueles identificados na base de dados espectral de massa NIST MS Search 2.0 (SUMNER et al., 2007). A temperatura linear experimental de cada composto foi calculada usando uma série de *n*-alcanos (C10-C30) nas mesmas condições experimentais das amostras. Os resultados foram expressos de forma semiquantitativa e expressos em μg kg^{-1} utilizando 1-heptanol como padrão interno.

5.2.8 Análise de dados

As avaliações foram realizadas com o material coletado em dois anos, assim, foi considerado como diferencialmente expressos, somente os metabolitos encontrados em comum para os dois anos avaliados. A análise estatística e a visualização dos dados foram realizadas em linguagem R (R CORE TEAM, 2019). Valores ausentes foram imputados com um valor aleatório entre zero e o limite da quantificação. As concentrações foram transformadas para logaritmo de *x* na base 10, com a finalidade de tornar a distribuição dos dados mais próximas da aderência a distribuição normal (VAN DEN BERG et al., 2006). A análise de componentes principais (PCA) foi realizada no conjunto de dados multidimensional obtidos, após a centralização da média e escala unitária, utilizando os pacotes FactoMineR e Factoextra implementados na linguagem R (KASSAMBARA; MUNDT, 2020; LÊ; JOSSE; HUSSON, 2008). A estatística t foi calculada utilizando o pacote Stats implementado na linguagem R.

5.3 RESULTADOS E DISCUSSÃO

Nos genótipos portadores de resistência, utilizados neste estudo, foram identificados ao total a alteração em 144 metabólitos. Destes, 48 são compostos voláteis, 47 compostos primários, 40 compostos fenólicos e 9 compostos lipídicos. Dentre os compostos voláteis, a classe com maior número de metabolitos que sofreram alterações nos níveis de expressão foram os aldeídos (10) e álcoois (8), além de 9 metabólitos desconhecidos, as demais classes de

compostos voláteis possuíram menor número de metabólitos alterados, como as cetonas (4), terpenoides (3), terpenos (3), ésteres (3), benzonoides (2), ácidos (2), hidrocarbonetos (1) e outros (3). Dentre os compostos primários, a classe dos ácidos orgânicos e dos açúcares possuíram ambos, 18 metabólitos com expressão alterada. Além destas, foi alterada também a concentração de metabólitos pertencentes a classe dos aminoácidos (8) e das aminas (3). Dentre os compostos fenólicos a principal classe alterada foram flavonoides e flavan-3-ols, que possuíram 9 e 8 metabólitos alterados, respectivamente, além destas, foram alterados também a expressão de metabólitos pertencentes as classes dos derivados do ácido benzoico (4), fenilpropanoides (4), stilbenos e estilbenoides (4), cumarina (3), dihidrocalcona (1), flavanona (1), flavona (1) e outros (5). Por fim, os compostos lipídicos foram apresentaram a menor alteração, para estes compostos, a maior alteração de metabólitos foi verificada na classe dos glicerolipídios (4) e dos ácidos graxos (3), além destes, também foi identificado um metabólito alterado na classe dos glicerofosfolipídios e outro na classe dos esfingolipídios (Figura 1).

5.3.1 Alterações metabólicas em 12 hpi

Em 12 hpi foi observada a alteração em 43 metabólitos, destes, a maior parte pertencia aos compostos primários (14) e fenólicos (14), seguido por compostos voláteis (11) e compostos lipídicos (4) (Figura 1 A). Dentre os compostos primários, açúcares foi a classe com maior alteração na concentração dos metabólitos (8), seguido por ácidos orgânicos (3), aminoácidos (2) e aminas/outros (1). Dentre os compostos fenólicos a classe dos flavonóides apresentou o maior número de metabólitos com expressão alterada (6), seguido pelos fenilpropanóides (4), derivados do ácido benzoico (2), flavonas (1) e flavan-3-ols (1). Dentre os compostos voláteis, foi observado maior número de classes com metabólitos alterados, dentre estes, destaca-se os álcoois (3) e aldeídos (2), além destes, as classes benzenoidos, cetonas, terpenos, outros e desconhecidos, apresentaram alteração em um metabólito, para cada classe. Os lipídeos apresentaram o menor número de metabólitos alterados, estes agrupam-se nas classes de ácidos graxos (2), glicerolipídios (1) e esfingolipídios (1).

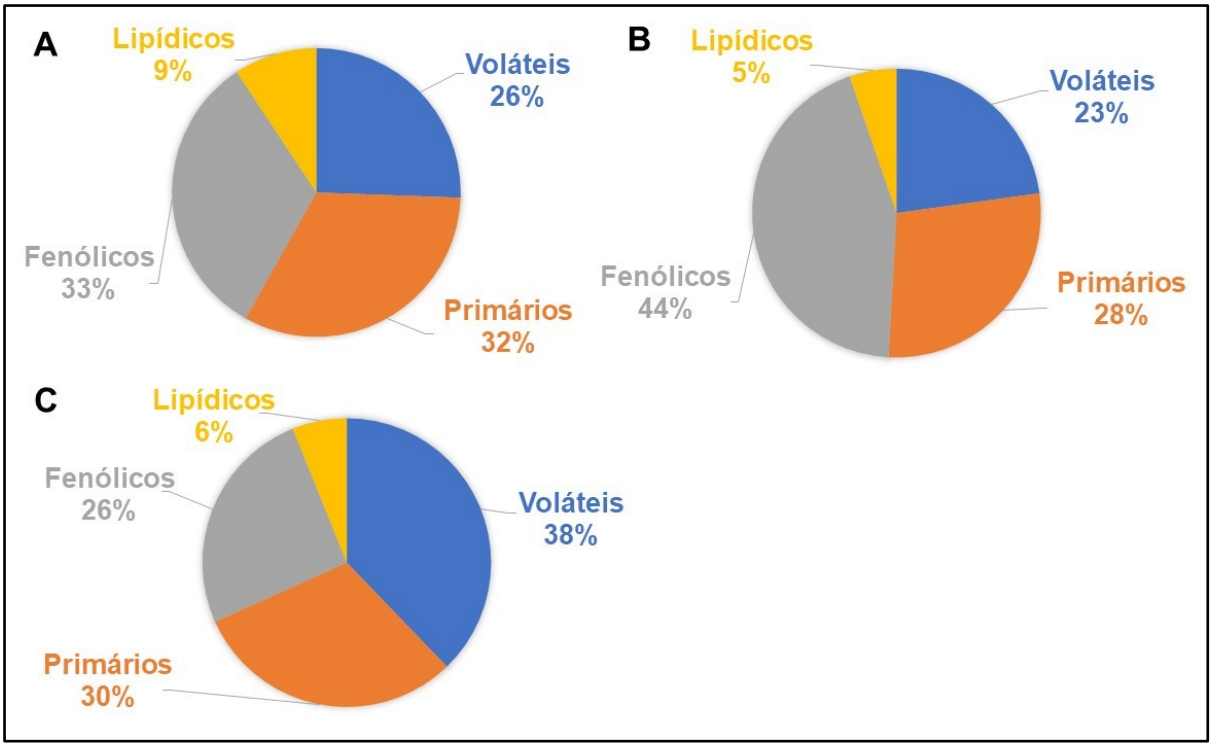

Figura 1. Distribuição relativa dos compostos metabólitos alterados em A) 12; B) 48 e; C) 96 horas após a inoculação do *Plasmopara viticola* em sete genótipos com diferentes constituições genéticas de resistência ao míldio. Neste estudo foram incluídos os genótipos *Rpv1*, *Rpv3-1*, *Rpv12*, *Rpv3-1+Rpv12*, *Rpv3-3+Rpv10*, *Rpv3-1+Rpv3-3+Rpv10*.

Neste ponto de coleta, a concentração do ácido docosahexaenoico foi regulado positivamente e este foi o único metabolito em que todos os genótipos deste estudo apresentaram a mesma variação. Com exceção da cv. Bianca, os demais genótipos apresentaram também elevação no conteúdo de ceramida, da mesma forma, com exceção do genótipo F12P127, os demais genótipos apresentaram elevação da concentração de ácido tartárico e redução da concentração de Cis-3-hexenylacetato. O genótipo F12P127 apresentou outras dissimilaridades em comparação aos demais, como, o único a elevar a concentração de 2-penten-1-ol, 2-heptenal e Ocimene-izomer2, além de ser o único a reduzir as concentrações de nonanal e trans-2-octenal (Figura 2).

Os genótipos BC4 e Bianca apresentaram redução do teor de ácido ascórbico, este comportamento pode estar relacionado a uma resposta muito precoce de indução da reação de hipersensibilidade, pois a deficiência de ácido ascórbico pode causar a morte celular (PAVET et al., 2005). A redução dos níveis de catechol em 'Jasmine' e mais fortemente no F12P127, que atua na rota do ácido salicílico, permite levantar duas hipóteses para estes genótipos, a menor catalização do ácido salicílico ou a elevação da atividade da enzima GUAIACOL O-METHYLTRANSFERASE, produzindo o guaiacol a partir da metilação do catechol (VAN

GELDER; FORRESTER; AKHTAR, 2020). Todavia, não foram observadas alterações significativas nos conteúdos destes outros metabólitos para estes genótipos. Não obstante, a redução nos níveis do catecol pode ser também devida a menor degradação das auxinas, em especial o ácido indol-3-acético (DONOSO et al., 2017).

O aumento da concentração do ácido docosahexaenoico em todos os genótipos, deve-se provavelmente a atuação do patógeno, tendo em vista que plantas terrestres não possuem a maquinaria enzimática para sintetizar este ácido graxo (WALSH et al., 2016). O cis-3-hexenilacetato é um composto volátil que desempenha um papel chave na indução da resistência via jasmonatos, principalmente em resposta a danos mecânicos ou por ataques entomológicos (FROST et al., 2008; ZHANG et al., 2013). Portanto a redução na concentração deste metabólito nas primeiras horas para a maioria dos genótipos, é um indício de que a nestes genótipos a via dos jasmonatos suprimida, ou, evitada, ao passo que tal alteração não é verificada para o genótipo F12P127. Além destas alterações metabólicas, destaca-se a elevação nos teores de ceramida em todos os genótipos, com exceção da cv. ‘Bianca’, este metabolito é um esfingolipídio que desempenha um papel fundamental na indução da morte celular, em resposta a reação de hipersensibilidade (HUBY et al., 2020). Este resultado aponta para uma rápida resposta na indução da morte celular para os genótipos BC4, Jasmine, Solaris, F12P60 e F12P127.

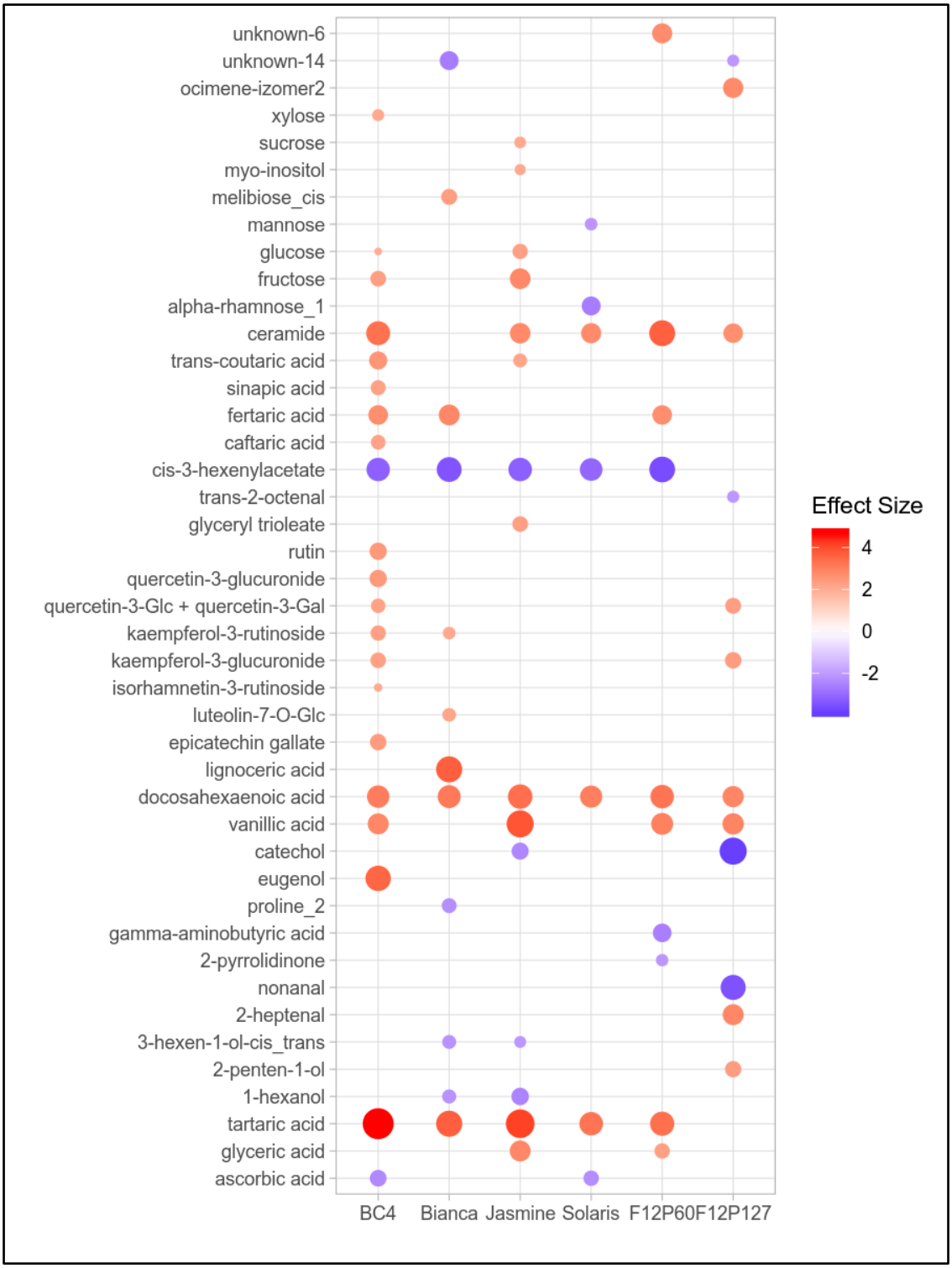

Figura 2. Alteração nas concentrações de metabólitos encontrados em folhas de videira com diferentes locos de resistência genética (*Rpv1*, *Rpv3-1*, *Rpv12*, *Rpv3-1+Rpv12*, *Rpv3-3+Rpv10*, *Rpv3-1+Rpv3-3+Rpv10*) 12 horas após a inoculação com *Plasmopara viticola*.

5.3.2 Alterações metabólicas em 48 hpi

Aos 48 hpi foi verificado alteração em 57 metabolitos, destacando-se a alteração nos compostos fenólicos (25), além destes foram observadas alterações em 16 compostos primários,

13 compostos voláteis e 3 compostos lipídicos (Figura 1 B). Dentre os compostos fenólicos, a maior classe de metabólitos alterados foram os flavonoides (9), seguido pelos Flavan-3-ols (5), fenilpropanoides (3) estilbenos + estilbenoides (3), cumarina (1), dihidrocalcona (1), flavonas (1) e outros (2). Dentre os compostos primários, os açúcares representaram novamente a classe com maior número de metabólitos alterados (7), seguido pelos ácidos orgânicos (5), aminoácidos (3) e aminas/outros (1). Dentre os compostos voláteis, foram encontrados 3 metabólitos alterados pertencentes a classe dos ésteres, classe com maior alteração dentre os compostos voláteis, além desta, foi observada alterações nos aldeídos (2), cetonas (2), álcoois (1), benzenoidos (1), terpenos (1), terpenoidos (1) e desconhecidos (2). Dentre os lipídeos, foi observada a alteração em um composto metabólito pertencente a classe dos glicerolipídeos, um glicerofosfolipídeo e um esfingolipídio.

A única alteração significativa para o mesmo metabolito em todos os genótipos avaliados, foi a elevação da concentração do açúcar cis melibiose (Figura 3). A alteração na concentração de açúcares nas células vegetais é comumente relatada durante a interação planta-patógeno (KANWAR; JHA, 2019; ROJAS et al., 2014). Para interação compatível entre a cv. 'Trincadeira' (*V. vinifera*) e o *P. viticola* resultou no acumulo de carboidratos ainda nas primeiras horas após a inoculação do patógeno (NASCIMENTO et al., 2019). Todavia a elevação na concentração dos açúcares, como entrada neste estudo, é também relatada para interações incompatíveis entre planta e patógeno (SCHARTE; SCHÖN; WEIS, 2005).

O acumulo do cis-melibiose, por outro lado, é melhor documentado em estudos envolvendo estresses abióticos, como o estresse por frio (YUANYUAN et al., 2009) e o estresse salino (ARIF et al., 2020; BENJAMIN et al., 2019), como resposta ao diferencial o de potencial, sendo relatado, durante o estresse salino, o acumulo da melibiose, bem como, de outros açúcares (BARNAWAL; SINGH; SINGH, 2019; KREPS et al., 2002). Todavia, não há relatos claros na literatura associando a cis melibiose e a resposta celular a interação compatível ou incompatível com patógenos.

Dentre os demais compostos fenólicos, resultado interessante foi observado para a elevação da concentração de trans- e cis-piceid exclusivamente para a cv. 'Bianca', enquanto as cvs. 'BC4', 'Jasmine' e 'Solaris' apresentaram incremento na concentração do trans-resveratrol. A presença em maior abundancia do trans-resveratrol demonstra que o mecanismo de identificação do patógeno já reconheceu o mesmo e iniciou a síntese de compostos de defesa, pois esta molécula é reconhecidamente associada com a defesa celular e a resposta de resistência (HIPSKIND; PAIVA, 2000; JEANDET; CLÉMENT; CORDELIER, 2019; LIU et al., 2019b). O piceid, por outro lado, é também um estilbeno produzido pela glicosilação do

resveratrol e seu conteúdo nos tecidos de videira é influenciado por fatores genéticos, pelo estágio fisiológico e fenológico e pelo ambiente (DUAN et al., 2015; LI et al., 2017a; PEZET et al., 2004). Todavia, o piceid apresenta atividade microbiana inferior ao resveratrol, estando normalmente associado a defesa da planta contra o estresse luminoso (ANDI et al., 2019; KOBAYASHI et al., 2000; PEZET et al., 2004; URBAN et al., 2018). Ainda assim, diversos estudos relatam o acumulo de piceid, como promotor da resistência contra patógenos (KRZYZANIAK et al., 2018; LIU et al., 2011; URBAN et al., 2018).

A presença de estilbenos está de acordo com o relatado na literatura e bem documentado para tecidos de videira atacados pelo *P. viticola* (CESCO et al., 2020; GOUVEIA et al., 2021; NOGUEIRA JÚNIOR et al., 2020). Estes compostos fenólicos desempenham importante atividade antimicrobiana em diversos organismos (DE FILIPPIS et al., 2019; GUTIÉRREZ-ESCOBAR et al., 2021; OLIVIER; SPRING; GINDRO, 2018; RIGHI et al., 2020). Contudo, além dos estilbenos, metabolitos ligados a morte celular também apresentaram importante alteração, mecanismo este que é reconhecidamente importante nos processos de defesa em plantas resistentes a patógenos biotróficos, como o *P. viticola* (COMBIER et al., 2019; MA et al., 2018). Desta forma, os resultados demonstram uma atuação em conjunta no tecido celular da videira, entre mecanismos de ação antimicrobiana e indução da morte celular da célula vegetal em genótipos portadores de genes associados com a resistência ao *P. viticola*.

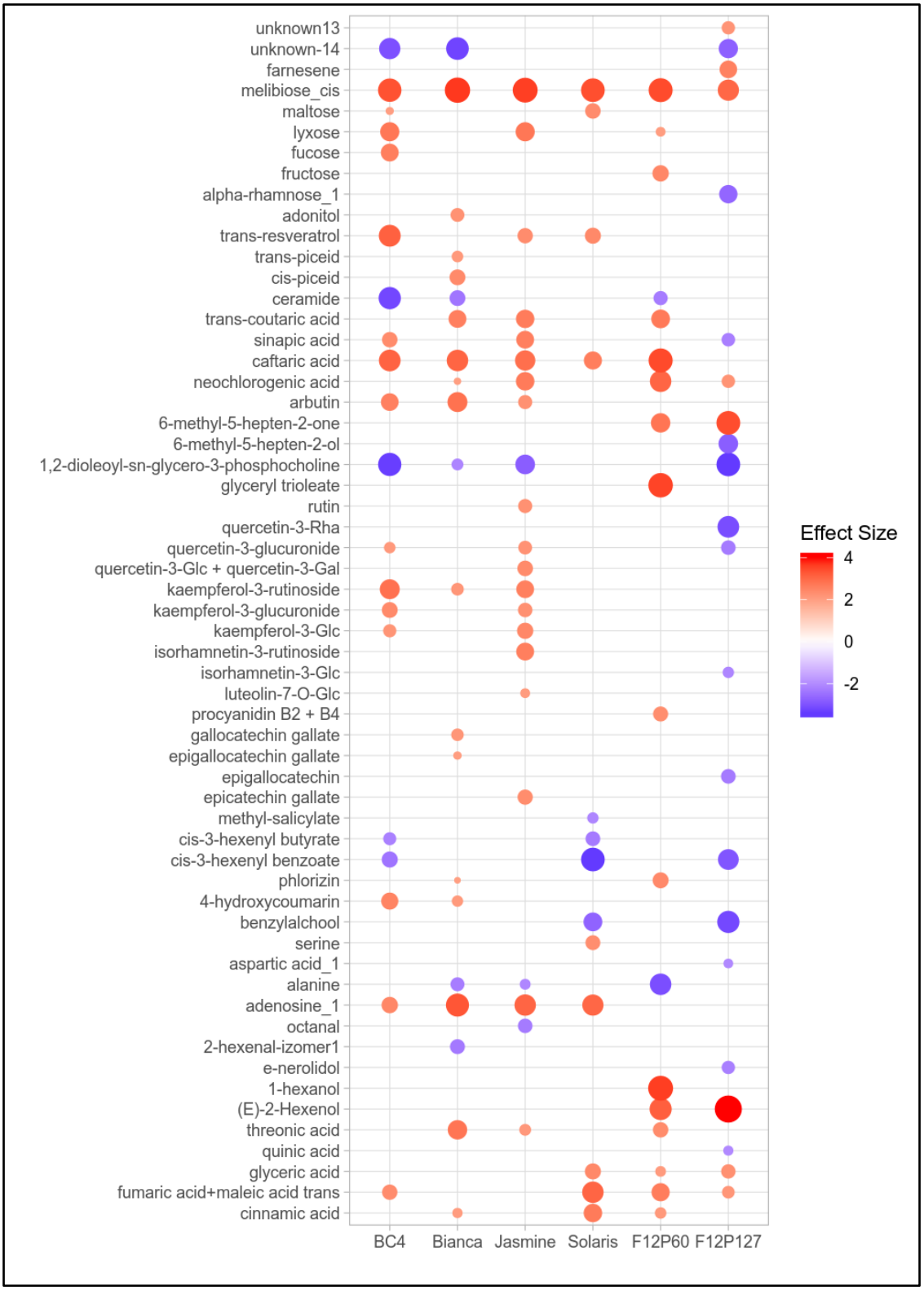

Figura 3. Alteração nas concentrações de metabólitos encontrados em folhas de videira com diferentes locos de resistência genética (*Rpv1*, *Rpv3-1*, *Rpv12*, *Rpv3-1+Rpv12*, *Rpv3-3+Rpv10*, *Rpv3-1+Rpv3-3+Rpv10*) 48 horas após a inoculação com *Plasmopara viticola*.

5.3.3 Alterações metabólicas em 96 hpi

O maior número de metabolitos alterados foi observado aos 96 hpi, neste ponto de observação foram encontrados 82 metabolitos alterados. Dentre estes, a maior parte pertencia aos compostos voláteis (31), seguido por compostos primários (25), fenólicos (21) e lipídicos (5) (Figura 1 C). Dentre os compostos voláteis foram observadas 11 classes metabólicas alteradas, destas a principais alterações foram observadas nos aldeídos (7), seguido pelos álcoois (5), desconhecidos (5), terpenos (3), ésteres (2), cetonas (2), terpenoides (2), ácidos (1), benzenoidos (1), hidrocarbonetos (1) e outros (2). Os compostos primários alterados agruparam-se em quatro classes de metabólitos, os ácidos orgânicos apresentaram o maior número de metabólitos alterados (13), seguido pelos açúcares (5), aminoácidos (4) e aminas/outros (3). Dentre os compostos fenólicos, foram observadas nove classes metabólicas, a classe com maior número de metabólitos alterados foram os flavonoides (9), seguido pelos derivados do ácido benzoico (2), cumarina (2), flavan-3-ols (2), fenilpropanoide (2), dihidrocalcona (1), flavonas (1), estilbenos (1) e outros (1). Dentre os compostos lipídicos, a classe dos glicerolipídios apresentou a maior alteração na concentração de metabólitos (3), além desta classe, foi observada também alteração em um ácido graxo e um esfingolipídio.

O aumento do número de metabólitos afetados em 96 hpi demonstra que muitos destes estão associados não somente com a resposta de resistência, mas também com o estresse celular causado em decorrência da interação incompatível planta patógeno. A redução nos níveis de ceramidas foi observada em todos os genótipos estudados, retornando aos valores normais, após o pico observado em 12 hpi. Indicando que o processo de indução da morte celular já havia cessado nestes genótipos, conforme discutido anteriormente para a atuação das ceramidas. Este processo é também evidenciado pela redução da concentração de açúcares, revertendo o efeito de concentração destes compostos, observado em 48 hpi.

Dentre os compostos metabólicos que tiveram sua concentração elevada no tecido vegetal neste período, destacam-se os compostos fenólicos, dentre estes, os flavonoides, principalmente os derivados do campferol, rutina e quercetina, bem como os compostos voláteis, principalmente aldeídos e álcoois (Figura 4). Os derivados do campferol, assim como, demais flavonoides, são reconhecidos na literatura por desempenhar importante papel durante a recuperação de estresses celulares, bióticos ou abióticos, principalmente atuando como antioxidantes (MODARRESI et al., 2020; YEDIDIA et al., 2019). A elevação no conteúdo de aldeídos, por sua vez, está associado também em resposta a recuperação celular, após o estresse oxidativo, sendo também uma forma de propagar o sinal, do dano causado pela atuação da

interação incompatível com o patógeno (ENGELBERTH; ENGELBERTH, 2020; YERGALIYEV et al., 2016). Portanto, de modo geral, a composição metabólica observada em 96 hpi, demonstra padrão de recuperação celular após a estresse biótico causado pela interação incompatível com o *P. viticola*.

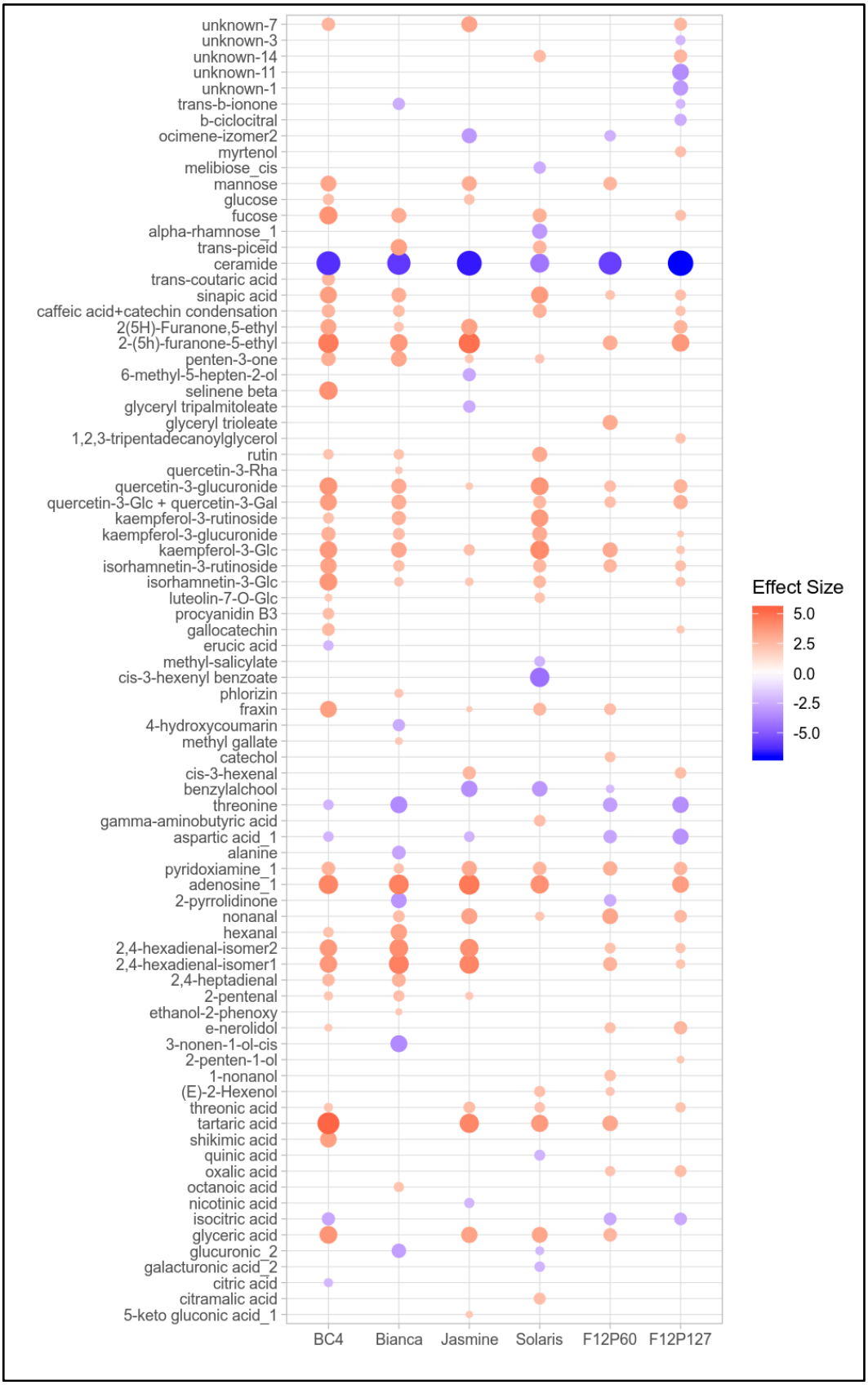

Figura 4. Alteração nas concentrações de metabólitos encontrados em folhas de videira com diferentes locos de resistência genética (*Rpv1*, *Rpv3-1*, *Rpv12*, *Rpv3-1+Rpv12*, *Rpv3-3+Rpv10*, *Rpv3-1+Rpv3-3+Rpv10*) 96 horas após a inoculação com *Plasmopara viticola*.

5.4 CONCLUSÕES

A alteração nos compostos metabólicos, em resposta a interação incompatível da *V. vinífera* com o *P. vitícola*, ocorre nas primeiras horas após o contato.

A resposta é heterogênea, pois genótipos com diferentes locos de resistência apresentam perfis metabólicos distintos quando expostos ao *P. viticola*.

De modo geral, a resposta na alteração metabólica ocorre nas primeiras 12 hpi, se intensificando até 48 hpi; em 96 hpi o perfil metabólico aponta para a recuperação após o estresse celular causado pela interação incompatível.

A resposta metabólica para a interação incompatível entre *V. vinífera* e *P. viticola* nas primeiras horas após a inoculação aponta para a indução da morte celular como mecanismo de hipersensibilidade nos genótipos estudados.

Utilizando os dados obtidos com este trabalho, futuros estudos podem focar esforços no reconhecimento de padrões associados com a morte celular nestes ou em outros genótipos, podendo ser adotadas novas abordagens como a transcriptômica, buscando entender melhor os processos envolvidos que culminaram com a geração destes perfis metabólicos.

6 CONSIDERAÇÕES FINAIS E PERSPECTIVAS

Com o trabalho desenvolvido foram abordadas três etapas das interações da videira (*V. vinifera*) e o patógeno agente causal do míldio (*P. viticola*), na presença de diferentes níveis de resistência genética do hospedeiro. Foi abordada a expressão de genes relacionados com as interações planta-patógeno, compatíveis e incompatíveis, principalmente aqueles ligados a via dos salicilatos e jasmonatos. Além disso, foi desenvolvido um estudo de proteômica em culturas celulares de videira, indicando as proteínas diferencialmente expressas em razão da resposta celular e um estudo de metabolômica, indicando os metabólitos alterados pela reação da planta ao patógeno.

Os resultados apresentados demonstram uma complexa interação do hospedeiro com o patógeno. A resposta de expressão dos genes relacionados a vias de defesa demonstrou atuação simultânea das vias do jasmonato e salicilato, ativadas diferencialmente em diferentes genótipos. O resultado da análise proteômica demonstrou que as proteínas diferencialmente expressas e os processos biológicos ativos variam de acordo com o genoma do hospedeiro. Quando expostos ao *P. viticola*, células com a presença de genes de resistência genética apresentaram menor número de rotas metabólicas afetadas, garantindo o funcionamento das vias metabólicas associadas com a resposta de defesa, enquanto em células suscetíveis, maior número de processos biológicos foram afetados. A análise metabolômica, realizada em cinética, permitiu inferir que a atuação do mecanismo de defesa, faz com que o perfil metabólico dos tecidos afetados pelo *P. viticola* seja modulado nas primeiras horas após a inoculação, com a ativação de compostos metabólicos relacionados com a indução da morte celular e do estresse oxidativo. Nos estágios finais, os metabolitos encontrados estão relacionados principalmente com a recuperação das células devido ao estresse causado pela reação incompatível com o patógeno.

Os resultados obtidos nestes estudos contribuem para o planejamento de estratégias de melhoramento genético da videira voltado para a produção de genótipos portadores de resistência genética ao míldio, principal causador de danos na viticultura. Em particular, os resultados auxiliam a definição de estratégias de combinações de locos associados com a resistência a este patógeno, via piramidação de genes. Não obstante, estes dados permitem avançar o conhecimento sobre o funcionamento dos mecanismos fisiológicos e bioquímicos, nos níveis de expressão gênica, mudanças no proteoma e modificações metabólicas que ocorrem devido a reação de resistência da videira ao *P. viticola*.

7 REFERÊNCIAS

ACANDA, Y. et al. Changes in abscisic acid metabolism in relation to the maturation of grapevine (Vitis vinifera L., cv. Mencía) somatic embryos. **BMC Plant Biology**, v. 20, n. 1, p. 487, 1 dez. 2020.

ALBERT, I. et al. An RLP23-SOBIR1-BAK1 complex mediates NLP-triggered immunity. **Nature Plants**, v. 1, n. 10, p. 1–9, 5 out. 2015.

ALI, K. et al. Alterations in grapevine leaf metabolism upon inoculation with Plasmopara viticola in different time-points. **Plant Science**, v. 191–192, p. 100–107, ago. 2012.

ALI, S. et al. Pathogenesis-related proteins and peptides as promising tools for engineering plants with multiple stress tolerance. **Microbiological Research**, v. 212–213, p. 29–37, 1 jul. 2018.

ALLÈGRE, M. et al. Stomatal deregulation in Plasmopara viticola-infected grapevine leaves. **New Phytologist**, v. 173, n. 4, p. 832–840, 1 mar. 2007.

ALONSO-VILLAVERDE, V. et al. The effectiveness of stilbenes in resistant Vitaceae: Ultrastructural and biochemical events during Plasmopara viticola infection process. **Plant Physiology and Biochemistry**, v. 49, n. 3, p. 265–274, 1 mar. 2011.

AMARO, T. M. M. M. et al. A Perspective on CRN Proteins in the Genomics Age: Evolution, Classification, Delivery and Function Revisited. **Frontiers in Plant Science**, v. 8, n. FEBRUARY, p. 99, 3 fev. 2017.

ANDERSON, J. P. et al. Antagonistic interaction between abscisic acid and jasmonate-ethylene signaling pathways modulates defense gene expression and disease resistance in arabidopsis. **Plant Cell**, v. 16, n. 12, p. 3460–3479, 1 dez. 2004.

ANDI, S. A. et al. The effect of light, phenylalanine and methyl jasmonate, alone or in combination, on growth and secondary metabolism in cell suspension cultures of Vitis vinifera. **Journal of Photochemistry and Photobiology B: Biology**, v. 199, p. 111625, 1 out. 2019.

ANTONIW, J. F. et al. Comparison of Three Pathogenesis-related Proteins from Plants of Two Cultivars of Tobacco Infected with TMV. **Journal of General Virology**, v. 47, n. 1, p. 79–87, 1 mar. 1980.

AOKI, Y. et al. Monitoring of a Single Point Mutation in the PvCesA3 Allele Conferring Resistance to Carboxylic Acid Amide Fungicides in Plasmopara viticola Populations In Yamanashi Prefecture, Japan. **PLANT HEALTH PROGRESS** □, v. 16, n. 2, 2015.

ARIF, Y. et al. **Salinity induced physiological and biochemical changes in plants: An omic approach towards salt stress tolerancePlant Physiology and Biochemistry**Elsevier Masson SAS, , 1 nov. 2020.

ASAI, T. et al. Map kinase signalling cascade in Arabidopsis innate immunity. **Nature**, v. 415, n. 6875, p. 977–983, 28 fev. 2002.

ATTARD, A. et al. Transcriptome dynamics of Arabidopsis thaliana root penetration by the oomycete pathogen Phytophthora parasitica. **BMC Genomics**, v. 15, n. 1, p. 1–20, 29 jun. 2014.

AZIZ, A. et al. **Editorial: Recent Advances on Grapevine-Microbe Interactions: From Signal Perception to Resistance ResponseFrontiers in Plant Science**Frontiers Media S.A., , 29 jul. 2020. Disponível em: <https://www.ncbi.nlm.nih.gov/pmc/articles/PMC7403216/>. Acesso em: 25 set. 2020

BARNAWAL, D.; SINGH, R.; SINGH, R. P. Role of Plant Growth Promoting Rhizobacteria in Drought Tolerance. In: **PGPR Amelioration in Sustainable Agriculture**. [s.l.] Elsevier, 2019. p. 107–128.

BATTISTON, E. et al. Innovative Delivery of Cu(II) Ions by a Nanostructured Hydroxyapatite: Potential Application in Planta to Enhance the Sustainable Control of *Plasmopara viticola*. **Phytopathology®**, v. 109, n. 5, p. 748–759, 1 maio 2019.

BAUDOIN, A. et al. QoI Resistance of Plasmopara viticola and Erysiphe necator in the Mid-Atlantic United States . **Plant Health Progress**, v. 9, n. 1, p. 25, 27 jan. 2008.

BELHADJ, A. et al. Methyl jasmonate induces defense responses in grapevine and triggers protection against Erysiphe necator. **Journal of Agricultural and Food Chemistry**, v. 54, n. 24, p. 9119–9125, 29 nov. 2006.

BELLIN, D. et al. Resistance to *Plasmopara viticola* in grapevine 'Bianca' is controlled by a major dominant gene causing localised necrosis at the infection site. **Theoretical and Applied Genetics**, v. 120, n. 1, p. 163–176, 11 dez. 2009.

BENJAMIN, J. J. et al. Metabolomic insights into the mechanisms underlying tolerance to salinity in different halophytes. **Plant Physiology and Biochemistry**, v. 135, p. 528–545, 1 fev. 2019.

BERNSDORFF, F. et al. Pipecolic Acid Orchestrates Plant Systemic Acquired Resistance and Defense Priming via Salicylic Acid-Dependent and -Independent Pathways. **The Plant cell**, v. 28, n. 1, p. 102–29, 1 jan. 2016.

BHATTARAI, G. et al. A Novel Grape Downy Mildew Resistance Locus from Vitis rupestris . **American Journal of Enology and Viticulture**, v. 72, n. 1, p. ajev.2020.20030, 20

ago. 2020.

BIAN, S. et al. Combinatorial regulation of CLF and SDG8 during Arabidopsis shoot branching. **Acta Physiologiae Plantarum**, v. 38, n. 7, 1 jul. 2016.

BILLET, K. et al. Semi-Targeted Metabolomics to Validate Biomarkers of Grape Downy Mildew Infection Under Field Conditions. **Plants**, v. 9, n. 8, p. 1008, 10 ago. 2020.

BLASI, P. et al. Construction of a reference linkage map of *Vitis amurensis* and genetic mapping of Rpv8, a locus conferring resistance to grapevine downy mildew. **Theor Appl Genet**, v. 123, p. 43–53, 2011.

BLASSER, M.; WELTZIEN, H. C. Epidemiologische Studien an Plasmopara viticola zur Verbesserung der Spritzterminbestimmung. **Journal of Plant Diseases and Protection**, v. 86, n. 8, p. 489–498, 1979.

BLUM, M.; WALDNER, M.; GISI, U. A single point mutation in the novel PvCesA3 gene confers resistance to the carboxylic acid amide fungicide mandipropamid in Plasmopara viticola. **Fungal Genetics and Biology**, v. 47, n. 6, p. 499–510, jun. 2010.

BOS, J. I. B. et al. The C-terminal half of Phytophthora infestans RXLR effector AVR3a is sufficient to trigger R3a-mediated hypersensitivity and suppress INF1-induced cell death in Nicotiana benthamiana. **Plant Journal**, v. 48, n. 2, p. 165–176, 1 out. 2006.

BOSO, S. et al. Susceptibility of 44 grapevine (Vitis vinifera L.) varieties to downy mildew in the field. **Australian Journal of Grape and Wine Research**, v. 17, n. 3, p. 394–400, 1 out. 2011.

BOVE, F. et al. Assessment of Resistance Components for Improved Phenotyping of Grapevine Varieties Resistant to Downy Mildew. **Frontiers in Plant Science**, v. 10, 27 nov. 2019.

BOVE, F.; ROSSI, V. components of partial resistance to *Plasmopara viticola* enable complete phenotypic characterization of grapevine varieties. **Scientific Reports**, v. 10, n. 585, 2020.

BOZKURT, T. O. et al. **Oomycetes, effectors, and all that jazzCurrent Opinion in Plant Biology**Elsevier Current Trends, , 1 ago. 2012.

BRILLI, M. et al. A multi-omics study of the grapevine-downy mildew (Plasmopara viticola) pathosystem unveils a complex protein coding-A nd noncoding-based arms race during infection. **Scientific Reports**, v. 8, n. 1, p. 1–12, 1 dez. 2018.

BUESO, E. et al. The single-subunit RING-type E3 ubiquitin ligase RSL1 targets PYL4 and PYR1 ABA receptors in plasma membrane to modulate abscisic acid signaling. **The Plant Journal**, v. 80, n. 6, p. 1057–1071, 1 dez. 2014.

BUONASSISI, D. et al. Breeding for grapevine downy mildew resistance: a review of “omics” approaches VITISANA View project COST FA1003 View project. 2017a.

BUONASSISI, D. et al. A new in vitro method for the assessment of *Plasmopara viticola* resistance on grapevine inflorescences. **Acta Horticulturae**, v. 1172, p. 21–26, 17 out. 2017b.

BURRIEZA, H. P. et al. Shotgun proteomic analysis of quinoa seeds reveals novel lysine-rich seed storage globulins. **Food Chemistry**, v. 293, p. 299–306, 30 set. 2019.

BURRUANO, S. The life-cycle of Plasmopara viticola, cause of downy mildew of vine. **Mycologist**, v. 14, p. 179–182, 2000.

CAARLS, L.; PIETERSE, C. M. J.; VAN WEES, S. C. M. How salicylic acid takes transcriptional control over jasmonic acid signaling. **Frontiers in Plant Science**, v. 6, n. MAR, p. 170, 25 mar. 2015.

CADLE-DAVIDSON, L. Variation Within and Between Vitis spp. for Foliar Resistance to the Downy Mildew Pathogen Plasmopara viticola. **Plant Disease**, v. 92, n. 11, p. 1577–1584, 13 nov. 2008.

CAI, X. et al. Mutant identification and characterization of the laccase gene family in Arabidopsis. **Journal of Experimental Botany**, v. 57, n. 11, p. 2563–2569, 1 ago. 2006.

CAMPBELL, S. E. et al. Fungicide Sensitivity Survey of *Plasmopara viticola* Populations in Georgia Vineyards. **Plant Health Progress**, v. 21, p. 256–261, 8 set. 2020.

CAMPBELL, S. E. et al. Efficacy of fungicide treatments for Plasmopara viticola control and occurrence of strobilurin field resistance in vineyards in Georgia, USA. **Crop Protection**, v. 139, p. 105371, 1 jan. 2021.

CANNON, S. B. et al. Diversity, Distribution, and Ancient Taxonomic Relationships Within the TIR and Non-TIR NBS-LRR Resistance Gene Subfamilies. **Journal of molecular evolution**, v. 54, p. 548–562, 2002.

CAO, H. et al. Characterization of an Arabidopsis mutant that is nonresponsive to inducers of systemic acquired resistance. **Plant Cell**, v. 6, n. 11, p. 1583–1592, 1 nov. 1994.

CAO, H. et al. Transcriptome analysis of methyl jasmonate-elicited panax ginseng adventitious roots to discover putative ginsenoside biosynthesis and transport genes. **International Journal of Molecular Sciences**, v. 16, n. 2, p. 3035–3057, 29 jan. 2015.

CASAGRANDE, K. et al. Defence responses in Rpv3-dependent resistance to grapevine downy mildew. **Planta**, v. 234, n. 6, p. 1097–1109, 7 dez. 2011.

CAUSIER, B. et al. The TOPLESS interactome: A framework for gene repression in Arabidopsis. **Plant Physiology**, v. 158, n. 1, p. 423–438, 1 jan. 2012.

CESCO, S. et al. Plasmopara viticola infection affects mineral elements allocation and distribution in Vitis vinifera leaves. **Scientific Reports**, v. 10, n. 1, p. 1–18, 1 dez. 2020.

CEVALLOS-CEVALLOS, J. M. et al. **Metabolomic analysis in food science: a reviewTrends in Food Science and Technology**Elsevier, , 1 dez. 2009.

CHATTERJEE, M.; CHAKRABORTY, J.; DAS, S. Abscisic Acid–Responsive 18 (CaABR18) Protein from Chickpea Inhibits the Growth of the Wilt-Causing Fusarium oxysporum f. sp. ciceri Race1. **Plant Molecular Biology Reporter**, v. 37, n. 3, p. 170–185, 15 jun. 2019.

CHEN, F.; MA, R.; CHEN, X. L. **Advances of metabolomics in fungal pathogen–plant interactionsMetabolites**MDPI AG, , 1 ago. 2019. Disponível em: <www.mdpi.com/journal/metabolites>. Acesso em: 22 nov. 2020

CHEN, J. et al. A novel *Meloidogyne graminicola* effector, MgMO237, interacts with multiple host defence-related proteins to manipulate plant basal immunity and promote parasitism. **Molecular Plant Pathology**, v. 19, n. 8, p. 1942–1955, 1 ago. 2018.

CHEN, T. et al. Insight Into Function and Subcellular Localization of Plasmopara viticola Putative RxLR Effectors. **Frontiers in Microbiology**, v. 11, p. 692, 21 abr. 2020.

CHEN, X. et al. A multilayered regulatory mechanism for the autoinhibition and activation of a plant CC-NB-LRR resistance protein with an extra N-terminal domain. **New Phytologist**, v. 212, n. 1, p. 161–175, 1 out. 2016.

CHENG, S. et al. Genetic transformation of a fruit-specific, highly expressed stilbene synthase gene from Chinese wild Vitis quinquangularis. **Planta**, v. 243, n. 4, p. 1041–1053, 1 abr. 2016.

CHESTER, K. S. The Problem of Acquired Physiological Immunity in Plants. **The Quarterly Review of Biology**, v. 8, n. 3, p. 275–324, 30 set. 1933.

CHINI, A. et al. The JAZ family of repressors is the missing link in jasmonate signalling. **Nature**, v. 448, n. 7154, p. 666–671, 9 ago. 2007.

CHINI, A. et al. The ZIM domain mediates homo- and heteromeric interactions between Arabidopsis JAZ proteins. **The Plant Journal**, v. 59, n. 1, p. 77–87, 1 jul. 2009.

CHITARRINI, G. et al. Identification of Biomarkers for Defense Response to Plasmopara viticola in a Resistant Grape Variety. **Frontiers in Plant Science**, v. 8, p. 1524, 5 set. 2017.

CHITARRINI, G. et al. Two-omics data revealed commonalities and differences between Rpv12-and Rpv3-mediated resistance in grapevine. **Scientific reports**, v. 10, p. 12193, 2020.

CHOI, J. et al. Cytokinins and plant immunity: Old foes or new friends? **Trends in Plant Science**, v. 16, n. 7, p. 388–394, jul. 2011.

CHONG, J.; POUTARAUD, A.; HUGUENEY, P. **Metabolism and roles of stilbenes in plantsPlant Science**Elsevier, , 1 set. 2009.

CHOUDHURY, F. K. et al. Reactive oxygen species, abiotic stress and stress combination. **The Plant Journal**, v. 90, n. 5, p. 856–867, 1 jun. 2017.

CLUZET, S.; MÉRILLON, J.-M.; RAMAWAT, K. G. Specialized Metabolites and Plant Defence. In: [s.l.] Springer, Cham, 2020. p. 45–80.

COLL, N. S.; EPPLE, P.; DANGL, J. L. **Programmed cell death in the plant immune systemCell Death and Differentiation**, ago. 2011.

COMBIER, M. et al. A secreted WY-domain-containing protein present in European isolates of the oomycete Plasmopara viticola induces cell death in grapevine and tobacco species. **PLOS ONE**, v. 14, n. 7, p. e0220184, 29 jul. 2019.

CORIO-COSTET, M. F. et al. Diversity and fitness of Plasmopara viticola isolates resistant to QoI fungicides. **European Journal of Plant Pathology**, v. 129, n. 2, p. 315–329, 17 nov. 2011.

CZARNOCKA, W.; KARPIŃSKI, S. **Friend or foe? Reactive oxygen species production, scavenging and signaling in plant response to environmental stressesFree Radical Biology and Medicine**Elsevier Inc., , 1 jul. 2018.

DAI, L. et al. The Novel Gene VpPR4-1 from Vitis pseudoreticulata Increases Powdery Mildew Resistance in Transgenic Vitis vinifera L. **Frontiers in Plant Science**, v. 7, p. 695, 27 maio 2016.

DAMERVAL, C. et al. Technical improvements in two-dimensional electrophoresis increase the level of genetic variation detected in wheat-seedling proteins. **ELECTROPHORESIS**, v. 7, n. 1, p. 52–54, 1 jan. 1986.

DANGL, J. L.; JONES, J. D. G. Plant pathogens and integrated defence responses to infection. **Nature**, v. 411, n. 6839, p. 826–833, jun. 2001.

DAS, D. et al. An efficient leaf-disc culture method for the regeneration via somatic embryogenesis and transformation of grape (Vitis vinifera L.). **Plant Cell Reports**, v. 20, n. 11, p. 999–1005, 1 maio 2002.

DASZKOWSKA-GOLEC, A.; SZAREJKO, I. **Open or close the gate - Stomata action under the control of phytohormones in drought stress conditionsFrontiers in Plant Science**Frontiers Research Foundation, , 13 maio 2013.

DE FILIPPIS, B. et al. Stilbene derivatives as new perspective in antifungal medicinal

chemistry. **Drug Development Research**, v. 80, n. 3, p. 285–293, 20 maio 2019.

DE GEYTER, N. et al. **Transcriptional machineries in jasmonate-elicited plant secondary metabolismTrends in Plant Science**Elsevier Current Trends, , 1 jun. 2012.

DEAN, R. A.; KUĆ, J. Induced systemic protection in cucumbers: the source of the "signal". **Physiological and Molecular Plant Pathology**, v. 28, n. 2, p. 227–233, 1 mar. 1986.

DELLA CORTE, A. et al. A rapid LC-MS/MS method for quantitative profiling of fatty acids, sterols, glycerolipids, glycerophospholipids and sphingolipids in grapes. **Talanta**, v. 140, p. 52–61, 1 ago. 2015.

DELMOTTE, F. et al. Rapid and multiregional adaptation to host partial resistance in a plant pathogenic oomycete: Evidence from European populations of Plasmopara viticola, the causal agent of grapevine downy mildew. **Infection, Genetics and Evolution**, v. 27, p. 500–508, 1 out. 2014.

DEMIANSKI, A. J.; CHUNG, K. M.; KUNKEL, B. N. Analysis of Arabidopsis JAZ gene expression during Pseudomonas syringae pathogenesis. **Molecular Plant Pathology**, v. 13, n. 1, p. 46–57, 1 jan. 2012.

DEMPSEY, D. A. et al. Salicylic Acid Biosynthesis and Metabolism. **The Arabidopsis Book**, v. 9, p. e0156, jan. 2011.

DENANCÉ, N. et al. **Disease resistance or growth: The role of plant hormones in balancing immune responses and fitness costsFrontiers in Plant Science**Frontiers Research Foundation, , 24 maio 2013.

DERCKS, W.; CREASY, L. L. Influence of fosetyl-Al on phytoalexin accumulation in the Plasmopara viticola-grapevine interaction. **Physiological and Molecular Plant Pathology**, v. 34, n. 3, p. 203–213, 1989.

DEVENDRAKUMAR, K. T.; LI, X.; ZHANG, Y. MAP kinase signalling: interplays between plant PAMP- and effector-triggered immunity. **Cellular and Molecular Life Sciences**, v. 75, n. 16, p. 2981–2989, 1 ago. 2018.

DEY, S. et al. Bacteria-triggered systemic immunity in barley is associated with WRKY and ETHYLENE RESPONSIVE FACTORs but not with salicylic acid. **Plant physiology**, v. 166, n. 4, p. 2133–51, 1 dez. 2014.

DEYETT, E. et al. Assessment of Pierce's disease susceptibility in *Vitis vinifera* cultivars with different pedigrees. **Plant Pathology**, v. 68, n. 6, p. 1079–1087, 24 ago. 2019.

DI GASPERO, G. et al. Selective sweep at the Rpv3 locus during grapevine breeding for downy mildew resistance. **Theoretical and Applied Genetics**, v. 124, n. 2, p. 277–286, 27 fev. 2012.

DICK, M. W. Towards and Understanding of the Evolution of the Downy Mildews. In: GISI, U.; LEBEDA, A. (Eds.). . **Advances in Downy Mildew Research**. 1. ed. Heidelberg: Springer Netherlands, 2002. p. 1–57.

DÍEZ-NAVAJAS, A. M. et al. Nonhost versus host resistance to the grapevine downy mildew, Plasmopara viticola, studied at the tissue level. **Phytopathology**, v. 98, n. 7, p. 776–780, 11 jul. 2008.

DING, X. et al. Activation of the indole-3-acetic acid-amido synthetase GH3-8 suppresses expansin expression and promotes salicylate- and jasmonate-independent basal immunity in rice. **Plant Cell**, v. 20, n. 1, p. 228–240, 1 jan. 2008.

DING, Y. et al. Opposite Roles of Salicylic Acid Receptors NPR1 and NPR3/NPR4 in Transcriptional Regulation of Plant Immunity. **Cell**, v. 173, n. 6, p. 1454- 1467.e10, 31 maio 2018.

DING, Y. et al. Differential Quantitative Requirements for NPR1 Between Basal Immunity and Systemic Acquired Resistance in Arabidopsis thaliana. **Frontiers in Plant Science**, v. 11, p. 1, 18 set. 2020.

DISTLER, U. et al. Drift time-specific collision energies enable deep-coverage data-independent acquisition proteomics. **Nature Methods**, v. 11, n. 2, p. 167–170, fev. 2014.

DISTLER, U. et al. Label-free quantification in ion mobility-enhanced data-independent acquisition proteomics. **Nature Protocols**, v. 11, n. 4, p. 795–812, 1 abr. 2016.

DIVILOV, K. et al. Single and multiple phenotype QTL analyses of downy mildew resistance in interspecific grapevines. **Theoretical and Applied Genetics**, v. 131, n. 5, p. 1133–1143, 7 maio 2018.

DONG, X. **NPR1, all things consideredCurrent Opinion in Plant Biology**Elsevier Current Trends, , 1 out. 2004.

DONOSO, R. et al. Biochemical and genetic bases of indole-3-acetic acid (auxin phytohormone) degradation by the plantgrowth- promoting rhizobacterium Paraburkholderia phytofirmans PsJN. **Applied and Environmental Microbiology**, v. 83, n. 1, 1 jan. 2017.

DOUGLAS, C. J. **Phenylpropanoid metabolism and lignin biosynthesis: From weeds to treesTrends in Plant Science**Elsevier Ltd, , jun. 1996. Disponível em: <https://linkinghub.elsevier.com/retrieve/pii/1360138596100194>. Acesso em: 16 nov. 2020

DUAN, D. et al. Genetic diversity of stilbene metabolism in Vitis sylvestris. **Journal of Experimental Botany**, v. 66, n. 11, p. 3243–3257, 1 jun. 2015.

DUFOUR, M. C. et al. Benzothiadiazole-primed defence responses and enhanced differential expression of defence genes in Vitis vinifera infected with biotrophic pathogens

Erysiphe necator and Plasmopara viticola. **Plant Pathology**, v. 62, n. 2, p. 370–382, 1 abr. 2013.

DUPLAN, V.; RIVAS, S. E3 ubiquitin-ligases and their target proteins during the regulation of plant innate immunity. **Frontiers in Plant Science**, v. 5, n. FEB, p. 42, 13 fev. 2014.

DURRANT, W. E.; DONG, X. SYSTEMIC ACQUIRED RESISTANCE. **Annual Review of Phytopathology**, v. 42, n. 1, p. 185–209, 29 set. 2004.

EIBACH, R. et al. The use of molecular markers for pyramidizing resistance genes in grapevine breeding. **Vitis**, v. 46, n. 3, p. 120–124, 2006.

EIBACH, R. et al. The use of molecular markers for pyramiding resistance genes in grapevine breeding. **Vitis**, v. 46, n. 3, p. 120–124, 2007.

EISENMANN, B. et al. Rpv3-1 mediated resistance to grapevine downy mildew is associated with specific host transcriptional responses and the accumulation of stilbenes. **BMC Plant Biology**, v. 19, n. 1, p. 1–17, 6 ago. 2019.

EMANUELLI, F. et al. A candidate gene association study on muscat flavor in grapevine (Vitis vinifera L.). **BMC Plant Biology**, v. 10, n. 1, p. 1–17, 9 nov. 2010.

EMANUELLI, F. et al. Genetic diversity and population structure assessed by SSR and SNP markers in a large germplasm collection of grape. **BMC Plant Biology**, v. 13, n. 1, p. 39, 7 mar. 2013.

ENGELBERTH, J.; ENGELBERTH, M. Variability in the Capacity to Produce Damage-Induced Aldehyde Green Leaf Volatiles among Different Plant Species Provides Novel Insights into Biosynthetic Diversity. **Plants**, v. 9, n. 2, p. 213, 6 fev. 2020.

EPPLE, P.; APEL, K.; BOHLMANN, H. An Arabidopsis thaliana thionin gene is inducible via a signal transduction pathway different from that for pathogenesis-related proteins. **Plant physiology**, v. 109, n. 3, p. 813–20, 1 nov. 1995.

FEECHAN, A. et al. Genetic dissection of a TIR-NB-LRR locus from the wild North American grapevine species Muscadinia rotundifolia identifies paralogous genes conferring resistance to major fungal and oomycete pathogens in cultivated grapevine. **Plant Journal**, v. 76, n. 4, p. 661–674, 1 nov. 2013.

FENG, J. et al. Salicylic acid-primed defence response in octoploid strawberry “Benihoppe” leaves induces resistance against Podosphaera aphanis through enhanced accumulation of proanthocyanidins and upregulation of pathogenesis-related genes. 2020.

FENG, S. et al. The COP9 signalosome interacts physically with SCFCOI1 and modulates jasmonate responses. **Plant Cell**, v. 15, n. 5, p. 1083–1094, 1 maio 2003.

FERNÁNDEZ-CALVO, P. et al. The Arabidopsis bHLH transcription factors MYC3 and MYC4 are targets of JAZ repressors and act additively with MYC2 in the activation of jasmonate responses. **Plant Cell**, v. 23, n. 2, p. 701–715, 1 fev. 2011.

FIEHN, O. et al. Quality control for plant metabolomics: Reporting MSI-compliant studies. **Plant Journal**, v. 53, n. 4, p. 691–704, 1 fev. 2008.

FIGUEIREDO, A. et al. Specific adjustments in grapevine leaf proteome discriminating resistant and susceptible grapevine genotypes to Plasmopara viticola. **Journal of Proteomics**, v. 152, p. 48–57, jan. 2017.

FIGUEIREDO, J. et al. Revisiting Vitis vinifera subtilase gene family: A possible role in grapevine resistance against plasmopara viticola. **Frontiers in Plant Science**, v. 7, n. NOVEMBER2016, p. 1783, 25 nov. 2016.

FIGUEIREDO, J.; SOUSA SILVA, M.; FIGUEIREDO, A. **Subtilisin-like proteases in plant defence: the past, the present and beyondMolecular Plant Pathology**Blackwell Publishing Ltd, , 1 abr. 2018. Disponível em: <http://doi.wiley.com/10.1111/mpp.12567>. Acesso em: 5 mar. 2020

FOLCH, J.; LEES, M.; SLOANE, G. H. A SIMPLE METHOD FOR THE ISOLATION AND PURIFICATION OF TOTAL LIPIDES FROM ANIMAL TISSUES* Downloaded from. **Journal of Biological Chemestryo**, v. 226, p. 497–509, 1957.

FORIA, S. et al. The genetic background modulates the intensity of Rpv3-dependent downy mildew resistance in grapevine. **Plant Breeding**, v. 137, n. 2, p. 220–228, 1 abr. 2018a.

FORIA, S. et al. InDel markers for monitoring the introgression of downy mildew resistance from wild relatives into grape varieties. **Molecular Breeding**, v. 38, n. 10, p. 1–12, 1 out. 2018b.

FRÖBEL, S. et al. Transcriptome analysis of early downy mildew (Plasmopara viticola) defense in grapevines carrying the Asian resistance locus Rpv10. **Euphytica**, v. 215, n. 2, 2019.

FROST, C. J. et al. Priming defense genes and metabolites in hybrid poplar by the green leaf volatile cis-3-hexenyl acetate. **New Phytologist**, v. 180, n. 3, p. 722–734, 1 nov. 2008.

FU, J. et al. Manipulating broad-spectrum disease resistance by suppressing pathogen-induced auxin accumulation in rice. **Plant Physiology**, v. 155, n. 1, p. 589–602, 1 jan. 2011.

FU, P. et al. Identifying Plasmopara viticola resistance Loci in grapevine (Vitis amurensis) via genotyping-by-sequencing-based QTL mapping. **Plant Physiology and Biochemistry**, v. 154, p. 75–84, 1 set. 2020.

GAMM, M. et al. Changes in Carbohydrate Metabolism in Plasmopara viticola-Infected Grapevine Leaves. **/ 1061 MPMI**, v. 24, n. 9, p. 1061–1073, 2011.

GAO, Q.-M. et al. Signal regulators of systemic acquired resistance. **Frontiers in Plant Science**, v. 06, p. 228, 13 abr. 2015.

GARCÍA-OLMEDO, F. et al. The defensive role of nonspecific lipid-transfer proteins in plants. **Trends in Microbiology**, v. 3, n. 2, p. 72–74, 1 fev. 1995.

GASCUEL, Q. et al. RXLR and CRN Effectors from the Sunflower Downy Mildew Pathogen Plasmopara halstedii Induce Hypersensitive-Like Responses in Resistant Sunflower Lines. **Frontiers in Plant Science**, v. 7, n. DECEMBER2016, p. 1887, 19 dez. 2016.

GAUTAM, J. K.; NANDI, A. K. APD1, the unique member of Arabidopsis AP2 family influences systemic acquired resistance and ethylene-jasmonic acid signaling. **Plant Physiology and Biochemistry**, v. 133, p. 92–99, 1 dez. 2018.

GAVNHOLT, B.; LARSEN, K. **Molecular biology of plant laccases in relation to lignin formationPhysiologia Plantarum**, 1 nov. 2002. Disponível em: <http://doi.wiley.com/10.1034/j.1399-3054.2002.1160301.x>. Acesso em: 16 nov. 2020

GESSLER, C.; PERTOT, I.; PERAZZOLLI, M. *Plasmopara viticola*: a review of knowledge on downy mildew of grapevine and effective disease management. **Phytopathologia Mediterranea**, v. 50, n. 1, p. 3–44, abr. 2011.

GINDRO, K.; PEZET, R.; VIRET, O. Histological study of the responses of two *Vitis vinifera* cultivars (resistant and susceptible) to *Plasmopara viticola* infections. 2003.

GÓMEZ-ZELEDÓN, J.; SPRING, O. Up-regulated RxLR effector genes of Plasmopara viticola in synchronized host-free stages and infected leaves of hosts with different susceptibility. **Fungal Biology**, v. 122, n. 12, p. 1125–1133, 1 dez. 2018.

GONZÁLEZ-LAMOTHE, R. et al. The Conjugated Auxin Indole-3-Acetic Acid-Aspartic Acid Promotes Plant Disease Development. **The Plant Cell**, v. 24, n. 2, p. 762–777, 2012.

GOUVEIA, C. et al. Subtilisin like proteins in the war between Grapevine and Plasmopara viticola isolates with contrasting aggressiveness. **European Journal of Plant Pathology**, v. 159, n. 2, p. 433–439, 1 fev. 2021.

GRAY, D. J.; MORTENSEN, J. A. Initiation and maintenance of long term somatic embryogenesis from anthers and ovaries of Vitis longii "Microsperma". **Plant Cell, Tissue and Organ Culture**, v. 9, n. 1, p. 73–80, jan. 1987.

GREEN, T. R.; RYAN, C. A. Wound-Induced Proteinase Inhibitor in Plant Leaves: A Possible Defense Mechanism against Insects. **Science (New York, N.Y.)**, v. 175, n. 4023, p.

776–7, 18 fev. 1972.

GRENVILLE-BRIGGS, L. J.; WEST, P. VAN. The Biotrophic Stages of Oomycete–Plant Interactions. **Advances in Applied Microbiology**, v. 57, p. 217–243, 1 jan. 2005.

GUAN, C. et al. LcSABP2, a salicylic acid binding protein 2 gene from Lycium chinense, confers resistance to triclosan stress in Nicotiana tabacum. **Ecotoxicology and Environmental Safety**, v. 183, p. 109516, 15 nov. 2019.

GUERREIRO, A. et al. Linking Jasmonic Acid to Grapevine Resistance against the Biotrophic Oomycete *Plasmopara viticola*. **Frontiers in Plant Science**, v. 7, p. 565, 28 abr. 2016.

GUTIÉRREZ-ESCOBAR, R. et al. Development and characterization of a pure stilbene extract from grapevine shoots for use as a preservative in wine. **Food Control**, v. 121, p. 107684, 1 mar. 2021.

HADWIGER, L. A. **Localization predictions for gene products involved in non-host resistance responses in a model plant/fungal pathogen interactionPlant Science**Elsevier, , 1 out. 2009.

HALL, D.; DE LUCA, V. Mesocarp localization of a bi-functional resveratrol/hydroxycinnamic acid glucosyltransferase of Concord grape (Vitis labrusca). **Plant Journal**, v. 49, n. 4, p. 579–591, 19 fev. 2007.

HARA-NISHIMURA, I.; HATSUGAI, N. **The role of vacuole in plant cell deathCell Death and Differentiation**Nature Publishing Group, , 3 jun. 2011.

HARTMANN, M. et al. Flavin Monooxygenase-Generated N-Hydroxypipecolic Acid Is a Critical Element of Plant Systemic Immunity. **Cell**, v. 173, n. 2, p. 456- 469.e16, 5 abr. 2018.

HARTMANN, M.; ZEIER, J. N-hydroxypipecolic acid and salicylic acid: a metabolic duo for systemic acquired resistance. **Current Opinion in Plant Biology**, v. 50, p. 44–57, 1 ago. 2019.

HE, R. et al. Overexpression of a thaumatin-like protein gene from Vitis amurensis improves downy mildew resistance in Vitis vinifera grapevine. **Protoplasma**, v. 254, n. 4, p. 1579–1589, 30 jul. 2017.

HE, X. et al. GhJAZ2 attenuates cotton resistance to biotic stresses via the inhibition of the transcriptional activity of GhbHLH171. **Molecular Plant Pathology**, v. 19, n. 4, p. 896–908, 1 abr. 2018a.

HE, X. et al. Overexpressing fusion proteins of 4-coumaroyl-CoA ligase (4CL) and stilbene synthase (STS) in tobacco plants leading to resveratrol accumulation and improved

stress tolerance. **Plant Biotechnology Reports**, v. 12, n. 5, p. 295–302, 1 out. 2018b.

HERNANDEZ-VALLADARES, M. et al. Reliable FASP-based procedures for optimal quantitative proteomic and phosphoproteomic analysis on samples from acute myeloid leukemia patients. **Biological Procedures Online**, v. 18, n. 1, p. 1–10, 21 jun. 2016.

HERRERA-VÁSQUEZ, A.; SALINAS, P.; HOLUIGUE, L. Salicylic acid and reactive oxygen species interplay in the transcriptional control of defense genes expression. **Frontiers in Plant Science**, v. 6, p. 171, 19 mar. 2015.

HIPSKIND, J. D.; PAIVA, N. L. Constitutive accumulation of a resveratrol-glucoside in transgenic alfalfa increases resistance to Phoma medicaginis. **Molecular Plant-Microbe Interactions**, v. 13, n. 5, p. 551–562, 19 fev. 2000.

HOFFMANN, N. et al. Laccases and peroxidases co-localize in lignified secondary cell walls throughout stem development. **Plant Physiology**, v. 184, n. 2, p. 806–822, 1 out. 2020.

HOFIUS, D. et al. **Role of autophagy in disease resistance and hypersensitive response-associated cell deathCell Death and Differentiation**Nature Publishing Group, , 29 ago. 2011.

HOFMANN, K. The Evolutionary Origins of Programmed Cell Death Signaling. **Cold Spring Harbor Perspectives in Biology**, p. a036442, 9 dez. 2019.

HONG, Y. S. et al. Metabolomics reveals simultaneous influences of plant defence system and fungal growth in Botrytis cinerea-infected Vitis vinifera cv. Chardonnay berries. **Journal of Experimental Botany**, v. 63, n. 16, p. 5773–5785, 1 set. 2012.

HOO, S. C.; HOWE, G. A. A critical role for the TIFY motif in repression of jasmonate signaling by a stabilized splice variant of the JASMONATE ZIM-domain protein JAZ10 in Arabidopsis. **Plant Cell**, v. 21, n. 1, p. 131–145, 1 jan. 2009.

HORSEFIELD, S. et al. NAD+ cleavage activity by animal and plant TIR domains in cell death pathways. **Science**, v. 365, n. 6455, p. 793–799, 23 ago. 2019.

HU, K. M. et al. Isolation and manipulation of Quantitative trait loci for disease resistance in rice using a candidate gene approach. **Molecular Plant**, v. 1, n. 5, p. 786–793, 1 set. 2008.

HUBY, E. et al. Sphingolipids: towards an integrated view of metabolism during the plant stress response. **New Phytologist**, v. 225, n. 2, p. 659–670, 15 jan. 2020.

IMAZIO, S. et al. From the cradle of grapevine domestication: Molecular overview and description of Georgian grapevine (Vitis vinifera L.) germplasm. **Tree Genetics and Genomes**, v. 9, n. 3, p. 641–658, 26 fev. 2013.

JAILLON, O. et al. The grapevine genome sequence suggests ancestral hexaploidization in major angiosperm phyla. **Nature**, v. 449, n. 7161, p. 463–467, 26 set. 2007.

JANEWAY, C. A.; MEDZHITOV, R. INNATE IMMUNE RECOGNITION. **Annu. Rev. Immunol**, v. 20, p. 197–216, 2002.

JEANDET, P. et al. Phytoalexins from the Vitaceae: Biosynthesis, Phytoalexin Gene Expression in Transgenic Plants, Antifungal Activity, and Metabolism. 2002.

JEANDET, P.; CLÉMENT, C.; CORDELIER, S. Regulation of resveratrol biosynthesis in grapevine: new approaches for disease resistance? **Journal of Experimental Botany**, v. 70, n. 2, p. 375–378, 7 jan. 2019.

JIAO, Y. et al. A stilbene synthase allele from a Chinese wild grapevine confers resistance to powdery mildew by recruiting salicylic acid signalling for efficient defence. **Journal of Experimental Botany**, v. 67, n. 19, p. 5841–5856, 1 out. 2016.

JIU, S. T. et al. Characterization of VvPAL-like promoter from grapevine using transgenic tobacco plants. **Functional and Integrative Genomics**, v. 16, n. 6, p. 595–617, 1 nov. 2016.

JONES, J. D. G.; DANGL, J. L. **The plant immune systemNature**Nature Publishing Group, , 16 nov. 2006.

JONES, P. et al. UGT73C6 and UGT78D1, Glycosyltransferases Involved in Flavonol Glycoside Biosynthesis in Arabidopsis thaliana. **Journal of Biological Chemistry**, v. 278, n. 45, p. 43910–43918, 7 nov. 2003.

JUNG, C. et al. Overexpression of AtMYB44 enhances stomatal closure to confer abiotic stress tolerance in transgenic Arabidopsis. **Plant Physiology**, v. 146, n. 2, p. 623–635, 1 fev. 2008.

JÜRGES, G. et al. The mode of interaction between *Vitis* and *Plasmopara viticola* Berk. & Curt. Ex de Bary depends on the host species. **Plant Biology**, v. 11, n. 6, p. 886–898, nov. 2009.

KAMOUN, S. et al. The Top 10 oomycete pathogens in molecular plant pathology. **Molecular Plant Pathology**, v. 16, n. 4, p. 413–434, 1 maio 2015.

KANWAR, P.; JHA, G. **Alterations in plant sugar metabolism: signatory of pathogen attackPlanta**Springer Verlag, , 8 fev. 2019. Disponível em: <https://doi.org/10.1007/s00425-018-3018-3>. Acesso em: 5 dez. 2020

KARASOV, T. L. et al. **Mechanisms to mitigate the trade-off between growth and defensePlant Cell**American Society of Plant Biologists, , 1 abr. 2017.

KASSAMBARA, A.; MUNDT, F. **factoextra: Extract and Visualize the Results of**

Multivariate Data Analyses. R package version 1.0.3 Comprehensive R Archive Network (CRAN), , 1 abr. 2020. Disponível em: <https://cran.r-project.org/package=factoextra>. Acesso em: 25 nov. 2020

KHAFIF, M. et al. An essential role for the VASt domain of the Arabidopsis VAD1 protein in the regulation of defense and cell death in response to pathogens. **PLOS ONE**, v. 12, n. 7, p. e0179782, 6 jul. 2017.

KIEFER, B. et al. The host guides morphogenesis and stomatal targeting in the grapevine pathogen Plasmopara viticola. **Planta**, v. 215, n. 3, p. 387–393, 2002.

KIM, H.-I. et al. Genome-Wide Identification and Characterization of Novel Laccase Genes in the White-Rot Fungus Flammulina velutipes. 2018.

KIM, J. H. et al. Molecular cloning, expression, and characterization of a flavonoid glycosyltransferase from Arabidopsis thaliana. **Plant Science**, v. 170, n. 4, p. 897–903, 1 abr. 2006.

KING, S. R. F. et al. Phytophthora infestans RXLR effector PexRD2 interacts with host MAPKKKε to suppress plant immune signaling. **Plant Cell**, v. 26, n. 3, p. 1345–1359, 1 mar. 2014.

KLESSIG, D. F. et al. Systemic Acquired Resistance and Salicylic Acid: Past, Present, and Future. v. 31, n. 9, 2018.

KOBAYASHI, S. et al. Kiwifruits (Actinidia deliciosa) transformed with a Vitis stilbene synthase gene produce piceid (resveratrol-glucoside). **Plant Cell Reports**, v. 19, n. 9, p. 904–910, 2000.

KORTEKAMP, A. Expression analysis of defence-related genes in grapevine leaves after inoculation with a host and a non-host pathogen. **Plant Physiology and Biochemistry**, v. 44, p. 58–67, 2006.

KORTEKAMP, A. et al. Identification, isolation and characterization of a CC-NBS-LRR candidate disease resistance gene family in grapevine. **Molecular Breeding**, v. 22, p. 421–432, 13 out. 2008.

KOSEV, K. et al. Phenotypic and molecular characterization of 18 Bulgarian newly bred grapevine varieties in relation to their resistance to downy mildew. **Biotechnology and Biotechnological Equipment**, v. 31, n. 1, p. 68–74, 2 jan. 2017.

KREPS, J. A. et al. Transcriptome changes for Arabidopsis in response to salt, osmotic, and cold stress. **Plant Physiology**, v. 130, n. 4, p. 2129–2141, 1 dez. 2002.

KRZYZANIAK, Y. et al. A plant extract acts both as a resistance inducer and an oomycide against grapevine downy mildew. **Frontiers in Plant Science**, v. 9, 25 jul. 2018.

KUO, C.-H. et al. Production of Resveratrol by Piceid Deglycosylation Using Cellulase. **Catalysts**, v. 6, n. 3, p. 32, 24 fev. 2016.

LAGRIMINI, L. M. et al. Molecular cloning of complementary DNA encoding the lignin-forming peroxidase from tobacco: Molecular analysis and tissue-specific expression. **Proceedings of the National Academy of Sciences of the United States of America**, v. 84, n. 21, p. 7542–6, 1 nov. 1987.

LALANCETTE, N.; ELLIS, M. A.; MADDEN, L. V. Development of an infection efficiency model for *Plasmopara viticola* on American grape based on termerature and duration of leaf wetness. **Phytopathology**, v. 78, p. 794–800, 1988.

LALANCETTE, N.; MADDEN, L. V.; ELLIS, M. A. A Quantitative Model for Describing the Sporulation of Plasmopara viticola on Grape Leaves. **Phytopathology**, v. 78, p. 1316–1321, 1988.

LASSNIGG, A. et al. Minimal changes of serum creatinine predict prognosis in patients after cardiothoracic surgery: A prospective cohort study. **Journal of the American Society of Nephrology**, v. 15, n. 6, p. 1597–1605, 1 jun. 2004.

LE HENANFF, G. et al. Characterization of vitis vinifera NPR1 homologs involved in the regulation of pathogenesis-related gene expression. **BMC Plant Biology**, v. 9, n. 1, p. 1–14, 11 maio 2009.

LÊ, S.; JOSSE, J.; HUSSON, F. FactoMineR: An R package for multivariate analysis. **Journal of Statistical Software**, v. 25, n. 1, p. 1–18, 18 mar. 2008.

LEI, Z. et al. Comparative proteomics of yeast-elicited medicago truncatula cell suspensions reveals induction of isoflavonoid biosynthesis and cell wall modifications. **Journal of Proteome Research**, v. 9, n. 12, p. 6220–6231, 3 dez. 2010.

LEMAITRE-GUILLIER, C. et al. Cultivar- and Wood Area-Dependent Metabolomic Fingerprints of Grapevine Infected by Botryosphaeria Dieback. **Phytopathology®**, v. 110, n. 11, p. 1821–1837, 6 nov. 2020.

LEMAÎTRE-GUILLIER, C. et al. Proteomics towards the understanding of elicitor induced resistance of grapevine against downy mildew. **Journal of Proteomics**, v. 156, p. 113–125, 6 mar. 2017.

LI, J.; BRADER, G.; PALVA, E. T. The WRKY70 Transcription Factor: A Node of Convergence for Jasmonate-Mediated and Salicylate-Mediated Signals in Plant Defense W. **The Plant cell**, v. 16, p. 319–331, 2004.

LI, M. et al. TCP Transcription Factors Interact With NPR1 and Contribute Redundantly to Systemic Acquired Resistance. **Frontiers in Plant Science**, v. 9, p. 1153, 14

ago. 2018.

LI, N. et al. **Signaling crosstalk between salicylic acid and ethylene/Jasmonate in plant defense: Do we understand what they are whispering?International Journal of Molecular Sciences**MDPI AG, , 4 fev. 2019. Disponível em: <www.mdpi.com/journal/ijms>. Acesso em: 22 ago. 2020

LI, R. et al. Resveratrol accumulation and its involvement in stilbene synthetic pathway of Chinese wild grapes during berry development using quantitative proteome analysis. **Scientific Reports**, v. 7, n. 1, p. 9295, 1 dez. 2017a.

LI, X. et al. Overexpression of pathogen-induced grapevine TIR-NB-LRR gene VaRGA1 enhances disease resistance and drought and salt tolerance in Nicotiana benthamiana. **Protoplasma**, v. 254, p. 957–969, 2017b.

LIANG, Z. et al. Whole-genome resequencing of 472 Vitis accessions for grapevine diversity and demographic history analyses. **NATURE COMMUNICATIONS**, v. 10, n. 1190, 2019.

LIECHTI, R.; FARMER, E. E. **The Jasmonate pathwayScience**American Association for the Advancement of Science, , 31 maio 2002.

LIN, H. et al. QTLs and candidate genes for downy mildew resistance conferred by interspecific grape (V. vinifera L. × V. amurensis Rupr.) crossing. **Scientia Horticulturae**, v. 244, p. 200–207, 26 jan. 2019.

LIPECKA, J. et al. Sensitivity of mass spectrometry analysis depends on the shape of the filtration unit used for filter aided sample preparation (FASP). **PROTEOMICS**, v. 16, n. 13, p. 1852–1857, 1 jul. 2016.

LIU, C. et al. Resveratrols in Vitis berry skins and leaves: Their extraction and analysis by HPLC. **Food Chemistry**, v. 136, n. 2, p. 643–649, 15 jan. 2013.

LIU, L. et al. Salicylic acid receptors activate jasmonic acid signalling through a non-canonical pathway to promote effector-triggered immunity. **Nature Communications**, v. 7, n. 1, p. 1–10, 11 out. 2016a.

LIU, L. et al. **Arms race: diverse effector proteins with conserved motifsPlant Signaling and Behavior**Taylor and Francis Inc., , 1 fev. 2019a. Disponível em: <https://www.tandfonline.com/action/journalInformation?journalCode=kpsb20>. Acesso em: 15 out. 2020

LIU, M. et al. Expression of stilbene synthase VqSTS6 from wild Chinese Vitis quinquangularis in grapevine enhances resveratrol production and powdery mildew resistance. **Planta**, v. 250, n. 6, p. 1997–2007, 1 dez. 2019b.

LIU, X. Q. et al. Phylogeny of the Ampelocissus-Vitis clade in Vitaceae supports the New World origin of the grape genus. **Molecular Phylogenetics and Evolution**, v. 95, p. 217–228, 1 fev. 2016b.

LIU, Z. et al. Overexpression of a resveratrol synthase gene (PcRS) from Polygonum cuspidatum in transgenic Arabidopsis causes the accumulation of trans-piceid with antifungal activity. **Plant Cell Reports**, v. 30, n. 11, p. 2027–2036, 30 nov. 2011.

LIVAK, K. J.; SCHMITTGEN, T. D. Analysis of relative gene expression data using real-time quantitative PCR and the 2-ΔΔCT method. **Methods**, v. 25, n. 4, p. 402–408, dez. 2001.

LOLLE, S.; STEVENS, D.; COAKER, G. Plant NLR-triggered immunity: from receptor activation to downstream signaling. **Current Opinion in Immunology**, v. 62, p. 99–105, 1 fev. 2020.

LOON, L. C. VAN. **Regulation of changes in proteins and enzymes associated with active defense against virus infection**Plenum Press, , 1981. Disponível em: <https://library.wur.nl/WebQuery/wurpubs/74919>. Acesso em: 31 jul. 2019

LORENZO, O. et al. JASMONATE-INSENSITIVE1 encodes a MYC transcription factor essential to discriminate between different jasmonate-regulated defense responses in arabidopsis. **Plant Cell**, v. 16, n. 7, p. 1938–1950, 1 jul. 2004.

MA, F. et al. Dynamic translocation of stilbene synthase VpSTS29 from a Chinese wild Vitis species upon UV irradiation. **Phytochemistry**, v. 159, p. 137–147, 1 mar. 2019.

MA, H. et al. Grapevine VpPR10.1 functions in resistance to *Plasmopara viticola* through triggering a cell death-like defence response by interacting with VpVDAC3. **Plant Biotechnology Journal**, v. 16, n. 8, p. 1488–1501, 1 ago. 2018.

MACHO, A. P.; ZIPFEL, C. **Plant PRRs and the activation of innate immune signalingMolecular Cell**Cell Press, , 24 abr. 2014.

MAJOR, I. T. et al. Regulation of growth-defense balance by the JASMONATE ZIM-DOMAIN (JAZ)-MYC transcriptional module. **New Phytologist**, v. 215, n. 4, p. 1533–1547, 1 set. 2017.

MAMMARELLA, N. D. et al. Apoplastic peroxidases are required for salicylic acid-mediated defense against Pseudomonas syringae. **Phytochemistry**, v. 112, p. 110–121, 1 abr. 2015.

MARGUERIT, E. et al. Genetic dissection of sex determinism, inXorescence morphology and downy mildew resistance in grapevine. **Theor Appl Genet**, v. 118, p. 1261–1278, 2009.

MARINHO, M. DA C. et al. Ecotoxicological evaluation of fungicides used in viticulture in non-target organisms. **Environmental Science and Pollution Research**, v. 27, n. 35, p. 43958–43969, 3 ago. 2020.

MARINO, D.; PEETERS, N.; RIVAS, S. Ubiquitination during plant immune signaling. **Plant Physiology**, v. 160, n. 1, p. 15–27, 1 set. 2012.

MARTÍNEZ-MÁRQUEZ, A. et al. Production of highly bioactive resveratrol analogues pterostilbene and piceatannol in metabolically engineered grapevine cell cultures. **Plant Biotechnology Journal**, v. 14, n. 9, p. 1813–1825, 1 set. 2016.

MATARESE, F. et al. Expression of terpene synthase genes associated with the formation of volatiles in different organs of Vitis vinifera. **Phytochemistry**, v. 105, p. 12–24, 1 set. 2014.

MATASCI, C. L. et al. Selection for fungicide resistance throughout a growing season in populations of Plasmopara viticola. **European Journal of Plant Pathology**, v. 120, n. 1, p. 79–83, 21 jan. 2008.

MATZINGER, P. **The danger model: A renewed sense of selfScience**American Association for the Advancement of Science, , 12 abr. 2002. Disponível em: <https://science.sciencemag.org/content/296/5566/301>. Acesso em: 9 mar. 2021

MAUL ET AL. **Vitis International Variety Catalogue**. Disponível em: <http://www.vivc.de/>. Acesso em: 6 maio. 2020.

MELCHERS, L. S. et al. A new class of tobacco chitinases homologous to bacterial exo-chitinases displays antifungal activity. **The Plant Journal**, v. 5, n. 4, p. 469–480, 1 abr. 1994.

MÉNARD, R. et al. b-1,3 Glucan Sulfate, but Not b-1,3 Glucan, Induces the Salicylic Acid Signaling Pathway in Tobacco and Arabidopsis. **The Plant Cell**, v. 16, p. 3020–3032, nov. 2004.

MERDINOGLU, D. et al. Genetic analysis of downy mildew resistance derived from *Muscadinia rotundifolia*. **Acta Horticulturae**, n. 603, p. 451–456, abr. 2003.

MERDINOGLU, D. et al. Breeding for durable resistance to downy and powdery mildew in grapevine. **Oeno One**, v. 52, n. 3, p. 189–195, 2 ago. 2018.

MERZ, P. R. et al. The transcription factor VvWRKY33 is involved in the regulation of grapevine (*Vitis vinifera*) defense against the oomycete pathogen Plasmopara viticola. **Physiologia Plantarum**, v. 153, n. 3, p. 365–380, 1 mar. 2015.

MESTRE, P. et al. Comparative analysis of expressed CRN and RXLR effectors from two *Plasmopara* species causing grapevine and sunflower downy mildew. **Plant Pathology**, v.

65, n. 5, p. 767–781, 1 jun. 2016.

MESTRE, P. et al. Identification of a Vitis vinifera endo-β-1,3-glucanase with antimicrobial activity against Plasmopara viticola. **Molecular Plant Pathology**, v. 18, n. 5, p. 708–719, 1 jun. 2017.

MÉTRAUX, J. P.; STREIT, L.; STAUB, T. A pathogenesis-related protein in cucumber is a chitinase. **Physiological and Molecular Plant Pathology**, v. 33, n. 1, p. 1–9, 1 jul. 1988.

MIKULSKI, D.; MOLSKI, M. Quantitative structure-antioxidant activity relationship of trans-resveratrol oligomers, trans-4,4′-dihydroxystilbene dimer, trans-resveratrol-3-O-glucuronide, glucosides: Trans-piceid, cis-piceid, trans-astringin and trans-resveratrol-4′-O-β-D-glucopyranoside. **European Journal of Medicinal Chemistry**, v. 45, n. 6, p. 2366–2380, 1 jun. 2010.

MILLI, A. et al. Proteomic analysis of the compatible interaction between Vitis vinifera and Plasmopara viticola. **Journal of Proteomics**, v. 75, n. 4, p. 1284–1302, 2 fev. 2012.

MITTLER, R.; BLUMWALD, E. The roles of ROS and ABA in systemic acquired acclimation. **The Plant cell**, v. 27, n. 1, p. 64–70, 1 jan. 2015.

MODARRESI, M. et al. Variations of glaucine, quercetin and kaempferol contents in Nigella arvensis against Al2O3, NiO, and TiO2 nanoparticles. **Heliyon**, v. 6, n. 6, p. e04265, 1 jun. 2020.

MONTEIRO, F. et al. Reference Gene Selection and Validation for the Early Responses to Downy Mildew Infection in Susceptible and Resistant Vitis vinifera Cultivars. **PLoS ONE**, v. 8, n. 9, 4 set. 2013.

MOORE, N. O. CLASSIFICATION AND SYSTEMATICS OF EASTERN NORTH AMERICAN VITIS L. (VITACEAE) NORTH OF MEXICO. **SIDA**, v. 14, n. 3, p. 339–367, ago. 1991.

MOREIRA, F. M. et al. Genetic linkage maps of two interspecific grape crosses (Vitis spp.) used to localize quantitative trait loci for downy mildew resistance. **Tree Genetics & Genomes**, v. 7, p. 153–167, 2011.

NANJO, Y. et al. Mass spectrometry-based analysis of proteomic changes in the root tips of flooded soybean seedlings. **Journal of Proteome Research**, v. 11, n. 1, p. 372–385, 1 jan. 2012.

NASCIMENTO-GAVIOLI, M. C. A. et al. Proteome of Plasmopara viticola -infected Vitis vinifera provides insights into grapevine Rpv1 / Rpv3 pyramided resistance to downy

mildew. **Journal of Proteomics**, v. 151, p. 264–274, jan. 2017.

NASCIMENTO-GAVIOLI, M. C. A. et al. Histopathological study of resistant (*Vitis labrusca* L.) and susceptible (*Vitis vinifera* L.) cultivars of grapevine to the infection by downy mildew. **The Journal of Horticultural Science and Biotechnology**, v. 95, n. 4, p. 521–531, 3 jul. 2020.

NASCIMENTO, R. et al. Early stage metabolic events associated with the establishment of Vitis vinifera – Plasmopara viticola compatible interaction. **Plant Physiology and Biochemistry**, v. 137, p. 1–13, 1 abr. 2019.

NEGREL, L. et al. Identification of Lipid Markers of Plasmopara viticola Infection in Grapevine Using a Non-targeted Metabolomic Approach. **Frontiers in Plant Science**, v. 9, p. 360, 21 mar. 2018.

NOGUEIRA JÚNIOR, A. F. et al. Virtual lesions and photosynthetic damage caused by Plasmopara viticola in Vitis labrusca. **European Journal of Plant Pathology**, v. 155, n. 2, p. 545–555, 1 out. 2019.

NOGUEIRA JÚNIOR, A. F. et al. Photosynthetic Cost Associated With Induced Defense to Plasmopara viticola in Grapevine. **Frontiers in Plant Science**, v. 11, p. 235, 19 mar. 2020.

O'BRIEN, J. A. et al. A Peroxidase-Dependent Apoplastic Oxidative Burst in Cultured Arabidopsis Cells Functions in MAMP-Elicited Defense. **Plant Physiology**, v. 158, p. 2013–2027, 2012.

OCHSSNER, I.; HAUSMANN, L.; TÖPFER, R. Rpv14, a new genetic source for Plasmopara viticola resistance conferred by Vitis cinerea. **Vitis: Journal of Grapevine Research**, v. 55, n. 2, p. 79–81, 2016.

OKUSHIMA, Y. et al. Secreted proteins of tobacco cultured BY2 cells: identification of a new member of pathogenesis-related proteins. **Plant Molecular Biology**, v. 42, n. 3, p. 479–488, 2000.

OLIVIER, V.; SPRING, J.-L.; GINDRO, K. Stilbenes: biomarkers of grapevine resistance to fungal diseases. **OENO One**, v. 52, n. 3, p. 235–241, 25 set. 2018.

ONAGA, G.; WYDRA, K. Advances in Plant Tolerance to Biotic Stresses. In: **Plant Genomics**. [s.l.] InTech, 2016.

PALMIERI, M. C. et al. Proteomic analysis of grapevine resistance induced by Trichoderma harzianum T39 reveals specific defence pathways activated against downy mildew. **Journal of Experimental Botany**, v. 63, n. 17, p. 6237–6251, 1 out. 2012.

PAOLACCI, A. R. et al. Jasmonate-mediated defence responses, unlike salicylate-

mediated responses, are involved in the recovery of grapevine from bois noir disease. **BMC Plant Biology**, v. 17, n. 1, p. 118, 10 dez. 2017.

PAUWELS, L. et al. NINJA connects the co-repressor TOPLESS to jasmonate signalling. **Nature**, v. 464, n. 7289, p. 788–791, 1 abr. 2010.

PAUWELS, L.; GOOSSENS, A. **The JAZ proteins: A crucial interface in the jasmonate signaling cascadePlant Cell**American Society of Plant Biologists, , 1 set. 2011. Disponível em: <www.plantcell.org/cgi/doi/10.1105/tpc.111.089300>. Acesso em: 7 out. 2020

PAVET, V. et al. Ascorbic acid deficiency activates cell death and disease resistance responses in Arabidopsis. **Plant Physiology**, v. 139, n. 3, p. 1291–1303, 1 nov. 2005.

PEART, J. R. et al. NRG1, a CC-NB-LRR protein, together with N, a TIR-NB-LRR protein, mediates resistance against tobacco mosaic virus. **Current Biology**, v. 15, n. 10, p. 968–973, 24 maio 2005.

PERAZZOLLI, M. et al. Induction of systemic resistance against Plasmopara viticola in grapevine by Trichoderma harzianum T39 and benzothiadiazole. **Biological Control**, v. 47, n. 2, p. 228–234, 1 nov. 2008.

PERESSOTTI, E. et al. Breakdown of resistance to grapevine downy mildew upon limited deployment of a resistant variety. **BMC Plant Biology**, v. 10, n. 1, p. 1–11, 15 jun. 2010.

PEZET, R. et al. Effects of resveratrol, viniferins and pterostilbene on Plasmopara viticola zoospore mobility and disease development. **Vitis**, v. 43, n. 2, p. 145–148, 2003.

PEZET, R. et al. Glycosylation and oxidative dimerization of resveratrol are respectively associated to sensitivity and resistance of grapevine cultivars to downy mildew. **Physiological and Molecular Plant Pathology**, v. 65, n. 6, p. 297–303, 1 dez. 2004.

PIRRELLO, C. et al. Emergent Ascomycetes in Viticulture: An Interdisciplinary Overview. **Frontiers in Plant Science**, v. 10, 22 nov. 2019.

PIRRELLO, C. et al. Mining downy mildew susceptibility genes: a diversity study in grapevine. **bioRxiv**, p. 2020.01.15.898700, 15 jan. 2020.

POLESANI, M. et al. cDNA-AFLP analysis of plant and pathogen genes expressed in grapevine infected with Plasmopara viticola. **BMC Genomics**, v. 9, 26 mar. 2008.

POLESANI, M. et al. General and species-specific transcriptional responses to downy mildew infection in a susceptible (Vitis vinifera) and a resistant (V. Riparia) grapevine species. **BMC Genomics**, v. 11, n. 1, p. 1–16, 18 fev. 2010.

PONCE DE LEÓN, I.; MONTESANO, M. Activation of Defense Mechanisms against Pathogens in Mosses and Flowering Plants. **International Journal of Molecular Sciences**, v.

14, n. 2, p. 3178–3200, 4 fev. 2013.

PONS, A. et al. Impact of Plasmopara viticola infection of Merlot and Cabernet Sauvignon grapes on wine composition and flavor. **Food Chemistry**, v. 239, p. 102–110, 15 jan. 2018.

POSSAMAI, T. et al. Rpv Mediated Defense Responses in Grapevine Offspring Resistant to Plasmopara viticola. **Plants**, v. 9, n. 6, p. 781, 22 jun. 2020.

POSTEL, S.; KEMMERLING, B. **Plant systems for recognition of pathogen-associated molecular patternsSeminars in Cell and Developmental Biology**Elsevier Ltd, , 1 dez. 2009.

POURCEL, L. et al. TRANSPARENT TESTA10 encodes a laccase-like enzyme involved in oxidative polymerization of flavonoids in Arabidopsis seed coat. **Plant Cell**, v. 17, n. 11, p. 2966–2980, 1 nov. 2005.

R CORE TEAM. **R: A Language and Environment for Statistical Computing**Vienna, AustriaR Foundation for Statistical Computing, , 2019. Disponível em: <https://www.r-project.org/>. Acesso em: 31 jan. 2020

RAINERI, J. et al. The rice transcription factor OsWRKY47 is a positive regulator of the response to water deficit stress. **Plant Molecular Biology**, v. 88, n. 4–5, p. 401–413, 1 jul. 2015.

RASMUSSEN, M. W. et al. MAP Kinase Cascades in Arabidopsis Innate Immunity. **Frontiers in Plant Science**, v. 3, n. JUL, p. 169, 24 jul. 2012.

RAUF, A. et al. **Proanthocyanidins: A comprehensive reviewBiomedicine and Pharmacotherapy**Elsevier Masson SAS, , 1 ago. 2019.

REID, K. E. et al. An optimized grapevine RNA isolation procedure and statistical determination of reference genes for real-time RT-PCR during berry development. **BMC Plant Biology**, v. 6, n. 1, p. 27, 14 nov. 2006.

RIAZ, S. et al. Genetic diversity analysis of cultivated and wild grapevine (Vitis vinifera L.) accessions around the Mediterranean basin and Central Asia. **BMC Plant Biology**, v. 18, n. 1, p. 137, 27 jun. 2018.

RICHTER, H. et al. Characterization of 3 new partial stilbene synthase genes out of over 20 expressed in Vitis vinifera during the interaction with Plasmopara viticola. **Physiological and Molecular Plant Pathology**, v. 67, n. 3–5, p. 248–260, 1 set. 2006.

RIEMANN, M. et al. Cytoskeletal responses during early development of the downy mildew of grapevine (Plasmopara viticola). **Protoplasma**, v. 219, p. 13–22, 2002.

RIGHI, D. et al. Generation of Stilbene Antimicrobials against Multiresistant Strains

of Staphylococcus aureus through Biotransformation by the Enzymatic Secretome of Botrytis cinerea. **Journal of Natural Products**, v. 83, n. 8, p. 2347–2356, 28 ago. 2020.

ROJAS, C. M. et al. **Regulation of primary plant metabolism during plant-pathogen interactions and its contribution to plant defenseFrontiers in Plant Science**Frontiers Research Foundation, , 10 fev. 2014. Disponível em: <www.frontiersin.org>. Acesso em: 5 dez. 2020

ROSS, A. F. Systemic acquired resistance induced by localized virus infections in plants. **Virology**, v. 14, n. 3, p. 340–358, 1 jul. 1961.

ROSS, A. F.; BOZARTH, R. F. Resistance induced in one plant part as a result of virus infection in another part. **Phytopathology**, v. 50, n. 9, p. 652, 1960.

ROSSI, V. et al. Estimating the germination dynamics of Plasmopara viticola oospores using hydro-thermal time. **Plant Pathology**, v. 57, n. 2, p. 216–226, 1 abr. 2008.

ROSSI, V.; CAFFI, T. The role of rain in dispersal of the primary inoculum of plasmopara viticola. **Phytopathology**, v. 102, n. 2, p. 158–165, fev. 2012.

ROSSI, V.; CAFFI, T.; GOBBIN, D. **Contribution of molecular studies to botanical epidemiology and disease modelling: Grapevine downy mildew as a case-studyEuropean Journal of Plant Pathology**Springer, , 18 abr. 2013. Disponível em: <https://link.springer.com/article/10.1007/s10658-012-0114-2>. Acesso em: 23 set. 2020

ROSSIN, G. et al. Grapevine downy mildew plasmopara viticola infection elicits the expression of allergenic pathogenesis-related proteins. **International Archives of Allergy and Immunology**, v. 168, n. 2, p. 90–95, 1 dez. 2015.

ROUXEL, M. et al. Phylogenetic and experimental evidence for host-specialized cryptic species in a biotrophic oomycete. **New Phytologist**, v. 197, n. 1, p. 251–263, 1 jan. 2013.

RUEHL, E. et al. Grapevine breeding programmes in Germany. In: **Grapevine Breeding Programs for the Wine Industry**. [s.l.] Elsevier Inc., 2015. p. 77–101.

RUMBOLZ, J. et al. Sporulation of Plasmopara viticola: Differentiation and light regulation. **Plant Biology**, v. 4, n. 3, p. 413–422, maio 2002.

RUSHTON, P. J. et al. Members of a new family of DNA-binding proteins bind to a conserved cis-element in the promoters of α-Amy2 genes. **Plant Molecular Biology**, v. 29, n. 4, p. 691–702, nov. 1995.

SAIFERT, L. et al. Marker-assisted pyramiding of resistance loci to grape downy mildew. **Pesquisa Agropecuaria Brasileira**, v. 53, n. 5, p. 602–610, 1 maio 2018.

SAITOU, N.; NEI, M. The Neighbor-joining Method: A New Method for

Reconstructing Phylogenetic Trees. **Molecular Biology and EvoluctionEvoluction**, v. 4, n. 4, p. 406–425, 1987.

SALINARI, F. et al. Downy mildew (*Plasmopara viticola*) epidemics on grapevine under climate change. **Global Change Biology**, v. 12, n. 7, p. 1299–1307, jul. 2006.

SALVAGNIN, U. et al. Homologous and heterologous expression of grapevine E-(β)-caryophyllene synthase (VvGwECar2). **Phytochemistry**, v. 131, p. 76–83, 1 nov. 2016.

SÁNCHEZ-MORA, F. D. et al. Behavior of grape breeding lines with distinct resistance alleles to downy mildew (*Plasmopara viticola*). **Crop Breeding and Applied Biotechnology**, v. 17, n. 2, p. 141–149, 2017.

SAPKOTA, S. et al. Construction of a high-density linkage map and QTL detection of downy mildew resistance in Vitis aestivalis-derived 'Norton'. **Theoretical and Applied Genetics**, v. 132, n. 1, p. 137–147, 19 jan. 2019.

SAPORTA, G. **Le monde des plantes avant l'apparition de l'homme - Gaston marquis de Saporta - Google Livros**. Paris: [s.n.].

SARGOLZAEI, M. et al. Rpv29, Rpv30 and Rpv31: Three Novel Genomic Loci Associated With Resistance to Plasmopara viticola in Vitis vinifera. **Frontiers in Plant Science**, v. 11, p. 1537, 8 out. 2020.

SARRIS, P. F. et al. A plant immune receptor detects pathogen effectors that target WRKY transcription factors. **Cell**, v. 161, n. 5, p. 1089–1100, 30 maio 2015.

SCHALLER, A.; STINTZI, A. **Enzymes in jasmonate biosynthesis - Structure, function, regulationPhytochemistry**Pergamon, , 1 set. 2009.

SCHARTE, J.; SCHÖN, H.; WEIS, E. Photosynthesis and carbohydrate metabolism in tobacco leaves during an incompatible interaction with Phytophthora nicotianae. **Plant, Cell and Environment**, v. 28, n. 11, p. 1421–1435, 1 nov. 2005.

SCHMIDLIN, L. et al. A stress-inducible resveratrol O-methyltransferase involved in the biosynthesis of pterostilbene in grapevine. **Plant Physiology**, v. 148, n. 3, p. 1630–1639, 1 nov. 2008.

SCHNEE, S.; VIRET, O.; GINDRO, K. Role of stilbenes in the resistance of grapevine to powdery mildew. **Physiological and Molecular Plant Pathology**, v. 72, n. 4–6, p. 128–133, 1 jul. 2008.

SCHORNACK, S. et al. Ancient class of translocated oomycete effectors targets the host nucleus. **Proceedings of the National Academy of Sciences of the United States of America**, v. 107, n. 40, p. 17421–17426, 5 out. 2010.

SCHWANDER, F. et al. Rpv10: a new locus from the Asian Vitis gene pool for

pyramiding downy mildew resistance loci in grapevine. **Theoretical and Applied Genetics**, v. 124, n. 1, p. 163–176, 21 jan. 2012.

SHAH, J. **The salicylic acid loop in plant defenseCurrent Opinion in Plant Biology**Elsevier Ltd, , 1 ago. 2003.

SHAH, J.; ZEIER, J. Long-distance communication and signal amplification in systemic acquired resistance. **Frontiers in Plant Science**, v. 4, p. 30, 22 fev. 2013.

SHARMA, M.; PANDEY, G. K. **Expansion and function of repeat domain proteins during stress and development in plantsFrontiers in Plant Science**Frontiers Research Foundation, , 11 jan. 2016.

SHEARD, L. B. et al. Jasmonate perception by inositol-phosphate-potentiated COI1-JAZ co-receptor. **Nature**, v. 468, n. 7322, p. 400–407, 18 nov. 2010.

SHI, J. et al. The comparative analysis of the potential relationship between resveratrol and stilbene synthase gene family in the development stages of grapes (Vitis quinquangularis and Vitis vinifera). **Plant Physiology and Biochemistry**, v. 74, p. 24–32, jan. 2014.

SHIM, J. S. et al. *AtMYB44* regulates *WRKY70* expression and modulates antagonistic interaction between salicylic acid and jasmonic acid signaling. **The Plant Journal**, v. 73, n. 3, p. 483–495, 1 fev. 2013.

SHIM, J. S.; CHOI, Y. DO. Direct regulation of WRKY70 by AtMYB44 in plant defense responses. **Plant Signaling & Behavior**, v. 8, n. 6, p. e24509, 3 jun. 2013.

SHIMONO, M. et al. Rice WRKY45 Plays a Crucial Role in Benzothiadiazole-Inducible Blast Resistance. **The Plant Cell**, v. 19, p. 2064–2076, 2007.

SILVA, A. L.; DOAZAN, J. P. Gamma-ray mutagenesis on grapevine rootstocks cultivated in vitro. **OENO One**, v. 29, n. 1, p. 9, 31 mar. 1995.

SINAPIDOU, E. et al. Two TIR:NB:LRR genes are required to specify resistance to Peronospora parasitica isolate Cala2 in Arabidopsis. **Plant Journal**, v. 38, n. 6, p. 898–909, 1 jun. 2004.

SOMSSICH, I. E. et al. Rapid activation by fungal elicitor of genes encoding "pathogenesis-related" proteins in cultured parsley cells. **Proceedings of the National Academy of Sciences of the United States of America**, v. 83, n. 8, p. 2427–30, 1 abr. 1986.

SONG, Z. et al. Genome-wide identification and characterization of UGT family in pigeonpea (Cajanus cajan) and expression analysis in abiotic stress. **Trees - Structure and Function**, v. 33, n. 4, p. 987–1002, 1 ago. 2019.

SPOEL, S. H. et al. NPR1 Modulates Cross-Talk between Salicylate-and Jasmonate-

Dependent Defense Pathways through a Novel Function in the Cytosol. **The Plant Cell**, v. 15, p. 760–770, 2003.

SPOEL, S. H. et al. Proteasome-Mediated Turnover of the Transcription Coactivator NPR1 Plays Dual Roles in Regulating Plant Immunity. **Cell**, v. 137, n. 5, p. 860–872, 29 maio 2009.

STAM, R. et al. Identification and Characterisation CRN Effectors in Phytophthora capsici Shows Modularity and Functional Diversity. **PLoS ONE**, v. 8, n. 3, p. e59517, 25 mar. 2013.

STASWICK, P. E. et al. Characterization of an Arabidopsis Enzyme Family That Conjugates Amino Acids to Indole-3-Acetic Acid W. **The Plant Cell**, v. 17, p. 616–627, 2005.

STAUDT, G.; KASSEMEYER, H. H. Evaluation of downy mildew resistance in various accessions of wild Vitis species. **Vitis**, v. 34, n. 4, p. 225–228, 1995.

STICHER, L.; MAUCH-MANI, B.; MÉTRAUX, AND J. SYSTEMIC ACQUIRED RESISTANCE. **Annual Review of Phytopathology**, v. 35, n. 1, p. 235–270, set. 1997.

SU, H. et al. Overexpression of VpPR10.1 by an efficient transformation method enhances downy mildew resistance in V. vinifera. **Plant Cell Reports**, v. 37, n. 5, p. 819–832, 6 maio 2018.

SUMNER, L. W. et al. Proposed minimum reporting standards for chemical analysis: Chemical Analysis Working Group (CAWG) Metabolomics Standards Initiative (MSI). **Metabolomics**, v. 3, n. 3, p. 211–221, 12 set. 2007.

SUN, H. et al. ITRAQ-based comparative proteomic analysis of differences in the protein profiles of stems and leaves from two alfalfa genotypes. **BMC Plant Biology**, v. 20, n. 1, p. 447, 29 set. 2020.

SWIDERSKI, M. R.; BIRKER, D.; JONES, J. D. G. The TIR domain of TIR-NB-LRR resistance proteins is a signaling domain involved in cell death induction. **Molecular Plant-Microbe Interactions**, v. 22, n. 2, p. 157–165, 8 fev. 2009.

TAURINO, M. et al. Jasmonates elicit different sets of stilbenes in Vitis vinifera cv. Negramaro cell cultures. **SpringerPlus**, v. 4, n. 1, p. 49, 1 dez. 2015.

TAYLOR, A. S.; COOK, D. C. An economic assessment of the impact on the Western Australian viticulture industry from the incursion of grapevine downy mildew. **Journal of Plant Diseases and Protection**, v. 125, n. 4, p. 397–403, 16 ago. 2018.

TERRAL, J. F. et al. Evolution and history of grapevine (Vitis vinifera) under domestication: new morphometric perspectives to understand seed domestication syndrome and reveal origins of ancient European cultivars. **Annals of botany**, v. 105, n. 3, p. 443–455, 1 mar.

2010.

TERRAS, F. R. et al. Small cysteine-rich antifungal proteins from radish: their role in host defense. **The Plant cell**, v. 7, n. 5, p. 573–88, 1 maio 1995.

THINES, B. et al. JAZ repressor proteins are targets of the SCFCOI1 complex during jasmonate signalling. **Nature**, v. 448, n. 7154, p. 661–665, 9 ago. 2007.

THIS, P.; LACOMBE, T.; THOMAS, M. R. Historical origins and genetic diversity of wine grapes. **Trends in Genetics**, v. 22, n. 9, p. 511–519, 1 set. 2006.

THOMMA, B. P. H. J.; NÜRNBERGER, T.; JOOSTEN, M. H. A. J. Of PAMPs and Effectors: The Blurred PTI-ETI Dichotomy OA. **The Plant Cell**, v. 23, p. 4–15, 2011.

THUERIG, B. et al. Reducing copper use in the environment: the use of larixol and larixyl acetate to treat downy mildew caused by *Plasmopara viticola* in viticulture. **Pest Management Science**, v. 74, n. 2, p. 477–488, 1 fev. 2018.

TOGNETTI, V. B. et al. Perturbation of indole-3-butyric acid homeostasis by the UDP-glucosyltransferase UGT74E2 modulates Arabidopsis architecture and water stress tolerance. **Plant Cell**, v. 22, n. 8, p. 2660–2679, 1 ago. 2010.

TÖPFER, R. et al. New Horizons for grapevine breeding. In: **Fruit, Vegetable and Cereal Science and Biotechnology**. [s.l.] New Horizons for grapevine breeding, 2011. p. 79–100.

ÜLKER, B.; SHAHID MUKHTAR, M.; SOMSSICH, I. E. The WRKY70 transcription factor of Arabidopsis influences both the plant senescence and defense signaling pathways. **Planta**, v. 226, n. 1, p. 125–137, 20 jun. 2007.

ÜLKER, B.; SOMSSICH, I. E. **WRKY transcription factors: From DNA binding towards biological functionCurrent Opinion in Plant Biology**Elsevier Current Trends, , 1 out. 2004.

UNGER, S. et al. The Course of Colonization of Two Different Vitis Genotypes by Plasmopara viticola Indicates Compatible and Incompatible Host-Pathogen Interactions. 2007.

UNUSAN, N. **Proanthocyanidins in grape seeds: An updated review of their health benefits and potential uses in the food industryJournal of Functional Foods**Elsevier Ltd, , 1 abr. 2020.

URBAN, L. et al. UV-C light and pulsed light as alternatives to chemical and biological elicitors for stimulating plant natural defenses against fungal diseases. **Scientia Horticulturae**, v. 235, p. 452–459, 17 maio 2018.

VALLEJO, A. et al. Fungicide distribution in vitiviniculture ecosystems according to different application strategies to reduce environmental impact. **Science of the Total**

Environment, v. 687, p. 319–329, 15 out. 2019.

VAN DEN BERG, R. A. et al. Centering, scaling, and transformations: Improving the biological information content of metabolomics data. **BMC Genomics**, v. 7, n. 1, p. 142, 8 jun. 2006.

VAN DER ENT, S. et al. 11 Induced Resistance - Orchestrating Defence Mechanisms through Crosstalk and Priming. In: **Annual Plant Reviews online**. Chichester, UK: John Wiley & Sons, Ltd, 2018. p. 334–370.

VAN ECK, L.; BRADEEN, J. M. The NB-LRR Disease Resistance Genes of Fragaria and Rubus. In: [s.l.] Springer, Cham, 2018. p. 63–75.

VAN GELDER, K.; FORRESTER, T.; AKHTAR, T. A. Evidence from stable-isotope labeling that catechol is an intermediate in salicylic acid catabolism in the flowers of Silene latifolia (white campion). **Planta**, v. 252, n. 1, p. 3, 1 jul. 2020.

VAN HEERDEN, C. J. et al. Detection of downy and powdery mildew resistance QTL in a “Regent” 3 “RedGlobe” population. **Euphytica**, v. 200, n. 2, p. 281–295, 2014.

VAN LOON, L. C. et al. Recommendations for naming plant pathogenesis-related proteins. **Plant Molecular Biology Reporter**, v. 12, n. 3, p. 245–264, set. 1994.

VAN LOON, L. C.; VAN KAMMEN, A. Polyacrylamide disc electrophoresis of the soluble leaf proteins from Nicotiana tabacum var. ‘Samsun’ and ‘Samsun NN’: II. Changes in protein constitution after infection with tobacco mosaic virus. **Virology**, v. 40, n. 2, p. 199–211, 1 fev. 1970.

VAN LOON, L. C.; VAN STRIEN, E. A. The families of pathogenesis-related proteins, their activities, and comparative analysis of PR-1 type proteins. **Physiological and Molecular Plant Pathology**, v. 55, n. 2, p. 85–97, ago. 1999.

VELASCO, R. et al. A High Quality Draft Consensus Sequence of the Genome of a Heterozygous Grapevine Variety. **PLoS ONE**, v. 2, n. 12, p. e1326, 19 dez. 2007.

VENUTI, S. et al. Historical Introgression of the Downy Mildew Resistance Gene Rpv12 from the Asian Species Vitis amurensis into Grapevine Varieties. **PLoS ONE**, v. 8, n. 4, p. e61228, 12 abr. 2013.

VERA, P.; CONEJERO, V. Pathogenesis-related proteins of tomato : p-69 as an alkaline endoproteinase. **Plant physiology**, v. 87, n. 1, p. 58–63, 1 maio 1988.

VEZZULLI, S. et al. The Rpv3-3 Haplotype and Stilbenoid Induction Mediate Downy Mildew Resistance in a Grapevine Interspecific Population. **Frontiers in Plant Science**, v. 10, p. 234, 6 mar. 2019.

VIVEROS SANTOS, I. et al. Regionalized Terrestrial Ecotoxicity Assessment of

Copper-Based Fungicides Applied in Viticulture. **Sustainability**, v. 10, n. 7, p. 2522, 19 jul. 2018.

VOGT, T.; JONES, P. **Glycosyltransferases in plant-natural product synthesis: Characterization of a supergene familyTrends in Plant Science**Elsevier Ltd, , 1 set. 2000.

VRHOVSEK, U. et al. **A versatile targeted metabolomics method for the rapid quantification of multiple classes of phenolics in fruits and beverages**. Journal of Agricultural and Food Chemistry. **Anais**...American Chemical Society, 12 set. 2012Disponível em: <www.ars.usda.gov/Services/docs.htm?docid=8964>. Acesso em: 25 nov. 2020

WALSH, T. A. et al. Canola engineered with a microalgal polyketide synthase-like system produces oil enriched in docosahexaenoic acid. **Nature Biotechnology**, v. 34, n. 8, p. 881–887, 8 jan. 2016.

WAN, Y. et al. A phylogenetic analysis of the grape genus (Vitis L.) reveals broad reticulation and concurrent diversification during neogene and quaternary climate change. **BMC Evolutionary Biology**, v. 13, n. 1, p. 1–20, 5 jul. 2013.

WANG, C. et al. Selection and regeneration of Vitis vinifera Chardonnay hydroxyproline-resistant calli. **Protoplasma**, v. 255, n. 5, p. 1413–1422, 1 set. 2018a.

WANG, D. et al. Salicylic Acid Inhibits Pathogen Growth in Plants through Repression of the Auxin Signaling Pathway. **Current Biology**, 2007.

WANG, K. et al. Two Abscisic Acid-Responsive Plastid Lipase Genes Involved in Jasmonic Acid Biosynthesis in Arabidopsis thaliana. **The Plant cell**, v. 30, p. 1006–1022, 2018b.

WANG, L. et al. RING-H2-type E3 gene VpRH2 from Vitis pseudoreticulata improves resistance to powdery mildew by interacting with VpGRP2A. **Journal of Experimental Botany**, v. 68, n. 7, p. 1669–1687, 1 mar. 2017a.

WANG, L.; YAO, W.; WANG, Y. The grape ubiquitin ligase VpRH2 is a negative regulator in response to ABA treatment. **Planta**, v. 251, n. 88, 1 abr. 2020.

WANG, T. et al. Overexpression of UGT74E2, an Arabidopsis IBA Glycosyltransferase, Enhances Seed Germination and Modulates Stress Tolerance via ABA Signaling in Rice. **International Journal of Molecular Sciences**, v. 21, n. 19, p. 7239, 30 set. 2020.

WANG, X. et al. Genomic analyses of primitive, wild and cultivated citrus provide insights into asexual reproduction. **Nature Genetics**, v. 49, n. 5, p. 765–772, 1 maio 2017b.

WANG, Z. et al. An oligo selection procedure for identification of sequence-specific DNA-binding activities associated with the plant defence response. **The Plant Journal**, v. 16,

n. 4, p. 515–522, 1 nov. 1998.

WASTERNACK, C.; HAUSE, B. Jasmonates: biosynthesis, perception, signal transduction and action in plant stress response, growth and development. An update to the 2007 review in Annals of Botany. **Annals of Botany**, v. 111, p. 1021–1058, 2013.

WAWRA, S. et al. **Secretion, delivery and function of oomycete effector proteinsCurrent Opinion in Microbiology**Elsevier Current Trends, , 1 dez. 2012.

WEI, Y. et al. An epidermis/papilla-specific oxalate oxidase-like protein in the defence response of barley attacked by the powdery mildew fungus. **Plant Molecular Biology**, v. 36, n. 1, p. 101–112, 1998.

WELTER, L. J. et al. Genetic mapping and localization of quantitative trait loci affecting fungal disease resistance and leaf morphology in grapevine (*Vitis vinifera* L). **Molecular Breeding**, v. 20, n. 4, p. 359–374, 25 set. 2007.

WEN, J. et al. A new phylogenetic tribal classification of the grape family (Vitaceae). **Journal of Systematics and Evolution**, v. 56, n. 4, p. 262–272, 1 jul. 2018a.

WEN, J. et al. Chloroplast phylogenomics of the New World grape species (*Vitis* , Vitaceae). **Journal of Systematics and Evolution**, v. 56, n. 4, p. 297–308, 1 jul. 2018b.

WHISSON, S. C. et al. A translocation signal for delivery of oomycete effector proteins into host plant cells. **Nature**, v. 450, n. 7166, p. 115–118, 1 nov. 2007.

WIEDEMANN-MERDINOGLU, S. et al. Resistance to downy mildew derived from *Muscadinia rotundifolia*: genetic analysis and use of molecular markers for breeding. **5th International Workshop on Grapevine Downy and Powdery Mildew**, p. 28, 2006.

WIŚNIEWSKI, J. R. et al. Universal sample preparation method for proteome analysis. **Nature Methods**, v. 6, n. 5, p. 359–362, 2009.

WITHERS, J.; DONG, X. **Posttranslational Modifications of NPR1: A Single Protein Playing Multiple Roles in Plant Immunity and PhysiologyPLoS Pathogens**Public Library of Science, , 1 ago. 2016.

WONG, F. P.; BURR, H. N.; WILCOX, W. F. Heterothallism in *Plasmopara viticola*. **Plant Pathology**, v. 50, n. 4, p. 427–432, 1 ago. 2001.

WU, L. et al. **Go in for the kill: How plants deploy effector-triggered immunity to combat pathogensVirulence**Landes Bioscience, , 2014. Disponível em: <https://www.tandfonline.com/doi/abs/10.4161/viru.29755>. Acesso em: 4 out. 2020

XIANG, J. et al. Studying the Mechanism of Plasmopara viticola RxLR Effectors on Suppressing Plant Immunity. **Frontiers in Microbiology**, v. 7, n. MAY, p. 709, 18 maio 2016.

XU, D. et al. Biological activity of pterostilbene against Peronophythora litchii, the

litchi downy blight pathogen. **Postharvest Biology and Technology**, v. 144, p. 29–35, 1 out. 2018.

XU, W. et al. VpSTS29/STS2 enhances fungal tolerance in grapevine through a positive feedback loop. **Plant Cell and Environment**, v. 42, n. 11, p. 2979–2998, 1 nov. 2019a.

XU, Y. et al. Transcriptome sequencing analyses reveals mechanisms of eliminated russet by applying GA 3 and CPPU on 'shine Muscat' grape. **Scientia Horticulturae**, v. 250, p. 94–103, 10 maio 2019b.

XUE, H. et al. The mechanism of induced resistance against Fusarium dry rot in potato tubers by the T-2 toxin. **Postharvest Biology and Technology**, v. 153, p. 69–78, 1 jul. 2019.

YAN, X. et al. Analysis of the grape (Vitis vinifera L.) thaumatin-like protein (TLP) gene family and demonstration that TLP29 contributes to disease resistance. **Scientific Reports**, v. 7, n. 1, p. 4269, 27 dez. 2017.

YEDIDIA et al. Structural Elucidation of Three Novel Kaempferol O-tri-Glycosides that Are Involved in the Defense Response of Hybrid Ornithogalum to Pectobacterium carotovorum. **Molecules**, v. 24, n. 16, p. 2910, 10 ago. 2019.

YERGALIYEV, T. M. et al. The involvement of ROS producing aldehyde oxidase in plant response to Tombusvirus infection. **Plant Physiology and Biochemistry**, v. 109, p. 36–44, 1 dez. 2016.

YIN, L. et al. Genome sequence of Plasmopara viticola and insight into the pathogenic mechanism. **Scientific Reports**, v. 7, 18 abr. 2017.

YU, C. K. Y. et al. A stilbene synthase gene (SbSTS1) is involved in host and nonhost defense responses in sorghum. **Plant Physiology**, v. 138, n. 1, p. 393–401, 1 maio 2005.

YU, D.; CHEN, C.; CHEN, Z. **Evidence for an Important Role of WRKY DNA Binding Proteins in the Regulation of NPR1 Gene ExpressionThe Plant Cell**. [s.l: s.n.]. Disponível em: <www.plantcell.org>. Acesso em: 1 ago. 2019.

YU, Y. et al. The grapevine R2R3-type MYB transcription factor VdMYB1 positively regulates defense responses by activating the stilbene synthase gene 2 (VdSTS2). **BMC Plant Biology**, v. 19, n. 1, p. 1–15, 7 nov. 2019.

YUAN, Y. et al. Functional analysis of rice NPR1-like genes reveals that OsNPR1/NH1 is the rice orthologue conferring disease resistance with enhanced herbivore susceptibility. **Plant Biotechnology Journal**, v. 5, n. 2, p. 313–324, 1 mar. 2007.

YUANYUAN, M. et al. Roles of plant soluble sugars and their responses to plant cold stress. **African Journal of Biotechnology**, v. 8, n. 10, 2009.

ZANGHELINI, J. A. et al. Response of PIWI grapevine cultivars to downy mildew in

highland region of southern Brazil. **European Journal of Plant Pathology**, v. 154, n. 4, p. 1051–1058, 15 ago. 2019.

ZEIER, J. et al. Light conditions influence specific defence responses in incompatible plant-pathogen interactions: Uncoupling systemic resistance from salicylic acid and PR-1 accumulation. **Planta**, v. 219, n. 4, p. 673–683, 20 abr. 2004.

ZHANG, H. et al. Investigating Proteome and Transcriptome Defense Response of Apples Induced by *Yarrowia lipolytica*. **Molecular Plant-Microbe Interactions®**, v. 30, n. 4, p. 301–311, 1 abr. 2017.

ZHANG, J. et al. An odorant receptor from the common cutworm (*Spodoptera litura*) exclusively tuned to the important plant volatile cis-3-Hexenyl acetate. **Insect Molecular Biology**, v. 22, n. 4, p. 424–432, 1 ago. 2013.

ZHANG, S. et al. Molecular cloning of a CC–NBS–LRR gene from Vitis quinquangularis and its expression pattern in response to downy mildew pathogen infection. **Molecular Genetics and Genomics**, v. 293, n. 1, p. 61–68, 1 fev. 2018.

ZHANG, Y. et al. Identification of the defense-related gene VdWRKY53 from the wild grapevine *Vitis davidii* using RNA sequencing and ectopic expression analysis in Arabidopsis. **Hereditas**, v. 156, n. 1, p. 14, 26 dez. 2019a.

ZHANG, Y. et al. Enhancement of methyl salicylate accumulation promotes early flowering in transgenic tobacco plants by overexpressing a carboxymethyl transferase (SAMT) gene from Lycium chinense. **Molecular Breeding**, v. 40, n. 6, p. 1–16, 1 jun. 2020.

ZHANG, Z. et al. Dual Regulation Role of GH3.5 in Salicylic Acid and Auxin Signaling during Arabidopsis-Pseudomonas syringae Interaction 1. **Plant Physiology**, v. 145, p. 450–464, out. 2007.

ZHANG, Z. et al. Red anthocyanins contents and the relationships with phenylalanine ammonia lyase (PAL) activity, soluble sugar and chlorophyll contents in carmine radish (Raphanus sativus L.). **Horticultural Science**, v. 46, n. 1, p. 17–25, 29 mar. 2019b.

ZHANG, Z.; COLLINGE, D. B.; THORDAL-CHRISTENSEN, H. Germin-like oxalate oxidase, a H2O2-producing enzyme, accumulates in barley attacked by the powdery mildew fungus. **The Plant Journal**, v. 8, n. 1, p. 139–145, 1 jul. 1995.

ZHAO, H. et al. Downy mildew resistance identification and SSR molecular marker screening of different grape germplasm resources. **Scientia Horticulturae**, v. 252, p. 212–221, 27 jun. 2019.

ZINI, E. et al. R-Loci Arrangement Versus Downy and Powdery Mildew Resistance Level: A *Vitis* Hybrid Survey. **International Journal of Molecular Sciences**, v. 20, n. 14, p.

3526, 18 jul. 2019.

ZIPFEL, C.; FELIX, G. **Plants and animals: A different taste for microbes?Current Opinion in Plant Biology**Elsevier Current Trends, , 1 ago. 2005.

ZOU, B. et al. AtMYB44 positively modulates disease resistance to Pseudomonas syringae through the salicylic acid signalling pathway in Arabidopsis. **Functional Plant Biology**, v. 40, n. 3, p. 304, 3 abr. 2013.

ZYPRIAN, E. et al. Quantitative trait loci affecting pathogen resistance and ripening of grapevines. **Molecular Genetics and Genomics**, v. 291, p. 1573–1594, 2016.